Physical Ageing of Epoxy Resin - Polyethersulphone Blends

by

Christopher David Breach

A Dissertation submitted to
Brunel University for the
Degree of
Doctor of Philosophy
1993

Preface

Writing this thesis has been a hard work. There are many aspects of the presentation which I feel could be significantly better and I am not satisfied with its structure, some of the data presentation and the relatively small amount of work it contains. This is not at all a reflection on my supervisor, Dr. Michael Folkes, who was very encouraging during the Ph.D and who has also had to struggle to find time in his busy schedule to read and correct the thesis. His support and numerous discussions and ideas have been invaluable during the Ph.D period and in the writing stages. The main problem is that I am just never satisfied with my own efforts.

I must express my gratitude to my friend Mr. Paulo Cezar Frangiosa, who spent 6 months in our research group working on a project directly related to mine and which I partly supervised. As a professional chemist qualified to M.S. level I found his help and ideas invaluable in the chemical preparation stages and mechanical testing and we had several interesting discussions. He deserves a medal for putting up with my rather moody behaviour at a time when all my thoughts were concentrated on completing experimental work in good time. Part of this moodiness was also due to the fact that I and my fiancee at that time (now my wife) were separated by some several thousand miles and Caroline's love, understanding and tolerance were a major factor in helping me to survive this period.

Several other people deserve mention. Many thanks to Dr. Sue Woodisse for support, assistance and discussions concerning thermal analysis and to Dr. Dudley Finch for kind permission to use his FTIR microscope and spectrometer. Dudley aroused in me an interest in biomedical polyurethanes (an interest still retained) and this has led to interesting discussions. Geoff Harris and his wife Linda deserve a mention as friends and for introducing me to Jujitsu. Thanks also to Dr. Henrik Lund for his company and interesting discussions as well as his BASF connections. Mr. J.F. Tung (hopefully Dr. Tung in the near future) also deserves special mention as a very good friend and colleague with whom I have had several interesting discussions concerning nylon 6, amongst other things. I am grateful also to Dr. D. Vesely for discussions and the interest he has shown in my work. Thanks also to my external supervisor Dr. J.M. Barton of the Defence Research Agency, the organisation which sponsored this work. Dr. Barton

kindly arranged for me to conduct dielectric measurements at the Defence Research Agency, Farnborough.

I must of course thank my family. Being the only scientist in the family (as far as I know) they have had to put up with some eccentric behaviour on my part (aren't all scientists a little eccentric?). My Sister also had to put up with me living with her in London for what was initially 'a few weeks' but which became about 2 years. I am grateful even though I may not show it.

Finally, I would like to include a quote. I can't quite recall the exact words or where I read them, but I know they were spoken by the late Richard Feynman about science, in particular, physics and they go something like

"..what one fool can do another can also...."

This is very easy for a man of Feynman's genius to say but the point of it is that although science is difficult, many people have a lot more potential than they realise and no matter how bright the scientist, they nearly all work very hard. Hard work brings understanding and any determined "*fool* " with an interest in a subject can eventually understand at least some part of it.

Christopher David Breach
1993

Para sa Pinakamamahal kong asawa Caroline

And for my Family

Contents

Summary

In view of an increasing number of reports describing epoxy resin-thermoplastic blends, it is clearly important to identify the effects of the thermoplastic on the blend properties. In this work difunctional epoxy resin monomer (Epikote 828) cured with diaminodiphenylsulphone (DDS) or dicyandiamide (DICY) are the model systems used. The thermoplastic is a polyethersulphone (PES) with either hydroxyl terminations (Victrex 5003P, ICI) capable of reaction with epoxy monomer or chlorine terminated (Ultrason E2010, BASF) which is incapable of reaction. The glass transition characteristics of the PES materials are very similar but the Ultrason E2010 is of lower average molecular weight and can be expected to contain more chain ends.

Epoxy-DDS-PES systems were prepared with 20phr and 30phr of PES. The effects of the PES on crosslinking and isothermal physical ageing behaviour were examined. Enthalpy relaxation data were curve fitted using a Kohlrausch function. Mechanical and dielectric spectroscopy data were analysed using W-L-F and power law methods. Despite a tendency for the PES to reduce the crosslink density of the network, the blends had glass transition temperatures almost identical to the unmodified resin. The reduction in crosslink density improved G_{1C} compared to the unmodified resin but promoted faster physical ageing and more rapid embrittlement when the blends were aged at the same temperature as the neat resin.

The epoxy-DICY-PES system was studied at one composition of 30phr PES. The system was two phase but fast curing led to premature arrest of the phase separation process. Annealing at various temperatures from below the glass transition of the low temperature phase to just below the glass transition of the high temperature phase resulted in what is believed to be microscopic morphological changes detectable only barely by DSC and quite clearly from dynamic mechanical analysis. These changes were not manifest in the morphology of fracture surfaces. Annealing was found to decrease G_{1C} .

Presentations

Physical Ageing of Epoxy- Resin -PES Blends
A presentation of research results made to an audience at the Department of Materials Technology, Brunel University, Uxbridge, November 1991.

Two Phase Epoxy-PES Blends
A presentation of research results made at a discussion meeting between C.D.Breach, M.J. Folkes and representatives of Westland Helicopters, Ciba-Geigy and the Defence Research Agency, Farnborough, September 1991.

Publications

Physical Ageing of an Epoxy Resin-Polyethersulphone Blend
C.D. Breach, M.J. Folkes and J.M. Barton, Polymer, 33 3080 (1992)

Epoxy Resin-Polyethersulphone Blends 1: As Cured Materials
C.D. Breach, M.J. Folkes and J.M. Barton (to be published).

Epoxy Resin-Polyethersulphone Blends 2: Enthalpy Relaxation
C.D. Breach, M.J. Folkes and J.M. Barton (to be published).

Epoxy Resin-Polyethersulphone Blends 3: Dynamic Mechanical Observations of Physical Ageing
C.D. Breach, M.J. Folkes and J.M. Barton (to be published).

The Effects of Annealing on the Mechanical Spectra of a Two Phase Epoxy Resin-Polyethersulphone Blend
C.D. Breach, M.J. Folkes and J.M. Barton (to be published).

Chapter 1
Review of Objectives, Elementary Physics of Non-Crystalline Solids and Experimental Investigations of Blending and Physical Ageing in Epoxy Resins

1.0 Introduction and Objectives

Structural relaxation or *physical ageing* of glasses is of great interest to condensed matter scientists, particularly those involved in polymer science. Physical ageing is a universal process in non-crystalline solids which occurs when a glass is held at a temperature below the glass transition range (Struik, 1978). It is when the physical structure of a glass at molecular or atomic level tries to relax towards an equilibrium configuration by means of small local motions rather than large scale diffusional motion (Ngai, 1987). The equilibrium state towards which the structure is driven is characteristic of the storage or annealing temperature. The origin of the driving force for relaxation is supercooling of the glass from a temperature above the glass transition to a temperature below the glass transition and is caused by the inability of the molecular structure to reach equilibrium during the cooling process. Faster cooling rates cause greater perturbations from equilibrium whilst slower cooling rates allow more time for the glass to achieve a topological structure nearer to the equilibrium state. As the cooling rate decreases so the excess stored energy and thermodynamic driving force for physical ageing get smaller. Ultimately, infinitely slow cooling would permit the glass structure to remain in equilibrium at all times but this of course is an idealisation.

The slow physical rearrangement of the molecular structure involves spatial changes, increases in packing density and decreases in internal viscosity as excess energy is slowly eliminated. This process affects mechanical properties below the glass transition range, in particular the ability of the molecular structure to respond to externally applied bulk stresses. As the structure becomes more densely packed the specific volume and the molecular mobility decrease so that the molecular structure becomes gradually more unable to transmit external forces to its neighbours and share the load, and is thus unable to dissipate the energy due to the applied force by undergoing motion. Transmission of stress becomes increasingly more difficult as packing density increases because of the smaller space available for motion. The result of this is that with physical ageing a glassy material becomes more brittle (Struik, 1978) and many other properties also change, such as conductivity and dielectric characteristics (Ngai, 1987) and they change in a manner that tends to be non-linear. The rate of the ageing process is dependent upon the driving force which depends upon the cooling rate as well as the sub glass transition temperature at which the material is annealed (Struik, 1978). At temperatures far below the glass transition range the ageing is very slow and stops at temperatures below which local relaxations are not active. Physical ageing is a thermoreversible effect and its effects can be erased by heating the solid to above the glass transition temperature, holding for a short period of time and requenching.

Physical ageing has very important effects on the properties of all glassy polymers. Its effects can be particularly catastrophic in the automotive and aerospace industries where durability and long service life are often required. This is especially true for aerospace applications where polymers are used as structural load bearing components in jet aircraft. Polymers used for the outer skins of aircraft or as helicopter rotor blades need to be able to cope with wide extremes of temperature and with impact damage from birds. For military aircraft the outer regions of the structure may be encounter temperatures from -70°C to 150°C. Some components may also be exposed to the heat from aero engines and clearly these materials may be susceptible to intermittent physical ageing possibly leading to premature failure.

Epoxy resins are used extensively in aerospace applications as matrices for carbon fibres and are chosen because of their excellent tensile strength and elastic modulus (Morgan, 1979) but are brittle. Physical ageing makes the

brittleness worse. Rubber toughened resins have greatly improved toughnesses but at the expense of a slight depression in the glass transition range which limits their upper use temperature (Raghava, 1987). In an attempt to improve on rubber modified systems, tough engineering thermoplastics are being used as toughening agents for epoxies . In systems of practical use, the thermoplastic forms a dispersed second phase which stops or slows down crack propagation. A thermoplastic which has been favoured as a toughening agent is polyethersulphone (PES), (Bucknall and Partridge, 1983, 1984, 1986, Raghava, 1987, 1988, Hedrick et al, 1985, 1987, Sefton et al, 1987) because of its high toughness (330-420 J/m^2 in tensile impact) and excellent mechanical properties. It can also aid adhesion of the uncured epoxy system to fibres.

The *objectives* of this research are strongly linked to the fact that epoxy resins and epoxy resin-PES blends are amorphous systems which are supposedly suitable for use as structural materials at elevated temperatures. Single phase epoxy-PES blends have been produced with T_g's almost identical to the unmodified resin. Two phase epoxy-PES blends have been reported with high glass transition temperatures characteristic of the unmodified resin and the PES. Whether the blend is single or two phase, the idea is to produce a material with mechanical and thermal properties at least as good as and preferably better than the unmodified resin. This can apparently be achieved in some cases and the as cured blends can offer improved properties. What is unclear is *how does the presence of the PES affect the long term physical properties at elevated temperatures?* This is at present an unknown quantity and accordingly, the objectives of this research are firstly, to examine the effects of the PES on the formation of the epoxy network and secondly, to determine how the PES affects the physical ageing behaviour of blends in comparison to the unmodified resin. However, this work extends beyond a consideration of simply epoxy-PES blends. Increasingly, other thermoplastics are being used for blending with epoxy resins, some of them derived from polysulphones or other polymers. Irrespective of the thermoplastic used it is likely that similar effects occur. Therefore, another important objective of this work is to stimulate further investigation into the physical ageing behaviour of many different epoxy-thermoplastic systems, including those commercially available.

1.1 Fundamental Ideas of the Glassy State

Physical ageing of glasses is a universal phenomenon. All glasses exhibit certain general features irrespective of whether the material in question is organic or inorganic, composed of simple molecules or long polymeric molecules. In fact, amorphous polystyrene exhibits similar viscosity characteristics to a low molecular weight organic glass, glycerol, over a similar temperature range (Brawer, 1985). The basic behaviour of glasses is easily understood in terms of model systems and in the following sections a model example of a glass is used to illustrate the general behaviour.

1.2 Basic Features of the Glassy State

It should be remembered that many materials are glasses only because they have been cooled so rapidly that crystallisation is prevented. In other systems, the stereochemistry is such that crystallisation is impossible, an example being PMMA. In many polymers, crystallisation is possible but even crystallisable polymers contain substantial regions of glassy material because of topological constraints on chain motion due to entanglements (DeGennes, 1979). There are two phases present and therefore a melting temperature range and a glassy temperature range are observed. For simplicity we consider next a system in which the structure is either completely glassy or crystalline. The behaviour of the thermal expansion of such a glass on heating or cooling illustrates well the common properties of glasses and figure 1.1 shows a dilatometry curve that might be obtained for a typical glassy material that is also crystallisable (Elliot, 1984).

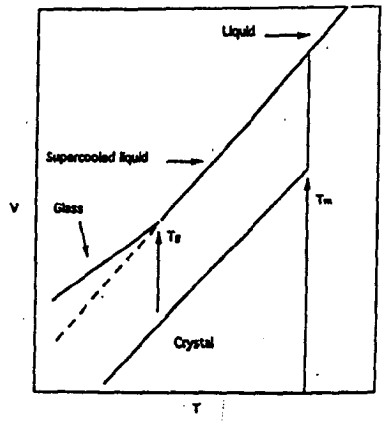

Figure 1.1: Typical volume dilatometry curve for a glassy material

Slow cooling allows crystallisation to occur and as crystals form there is an abrupt discontinuity in volume but bypassing crystallisation by very fast cooling leads to a continuous change in volume (c.f. figure 1.1). The supercooled curve is divided into two linear regions and a region of slight curvature. Extrapolating the high temperature line and interpolating the low temperature line cause them to intersect very nearly in the middle of this region of curvature, and this temperature of intersection is used to define the fictive temperature T_f (Davies and Jones, 1953) or the glass transition temperature T_g. The start of the curvature marks the point where the structure of the glass falls out of equilibrium and the region over which the curvature occurs defines the glass transformation range, the breadth of which is often larger at higher cooling rates as well as starting at higher temperatures because the glass falls out of equilibrium faster at higher cooling rates (Jäckle, 1986).

A supercooled glassy material which is normally crystalline will ultimately age towards a state of crystallinity, passing through many metastable configurations during sub glass transition annealing, each configuration being characterised by increasing amounts of crystallinity. Therefore the dilatometry curve would exhibit at various times, both a glass transition and a melting point, and eventually only a melting point. In many semi-crystalline polymers a glass transition and a melting point are always observed but annealing at temperatures between the glass transition and the melting point can improve the degree of crystallinity. However, for some materials, and in particular the polymers used for the work in this thesis, molecular architecture prevents crystallisation and annealing drives the glass towards an equilibrium glass state of minimum energy appropriate to the temperature. During a change of temperature the total system of molecules must change its configuration to one of lower energy which is in equilibrium with the final temperature. To do this requires that the individual molecules adjust their positions. Each molecule will be able to do so with a similar relaxation time in monatomic systems, so that the effect of local environment is to perhaps lead to a very narrow distribution of response or relaxation times. In long chain materials each macromolecule is made up of segments and each segment of smaller constituents, so that the macromolecular chain has a relaxation time that depends on the relaxation times of the constituents. Join the chains together in an entangled mass and the single macromolecule relaxation time becomes longer due to entanglements with other chains as

well as specific interactions such as secondary bonding. However the main effect is having to move in a way that depends upon movement of neighbouring chains. This is known as *cooperativity* and since entanglements can lead potentially to a wide variety of local environments, the global or total relaxation time of a bulk homopolymer in response to an external force is considerably longer than for a single macromolecule of the same substance. Of course some of the local motions can still occur along the chains because the segments or sidegroups are small. The global relaxation time (of any glass irrespective of type) is related to the structure of a material and the temperature and is also affected by the local environment. The cooling rate defined by the following equation

$$q = \Delta T / \Delta t \qquad (1.0)$$

is important in determining the structure formed during the cooling process. If cooling is considered as a series of incremental steps in temperature ΔT over a given time Δt, then as long as the global relaxation time is less than or equal to Δt, the system will relax into an equilibrium state. However as temperature decreases, so inevitably does molecular mobility and a point is reached at which the global relaxation time is larger than Δt and the system cannot reach equilibrium in the time allowed. The faster the cooling rate the sooner this occurs.

1.3 Cooling Rate, Fictive Temperature and Some Thermodynamic Observations

The increase of fictive temperature with cooling rate is a means of characterising the state of a glass (Davies and Jones, 1953) and for a given material cooled at different rates, a higher fictive temperature can be associated with greater perturbations from equilibrium. During ageing the fictive temperature, because of its kinetic nature also relaxes towards a minimum limiting value. Figure 1.2 depicts the typical curve obtained for the enthalpy during cooling of a glass (Petrie, 1972).

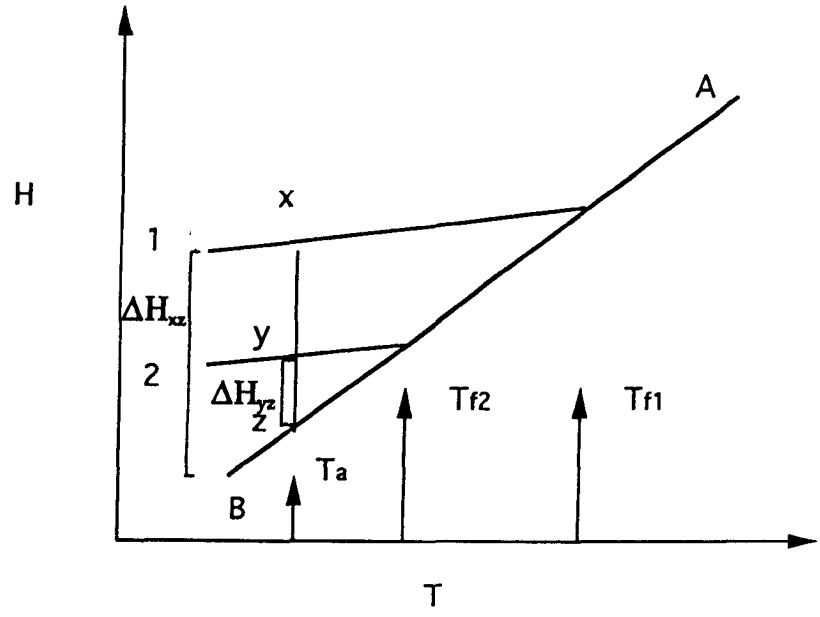

Figure 1.2: Typical enthalpy cooling curve for a glassy material

The curve AB is an equilibrium cooling curve for a glass that would be obtained during infinitely slow cooling. Suppose now that a glass is cooled along path 1, it will have fictive temperature T_{f1}. If this glass is annealed at temperature T_a the amount of excess enthalpy to be lost in order to attain equilibrium is given by ΔH_{xz} and the excess enthalpy decreases along path xz. Similarly the fictive temperature changes slowly along the path AB between T_{f1} and T_a. If the glass is cooled along path 2, ΔH_{yz} enthalpy needs to be lost at the temperature T_a and the material now has a fictive temperature T_{f2}.

Annealing simultaneously reduces the excess stored enthalpy, the excess entropy and the fictive temperature, the lower limit of T_f being the annealing temperature. It must be remembered that a different value of the fictive temperature exists for different quantities and the excess enthalpy and excess volume for example, will not necessarily yield similar values of the fictive temperature (Brawer, 1985). Clearly however, the same state of excess enthalpy could in principle be achieved by cooling or by cooling and annealing.

The amount of excess enthalpy stored prior to ageing and the enthalpy changes as a function of time can be calculated from calorimetric measurements of the heat capacity (Petrie, 1972, Richardson and Saville, 1977). The heat capacity curve of a rapidly quenched glass shows only an

approximate step change as the glass transformation is passed through. Physical ageing results in the development of an endothermic peak in the region of the glass transition which grows in magnitude and shifts to higher temperatures as the sub-glass transition ageing time is increased (Petrie, 1972, Struik, 1978, Scherer, 1986) and this is shown schematically in figure 1.3. Above and below the glass transition the change in heat capacity is usually quite linear and the amount of excess enthalpy lost during ageing can be calculated by subtraction of the aged and unaged heat capacity curves (Richardson and Saville, 1977).

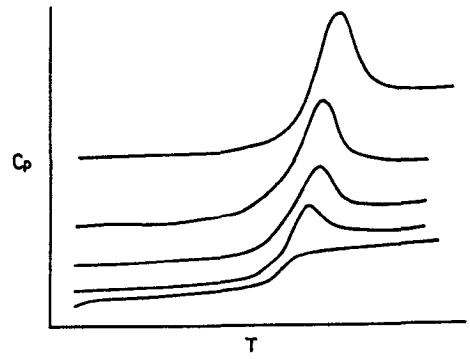

Figure 1.3: Development of the endothermic peak in the heat capacity as a glass is annealed below T_g

The presence of the endothermic peak is important. A change in temperature is a kind of generalised force or potential to which the structure of the glass must respond by adjusting to a new configuration. In a quenched glass molecular mobility is high because of the excess free energy (enthalpy) and excess 'free' volume, or space between molecules. These factors allow an almost immediate response (expansion) of the glass structure at low to moderate heating rates so that a peak does not appear on the heat capacity curve of a rapidly quenched glass, or if it does it is only very slight (c.f. figure 1.3). In this instance the relaxation time of the glass structure is such that $\tau \leq \Delta t$ and the structure can relax very quickly as temperature changes.

If the same glass is heated at a very fast rate then $\tau \succ \Delta t$ and the structure never quite has enough time to adjust and changes slowly relative to the heating rate. This leads to superheating of the glass initially but as temperature is increased the molecular mobility becomes greater and at some

particular temperature the global relaxation time shortens so that $\tau \leq \Delta t$. At this point the glass structure is able to 'catch up' and can absorb almost at once, all of the energy it lacks. Up to this point the glass has been superheated. It is important to realise that the relaxation time is structurally dependent so that denser packing increases the global relaxation time in a polymer

If a constant low heating rate is used to characterise the unaged and aged glass system, the enthalpy change can be measured as a function of time. Physical ageing causes molecular mobility, free volume and entropy to decrease which is accompanied by denser packing and an increased average relaxation time (Struik, 1978). Therefore when the same heating rate is applied to samples of the same material which are aged for longer times at the same temperature, the response time of the aged glass structure becomes longer during the heat capacity measurement. This is the cause of the heat capacity endothermic peak (Petrie, 1972, Brawer, 1985).

The specific volume behaves in the same way as the enthalpy and decreases because free volume is eliminated and packing increases. Hysteresis is observed with volume dilatometry measurements even at equal heating and cooling rates as shown in figure 1.4.

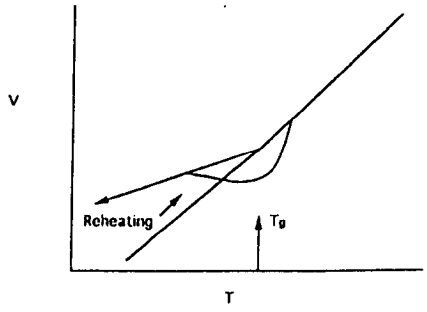

Figure 1.4: Volume hysteresis in a typical glass

On cooling the glass the volume curve follows curve 1 but during reheating at the same rate , at a point near the glass transformation range the glass structure acquires sufficient mobility that it starts to relax and dissipate excess volume in order to try to attain equilibrium by reaching the equilibrium volume curve. However, in doing so the volume starts to decrease below the volume previously achieved during cooling (Rehage and Borchard, 1973).

1.4 Basic Equilibrium Thermodynamics of Glasses

Clearly extensive parameters such as volume, enthalpy and entropy undergo important changes in a glass during cooling, reheating and sub-glass transition annealing. This suggests that it is necessary to understand 'why' glasses form during cooling in terms of thermodynamics, which will give greater insight into the physics of glass formation.

A system which illustrates very well the general properties of almost all glasses is o-terphenyl. Figure 1.5 illustrates the observed changes that occur in the enthalpy of o-terphenyl and figure 1.6 shows the effects on the entropy and heat capacity of this material as a function of temperature.

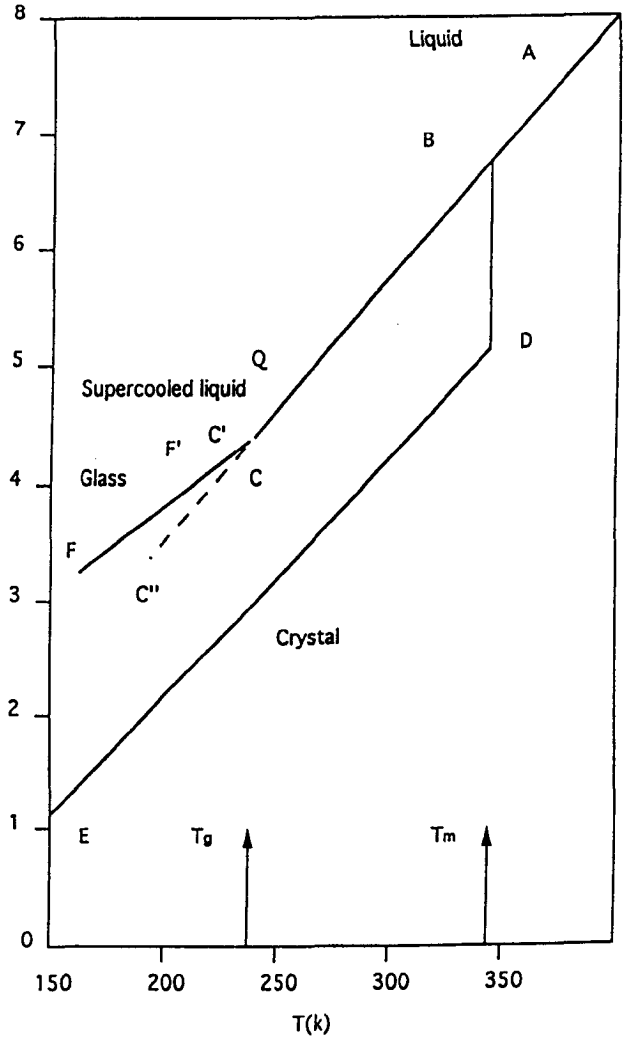

Figure 1.5: Enthalpy of o-terphenyl as a function of temperature (Brawer, 1985)

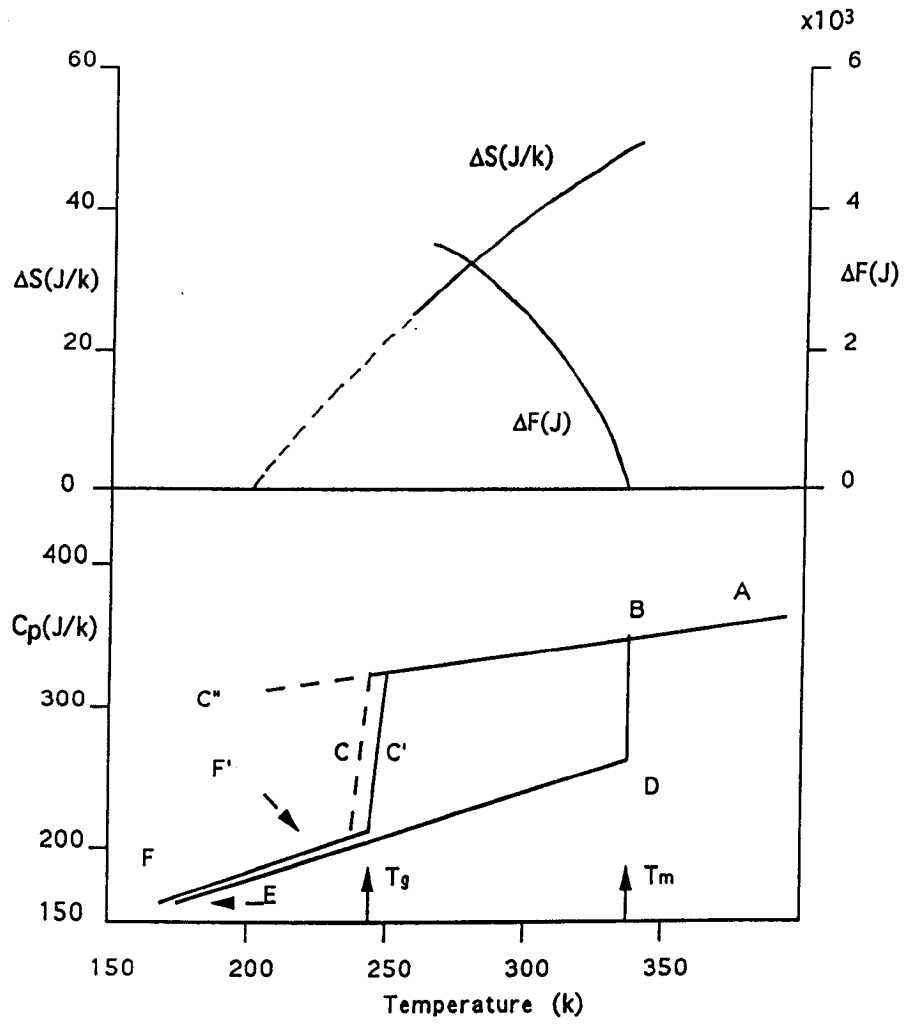

Figure 1.6: Entropy and heat capacity of o-terphenyl as a function of temperature (Brawer, 1985)

The pV term of the enthalpy of liquids is usually quite small because volume changes on heating a liquid are not large compared to a solid so that the enthalpy is approximately equal to the internal energy U. During heating, the enthalpy of crystalline o-terphenyl follows the line ED and at the melting point it jumps to point B, changing by an amount equal to the enthalpy of fusion. The absorption of enthalpy at the melting point disrupts the physical bonds between o-terphenyl molecules (as indeed it does in polymers). For the case of inorganic glasses, the energy is used to break up the chemical bonds (Brawer, 1985, Bartenev, 1988).

The slope of the enthalpy from A to B is steeper than from E to D and occurs in many materials due to the fact that the fluid structure changes with temperature (Brawer, 1985). Atoms or molecules in the fluid form small clusters and during heating the co-ordination number changes. The extent of the bonding interactions between molecules will decrease as the molecules reorient, causing the disruption of molecular packing by increasing the number and frequency of molecular motions and thereby increasing the configurational energies of the molecules in the liquid. Vibrational motions in most liquids are not important and do not contribute to the properties but in the clustered regions there is a limited amount of bonding and short range structure and further addition of heat increases the vibrational amplitudes of the molecules in the clusters (Brawer, 1985). This will eventually lead to the disruption of the clusters. In the solid, heating affects the vibrational amplitude of the molecules considerably but the difference between the heat capacities of the liquid and solid, ΔC_p, arises from the contributions of configurational changes, given by the equation

$$\Delta C_p = C_{p,liq} - C_{p,glass} \qquad (1.1)$$

The specific heats of the crystal and glass forms of the same material differ by only a few percent below the glass transformation and it is likely that the crystal specific heat gives a reasonable estimate of the vibrational contribution to the liquid specific heat at higher temperatures. This equation implies an entropy difference between the two forms of the material, ΔS, given by the equation

$$\Delta S = S_{liq} - S_{crystal} \qquad (1.2)$$

At the point A on the diagram the fluid is in thermal equilibrium but rapid cooling can bypass crystallisation and the material can be brought to temperatures below the melting temperature without crystallising. Along the line BQC' the supercooled fluid behaves like a fluid in thermal equilibrium and the enthalpy measured between points C' and T_m is reproducible and independent of thermal history if sufficient time is allowed for thermal equilibrium to be achieved (Brawer, 1985). If the supercooled liquid line is extrapolated the equilibrium line for the metastable fluid is obtained and in the absence of crystallisation the fluid is in thermodynamic equilibrium along this line.

An interesting feature of the entropy curve is that if it is extrapolated to below the glass transformation it vanishes at about 200K for o-terphenyl. This behaviour has been observed for many glasses and in several cases the entropy vanishes at only 20K below the glass transformation (Jäckle, 1986). This behaviour was highlighted by Kauzmann (1948) and is known as the *Kauzmann Paradox*. If is assumed that the vibrational and configurational contributions to the specific heat are uncoupled, the vanishing of the configurational entropy is an apparent violation of Nernst's theorem (Callen, 1989) but this applies only to phases that are in complete thermodynamic equilibrium with regard to the order and distribution of molecules down to absolute zero. However, it is obvious that a supercooled liquid solidifying as a glass has an almost fixed degree of order after the glass transformation and therefore it must have an excess or residual entropy. This presents an obvious dilemma (Kauzmann, 1948).

1.5 Glass Formation as a Phase Transition

The way in which enthalpy and volume change in a glass are suggestive of a phase transition. A second order phase transition in the sense of Ehrenfest (1933) also exhibit continuous changes in these quantities. Ehrenfest defined the order of a transition by the lowest derivative of a thermodynamic potential at which there is a discontinuity but problems with this approach have led to a different modern definition in terms of whether or not a latent heat exists for the transition (Binney et al, 1992). The heat capacity in glasses over the glass transformation also exhibits what could be called a rounded discontinuity suggesting that there may be similarities between the glass transformation and a second order phase transition (Davies and Jones, 1953, Cusack, 1987). The glass transformation is clearly not a first order phase transition and although it has similarities with second order phase transitions, it exhibits kinetic dependence: second order phase transitions are not kinetically dependent (Rehage and Borchard, 1973).

Phase transition theory can, however, provide a framework within which glass transformations can be modelled and such models are a means of avoiding vanishing configurational entropy. Davies and Jones (1953) reasoned that there must either be a thermodynamic discontinuity at some temperature below the glass transformation range or else the thermodynamic properties of the fluid change very rapidly. It has been suggested that the glass transformation pre-empts some phase transition which lies at a

temperature slightly below the glass transformation range (Kauzmann, 1948). Davies and Jones (1953), Goldstein (1963) and Gupta and Moynihan (1976) explored the correspondence between glass transformations and second order phase transitions using the Ehrenfest relations. It was found that only the first of the Ehrenfest relations was in agreement with the observed properties of glasses and that instead of the 1st and 2nd relations being equal, they obeyed the following inequality

$$\frac{TV\Delta\alpha(T_g)}{\Delta C_p(T_g)} \prec \frac{\Delta\beta(T_g)}{\Delta\alpha(T_g)} \qquad (1.3)$$

RELATION 1 RELATION 2

Where $\Delta\alpha$, $\Delta\beta$ and ΔC_p are the differences between the thermal expansion, compressibility and heat capacity of the liquid and glass respectively. The first relation implies that during glass formation the entropy of the liquid and glass are the same on either side of the transition, irrespective of the pressure at which the glasses are formed. Furthermore, the Prigogine-Defay ratio (Elliot, 1984) given by

$$R = \frac{\Delta\beta(T_g)\Delta C_p(T_g)}{TV[\Delta\alpha(T_g)]^2} \qquad (1.4)$$

which should be 1, is found to lie between 2 and 5 in general for glasses.

The violation of the Ehrenfest relations makes clear the fact that the glass transformation is not a second order phase transition but phase transition theory provides a good framework for thermodynamic analysis of glasses. Davies and Jones (1953) used order parameters in a theory based on phase transitions. An order parameter is some quantity that becomes fixed as the material undergoes a second order transition and is therefore a quantity that can characterise the state of the material. As the glass transformation range is crossed the internal ordering parameters become fixed and in practice a minimum of two ordering parameters, corresponding to fictive temperature and pressure are required (Brawer, 1985). The ordering parameters can be used to specify the glass structure and may be for example, average co-ordination number or the excess volume. Critical values of entropy or volume may also be used and in these cases the relaxation of the fluid corresponds to a time dependent change in the ordering parameter. Single

order parameter models can be used if a mean field theory is required (Chandler, 1987, Thompson, 1988).

To further illustrate the use of order parameters consider firstly the thermodynamic properties of viscous fluids in terms of vibrational and configurational terms. For example, the heat capacity may be written as (Brawer, 1985)

$$C_p = C_{p,vibrational} + C_{p,configurational} \qquad (1.5)$$

The contribution to the heat capacity due to vibrational motions relaxes on a time scale of the order of picoseconds following a temperature shift. The configurational heat capacity relaxes very slowly and configurational properties can be considered as unique functions of the order parameter (Davies and Jones, 1953, Brawer, 1985). Thus, for an order parameter Z, the expression for a property Q in terms of vibrational and configurational terms is given by

$$Q = Q_v(T,P) + Q_c(Z(T,P)) \qquad (1.6)$$

where v and c refer to vibrational and configurational quantities. The order parameter Z(T,P) changes rapidly at high temperatures but the rate of change of Z becomes so slow at lower temperatures that it can no longer follow the temperature change. At the point where a significant change in the properties of the fluid occurs, at the fictive temperature for example, the order parameter perhaps entropy, becomes fixed. This view of the glass transition then attributes any further changes in Q below the glass transition temperature to be due only to molecular vibrations (Brawer, 1985). This of course is not strictly correct because physical ageing can occur at temperatures well below the glass transformation range. The single order parameter approach implies that if two glasses are prepared with exactly the order parameter, then all other properties will be equal. This is not true and two glasses may be prepared with the same refractive index for example, but totally different in other properties. For this reason at least two order parameters are required. The effectiveness of order parameter theories has been considered by Goldstein (1973) and such theories are commonly encountered in the models of Cohen and Turnbull (1959, 1961), Gibbs and DiMarzio (1958) and Adam and Gibbs (1965) as well as others. The most

important of these phenomenological models in terms of glass formation will be described next.

1.6 Important Phenomenological Models of the Glass Transition

The phenomenological models most frequently encountered in describing why glasses are formed use thermodynamics or statistical mechanics to attempt to describe the dramatic property changes that occur in supercooled liquids. Another characteristic change in glass forming liquids is the increase in viscosity as well as the temperature dependence of the shear relaxation time (Jäckle, 1986). This type of behaviour is observed in a broad class of materials of widely differing molecular structure. For a small number of network forming glasses such as fused quartz, the viscosity formula follows an Arrhenius form with a high nearly constant activation energy. However, the majority of glass forming liquids show strong deviations from Arrhenius behaviour, following the Fulcher law for the viscosity

$$\eta(T) = C\exp[A / k_B(T - T_0)] \qquad (1.7)$$

These deviations correspond to a strong increase in apparent activation energy between the melting point and the glass transformation. Close to the T_g however, the temperature dependence of the viscosity is again observed to be Arrhenius like (Elliot, 1984, Cusack, 1987). It is a striking coincidence that liquids which follow the Arrhenius viscosity formula are also conspicuous by the absence of a configurational specific heat (Angell and Sichina, 1976). This fact suggests that the increase in the apparent activation energy for viscous flow is somehow connected with the structural changes.

There have been many attempts to correlate the viscous behaviour with the elementary thermodynamic properties of glasses and two classical theories have had some success in reproducing experimental data. These are the free volume theory of Cohen and Turnbull (1959, 1961) and the entropy theory of Gibbs and DiMarzio (1958) and Adam and Gibbs (1965). Also very important in polymer physics is the empirical equation of Williams, Landel and Ferry (1955). Although theoretical developments have occurred with regard to these theories, the original works will now be described.

1.6.1 Free Volume Theory

In 1935 Hirschfelder argued that 'the surplus volume in one part of the liquid becomes available in another part without appreciable activation energy as compared to k_BT. Accordingly, the slowness of molecular transport in liquids is attributed to the scarcity of free volume rather than the existence of free energy barriers. The free volume idea is largely based on intuition but the work of Doolittle (1951) on non-polymeric fluids provided evidence for its existence. Doolittle defined the free volume as

$$v_f = (v - v_o) \qquad (1.8)$$

where v is the total volume of the liquid at temperature T and v_o is the theoretical volume of closest packing at 0 k. The volume v_o is that part of the total volume occupied by the molecules and v_f is the free volume referred to by Hirschfelder (1935), which permits diffusive motion. Doolittle obtained good values of v_o by extrapolating density data for liquids to 0 k and obtained a good fit to the viscosity equation

$$\eta = A\exp(Bv_o / v_f) \qquad (1.9)$$

where A and B are empirical constants.

The free volume idea is most plausible for van der Waals liquids of non-interlocking molecules but the concept was extended to polymers by Fox and Flory (1950, 1951, 1954) who suggested that the glass transition was characterised by the freezing in of a critical free volume. It is more usual to discuss the free volume in terms of the fractional free volume $f=v_f/v$ and at and below the glass transition the free volume f is defined as

$$f_g = \frac{v_f^*}{v} \qquad (1.10)$$

and was originally considered effectively constant. Above the glass transition the expansion of the polymer melt contributes to v_f such that

$$v_f = v_f^* + (T - T_g)(\partial V/\partial T) \qquad (1.11)$$

which leads to

$$f = f_g + (T - T_g)\alpha_f \qquad (1.12)$$

where α_f is the free volume thermal expansion. The fractional free volume at the glass transition, f_g, was originally supposed to be a universal constant but is now known to vary between materials (Ferry, 1980). From these free volume ideas it is possible to derive the empirical W-L-F equation (Williams et al, 1955, Ferry, 1980) which can be obtained in the following form

$$\log_{10} a_T = \frac{-(B / 2.303 f_g)(T - T_g)}{f_g / \alpha_f + (T - T_g)} \qquad (1.13)$$

where B is the same constant that appears in equation 1.9 and the other symbols have their usual meaning. This theory accounts well for the frequency dependence and time-temperature superposition behaviour of many polymers and may also be obtained in other forms (Ferry, 1980).

Cohen and Turnbull (1959) used the free volume idea in a model based on the hypothesis of Hirschfelder that molecular transport in liquids occurs by movement of molecules into voids with the additional condition that this only occurs if voids of volume greater than some critical free volume are present, so that the redistribution of free volume does not involve any free energy change. The model assumes that the liquid molecules are hard spheres and a self diffusion coefficient was derived as

$$D = D_o \exp(-\gamma v^* / v_f) \qquad (1.14)$$

where D_0 is proportional to the molecular diameter and the gas kinetic velocity and $0 < \gamma \leq 1$. The Doolittle equation can be derived from this because Doolittle's form of the free volume equation is used.

In a later paper Turnbull and Cohen (1961) extended this analysis by assuming each molecule to be confined to a cage formed by its neighbours. The potential energy of each molecule was assumed to be of a Lennard-Jones form and to be a function of the cage radius. For small cage radii a large free energy would be required to redistribute the excess volume but at sufficiently large radii corresponding to the linear portion of the potential energy curve, no free energy is required. This idea is expressed as

$$v = v_o + \Delta v_c + v_f \qquad (1.15)$$

where Δv_C is the part of the excess volume which requires free energy for redistribution. At and below some critical temperature T_0 the cage radius is so small that the energy required for redistribution of any excess volume is large so that $v_f=0$ and $v-v_0=\Delta v_C$. Above T_0 where the cage radii are large most of the volume added by the thermal expansion is free. Turnbull and Cohen wrote

$$v_f = \alpha \bar{v}_m (T - T_o) \qquad T \geq T_o \qquad (1.16a)$$

$$v_f = 0 \qquad T < T_o \qquad (1.16b)$$

where α and v_m are the average thermal expansion coefficient and average molecular volume respectively, taken over the temperature range T_0 to T. Substituting equations 1.16a,b into equation 1.15 gives values of γv^* which closely match the volume v_0 in many van der Waals liquids.

Cohen and Turnbull's theory fits experimental data on many systems and predicts that the relaxation time tends to infinity (a singularity) as the temperature approaches T_0 due to the scarcity of free volume. The glass transition at T_0 is therefore unattainable because the volume relaxation time becomes infinite.

The model of Turnbull and Cohen was further developed by Grest and Cohen (1981) in terms of percolation theory but although it predicts the relaxational nature of glasses very well it classes the glass transition as a first order phase transition which clearly it is not.

1.6.2 Entropy Theory

The free volume theory is not satisfactory in describing the P-T behaviour of polymers (Goldstein, 1973) but the equations can be modified to agree by introducing what amounts to quantities that act as correction factors (Ferry, 1980). A method of describing the glass transition which has no need of such artificial hypotheses (Goldstein, 1963, 1973) is the Gibbs-DiMarzio theory (1958) which considers that if it was possible to cool a polymeric liquid so that it remained in equilibrium at all times, a point would be reached at which the

material would undergo a second order phase transition. This would account for the vanishing of the configurational entropy. The hypothetical second order transition temperature is never reached because as it is approached the viscosity becomes very large and limits the number of conformational states of the molecules, which decrease sharply in number. Therefore viscosity induced sluggishness rather than limited availability of holes is responsible for the transition. This entropy effect therefore prevents the true transition temperature being reached on accessible time scales and instead the material undergoes a gradual change of slope over the glass transformation range.

The Gibbs-DiMarzio theory is a lattice theory which uses two components to describe the stored energy of the system. The chain bonds may store energy and are then flexed into configurations higher than the minimum energy configuration and energy may also be brought into the system by the creation of holes. There is then a hole energy which is proportional to the number of van der Waals interactions lost on the introduction of lattice vacancies. Using these concepts, partition functions were derived from which thermodynamic properties were determined. The theory was the used to describe the cooling of a polymer melt: as temperature decreases and there is less energy in the system, firstly the low energy molecular conformations begin to dominate and secondly the number of holes decreases. The number of ways to pack the molecules in the bulk phase is reduced because the tube of empty volume required by the molecular chains must satisfy strict geometrical requirements. As the temperature is further decreased the polymer system reaches a point where amorphous polymer packing would become impossible if both of these processes continued thereby giving rise to the glass transformation.

The theory was taken a stage further by Adam and Gibbs(1965) who also managed to derive an equation like the W-L-F equation. They related the temperature dependence of the relaxation process to the size of a region defined as a volume large enough to allow relaxation to take place without affecting neighbouring regions. The co-operatively rearranging region is large enough to allow a transition to a new configuration and is therefore determined by chain configuration. The size of the co-operatively rearranging region will equal the sample size at a critical temperature T_c where only one conformation is available to each molecule. It is possible using the equations derived by Adam and Gibbs in this molecular kinetic

theory to calculate the size of a co-operatively rearranging region and the temperature T_c.

1.6.3 Do the Theories Agree with Experiment?

Goldstein (1963, 1973, 1976, 1977) considered the merits of the free volume and entropy approaches in understanding glass transformations. In their original forms, the two theories predict about the same temperature dependence of the viscosity near to the glass transition. Critical comparison of the theories, particularly with regard to the effects of pressure on the glass transition show that the free volume theory fails rather badly whilst the entropy theory, on the basis of limited data, agrees fairly well. Secondly, in the glass transformation range, the entropy theory allows the effect of thermodynamic and kinetic contributions to the glass transition to be separated as the system can be studied out of equilibrium. The relative importance of the thermodynamic state with regard to volume or entropy can then be evaluated. In this respect the free volume theory fails badly whilst the entropy theory gives a qualitatively correct answer. It is also observed that the second order transition temperature T_2 of the entropy theory agrees rather well with the temperature T_0 of the Fulcher equation (Goldstein, 1969, Matsuoka, 1986).

In practice it seems that a theory encompassing the good aspects of both theories is required since both entropy and free volume are important. The theory of Chow (1989a) is based on the Gibbs-DiMarzio theory but removes the dependence of the glass transition on a second order phase transition and is general enough to account for the behaviour of non-polymeric glasses which the Gibbs theory was unable to do. Chow treated the phase transition temperature T_2 of the entropy theory as a thermodynamic anomaly by utilising Flory's lattice statistics of chain molecules (Flory, 1953). The temperature T_2 is considered to occur when the most stable hole configuration is reached under the co-operative constraints of linear chains. The analysis showed that the equilibrium glass transition temperature is determined mainly by the stiffness of the polymeric chains (determined in turn by the height of the rotational energy barrier) which is consistent with the Gibbs-DiMarzio theory. It also showed that the ratio of the hole (intermolecular) and flex (intramolecular) energies varies only between 2 and 2.3. This supports the idea that the conformational theory is experimentally equivalent to the free volume theory and the results of calculations agree well

with molecular parameters calculated for polymers using the Gibbs-DiMarzio theory. Matsuoka (1992) has also developed a theory of the glass transition which incorporates free volume and entropy ideas and derives equations similar to those of Adam and Gibbs (1965).

1.7 Time Dependent Relaxation below the Glass Transition: Physical Ageing

1.7.1 Non-Linearity in Physical Ageing

The equilibrium approaches used to formulate the free volume and entropy theories can explain why glasses form and what their expected equilibrium properties should be but are unable to account for the kinetic dependence of the glass transition or describe time dependent relaxation at sub-glass transition temperatures. The relaxation of various material properties through and below the glass transition is a non-linear process that is not describable by linear relaxation theory and is therefore inaccessible to *equilibrium* thermodynamics (Lindenmeyer, 1981). In the region of the glass transition the diffusive thermal motion of the molecules of a liquid is not exponential (Struik, 1978). Equilibrium (linear) theories of the glass transition can describe the equilibrium behaviour of glasses above and below the glass transition but not as the transition is passed through and nor can they describe physical ageing (Cusack, 1987). Non-linearity occurs frequently, particularly in spectroscopic techniques and linear behaviour is assumed in the form of $\omega\tau=1$, where ω is the frequency and τ the periodic time (McCrum, Read and Williams, 1967). However, spectra are rarely observed to conform to Debye behaviour. Explanations for the non-linearity appear in the form of suggestions that the relaxation behaviour at a molecular level is non-exponential as a result of the co-operative motions (Williams, Cook and Hains , 1972, Jonscher, 1977) or that the non-exponential behaviour results from a superposition of exponential relaxation processes, leading to a distribution of relaxation times (Struik, 1978). The recent theory of complex correlated processes due to Ngai et al (1984-1988) and Rajagopal et al (1984-1990) allows for an initially exponential relaxation process which crosses over to non-exponential relaxation at some later stage . This allows for initially uncorrelated relaxation but introduces cooperativity at some critical stage. The distribution of relaxation times approach is however the oldest and most widely accepted amongst polymer scientists (Lindsay and Patterson, 1980). Struik (1978) uses a distribution of relaxation times approach and equates

this with free volume, summing up the non-linearity in structural relaxation as shown schematically in figure 1.7.

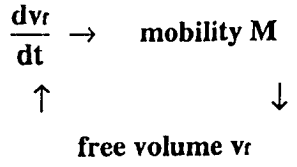

Figure 1.7: Interdependence of mobility, free volume and free volume relaxation rate (Struik, 1978)

Physical ageing is a thermoreversible process so that the relaxations of the various quantities can be erased simply by removing the thermal history, which is easily accomplished by annealing the glass at about 20°C above the glass transformation range and requenching (Petrie, 1972).

There is a vast amount of literature describing experimental investigations of the non-linearity in relaxing physical properties, the classic experiment being that of Kovacs (1963) who examined volume relaxation. Kovacs cooled or heated samples of PVa from either 40°C or 30°C to a final temperature of 35°C and monitored the changes in specific volume. He observed that the curves for contraction of the volume towards the equilibrium volume at 35°C and the curve for the expansion of the volume towards the same equilibrium state were not mirror images of each other but were symmetrical, with the expansion curve exhibiting a greater rate of relaxation towards the new equilibrium. This was attributed to the fact that contraction towards equilibrium is an autoretarded process during which the relaxation times become longer as packing density increases. Conversely, in expanding, the structure of the glass becomes less dense and the relaxation times become shorter (an autocatalytic process) thereby accounting qualitatively for the asymmetry. There is far too much to describe but the review by Ngai (1987) and Tant and Wilkes (1981) provides many references and there should be no doubt that few properties of glasses follow a Debye relaxation theory.

The non-linearity has led to many attempts to derive mathematical functions that allow empirical predictions of how properties relax. A function that has been frequently used is the Kohlrausch function (Kohlrausch, 1847) although this has now been derived theoretically and given a more sound physical

basis by Ngai et al (1984-1988) and Rajagopal et al (1984-1990). Some attempt has also been made to understand the glass transformation in terms of non-linear thermodynamics (Baur, 1989) but the applicability of this approach is limited at the present time.

1.7.2 Free Volume and Entropy in Physical Ageing

The free volume theory argues that the scarcity of free volume leads to low molecular mobility and an inability to relax towards the transition. The entropy theory argues that it is the increase in viscosity and reduction in molecular mobility at lower temperatures that reduces the conformational entropy, since fewer conformations are available as temperature decreases. In terms of physical ageing, both concepts are useful because the elimination of free volume leads to a reduction in bulk entropy and less space for molecular motion, therefore limiting the conformations available to the segments.

The interpretation of physical ageing in terms of free volume is however, the most common and has proven extremely useful. Kovacs (1963) used a single order parameter model to describe isobaric volume recovery and proposed the equation

$$\frac{dV}{dt} = \alpha_g V_o q - \frac{(V - V_e)}{\tau} \qquad (1.17)$$

where q=dT/dt, V and V_0 are the actual and equilibrium specific volumes respectively, α_g is the volumetric thermal expansion coefficient of the glass and t is the volume retardation time at pressure P. Enthalpy relaxation is described by replacing the bracketed term in 1.17 by $(H-H_0)/H_0$. Hutchinson and Kovacs (1976) also derived a similar equation which involves conformational entropy instead of volume.

The equation 1.17 is a single parameter model but despite limitations it has proven quite successful in describing the effects of ageing on polymers. Tensile deformations, uniaxial compressions and shear deformations have been observed to erase the ageing of polymers (Matsuoka et al, 1977, 1978). Struik (1978) has suggested that any deformation creates free volume. Matsuoka and Bair (1977) stressed polycarbonate in pure shear and found that there was an increase in the enthalpy with deformation, suggesting an increase in free volume with shear and Matsuoka et al (1978) proposed a model relating free volume to the tensile strain and Poisson's ratio. They

found good agreement with experimental data. Struik (1978) suggested that the rate of generation of free volume is proportional to the rate of dissipation of mechanical energy. Generally, the free volume theory predicts that with an increase in free volume, ageing is totally or partially erased.

Matsuoka and Bair (1977) also found support for the free volume by monitoring the temperature of polycarbonate during tensile and shear deformation. They reasoned that with an increase in free volume during deformation the excess enthalpy would increase with a parallel decrease in the temperature. The temperature was found to reach a minimum value when the polymer began to yield. At this point there was a temperature increase due to frictional heat generation. Creep behaviour has also been described by Matsuoka et al (1978). Free volume equations were found to quite accurately reproduce creep curves. The dependence of the mode of failure of a polymer on free volume has been demonstrated by Mininni et al (1973) in a study of amorphous PET. With a large excess free volume ductile behaviour was observed but the material became more brittle when aged.

The free volume theory is a useful qualitative concept in describing the changes that occur when polymers are physically aged. There has been limited success in describing quantitative behaviour but there are drawbacks, as already briefly mentioned in section 1.5.1. However, the free volume theory allows for a distribution of hole sizes as described in the models of Cohen and Turnbull (1959) and Turnbull and Cohen (1961), which allows for a distribution of molecular mobilities and relaxation times. This means that the existence of sufficient mobility for local molecular relaxations depends upon the presence of holes that exceed a critical free volume. Struik (1978) has used this idea to consider that during the cooling or ageing of a polymer the distribution of relaxation times shifts to longer time scale, the shape of the distribution remaining unchanged. This is described as thermorheological simplicity (TRS) in some work (Scherer, 1986).

The idea of TRS simplifies analysis of phenomena and is applied also to the shift of spectra under changes of applied field (McCrum, Read and Williams , 1967), although of course, like linearity and Debye relaxation, TRS is rarely observed. In the initial development of physical models this assumption was necessary to provide a framework for theoretical development. However, there is a need to take the understanding further by attempting to incorporate

the established non-linearity of relaxations which in the case of polymer chains are complicated by the presence of entanglements. The entanglements couple very strongly the motions of one chain with another (DeGennes, 1979, Ngai et al, 1986) and although exponential relaxation may proceed at short times (Ngai et al, 1986) the crossover to non-linear relaxation occurs quite rapidly. Prior to the crossover it can be argued that the local free volume is sufficiently large that relaxing segments of chains do not rely on the motions of their neighbours in order to create space for movement. The crossover to non-linearity may be due to the free volume reaching levels that require co-operative motions to occur. For these reasons it seems unlikely that Struik's argument can always be valid and the distribution of relaxation times may well be expected to change with ageing as well as shifting to longer time scales (see Appendix A1.1).

Multiparameter free volume models have been successfully used for glasses by DeBolt et al (1976) in a model based on the work of Tool (1945,1946) and Narayanaswamy (1971). Kovacs et al (1979) produced a multiparameter model for recovery in polymers which contained parameters measurable by calorimetry and which was able to reproduce enthalpy curves for polystyrene quite well. Other models similar to this exist for polymers but they are not intended to predict glass transition ranges or properties (Chow and Prest, 1982), merely reproduce experimental data. Such models may incorporate the fictive temperature and are quite common (Brawer, 1985, Scherer, 1986) and also allow in principle the calculation of a relaxation time which depends upon the fictive temperature and a structure parameter x which is supposedly time independent and characterises the glass structure through its dependence on the fictive temperature. A method of determining this parameter for isothermal enthalpy relaxation, which uses variations in the endothermic peak temperature of a well annealed glass with DSC scanning rate has been described by Hutchinson and Ruddy (1988).

Chow's model (1989a) based on the-DiMarzio theory was further developed by the author (Chow, 1989b) to analyse non-equilibrium relaxation. The model is reasonably successful and shows how the kinetics of holes and bond rotations affect the enthalpy relaxation. Calculations show that the conformational activation energies are between 1 and 2 orders of magnitude less than the hole activation energy, thereby predicting that at short times the enthalpy relaxes much faster than volume. At longer times the model

predicts that the rates of relaxation of enthalpy and volume are similar, agreeing with experimental observations.

1.7.3 The Importance of Secondary Relaxations in Amorphous Polymers

Secondary relaxations have been shown to contribute significantly to the heat capacity of polymers because they provide an energy absorbing mechanism as they are passed through and represent extra degrees of freedom acquired by the system. These relaxations are known to vary in complexity from co-operative to non-cooperative depending on the particular segment involved and the local conditions, as reflected in the activation entropy (Starkweather, 1981, Starkweather and Avakian, 1989). Physical ageing reduces the free volume and relaxation peak intensity, therefore also reducing slightly the number of active secondary relaxations as the decrease in local density in some regions prevents relaxation. Simha et al (1972) showed that a reduction in the number of active secondary relaxations leads to less absorption of heat when the secondary relaxation is passed through and this in turn decreases the heat capacity. When passing through these relaxations a transition from brittle to ductile behaviour also occurs as a result of the extra molecular activity and the elastic modulus drops for the same reason (Bicerano, 1991a,b). The onset of ductile behaviour in tensile tests of BPAPC is correlated with low temperature relaxations (Bubeck et al, 1984) and the freeing of secondary motions in PVC and amorphous PET has been suggested as responsible for the brittle-ductile transition behaviour (Hiltner et al, 1974).

The dynamic mechanical properties also change, a maximum in the loss modulus being observed as the storage modulus decreases due to the additional dissipation of applied external work by the secondary relaxations. The dependence of yield stress also follows that of the elastic and shear modulus, loss modulus, etc., and reaches a peak as the relaxation is passed through. (Bicerano, 1991a). Failure of polymers is normally affected by the molecular mobility and therefore depends upon which molecular motions are active at the test temperature. The mode of failure of a polymer is determined by the competition between shear banding , which leads to shear yielding and ductile failure, and crazing, which leads to cracking and brittle failure (Kramer, 1983, Kambour, 1983a,b). The crazing stress is mainly determined by such factors as the chain entanglements and exhibits a weak temperature dependence so that it can be inferred that it is the yield strength at any given

temperature which is primarily affected by secondary relaxations (Kramer, 1983). Physical ageing increases the yield strength leaving the crazing stress unaffected. The yield stress is normally less than the crazing stress but physical ageing can reduce the number of active secondary relaxations as free volume is lost, causing the yield stress to exceed the crazing stress. Crazing then becomes the mode of failure in well aged samples because it requires less stress. Monitoring the secondary relaxations by mechanical or dielectric spectroscopy thus provides a means of observing the effect of physical ageing.

The ageing process results in a change in the number of accessible conformations, a phenomenon also associated with secondary relaxations and a small number of studies have examined conformational changes with physical ageing by using FTIR spectroscopy. Ito et al (1978) followed the conformational changes in PET and measured the changes in the intensity of an absorption band at 973 cm^{-1} , due to the CH_2-O vibration. They found that with increased physical ageing, the relative number of gauche conformations increased. Similar results were found by Moore and O'Loane (1981) also for PET.

1.7.4 Modelling of Relaxation Kinetics

Models have been used to curve fit the relaxation of quantities such as conductivity, enthalpy, volume etc., as a function of time or to reproduce the shapes of spectra, heat capacity curves and volume relaxation curves (Kovacs, 1963, Narayanaswamy, 1971,Brawer,1985, Ngai, 1987, Hodge, 1991). Many of these models use an exponential relaxation function to model the relaxation of a property Q (the specific volume for example) in an equation like the following.

$$Q(t) = Q_o(1 - \exp(-t/\tau)) \qquad (1.18)$$

where Q_0 is the value of property Q prior to the start of relaxation. The above equation describes the decay of the quantity Q so that Q_0 is the initial value and this equation is linear. However, a non-linear relaxation function called the Kohlrausch function (1847) has found increasing use in describing the non-linear or stretched exponential relaxation of many properties of glasses as well as reproducing non-Debye spectral shapes. This function is shown below and substituting it into equation 1.19 might be one way to describe the non-linear relaxation of property Q.

$$\phi(t) = \exp-(t/\tau_o)^{\beta} \qquad 0 \le \beta \le 1 \qquad (1.19)$$

where t_0 is an effective relaxation time (or correlation time) and β is a constant which is related to the width of the distribution of relaxation times and which increases with increasing sample temperature (Lindsay and Patterson, 1980 and Appendix A1.2). This equation was first used, although not in the above from, by Kohlrausch (1847) to describe mechanical and dielectric relaxations and was revived by Williams and Watts (1971) to describe the dielectric relaxation in viscous liquids and polymers. This function has been used extensively to curve fit data from mechanical and dielectric spectroscopies (Colmenero et al, 1991), NMR, photon correlation spectroscopy and many other quantities (Ngai, 1987).

The Kohlrausch function can be derived from a distribution of relaxation times model (see Appendix 1) and although it appears to be universally applicable to glasses in this form , the constant β is often time dependent and at times $t<t_0$ the function is not accurate . The Kohlrausch function has been derived more rigorously by Ngai et al (1984-1988) and Rajagopal et al (1984-

1990) by a method based on complex correlated processes. This approach derives the Kohlrausch function and additional equations for its satisfactory application, which lead to an exponential relaxation at $t<t_0$ and crossover to non-linear behaviour as described by the Kohlrausch equation at longer times, thus reproducing the observed properties of crossover and dominance common to polymers and glasses in general. However, the theory of Ngai, Rajagopal and co-workers is not based on a distribution of relaxation times approach. Rather it considers relaxation in terms of a primary relaxing species, which is the basic unit undergoing relaxation. In a polymer melt this could be a whole chain or just monomer units, depending upon the scale chosen and the primary species relaxes exponentially, in a Rouse like manner initially but crosses over to obey a Kohlrausch form after a critical time. Therefore the initial relaxation is uncoupled, but after the critical time entanglements for example may introduce coupling. Clearly the time at which crossover is observed depends upon the nature of the primary species and beyond this time the relaxation time of the primary species becomes a function of the increasing degree of coupling between the polymer molecules (Ngai, 1986). The model does however allow for a distribution of relaxation times (Rendell et al, 1984) and the basic physics of recovery in the Ngai model is essentially the same as in the Narayanaswamy , KAHR and Moynihan models and indeed its use in the description of physical ageing can entail the use of the fictive temperature (Ngai et al, 1984) although the forms of these equations differ slightly from those of the former.

Dynamic scaling equations have also been used to describe the shift of glass relaxation susceptibility peaks when the applied field is changed (Souletie and Thoulence, 1985). The scaling hypothesis is based on phase transition theory and assumes that under a change of applied field the shape of the relaxation spectrum is invariant, the only effect being to shift the spectrum to higher values of frequency or temperature, or whichever quantity is the independent variable (Thompson, 1988). Scaling theory has become extremely important in polymer physics, largely through the efforts of DeGennes and the scaling concepts derived from phase transition theory have been applied in the analysis of polymer chain dynamics or reptation (DeGennes, 1979, Doi and Edwards, 1987) as well as critical phenomena such as phase separation and gelation.

1.8 Epoxy Resins

Epoxy resins are used widely because when crosslinked they are isotropic with regard to their mechanical properties at elevated temperatures, are easy to process because they are prepared from low molar mass resins which are polymerised by the addition of a curing agent and are able to make good contact with fibres in composite materials because of their low viscosity (Morgan and O'Neal, 1977). Unfortunately they are brittle but a common means to overcome this drawback has been to incorporate a fine, randomly dispersed rubbery second phase in the epoxy matrix to improve toughness (Manzione et al, 1981, Yee and Pearson, 1989). This significantly improves the impact strength without seriously affecting other properties. The improvements observed in the systems are dependent upon the morphology and type of rubber used and whilst rubber toughening improves impact strength, it lowers the glass transformation range slightly (Raghava, 1987a). For this reason attempts have been made to incorporate tough, high temperature engineering thermoplastics into the resin as a reinforcing second phase. The relaxation of resins and resins blends is dependent upon the microstructure which in turn depends on the cure schedule. Curing will now be briefly described.

1.8.1 Cure of Epoxy Resins

The cure cycle of epoxy resins is important because it affects the morphology of both neat and modified epoxy systems (Lee and Neville, 1967). The cure process will be briefly described with regard to the primary reaction of a diglycidyl ether of bis-phenol A epoxy monomer (DGEBA), the structure of which is shown below.

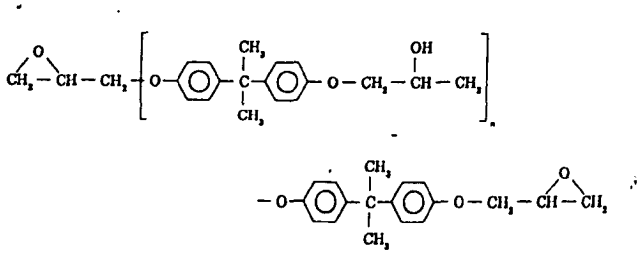

Figure 1.8: Chemical Structure of DGEBA Monomer

For crosslinking to occur , a suitable hardener such as a primary amine or acid anhydride must be present (Bucknall, 1977). The crosslinking reaction shown below occurs in the presence of several different types of hardener.

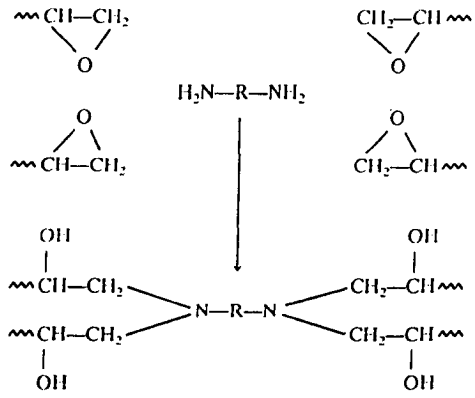

Figure 1.9: Primary Epoxy-Hardener Reaction

When acted upon by a suitable hardener, the epoxide ring opens in the manner shown above, each ring establishing a branching point in the molecular chain so that each DGEBA molecule becomes effectively tetrafunctional (Manzione et al, 1981). As the reaction proceeds the molecular weight of the material increases rapidly and eventually several chains become linked together into networks of infinite molecular weight. The primary reaction can be observed from infra-red spectroscopy by monitoring the disappearance of the epoxide vibration in the region of 910-915 cm^{-1} (Chang et al, 1982b, Allen and Sanderson, 1988, Choy and Plazek, 1990) and results in the formation of ether linkages, the characteristic vibration of which can be seen to appear in the IR spectrum as curing proceeds. The sudden and irreversible transformation from a viscous liquid to an elastic gel signifies the onset of gelation and can be monitored by dynamic mechanical measurements (Manzione et al, 1981, Pang and Gillham, 1989).

Gelation is an important characteristic of thermosets from a processing point of view because it is accompanied by a large increase in viscosity and beyond the gel point the polymer is no longer processable. Gelation occurs at a well defined and calculable stage in the course of the chemical reaction and the conversion needed to from a gel can be calculated from the functionality of the starting materials (Flory, 1953). Gelation typically occurs at 55-80% conversion and beyond the gel point reaction proceeds towards the formation

of a network with substantial increase in the crosslink density and glass transformation temperature.

The effects of cure temperature on the glass transformation temperature have been reported by Manzione et al (1981) who found that lower cure temperatures resulted in higher glass transformation temperatures and proposed that this was because of changing reaction kinetics causing the formation of different network structures. High temperature cure may also lead to different network structures because of volatilisation of the hardener.

Matsuoka (1992) has discussed the curing reaction in terms of simple thermodynamics. There are well defined changes that occur in the enthalpy and entropy of reacting epoxies. The initial low viscosity mixture of hardener and epoxy contains a large number of chain ends. A conformer at the end of a chain has a much higher energy level than the same conformer at the interior of the chain as well as a higher entropy and free volume. The low viscosity mixture has a low molecular weight and thus a low T_g because of the chain ends and the absence of appreciable entanglements. During cure the loss of epoxide chain ends by chemical reaction leads to a reduction in the free volume, enthalpy and entropy of the reacting mixture compared to the unreacted state. As the free volume decreases and molecular weight increases so the T_g of the system rises. The modulus of the material also increases and when every epoxy group has undergone at least one reaction the gel point is reached. The elastic modulus is proportional to the change of entropy per strain per unit volume, a result derived from rubber elasticity theory and so is proportional to the number of crosslinked chains per unit volume. The number of crosslinked chains per unit volume increases with reaction although a point is reached in a well cured material where the chemical reaction can cause the number of chains per unit volume to decrease even though the reaction continues, resulting in a decrease in the room temperature density and modulus (Enns and Gillham, 1983, Gupta and Brahatheeswaran, 1991).

The final structure of cured epoxies is complex and depends on the specific cure conditions because more than one reaction can occur and the kinetics of each reaction exhibit different temperature dependencies. The structure is affected by steric and diffusional restrictions of the reactants during cure (Morgan et al, 1978a,b, 1979), the presence of impurities that act as catalysts

(Whiting and Kline, 1974), the reactivity of the epoxide group and curing agent (Lee and Neville, 1967, Bell and McCavill, 1974), inhomogeneous mixing of the reactants and cyclic polymerisation of the growing chains (Lee and Neville, 1967, Morgan et al, 1979). Transetherification reactions (homopolymerisation of the epoxy) may also occur and means that fewer epoxy groups are available for primary reactions (Whiting and Kline, 1974). This results in lower crosslink densities. the microstructure is therefore heterogeneous, probably consisting of regions of varying crosslink density.

1.8.2 Properties of Cured Epoxies

The heterogeneity of cured epoxy resins was investigated by Erath and Robinson (1969) with transmission electron microscopy. Prior to this Flory's idea of a thermoset as an infinite network (c.f figure 1.10(a)) had been widely accepted as a plausible model. Flory also proposed that low molecular weight material segregated to various points throughout the network. However, experimental strengths for epoxies fall far short of the predicted ideal network strength which suggests gross heterogeneity probably due to the presence of microvoids (Morgan and O'Neal, 1978a,b, 1977a,b). Erath and Robinson observed regions of epoxy at which there appeared to be very small dense heterogeneities which they attributed to the presence gel particles. They considered that these regions might diffuse and agglomerate during the cure process. Morgan and O'Neal (1977b) used electron and optical microscopy to examine strained films and fracture topographies of DETA cured DGEBA resin and concluded that many epoxy resins failed by a crazing process, thereby inferring that the microstructure is heterogeneous and not completely crosslinked (c.f figure 1.10(b), (c)). Morgan (1979) found that a DGEBA resin cured with 9,11 and 13 phr of DETA showed mechanical property changes inconsistent with a highly crosslinked structure. The resins exhibited macroscopic yield stresses and elongations in excess of 10%. Calculated activation volume gave values comparable to those obtained for linear polymers. Various topographies have been suggested by Morgan and O'Neal (1979) and Nielsen (1969) in which the network structure contains dangling bonds and loops as well as segregated monomer.

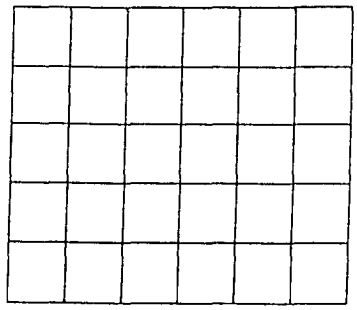

(a)

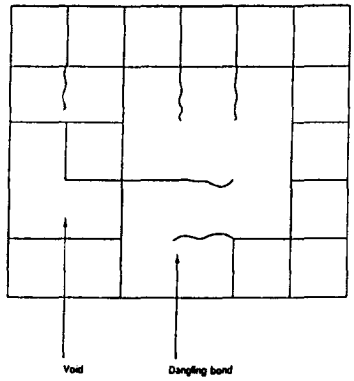

(b)

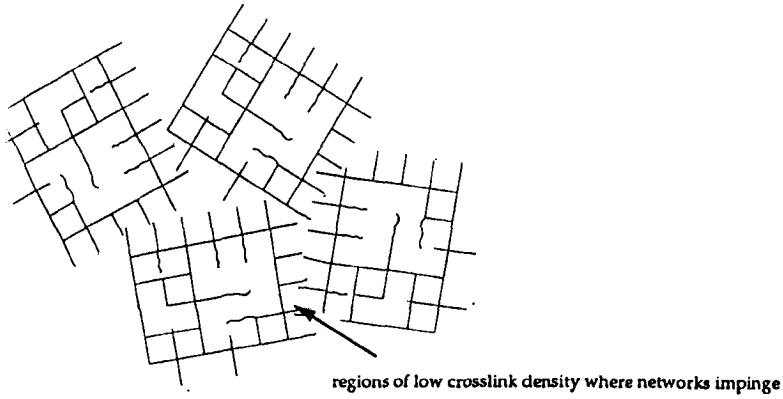

(c)

Figure 1.10: (a) Schematic illustration of epoxy structure as a perfect network. The network was assumed to extend in this form throughout the whole material and was also referred to as an infinite network. (b) Schematic illustration of the reality of epoxy resin structure i.e. voids and dangling (unreacted) bonds in the infinite network. (c) Further illustration of the more likely way in which the microstructure of epoxies develops. Several networks form at different points and impinge, each one containing imperfections. Further defects arise at the boundaries where the networks meet.

The properties of density, specific volume , thermal expansion , modulus etc., are highly dependent on the cure schedule and important for the service performance of the cured materials. An important factor which determines many of the properties is the crosslink density and a crude method of measuring this has been reported by Nielsen (1964). Crosslinking reduces the specific volume and thermal expansion coefficient (Mason, 1964). Relatively little work has addressed the effect of crosslink density on the properties of epoxies. It is known that the glass transformation range increases with crosslink density and Kenyon and Nielsen (1969) found that the mechanical spectroscopy relaxation peak reached its maximum at stoichiometric concentrations of hardener. Crosslinks can also decrease creep in rubbery materials as well as reduce the specific volume and density.

Most studies have sought to investigate the effects of crosslink density by varying the stoichiometric ratio of resin and curing agents but the results of such studies have been contradictory because of the effects of cure chemistry. Chang et al (1982a) overcame this problem by fixing the stoichiometric ratio and using the cure cycle to control the crosslink density. Crosslink density was monitored by following the change in concentration of epoxy groups using FTIR. The bulk density increased linearly with crosslink density and the modulus, upper and lower yield points and the degree of retraction were also found to increase with the degree of crosslinking. Thermally stimulated depolarisation data (TSD) showed that the β relaxation depended on the crosslink density but the g relaxation was unaffected. However, the mechanical b relaxation has been found to shift to higher temperature with postcuring or higher curing temperature due to its dependence on crosslinking (Lewis et al, 1979, Pogany, 1970). The question of the effect of stoichiometry on ultimate tensile strength has been determined by Mostovoy et al (1966) to reach a maximum at stoichiometric concentrations of hardener whilst Bell (1970) reported insensitivity to stoichiometry. Elastic modulus was found by Mostovoy (1966) and Bell (1970) to be independent of stoichiometric ratio and later confirmed by Kim et al (1978).

Enns and Gillham (1983) studied modulus, density, glass transition temperature and water absorption of a DDS cured DGEBA resin as a function of the extent of cure. Specimens of different degrees of cure were formed by curing for different times. The room temperature density of each cure state was measured after slow cooling and the moisture absorption was monitored

gravimetrically at 25°C for two months at several humidity levels. It was found that the room temperature density and modulus decreased with increasing extent of conversion whereas the glass transition and water absorption increased. Pogany (1970) had also reported a decrease in the room temperature modulus with increasing cure. The equilibrium water absorption increases linearly with the extent of cure and with specific volume. These anomalous results were explained by suggesting that as the glass transition temperature increases with extent of cure, the resulting material has a structure that becomes far removed from the room temperature equilibrium state, resulting in more free volume and water absorption. Increasing density with degree of cure is expected to reduce the water uptake as the volume decreases. Enns and Gillham suggested that as the glass is crosslinked , more free volume is produced because of the extra crosslinks preventing the closer packing of the molecules.

Similar results were observed by Gupta and Brahatheeswaran (1991). In an extensive study they cured a DGEBA type difunctional epoxy with different amounts of a tetrafunctional curing agent. The occupied molecular volume was determined by extrapolating the specific volume to O k or by estimating the van der Waals volume for the network and then calculating the empty volume, packing coefficient and the free volume fraction. Their results indicated that highly crosslinked samples showed good packing above the glass transition but poor packing in the glassy state. They suggested that after postcuring and during subsequent cooling, the crosslink density affects the rate at which the samples contract and that more highly crosslinked samples contract more slowly. Due to the slower contraction and higher glass transformation it was concluded that in more highly crosslinked samples a larger free volume fraction is frozen in when microbrownian motion ceases at T_g. With further cooling below the glass transition the intersegmental separation is considered to be higher in the highly crosslinked samples because the crosslinks prevent close packing.

Oleinik (1982) has suggested that the free volume in an epoxy resin is distributed over various hole sizes and that there exist different hole types, configurational and fluctuational. The former are considered to be always present because of the molecular architecture and are basically static in the sense that they are not free to migrate throughout the network. Fluctuational holes are kinetic and result from the freezing in of relatively high energy

conformational sequences of macromolecular segments and are termed dynamic because they are free to move via conformational rearrangements and are able to disappear at the sample surface. Static holes may limit the mobility of dynamic holes by merging with them. Brownian motion of the dynamic holes in the network is considered to take place by a mechanism of exchanging places much like vacancies in an atomic lattice. Oleinik suggests that a distribution of these hole sizes forms the basis of the observed distribution of relaxation times and that at any temperature there will be a thermodynamic equilibrium size distribution of holes and also that there will be a surface energy associated with the holes. In a non-equilibrium state excess hole sizes and excess hole surface energy may provide a driving force for the achievement of the equilibrium thermodynamic distribution. Free volume distributions in an epoxy have been determined recently by Deng et al (1992) using positron annihilation lifetime (PAL) spectroscopy and found that at room temperature, the free volume hole radii are distributed between 1.7 and 2.45 Å. The distributions of radii were found to shift to larger radius with temperature whilst the free volume distribution functions shifted to larger volume and appeared to broaden. The total fractional free volume of an epoxy can be estimated from mechanical spectroscopy using the W-L-F equation. This was done by Gerard et al (1991). They observed that as crosslink density decreased , both of these constants decreased and fractional free volume and free volume coefficient of expansion increased.

Mikolajczak et al (1987) examined the effects of network structure on the free volume of an epoxy. DGEBA resin was mechanically mixed with DDM hardener and cured or mixed with a solvent and hardener and then cured. Using dynamic mechanical spectroscopy, the effects of the solvent were examined. Three mechanical relaxations, α, β and γ, were observed for the cured resin prepared by either method. The solvent reduced the temperature and strength of the α and γ. relaxations. There was a decrease in the temperature and an increase in the strength of the β relaxation and a two fold decrease in the rubber modulus of the epoxy. They found that the decrease in the strength of the a relaxation and the decrease in the modulus was due to a decrease in the crosslink density caused by the solvent.

Plazek and Frund (1990) also studied the curing of a DGEBA resin cured with MDA using DSC and FTIR. The fictive temperature of the material was found to increase rapidly with the degree of cure but as it approached the

curing temperature (at about 80% conversion) the rate of increase slowed down and the material vitrified. Infra-red spectroscopy revealed that the slowing down of the reaction rate in the last 20% of cure was due to a depletion in the number of reactive epoxy groups and restrictions on diffusion of the hardener. The characteristic step in the heat capacity at the glass transformation was found to decrease in magnitude as the degree of cure increased.

Finally, the major drawback of epoxy resins, namely poor impact strength is well illustrated by the work of Bucknall and Partridge (1984) in which the fracture toughness as measured by G_{1C} was reported as 0.11 for a DICY cured resin and 0.18 for a DDS cured resin. Rubber toughening can improve this significantly typically to 0.26 (Manzione et al, 1981).

1.8.3 Secondary Relaxations in Epoxies and other Aromatics

The units that make up the chain structure of epoxy resins are common to other aromatic polymers, some of which possess similar relaxations to the cured epoxy resin, although this depends sometimes on the type of hardener that is incorporated into the epoxy network. Of the mechanically activated low temperature relaxations in epoxies it is known that at -143°C there is a relaxation termed the γ relaxation and at -67°C a β relaxation (Dammant and Kwei, 1967), but the precise location of these depends upon the chemical and physical structure of the cured resin. Charlesworth (1979) showed that the γ relaxation is limited to those epoxy networks containing long enough CH_2 sequences from the diepoxide but this may also be due to the curing agent (Ochi et al, 1982,1987). A mechanical β relaxation in diepoxide networks is observed irrespective of the chemical nature of the epoxide or whether the curing agent is amine or anhydride (Ochi et al, 1986). Dammant and Kwei (1967) proposed that this relaxation was due to the motion of the CH_2-CH(OH)-O- groups. Pogany (1970) studied the low temperature relaxations in DETA cured DGEBA and compared the relaxations with those of other aromatic polymers including phenoxy resin, polycarbonate and polysulphone. Pogany attributed a mechanical relaxation in the epoxy at -80°C to the crankshaft rotation of the CH_2-CH(OH)-O- groups although the position of this relaxation varied with the chemical structure of the epoxy.

Pogany suggested that the variation in the position of the peak occurred because of hydrogen bonding of the -OH group which may hinder the crankshaft rotations and also suggested that the broadness of the mechanical b relaxation may be due to two relaxations. In the same report it was also concluded that shifts in the low temperature relaxations with further crosslinking resulted from increased steric hindrance, thereby making necessary higher temperatures for the relaxations so as to create extra space by expansion of the free volume. A lower temperature relaxation that was found was attributed to oscillation or wagging of the phenyl groups.

Chang, Carr and Brittain (1982a,b,c) studied the relaxation behaviour of several different epoxy systems of different structure using TSD. Two peaks, g at -158°C and b at -88°C were found for resins cured with a diamine. Structural change in the resin molecule or hardener did not seem to affect these peaks. The TSD of neat uncured DGEBA showed only a small peak at -113°C, attributed to the epoxy ring. Postcuring increased the intensity of the b relaxation which was attributed to the formation of crosslinks. The effects of network flexibility on the mechanical β relaxation were studied by Cukierman et al (1991). They found that the motions responsible for the β relaxation began to develop at the same temperature irrespective of the crosslink density and calculated the activation energy using the method of Starkweather (1981). The activation energy was found to be independent of the crosslink density but the activation entropy, which is a measure of the cooperativity decreased with crosslink density indicative perhaps of increased free volume.

The effects of intermolecular interaction on the low temperature relaxations in several aromatic polymers containing the bisphenol A unit was investigated by Yee (1981). A relaxation was found at -100°C Yee suggested that if this relaxation was due to the motion of phenyl groups about the 1,4 axis, there should be two relaxation peaks in a tetra-methyl BPA polycarbonate copolymer. Conversely, if the relaxation was due movement of the entire monomer unit, co-operative motion would occur such that only one relaxation peak would be observed and experimental results showed the latter to be the case. Yee also investigated a piperidine cured epoxy and found that the γ relaxation shifted to higher temperatures , a result inconsistent with phenyl ring motion since it is suggestive of a dependence on crosslinking.

Phenyl ring motions in polycarbonates were also investigated by Yee and Smith (1981). Phenyl group motions are though to play a role in physical ageing processes and mechanical properties and secondary relaxations are known to make considerable contributions to the mechanical behaviour (Bicerano, 1991a). The authors found good correlation between the temperature dependence of plane strain fracture energy and the magnitude of the mechanical spectroscopy loss tangent. The study aimed to link the γ relaxation with phenyl ring motion but the secondary relaxations observed were broad possibly masking the simultaneous motions of phenyl rings, phenyl-carbonate and methylene groups.

Kurz, Woodbrey and Ohta (1970) investigated the relaxation behaviour of several polysulphones and observed low temperature mechanical relaxations $\beta_1$and β_2 at 0°C and -100°C. Whilst the exact origin of the β_1 relaxation was not established and it did not occur in all of the polysulphones, it was suggested that β_2 relaxation observed in all of the materials was connected with the motion of the -SO_2 groups. However, in regard to the β_1 relaxation it was suggested that it may involve a complex motion between phenyl rings and -C-O-C- groups. Dumais et al (1986) studied the phenyl ring motions in polysulphones using NMR and concluded that phenyl ring flips through 180° are important in ageing induced embrittlement , an opinion previously expressed by Legrand (1969). Dumais et al found that as the temperature was raised the number of phenyl groups involved in ring flips greatly increased but depended also on chain packing and prior thermal history. In polysulphones the rigidity of the -SO_2 group is responsible for the hindrance of these motions as well as chain packing. According to Yee and Smith (1981), the rotation of the phenyl ring in polycarbonate involves a larger fractional free volume and moment of inertia than the carbonate group so that with physical ageing, the volume available for ring rotation is reduced and some of the phenyl rings become inactive. Garroway et al (1986) specifically investigated the molecular motions of a piperidine cured DGEBA resin using NMR and concluded that 180° ring flips could occur. However, they found that if the phenyl rings were able to reorient by means of small diffusive steps, the correlation time was the same as observed for the mechanical relaxation at -40°C. and a frequency of 6 Hz. This suggested that small angle phenyl ring orientation occurs which may be identical to the dynamic mechanical relaxation.

1.8.4 Physical Ageing of Epoxy Resins

Physical ageing in epoxy resins is complicated by the fact that because the materials are never completely cured, and because the reactions become severely diffusion limited in the last 20% of cure (Plazek and Frund, 1990), long term annealing below the glass transition may cause physical and chemical ageing. Kriebich and Schmidt (1975) aged an epoxy resin and observed that the heat capacity curve in the region of the glass transition split into two regions. The heterogeneity of the epoxy structure led them to conclude that this phenomenon was phase separation of regions of the network which had different crosslink densities. The lower temperature part then remerged with high temperature portion on subsequent ageing, which led the authors to propose that the less dense networks underwent further reaction with diffusion of the reactants occurring at the same time as physical ageing, the latter process possibly assisting the diffusion. The shift in the lower transition was attributed to densification of the lower density material. Kaiser (1979) observed a similar splitting effect and when the epoxy was annealed at higher temperatures an endotherm was found below the glass transition which subsequently shifted to higher temperatures with longer times supposedly because of densification.

The occurrence of phase separation during the physical ageing of pure epoxies is possible but Ophir, Emerson and Wilkes (1978) suggested that if this was the case then the glass transformation temperatures should separate rather than merge, although this suggestion ignores the possibility of further chemical reaction. These authors examined the physical ageing of neat and rubber toughened DGEBA resin and observed the same ageing behaviour with regard to enthalpy in both materials but the yield point of the neat resin disappeared and the modulus increased, reflecting the annealing induced brittleness. The yield point of the rubber toughened material was retained but shifted to higher stresses. Stress, enthalpy and volume were found to have similar time-temperature dependencies in the materials. Morgan (1979) monitored the effects of ageing on the tensile properties of an epoxy and found that there was a decrease in elongation and an increase in the yield strength, similar results to those of Ophir et al (1978). Morgan also found that the mechanical property changes were thermoreversible. Kong, Tant and Wilkes (1979) investigated the time dependence of mechanical properties and found that the stress relaxation decreased linearly with log annealing time. From dynamic mechanical measurements, modulus and yield strength

increased with ageing whilst the magnitudes of loss modulus and damping peaks decreased.

Kong (1981) investigated the effects of ageing on the properties of an epoxy matrix-graphite fibre reinforced system which was annealed at 140°C. The ultimate tensile strength, strain to break and static toughness of the composite system decreased with time and no weight loss was observed after annealing, demonstrating that degradation did not occur. Kong et al (1981) also studied the effects of ageing on the mechanical properties of TGDDM-DDS epoxy-graphite composites and obtained similar results. In the same study TGDDM-DGOP resins cured with DDS, both with and without fibre reinforcement, were annealed at 80°, 110° and 140°C. The density and hardness of the materials increased, water absorption decreased and NMR results suggested that water can reside in the free volume or disrupt hydrogen bonds. A down field shift in the NMR spectra of the aromatic response was interpreted as molecular aggregation of the phenyl rings during volume relaxation. Dynamic mechanical results showed a decrease in damping and an increase in storage modulus after ageing. The mechanical β relaxation peak was observed to decrease in intensity but did not shift whilst the glass relaxation shifted upwards by 11°C. These effects were found to be thermoreversible.

Chang and Brittain (1982c) cured DGEBA with DDS and when material was annealed, the magnitude of the DSC endotherm, the material density and the upper yield point increased. In contrast, the lower yield point remained unchanged. After deforming the aged material the DSC peak disappeared, presumably due to the creation of free volume (Struik, 1978). The TSD peak corresponding to the glass relaxation decreased in magnitude after annealing in much the same way as observed for the mechanical glass relaxations in the works of Ophir et al (1978), Kong et al (1979) and Kong (1981). Further work by Kong (1983a,b) reported similar effects.

Resins of different structure but based on DGEBA were cured by Lin, Sautereau and Pascault (1986) with DICY using several different cure schedules and formulations to vary the final structure. The isothermal and dynamic enthalpy relaxation was studied using DSC. Unusually, the isothermal relaxation rates of the networks were found to fit an Arrhenius form. Endothermic peaks originated below the transition for precured

materials but at the transition for unprecured materials. The ductility of the unprecured networks was observed to decrease with ageing time but remained fairly stable for the precured and filled materials. This stability was explained as due to the competition between structural relaxation and the relaxation of thermic stresses.

Ellis and Karasz (1986) examined the physical ageing of DGEBA -MPDA in the dry and plasticised states using enthalpy recovery as a monitor. The results showed that water acts as plasticiser and accelerates ageing at any given temperature but no differences in the kinetics of the two states were established when the glass transition temperatures were used as reference temperatures . It was also found that introducing moisture into dry specimens has a dilatational effect which erases accumulated ageing.

A few studies have aimed to determine the changes in resin systems both during and after curing. Choy and Plazek (1986) produced a series of epoxy resins derived from DGEBA with differing chain lengths and studied these materials during and after curing with a diamine and DDS. Like Enns and Gillham (1983), with more advanced curing the room temperature density of the materials was found to decrease. During annealing of the fully cured material the creep compliance increased linearly with the cube root of time, following an Andrade form for the time scales explored. Pang and Gillham (1989) examined the dynamic mechanical properties of a DGEBA resin cured with a tetrafunctional amine during and after the curing process in an effort to establish the influence of thermal prehistory, annealing time and annealing temperature. The annealing temperatures ranged from -15°C to 130°C. the relative rigidity increased linearly with log time of annealing as a consequence of spontaneous densification of the glassy material. The rate of isothermal annealing of a fast quenched material was found to be higher during the early stages of annealing than for a slow cooled material, a fact attributed to the higher quenched in free volume of the fast quenched material and later confirmed in part by the work of Gupta and Brahatheeswaran (1991). However, at long times the annealing rates of fast and slow cooled materials were indistinguishable.

Plazek and Frund (1990) also monitored changes in an epoxy during and after cure. Fully cured materials were annealed at 37°C below the glass transition and using DSC endothermic peaks were observed after only 16 hours but

were also seen during curing after only 1 hour. The rate of physical ageing in the cured material slowed down as the annealing temperature was reduced. The fictive temperature of fully cured networks during annealing decreased with time.

Evidence that physical ageing occurs with some degree of simultaneous chemical reaction was presented by Mijovic and Liang (1984) who found that the mechanical spectra of annealed and requenched epoxy resins were not thermoreversible, perhaps giving credence to some of the suggestions made by Kriebich and Schmidt (1975).

1.9 Blending as a means to Toughen Epoxy Resins

Thermoset materials and in particular epoxy resins, currently dominate as matrices for composite materials. Rubber toughening has been used to overcome their brittleness (Bucknall, 1977, Sultan et al, 1971, 1979, Manzione et al, 1981) but Kinloch et al (1983) showed that it may not be necessary to use rubbery particles to toughen epoxy resins. Polymer blending to obtain synergistic properties is common (Fried, 1983) and following Kinloch's suggestions, attempts have been made to reinforce epoxies with a tough thermoplastic second phase. In epoxy-thermoplastic blends the two components are mixed together and the epoxy crosslinked in situ, although pre-reaction of the thermoplastic is performed first in many cases so that during subsequent crosslinking of the epoxy, the thermoplastic and epoxy phases are chemically joined by the small number of epoxy-thermoplastic copolymerised chains (Hedrick et al, 1985, 1991) Such systems may have various morphologies depending upon the amount of thermoplastic and the cure schedule. Some studies have initially examined systems where the pre-reaction stage is omitted and still claim a toughening effect (Sefton et al, 1987, Almen et al, 1988a,b) whilst others report no toughening or two phase morphology by using such a approach (Bucknall and Partridge, 1983, Raghava, 1987, 1988). Prior to examining these systems in more detail, the general requirements for obtaining a tough system as well as some consideration of the thermodynamics of blending will be presented.

1.9.1 General Toughening Criteria

In order to obtain significant toughening in a brittle material by incorporating either soft (rubbery) or hard inclusions, adhesion at the interface between the matrix and inclusion should exist in the form of molecular entanglements or chemical bonding (Olabisi et al, 1979). Also important is the ductility of the matrix and notch and triaxial stress sensitivity of the material, stress state at the interface, the difference between elastic moduli and Poisson's ratio of the materials (Raghava, 1988).

If a soft inclusion is present in a hard matrix, for example, rubber particles in an epoxy, a triaxial thermal stress state exists in the rubber particles after curing. Inadequate adhesion between the particles and the matrix at the interface may partially or fully debond the particle and a flaw may be generated, which under an external load may cause premature failure. If the matrix is ductile, the stress concentration due to the inhomogeneity may

cause plastic deformation in the matrix , manifested as shear yielding or shear band formation in the matrix. The energy absorbed by the yielding can blunt the crack tip thereby toughening the material.

Yee and Pearson (1989) studied a CTBN toughened epoxy resin and concluded that a reduction in the crosslink density of the epoxy by the presence of the rubber particles and rubber dissolved in the epoxy phase, renders these materials more ductile, thereby increasing their toughness. A high tensile stress exists at such rubber particles at their equator when under tension. Crazing in the interphase region may be initiated at the equator and is possible only if adhesion between the particle and matrix is very good, otherwise the two components will debond, generating a flaw. However, crazing occurs on condition that the matrix may also undergo some plastic deformation.

This is only one point of view as to the mechanism of rubber toughening in epoxies, which is greatly disputed. Sultan et al (1971, 1979) investigated the effect of rubber particle size and found that it affects both the increase in toughening and the toughening mechanism. Small rubber particles (<0.1μm) produced only marginal improvements in toughness compared to an unmodified epoxy whereas G_{1C} was found to increase by an order of magnitude with large rubber particles (1-22μm). from deformation experiments it was concluded that the mechanism of toughening was crazing at the crack tip. Bucknall and Smith (1965) reported that the observed increase in fracture toughness in a rubber modified glassy thermoplastic was due to crazing and that the rubber particles acted as craze initiators and stabilisers in the glassy phase, causing a far larger proportion of the glassy material to undergo crazing before gross fracture.

Pure crazing in thermosets has not been observed but the work of Sultan et al (1979) shows that particle size is important. Bucknall and Yoshii (1978) proposed that in rubber toughened thermosets the increased energy absorption arises from massive crazing and shear flow. Evidence of crazing was presented in the form of TEM micrographs which showed a craze like structure in the epoxy. Lilley et al (1973) and Morgan (1979) have also observed crazes but other reports doubt the ability of epoxy resins to undergo crazing (Kunz-Douglass et al, 1980, Mijovic and Kowtsky, 1979, Yee and Pearson, 1989). However the work of Morgan (1979) and the known fact that

epoxies are highly heterogeneous makes it very likely that in some systems crazing can occur.

It has also been proposed by Bascom et al (1976, 1981) that in rubber modified adhesives, the plastic zone sizes are directly related to the material toughness. They proposed that the triaxial tension ahead of the crack tip increases the size of the plastic zone and that plastic flow and elongation of the particles also contribute to the toughness. These conclusions have been supported by Kinloch et al (1983).

1.9.2 Thermodynamics of Miscibility

It is important when blending polymers to understand something of the thermodynamics of mixing, which is best approached in terms of the free energy of mixing. The variation of free energy with composition in a two component system is shown schematically in figure 1.11.

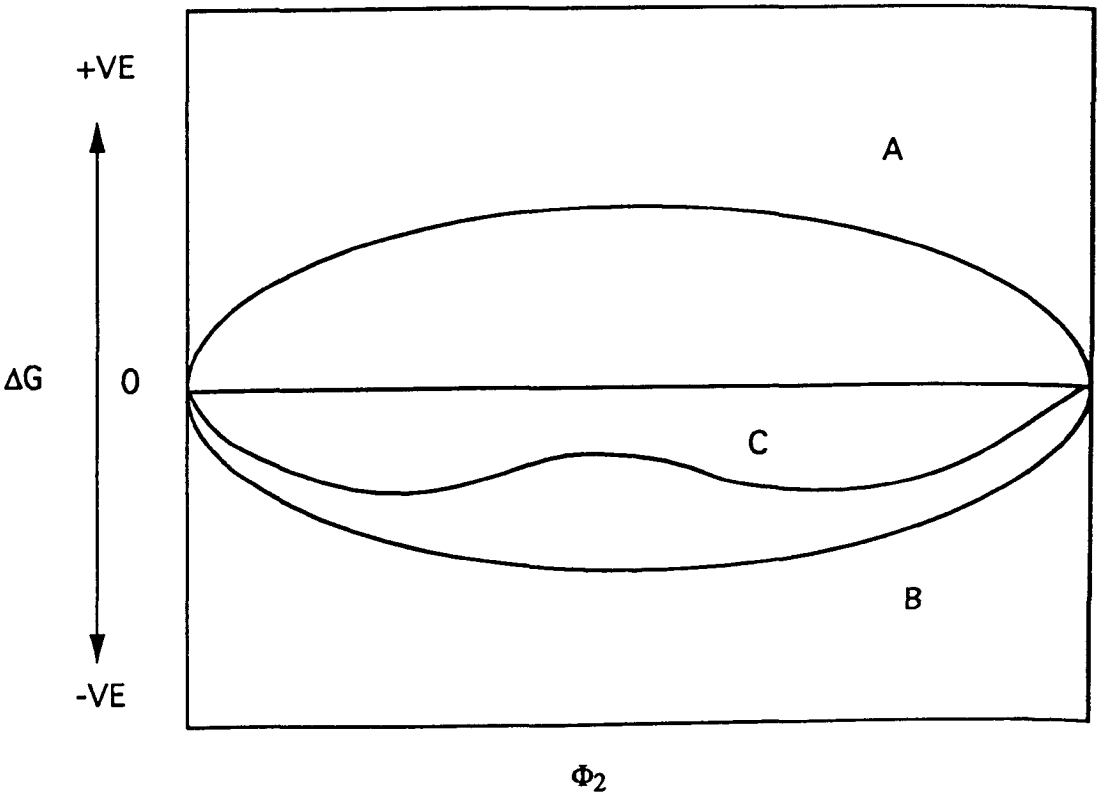

Figure 1.11: Free energy as a function of composition in a binary system of polymers.

Complete miscibility exists only if

$$\Delta G_m = 0$$
$$\frac{\partial^2 \Delta G_m}{\partial \phi^2} > 0 \qquad (1.20)$$

These criteria are met by curve B for all compositions. Blends described by curve A violate the above equations and are completely immiscible. A system described by curve C is partially miscible in that a single amorphous phase can be formed to the left and right of the minima of curve C. Two phase will be formed with compositions given by the minima when mixtures have compositions in the intermediate range. The free energy of mixing can be described in terms of enthalpic and entropic contributions as

$$\Delta G_m = \Delta H_m - T(\Delta S_m^c + \Delta S_m^e) \qquad (1.21)$$

where ΔH_m is the enthalpy of mixing, $\Delta S_m{}^c$ is the combinatorial entropy of mixing and $\Delta S_m{}^e$ is the excess entropy of mixing. If the blend constituents are capable of specific interactions of sufficient strength to promote solution, a single phase amorphous blend may well result which exhibits a single composition dependent glass transition range (Olabisi et al, 1979, Barlow and Paul, 1981). Since miscible blends are intimately mixed it may also be possible for chemical reactions to occur particularly in initially dilute solutions. The blend glass transition temperature can be estimated by various equations, a common example being the Flory-Fox equation (Fried, 1983), shown below.

$$1/T_g = w_1/T_{g1} + w_2/T_{g2} \qquad (1.22)$$

where T_{gi} is the glass transition temperature of component i and w_i its weight fraction in the blend.

However, not all blends are miscible and immiscibility is the more common case. Polymers can be miscible at high temperature but may phase separate during cooling or when held at a different temperature (Olabisi et al, 1979). If a blend is single phase at low temperature but phase separates at higher temperature, this phenomenon is called lower critical solution (LCST) behaviour and if it phase separates during cooling from higher temperature it is termed upper critical solution temperature (UCST) behaviour.

Alternatively, phase separation can be induced by crosslinking one of the components and in this case the incompatibility is caused by the increasing molecular weight of the network as well as its progressive change in chemical structure. Generally phase separation may be a process of two types, either a diffusional process called spinodal decomposition or a nucleation and growth process (Olabisi et al, 1979, Elliot, 1984). If a non-reactive system is brought from a single phase region of the phase diagram into a two phase field and held there, either or both of these processes may occur (Zarzycki, 1991). The structure that results from these different mechanisms is different the spinodal morphology appearing interconnected whereas the nucleation and growth morphology is one of separate particles.

Spinodal decomposition is a kinetic process of generating a spontaneous and continuous growth of a phase within an unstable parent phase (Olabisi et al, 1979). The growth originates from small amplitude compositional fluctuations which statistically promote continuous and rapid growth of a sinusoidal composition modulation with a certain maximum wavelength. Phase connectivity is a characteristic of this type of phase separation but an interconnected structure can also arise from shearing during nucleation and growth. The theory of Cahn (1965) describes the theory of spinodal decomposition in more detail.

1.9.3 When is a Polymer Phase Separated?

A phase is defined as a piece of matter which is homogeneous and has reproducible and stable thermodynamic properties (Callen, 1989) but stability criteria in thermodynamics allow for small fluctuations in density and concentration (ter Haar and Wergeland, 1962, Callen, 1989). It would seem from this definition of a phase that phase separation is easy to detect but there is some debate as to how large must the minimum size of a 'separate' phase be in a polymer blend to make it distinct? The presence of 50-100 Å inhomogeneities in polymer-polymer solutions is expected but does not by itself constitute a phase separated system because such systems can satisfy the criteria for being single phase and heterogeneities (fluctuations in concentration and density) of this order have been observed in single component systems (Olabisi et al, 1979).

In polymer science certain macroscopic techniques are used to determine the extent of miscibility in blends. The most common method uses DSC and a

miscible polymer blend exhibits only a single glass transition at some point intermediate between the glass transition temperatures of the pure components. In the case of borderline miscibility the transition is observed to be single but broad (Olabisi et al, 1979). When limited miscibility occurs in a binary system two glass transition temperatures are observed. There is however a serious limitation to this technique that occurs when the glass transition temperatures of the two components are similar or differ by <20°C. The transitions on this case often overlap and detection of a two phase morphology becomes almost impossible.

There is some debate about the level of molecular mixing required to yield separate glass transition ranges. In some blends a single glass transformation range is observed where a two phase structure is resolved by some other technique such as SEM (Bucknall and Partridge, 1983, Fried, 1983) but physical ageing can make one or both of the components visible as an endotherm develops at the glass transition. Commonly used macroscopic techniques for detecting different phases in polymers include DSC (Stoetling et al, 1970, Zabrewzski, 1973, Landi, 1974), dynamic mechanical spectroscopy, (Paul et al, 1975, Shaw, 1974, Bucknall and Partridge, 1983, Hedrick et al, 1991) and dilatometry (Olabisi et al, 1979). Microscopic techniques consist largely of SEM and TEM (Manzione et al, 1981, Bucknall and Partridge, 1983, 1984, 1986, Sefton et al, 1987, Inoue et al, 1989, Hedrick et al, 1991) in which it is often necessary to stain or dissolve one of the phases to reveal the two phase morphology. The various techniques are discussed more fully by Olabisi et al (1979).

On the basis of the reported techniques , it seems that inhomogeneities must be of the order of 150A or more in order to be identifiable as a separate phase. Clearly, phases can exist which are smaller than this and these may not be detectable by conventional means such as DSC. It may also be the case that the two phases have similar glass transition temperatures which may lead to only a single glass transition range being detected. Results can be confusing, as reported by Bucknall and Partridge (1983) when phase separation was detected by mechanical spectroscopy but was not visible using electron microscopy. In the same publication, SEM revealed a two phase structure but the similar glass transition temperatures of the two phases showed a single mechanical relaxation peak. Clearly, 'seeing' is not always 'believing' and conventional techniques may be inadequate for detecting very small phases.

This is particularly important in the context of the work contained in chapter 3.

1.9.4 Cure and Phase Separation in Rubber Modified Epoxies

It is relevant in discussing phase separated epoxy-thermoplastic systems to examine the phase separation process in rubber toughened epoxies, which is fairly well understood because similarities exist even though the second component is vastly different. The effects of cure on epoxy resin have already been discussed and cure in the presence of a CTBN rubber modified epoxy will be examined.

The structure of CTBN rubber is shown in figure 1.12.

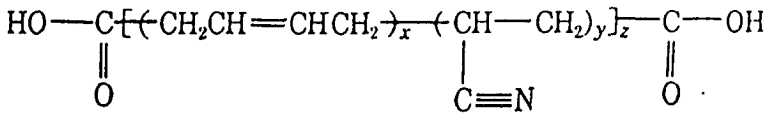

Figure 1.12: Chemical structure of CTBN rubber

An obvious requirement is that the rubber must be soluble in and well dispersed throughout the resin prior to curing so that a homogeneous phase exists. This requires that the solubility parameters of the rubber and liquid resin are similar prior to cure (Sultan et al, 1971,1979). The rubber has OH terminations which are able to react with the epoxy so that during phase separation there is some chemical bonding between the rubber rich phase and the epoxy matrix. In the presence of a hardener there should be a rapid reaction of the OH in the rubber with the epoxy, and the occurrence of this reaction in the presence of a large excess of epoxy monomer leads to the rubber chains being end capped at both ends by one unit of epoxy (Manzione et al, 1981). As the reactions are taking place there is a simultaneous increase in molecular weight and viscosity as the network structure develops. The rubber and epoxy become less compatible with cure because of the molecular

weight difference and a point is reached at which phase separation occurs and rubber rich domains precipitate into an epoxy rich matrix. At the gel point the system is too viscous to permit further phase separation and the morphology becomes effectively fixed (Bucknall, 1977, Rowe et al,1970, Gillham et al, 1977). Long gel times allow more time for complete phase separation but if the material gels too quickly the rubber domains may not have time to fully develop (Gillham et al, 1977).

The effect of using non-reactive chain terminations is that in the absence of a chemical reaction between the epoxy and rubber a weak interface results which does not improve fracture toughness (Siebert and Riew, 1971). Clearly, chemical bonding across the interface is an important criterion, not only in rubber toughened epoxies but in other blends including thermoplastic toughened epoxies.

1.9.5 Initial Development of Thermoplastic Toughened Epoxies

The use of polyaromatics as toughening agents for epoxy matrices was undertaken with some considerable degree of success by Sefton et al (1987) and Almen et al (1988a,b) but the commercial applications of these blends did not allow explicit details of the technique to be published by these researchers. However, other researchers also made progress in this area (Hedrick et al, 1985, 1991). Almen et al (1988a) stated that polyaromatics show distinct advantages over as toughening agents because of their high glass transformation ranges, higher thermal stability and moduli. A general formula for a polyaromatic is

$$-AR_1-X-AR_2-Y- \qquad (1.23)$$

The choice of the groups AR_1, AR_2, X and Y and their distribution along the backbone dictate the modulus of the polymer as well as the solubility and in some cases the crystallinity. All para linkages are preferred when a high modulus, high performance polymer is required but all meta linkages can be used to enhance processability and solubility. Incorporation of an ether or sulphide flexibilising group lowers the glass transition range and renders the polymer more processable. Inclusion of a sulphone group results in an increase in the glass transition temperature. Selection of the right flexible group for incorporation into the polymer is obviously very important because

it will have a significant effect on the mechanical and thermal characteristics of the polymer as well as its compatibility in a blend. When AR_1 and AR_2 are phenyl, X is ether and Y is sulphone, the polymer is polyethersulphone, which is tough possibly because of the β relaxation which occurs at circa -100°C (Dumais et al, 1986, Legrand, 1969), has a high glass transition in the region of 230°C and is stable up 200°C.

Polyethersulphones have many uses as low smoke emission plastics and tough coatings (Wu et al, 1988). In an early study of epoxy-thermoplastic blending Bucknall and Partridge (1983) blended a low molecular weight PES containing OH end groups with a tetrafunctional resin, a trifunctional resin and mixtures of these two resin types. The systems were cured with DICY or DDS. The hydroxyl end groups of the PES are capable of reacting with the epoxy groups to form a copolymer so that chemical bonding may be established across the interface as phase separation occurs. However, Bucknall and Partridge found that phase separation did not occur in the tetrafunctional resin cured with either hardener and the blend had poor fracture properties. A trifunctional resin cured with both hardeners showed phase separation by SEM and mechanical spectroscopy but blends of the two resins with the PES showed a two phase morphology by SEM but not by mechanical spectroscopy. In all cases there was little improvement in the blend fracture toughness compared to the resin. In a later report, Bucknall and Partridge (1986)again concluded that little improvement resulted in fracture toughness even in two phase blends.

Diamant and Maroum (1984) investigated the effects of toughening tetrafunctional epoxy resin with various ductile and tough thermoplastics possessing high glass transition temperatures but did not observe a two phase structure and found no improvement in fracture toughness. Hedrick et al (1985) modified a bisphenol A type of resin using phenolic hydroxy terminated polyethersulphone oligomers and reported a two fold increase in fracture toughness which they claimed to be dependent upon the block length of the PES oligomers. A nodular morphology was observed by SEM.

Raghava (1987, 1988) blended a tetrafunctional epoxy resin with PES and cured the system with an aromatic anhydride. A two phase bimodal particle distribution was observed by SEM. The glass transition of the blend and neat epoxy were observed to be the same. The author proposed that the lack of

improvement in fracture toughness was due to the fact that at low concentrations of PES the resin was still brittle. It was also suggested that hardener viscosity may affect the morphology of the blend and that PES may plasticise the epoxy and decrease the crosslink density, resulting in lower elastic moduli at all temperatures compared with the unmodified epoxy.

A study by Yamanaka and Inoue (1989) of blends of Epikote 828 and hydroxy terminated PES cured with DDM reported phase separated morphologies observed by light scattering, SEM and DSC. In the early stages of curing the ternary mixture was observed to change from single phase to phase separated and the authors proposed that this took place by spinodal decomposition because a supposedly interconnected morphology was observed by SEM. The blend showed much higher adhesive strength than the neat resin in both shear and peel modes.

A different approach was taken by Hedrick et al (1991) who obtained significant improvements in fracture toughness of epoxy-PES systems cured with DDS. The PES and epoxy were first pre-reacted before curing and a two phase structure was observed by SEM even though the blends were quite transparent.

1.9.6 Physical Ageing of Epoxy-PES Blends

There appears to be no published work concerning physical ageing of epoxy-thermoplastic blends although much work probably remains unpublished for commercial reasons. However, Breach, Folkes and Barton (1992) have produced a brief report concerning the enthalpy relaxation of single phase epoxy-PES blends annealed at 180°C. As the amount of PES in the blends was increased, the materials were observed to relax faster , a fact attributed to increased free volume introduced into the network through disruption of crosslinking and the excluded volume effect of the PES.

Chapter 2

Experimental Methods and Characteristics of Basic Materials

2.0 Characteristics of the Base Materials

2.1 Resin

Table 2.1 shows the manufacturers information concerning the properties of the Epikote (Shell) 828 Epoxy Resin oligomer. The chemical structure of the resin monomer is shown in figure 2.1.

Table 2.1: Properties of Epikote 828 Oligomer

Viscosity at 25°C (poise)	Specific Gravity (20°C)	Epoxide (eq/110g)	M_n (g/mol)	T_g(°C)	Functionality	Epoxy equivalent
110-150	1.1	0.52-0.54	380	-14	2	1.9

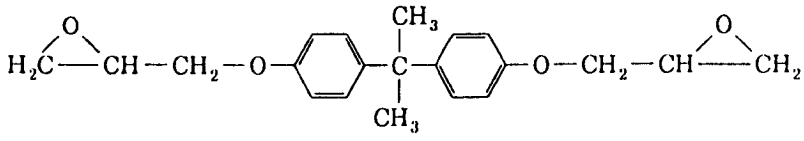

Figure 2.1: Chemical structure of Epikote 828 resin monomer

2.2 PES

The characteristics of the PES thermoplastics are shown in table 2.2 and the chemical structure is shown schematically in figure 2.2.

Table 2.2: Properties of PES Thermoplastics

Source	Source Identification	Chain Termination	T_g
ICI	Victrex 100P	-OH	230°C
BASF	Ultrason E2010	-Cl	230°C

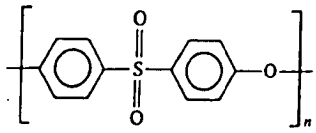

Figure 2.2: Chemical structure of PES

2.3 Curing Agents

Table 2.3 shows the properties of the curing agents and the chemical structures are shown in figure 2.3.

Table 2.3: Properties of Curing Agents

Material	Mol. Weight (g/mol)	Melting Range (°C)	Functionality	Molar Vol. (cm^3/mol)
DDS	248	175-177	4	193
DICY	84	----------	4	72

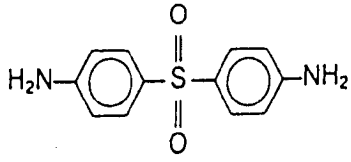

DDS

(a)

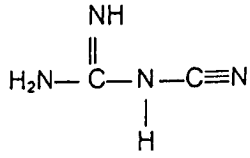

(b)

Figure 2.3: Chemical structures of curing agents (a) DDS (b) DICY

2.4 Blend Preparation

2.4.1 828/DDS Systems

The neat resin was prepared by gently heating 100g of resin at 50°C for several minutes, after which time 36 phr of DDS was added and the mixture stirred. The mixture was slowly heated to 130°C and held at this temperature for 3-5 minutes, at which point the DDS dissolved in the resin. The resin was transferred to steel moulds and then placed in a vacuum oven at 140°C and degassed under a vacuum of 25mm Hg for 10-15 minutes. After this time the resin was transferred to a fan assisted oven and cured for 2 hours at 180°C and postcured for 2 hours at 200°C.

The procedure for the blends was slightly different. Firstly the PES was dissolved in a mixture of dichloromethane/methanol (95/5 w/w) to 10% by weight. The resin and hardener were mixed together at 50°C with stirring for several minutes. The mixture was then cooled to 45°C and the PES/solvent mixture added at which point some of the solvent evaporated. The mixture was stirred vigorously and heated from 45°C to 130°C over a period of 45 minutes, stirring continuously. During this period much of the solvent is removed. The mixture was held at 130°C for 3-5 minutes until the DDS dissolved. At this point the mixture was viscous, homogeneous and quite clear. The mixture was poured into moulds (preheated at 140°C) to a depth of 3-4mm. The moulds were transferred to a vacuum oven at 140°C and the mixture degassed at 25mm Hg for 30 minutes. After this period the mouldings were relatively void free and were cured in the same way as the neat resin.

After curing the mouldings were machined to 2-3mm thick and cut into suitable sizes for the experimental work.

2.4.2 828/DICY Systems

Firstly the DICY hardener was ground with a mortar and pestle to remove any agglomerates. The epoxy resin monomer was heated gently at 50°C for several minutes and the hardener was added at a concentration of 5phr with continuous stirring. After cooling the mixture to 45°C the PES/solvent mixture as described in the previous section containing only 30 phr of PES, was added and the mixture vigorously stirred whilst heating to 100°C over a period of 45 minutes to remove a large amount of the solvent. The mixture was held at this temperature for 5 minutes to promote partial curing. The

mixture was transferred to preheated moulds and degassed in a vacuum oven under a vacuum of 25mm Hg at 130°C for a period of 30 minutes. The materials were then cured for 1 hour at 160°C followed by 16 hours at 180°C.

2.5 Characterisation of PES and Cured Materials

After preparation the specimens were characterised in the as cured state using the following experimental methods.

2.5.1 Differential Scanning Calorimetry

Samples of 10 mg in weight were cut from as cured plaques and scanned at 20°C/min on a Perkin-Elmer (PE) Model DSC II coupled to a PE 3600 data station. For heat capacity measurements a sapphire standard was first used for calibration and the necessary corrections applied. Five specimens of each sample of each material were used for experimentation. From the heat capacity measurements of aged materials the enthalpy change as a function of time was calculated.

2.5.2 Dynamic Mechanical Spectroscopy

Two instruments were used for mechanical spectroscopy. A Rheometrics RSA II coupled to an IBM workstation was used for testing at a frequency of 1Hz. Specimens were tested in the form of rectangular bars in dual cantilever or three point bend testing modes. The test bars were typically 50 x 2 x 2mm in measurement. A Polymer Laboratories DMTA II was also used for mechanical spectroscopy measurements. The standard test frequency was 1 Hz but for frequency scanning the RSA II was used to its maximum frequency of 15 Hz and the DMTA II to its maximum frequency of 100Hz. Activation energies were calculated according to the methods described by Starkweather (1981) from the relaxation peak position and the measurements were also used in a power law analysis described by Souletie and Thoulence (1985).

2.5.3 Impact Measurements

The impact test is a simple method of measuring the resistance of a material to crack propagation under shock loading. The energy absorbed by the specimen is a measure of the material toughness.

Samples of materials measuring 60 x 60 x 4 mm were machined and notch depths from 0.1 to 1mm were cut. The materials were tested using a Rosand Precision Falling Weight Impact Analysis System (Type 5) coupled with an IFW Data Analysis System.

From the energy absorbed during impact and the corresponding notch dimensions (see figure 2.4), the critical strain energy release rate G_c was calculated using the formulae

$$I = BWZG_c$$

where I = impact energy

G_c = critical strain energy release rate

and Z is given by

$$Z = \frac{a}{2W} + \frac{S}{18\pi a}$$

Plotting impact energy against BWZ yields the critical strain energy release rate G_c (Kinloch and Young, 1983,Williams, J.G., 1984).

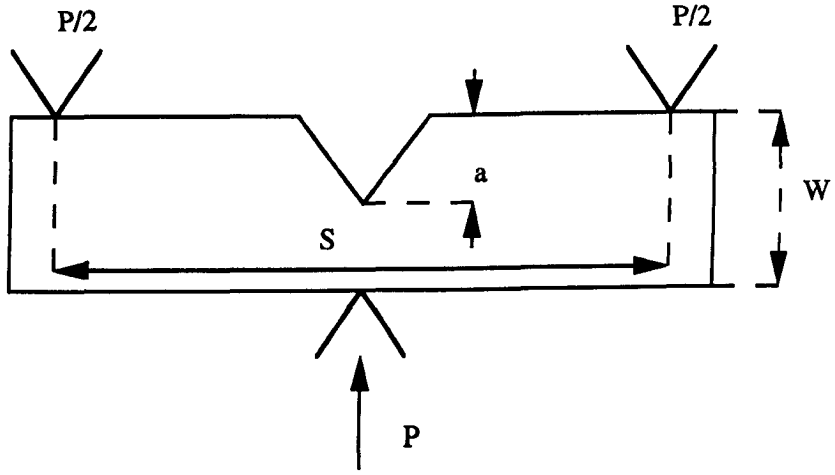

Figure 2.4: Charpy Geometry used for impact testing

2.5.4 Infra-Red Spectroscopy

A Nicolet FTIR Microscope was used for determining the infra-red spectra of the materials. The samples of cured materials and thermoplastics were powdered by cutting with a fine saw. This powder was placed under the FTIR microscope in absorbance mode and the spectra collected in 200 scans with a resolution of 2 cm^{-1}

2.5.5 Dielectric Spectroscopy

A Polymer Laboratories DETA 2 was used to collect dielectric spectra. The range of frequency used was from 50 to 100000 Hz. Thin samples were machined from the mouldings to a thickness of 1-2mm, 35 mm square and gold coated on both sides taking care to leave the edges uncoated. The samples were placed in the dielectric cell at various temperatures from ambient to 240°C for the 828/DDS systems and up to 180°C for the 828/DICY systems.

2.5.6 Scanning Electron Microscopy

A Cambridge Instruments S250 SEM was used for examination of fracture surfaces. The specimens were cut to about 5mm thick and mounted on an aluminium stub and gold coated. Conductive paint was applied to the coated specimen and the materials were observed under an accelerating voltage of 20 keV.

2.6 Method of Determining the Molecular Weight Characteristics of PES

2.6.1 Gel Permeation Chromatography (GPC)

Molecular weights of the two samples of PES were determined by GPC. Sample solutions were prepared by adding 10ml of solvent to 20mg of sample and gently heating the solutions to dissolve the materials. A small amount of acetone was added as an internal marker and after thorough mixing the solutions were filtered through a 0.45 micron PTFE membrane prior to chromatography. Each sample was run in duplicate. The following conditions were employed.

Columns-PL gel 2 X mixed gel , 10 microns, 30 cm
Solvent- dimethylformamide (DMF) with lithium bromide
Flow rate- 1.0 ml/min
Temperature - 80°C (nominal) Detector- refractive index

2.7 Conditioning and Annealing

2.7.1 828/DDS Systems

Once it had been determined that the materials were fully cured and the glass transformation ranges were known the blends were conditioned in the case of 828/DDS systems by annealing at 20°C above the calorimetric midpoint T_g for 10 minutes and quenched in air between steel plates at 25°C. This conditioning erases any prior thermal history. The materials were then aged at various times at 180°C for up to 28 days and each time the specimens were quenched between steel plates at 25°C. The same experimental techniques used for characterisation of the as cured materials were used to monitor the physical ageing behaviour.

2.7.2 828/DICY Systems

In the case of the 828/DICY systems no conditioning was applied because of the risk of thermal degradation. The samples were simply annealed at 120°, 140°, 160° and 180°C for various times up to 70 days and quenched in air between steel plates at 25°C after annealing.

2.8 PES Materials Characteristics

These are shown here to avoid confusion in the discussion of the results for the blends. The molecular weight distribution curves of ICI Victrex 100P and BASF Ultrason E2010 are shown in figure 2.5.

The values of molecular weight are shown in table 2.4.

Table 2.4: Molecular Weight Characteristics of PES Materials

Material	Chain Termination	M_n	M_w
ICI- 100P	-OH	2.8×10^4	6.05×10^4
BASF-E2010	-Cl	1.01×10^4	4.08×10^4

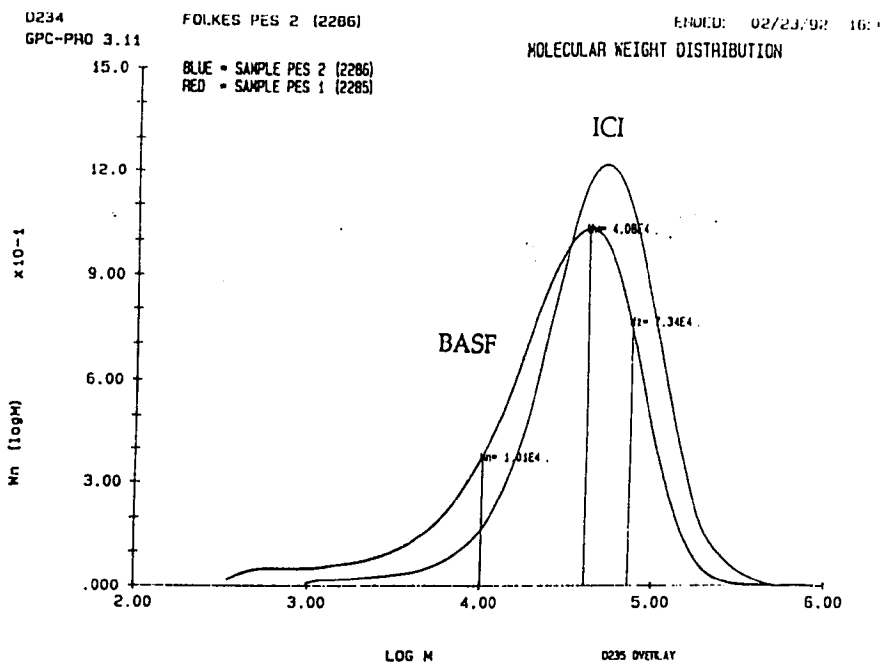

Figure 2.5: Molecular weight distribution curves of ICI and BASF PES

The heat capacity curves are shown in figure 2.6

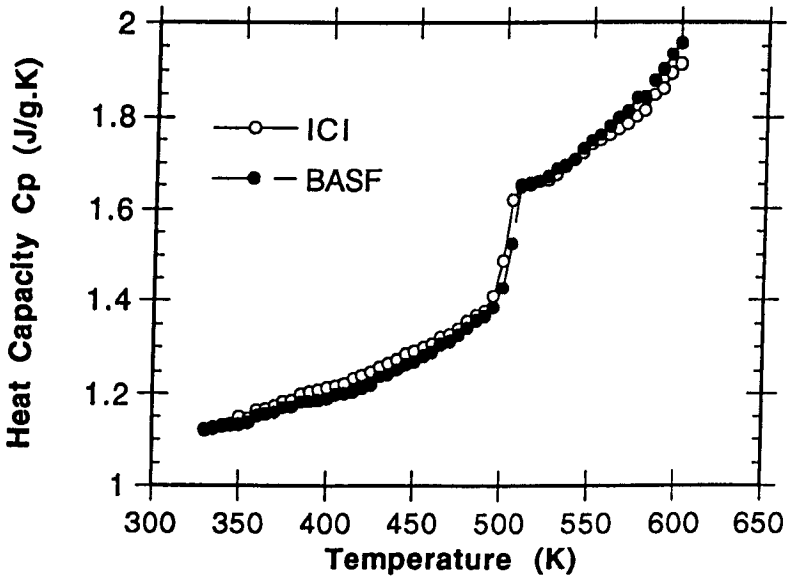

Figure 2.6: Heat Capacity Curves of PES

The thermogravimetric data are shown in figure 2.7

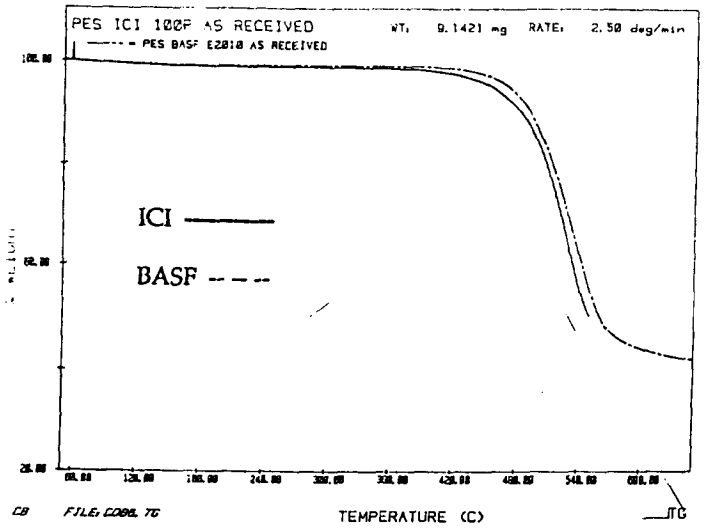

Figure 2.7: Thermogravimetric curves of ICI and BASF PES

The dynamic mechanical spectra are shown in figure 2.8

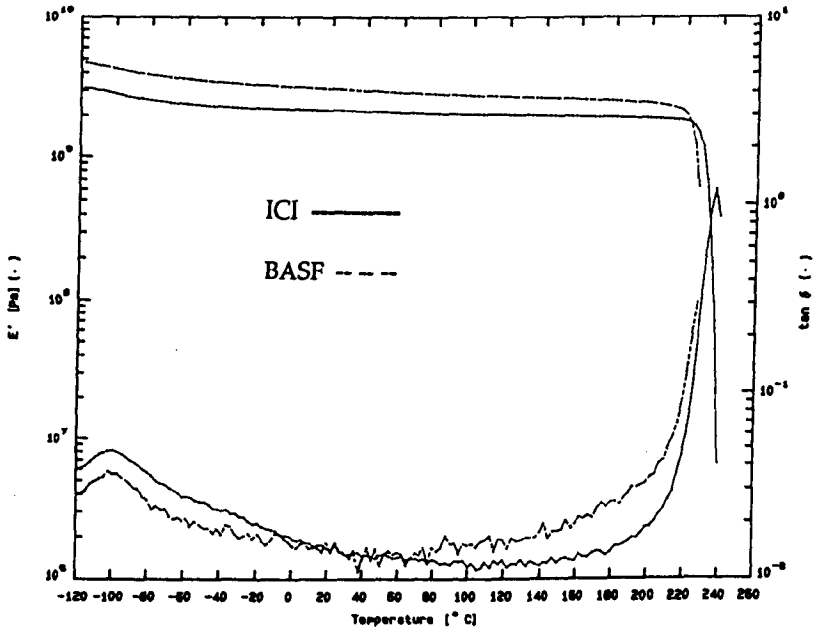

Figure 2.8: Dynamic mechanical spectra of ICI and BASF PES

The molecular weight of the ICI material is higher and the distribution narrower. The heat capacities are similar despite the differences in molecular weight and the materials have similar onset glass transitions. The ICI PES seems to start to degrade slightly earlier than the BASF PES, although the differences are not great. The dynamic mechanical spectra are also similar

but the ICI PES appears to have a higher dynamic storage modulus although the glass transition relaxation peaks occur at similar temperatures.

Chapter 3

Physical Ageing of Single Phase Epoxy Resin-Polyethersulphone Blends

3.0 Introduction

Although there has been a great drive towards developing epoxy-PES blends which are phase separated, the lack of an easily distinguishable reinforcing second phase is not necessarily a disadvantage and blends which are apparently single phase have fracture toughnesses at least as good as the unblended epoxy resins (Bucknall and Partridge, 1983, Diamant and Maroum, 1984, Hedrick et al, 1991) as well as comparable Young's moduli. These materials also make very good adhesives and depending upon the PES content, can give joint strengths which are as good as, if not better than the same epoxy without the PES additive. Such blends have potential applications and are not simply interesting academically.

In the first section of this chapter we characterise blends of an Epikote 828 difunctional epoxy cured with DDS and containing either ICI (Victrex 100P) PES or BASF (Ultrason E2010) PES. These blends appear to be single phase insofar as the analytical techniques used to study the blends did not reveal the presence of two distinct phases. For reasons discussed in section 1.9.3 this

is not of course entirely conclusive. Apparently single phase blends of PES and epoxies have been found (Diamant and Maroum, 1984, Hedrick et al, 1991) although Bucknall and Partridge (1983) found that phase separation was detectable with some experimental techniques but not with others. However, Hedrick et al (1991) have also produced clear blends (clarity suggesting single phase structure) which nevertheless exhibit very small (typically 2μm) PES rich particles.

The potential for commercial exploitation of these materials, does however, depend upon acquiring a good understanding not only of the initial 'as cured' properties of the blends, but also their time dependent properties under certain conditions. This is the concern of the second part of this chapter, which highlights some of physical ageing characteristics of these systems at high temperature. This is extremely important because it is pointless having blends which adhere as well as an unblended epoxy initially but which physically age more rapidly under the same service conditions. This has clear implications for aerospace structures which are bonded together by epoxy-PES blends and which may be exposed intermittently to moderate or high temperatures. The results presented in this chapter will show that the presence of the PES has major effects on the microstructure of the cured epoxy blends which in turn influences greatly the physical ageing behaviour of these materials at high temperature. In addition, the lower molecular weight of the BASF E2010 PES in comparison to the ICI 100P material, as well as its -Cl chain terminations, will be shown to significantly affect the physical ageing behaviour.

3.1 Unaged Materials: Results

3.1.1 Calorimetry and Thermogravimetry

The effects of PES on the heats of reaction of the blends are shown by the data in table 3.1.

Table 3.1: Heats of Reaction

Material	Heat of Reaction ΔH(kJ/mol)
828/DDS	351+/-10
20I	330+/-9.5
30I	313+/-9.8
20B	318+/-9.4
30B	305+/-9.5

Increasing the amount of PES decreases the heat of reaction relative to the neat resin but more so with the BASF PES. This effect is probably related to the lower molecular weight of the E2010 which is expected also to contain a higher number of chain ends for a given amount of material than the 100P. This means that the number of PES chain ends present in the BASF blends is likely to be greater than a blend of the same composition containing ICI PES.

In principle a small number of ICI PES hydroxy end groups may react with the epoxide groups but even if this can occur it will be limited and create a long flexible copolymer which can only act as a very flexible crosslink between epoxide molecules. The prevention of some chemical reactions will affect the thermodynamic properties of the cured blends via the heat capacity and the glass transformation characteristics, the extent depending upon the molecular weight characteristics of the PES. Figures 3.1 and 3.2 show the heat capacity curves of the ICI blends and BASF blends respectively, together with the curve obtained for the cured resin. All of the materials exhibit a single glass transformation range located at a similar position and over a similar temperature range. This suggests that the blends differ little from the neat resin and are apparently single phase .

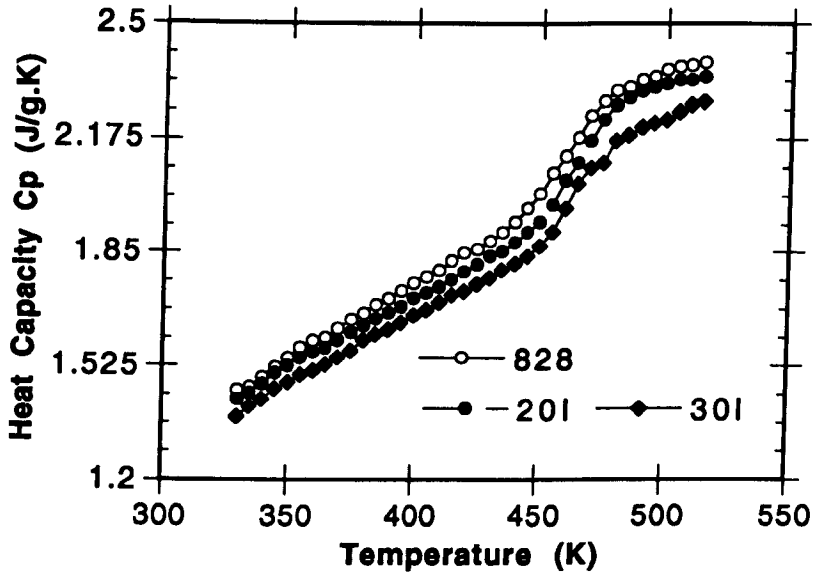

Figure 3.1: Heat capacity curves of the neat cured resin and ICI blends

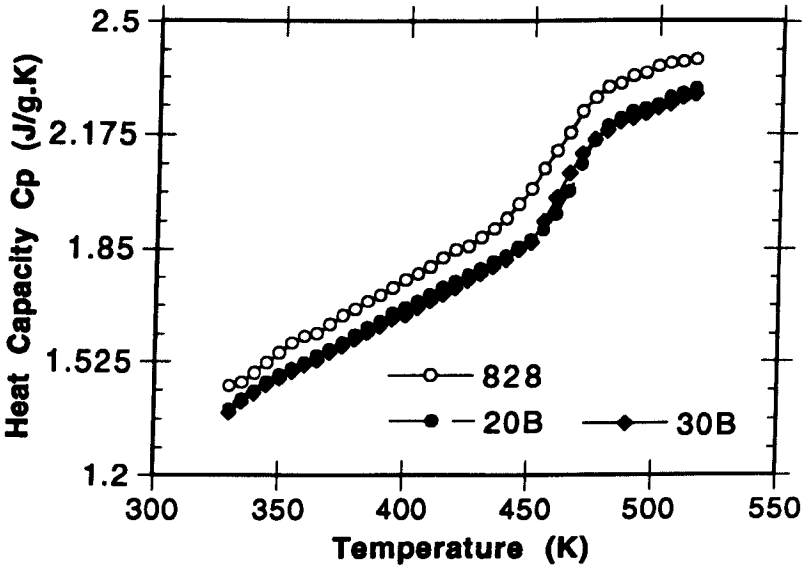

Figure 3.2: Heat capacity curves of neat cured resin and BASF blends

The curves appear similar in shape but the heat capacities differ slightly, falling approximately in the order C_p(RESIN)> C_p(20I)> C_p(30I)~C_p(20B,30B). The PES causes a decrease in the heat capacity but the effect is greater with the BASF PES.

The glass transformation temperatures of the blends were obtained using the Flory-Fox rule of mixtures (Fried, 1983) and table 3.2 shows that the glass transition temperatures are similar to the neat resin.

Table 3.2: Glass Transformation Temperatures

Material	T_{go}/T_{gmp} (°C)	Flory-Fox T_{go}/T_{gmp} (°C)
828/DDS	201/206	----------
20I	195/201	203/204
30I	199/202	205/205
20B	192/199	200/205
30B	198/203	205/210

The crosslink density measurements of the materials shown in table 3.3 suggest that there is no difference between the blends and the unmodified resin but these measurements were obtained by the method of measuring the glass transformation characteristics of the uncured and cured materials , as detailed by Nielsen (1964) which does not account for the copolymer effect of the hardener. Some work has reported that reaction between the epoxy end groups of the hydroxy terminated ICI PES can occur without pre-reaction prior to curing (Sefton et al, 1987) and if this does occur then copolymerisation of the thermoplastic and epoxy must be considered.

Table 3.3: Crosslink Density Measurements

Material	Mean Molecular Weight Between Crosslinks	Mean Crosslink Density
828/DDS	205	4.9
20I	205	4.9
30I	204	4.9
20B	204	4.9
30B	200	5

Even if the ICI PES chain ends can react with the epoxide groups, this does not apparently lead to a detectable phase separation in terms of calorimetric properties. The presence of the PES does not seem to have reduced the glass transition in comparison to the neat resin even though it reduces the extent of chemical reaction by a small but significant amount. In preparing the blends the PES also drastically increased the viscosity of the unreacted mixture. The effects of lower crosslink densities in the blends are more clearly seen in the thermodynamic properties of the glass transformation in table 3.4

Table 3.4: Calorimetric Data of Blends

Material	ΔH (T_{go}) (J/g)
828/DDS	12.26
20I	11.6
30I	10.2
20B	10.76
30B	11.07

The differences in enthalpy of the materials measured at the onset temperature decrease with the quantity of PES irrespective of type. Comparing equivalent blends, the differences are greater for the ICI materials which suggests a greater degree of structural freedom in the BASF blends during the cooling process and an ability to eliminate more energy and it seems logical that this should arise from fewer crosslinks in the BASF blends.

The effects of lower crosslink density should be observable in the thermal stability of the blends. The thermogravimetric curves in figures 3.3 and 3.4 show the weight loss of the ICI and BASF blends respectively with the neat cured resin superimposed. It appears that the decomposition process in the BASF blends starts later than in the ICI blends but the rate of decomposition is higher as seen from the increased slope of the decomposition region. The presence of a shift in the BASF materials appears rather odd but the faster decomposition is expected because of the lower crosslink density. In comparison to the neat resin both blends compare well, the ICI blend starting to decompose at a similar temperature to the resin.

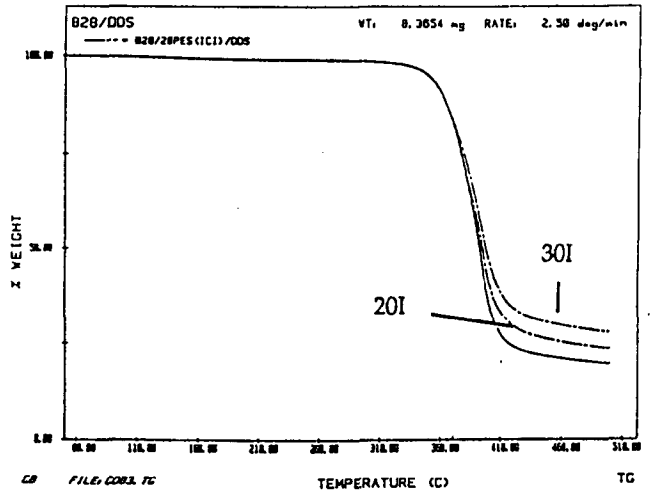

Figure 3.3: Thermogravimetric curves of neat resin and ICI blends

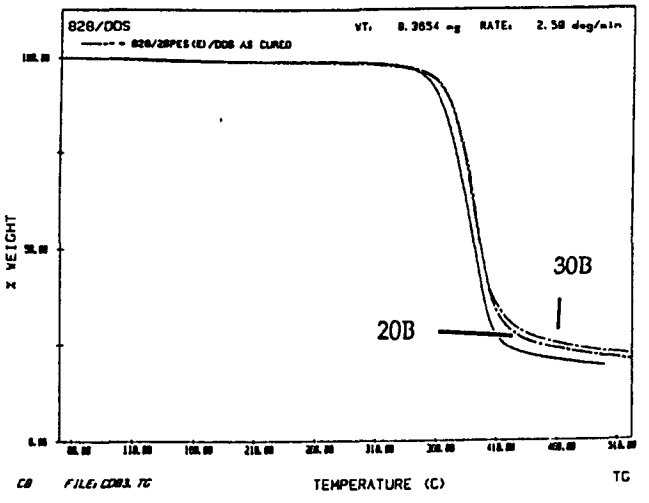

Figure 3.4: Thermogravimetric curves of neat resin and BASF blends

3.1.2 SEM Micrographs

Figures 3.5, 3.6 and 3.7 show the fracture surfaces of neat epoxy and blends of 30I and 30B respectively. These micrographs are representative of the fracture surfaces of the other blends. The fracture surfaces are featureless except for hyperbolic marks indicating the presence of primary and secondary fracture (Döll, 1989) and do not indicate the presence of two phases, much the same as those of Bucknall and Partridge (1983). Although etching was attempted in the vain hope of revealing a second phase the results were inconclusive.

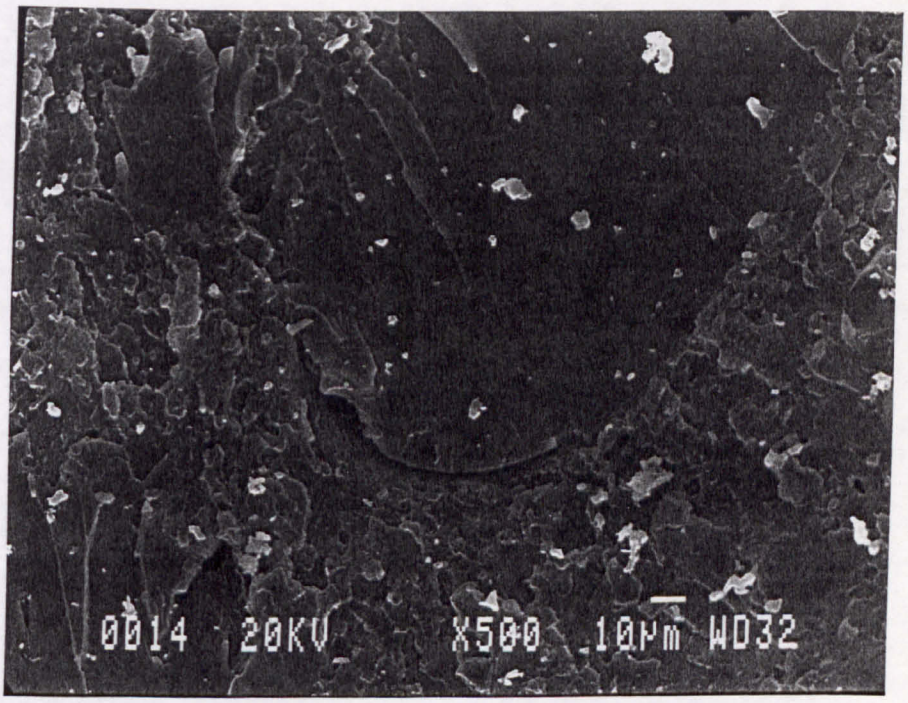

Figure 3.5: SEM micrograph of fracture surface of neat cured epoxy resin

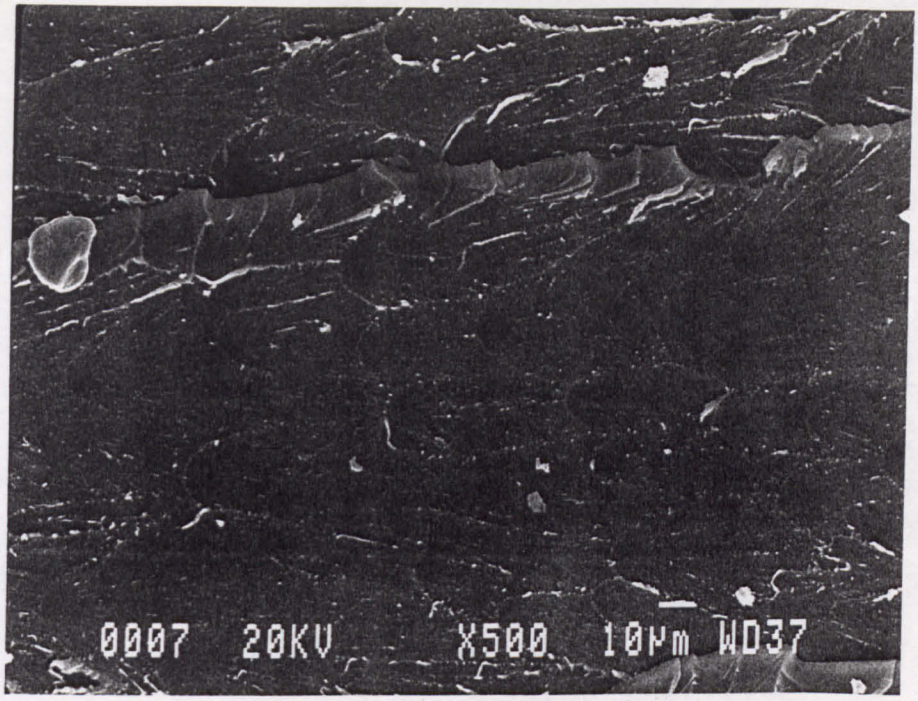

Figure 3.6: SEM micrograph of fracture surface of 30I blend

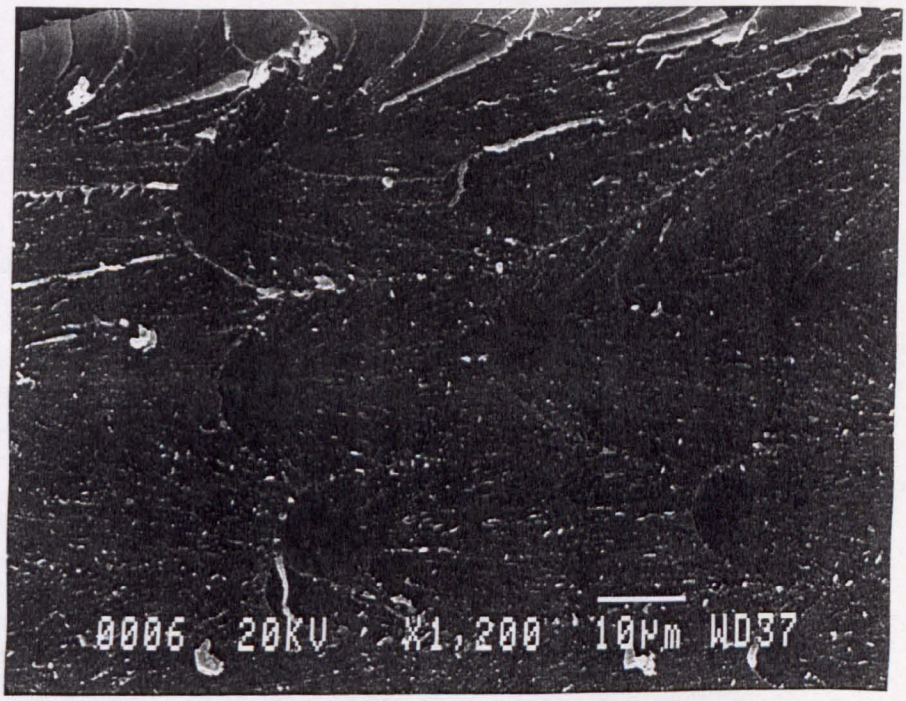

Figure 3.7: SEM micrograph of fracture surface of 30B blend

3.1.3 Infra-Red Spectroscopy

If the curing reaction also allowed the hydroxy end groups of the ICI PES to undergo reaction with some epoxide groups, in comparison to an equivalent BASF blend, the ICI blend should exhibit some increase in intensity in a characteristic region of the IR spectrum.

In rubber toughened systems the reaction between the end groups of the rubber and the epoxy is important in the phase separation process (Manzione et al, 1981) but the appearance of a single glass transition in the blends suggests that these materials are single phase. The problem with the blends of PES and epoxy is that both of these materials are polyethers. The result of a reaction between the ICI PES hydroxy end groups and the epoxy resin will be the formation of an ether segment, as shown below in figure 3.8.

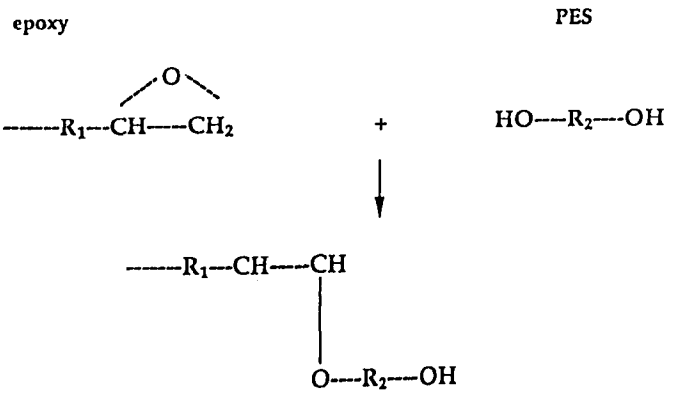

Figure 3.8: Schematic diagram showing mechanism of PES-epoxide reaction

This is a mono-aryl ether (Bellamy, 1976) but this type of group is already present in the PES and the epoxy oligomer as well as di-aryl ether structures. The formation of this type of structure has been examined by Wu et al (1988) in crosslinking of hydroxy terminated PES by heat where an increase in the characteristic di-aryl ether absorption at 1250 cm^{-1} was observed. However, this is a mono-aryl ether and will occur in a different part of the spectrum. The formation of an ether structure of the type $-CH_2-0-R-$ may be observed as an increase in the intensity of a vibration in the region 1150-1060 cm^{-1} (Bellamy, 1976). Given the abundance of ether vibrations, the only way to detect this vibration is by comparison of equivalent blends containing hydroxy and non-hydroxy terminated PES.

The spectra of the blends are shown in figure 3.9 for the neat cured resin, figures 3.10 and 3.11 for the 20I and30I and figures 3.12 and 3.13 for the 20B and 30B blends respectively. The IR spectra of the blends show two absorption peaks characteristic of the PES at 1490 cm^{-1} due to the C=C aromatic stretch and at 870cm^{-1} due to the -CH out of plane aromatic vibration and the appearance of the spectra is identical. Apart from these two additional PES vibrations, the blend spectra are also identical to the neat cured resin.

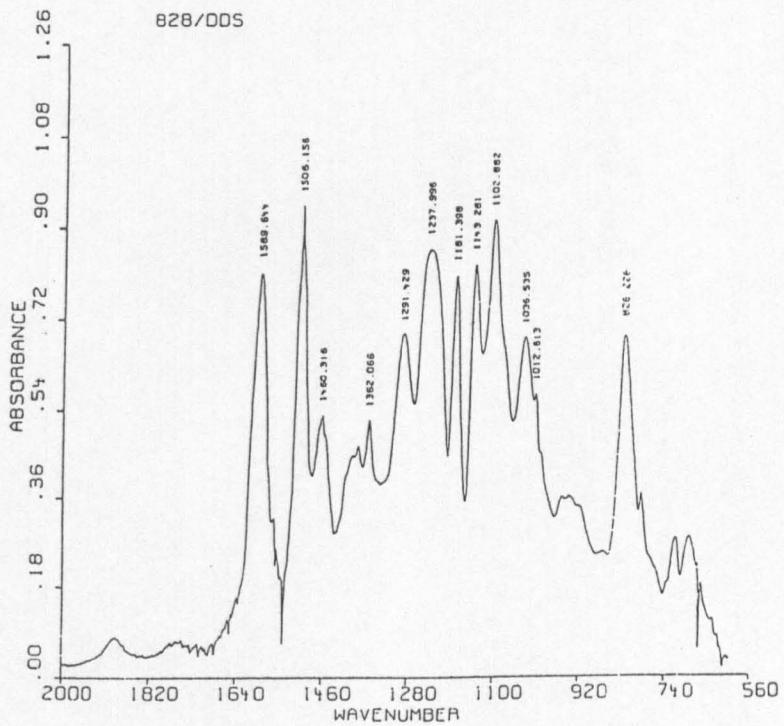

Figure 3.9: FTIR spectrum of neat cured resin

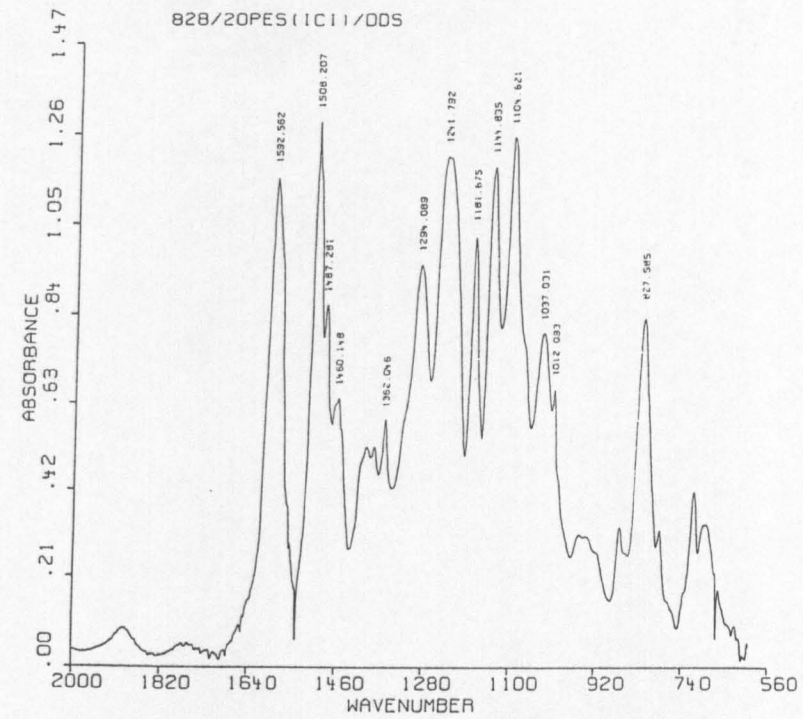

Figure 3.10: FTIR spectrum of 20I blend

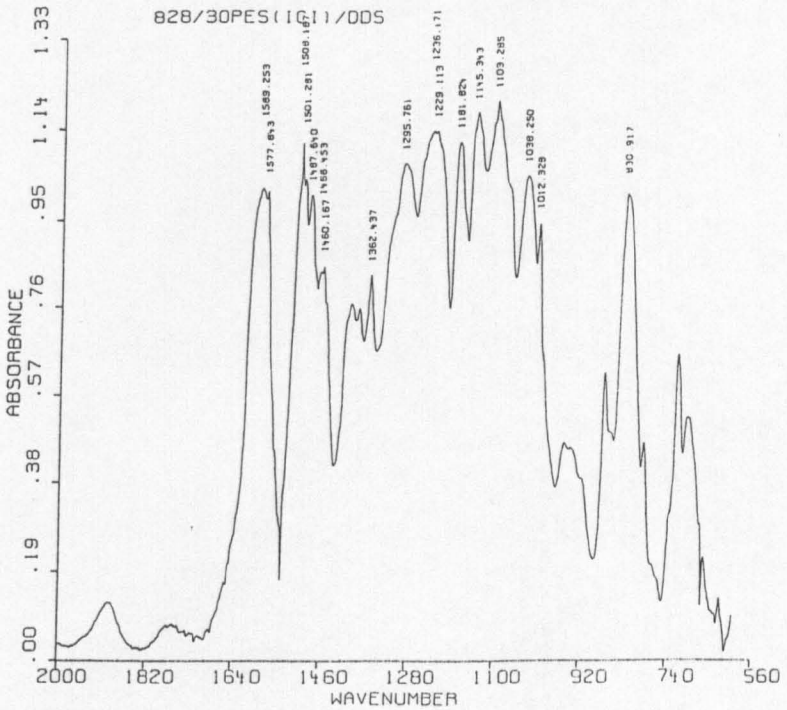

Figure 3.11: FTIR spectrum of 30I blend

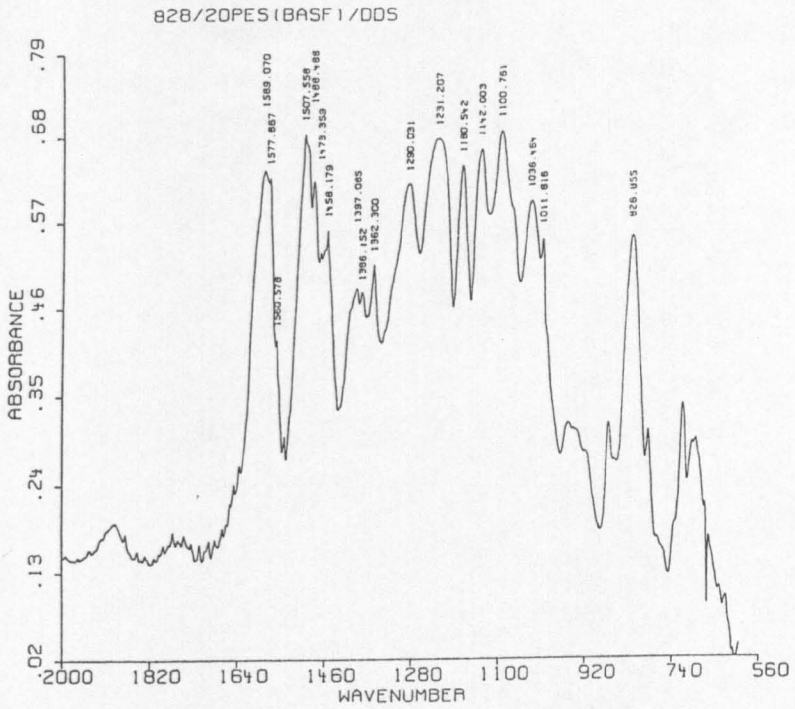

Figure 3.12: FTIR spectrum of 20B blend

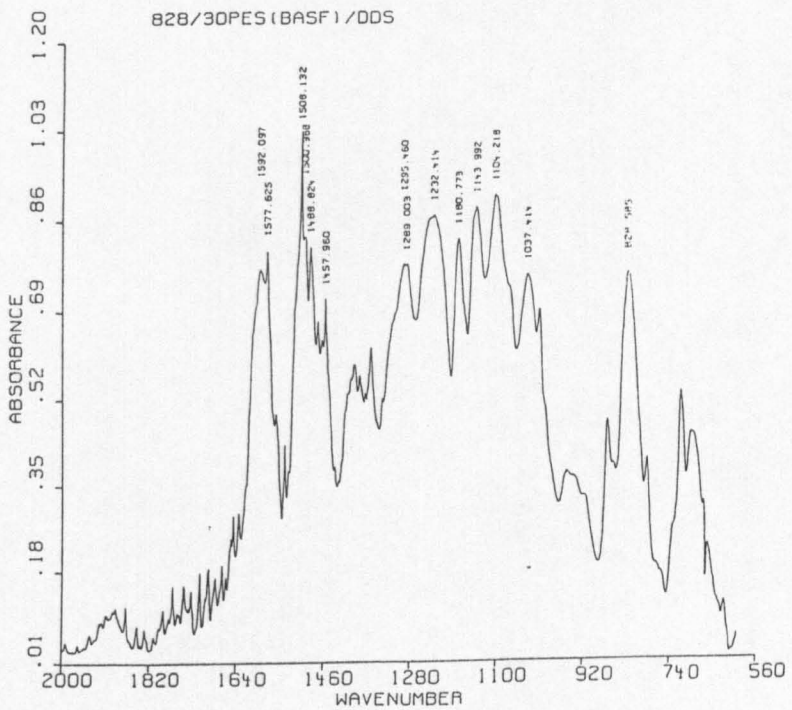

Figure 3.13: FTIR spectrum of 30B blend

Clearly the materials are cured since there is no significant epoxide vibration at 910-915 cm^{-1} .There is no apparent difference between the spectra of the blends in the ether regions and the only possible conclusion is that there is no detectable reaction between the hydroxy terminated ICI PES and the epoxide group.

3.1.4 Mechanical Spectroscopy

3.1.4.1 The Alpha (Glass) Relaxation

The tan δ curves of the blends are shown in figures 3.14 and 3.15 for ICI and BASF blends respectively with the neat resin for comparison.

The peak positions of the ICI blends reduce in temperature with PES and the peak intensity increases but the spectral shape does not change appreciably. In the BASF blends the shift is present only in the 30B blend where the peak broadens and reduces in intensity.

The widths of the E" relaxation at half height are a means of assessing the extent of the crosslinking in the materials, the relaxation transition becoming narrower with increasing molecular freedom or decreased crosslinking, as well as increasing in amplitude (Gerard et al, 1991). The loss moduli characteristics are shown in table 3.5 for a measurement frequency of 1Hz.

Table 3.5: E" Transition Widths and Intensities

Material	ΔW	E''_{max} ($x10^8 N/m^2$)	$T_{(E'')max}$ (°C)	Tan δ_{max}	$T_{\tan \delta\, max}$ (°C)
828/DDS	25.4	2.12	199	0.82	209
20I	21.6	2.3	200	0.81	209
30I	21.3	2.36	200	0.8	206
20B	18.4	2.3	199	0.81	209
30B	18.9	1.8	199	0.75	206

The width ΔW of the E" transition is approximately the same for both ICI materials, as indeed it is in the BASF blends. There is a decrease in ΔW relative to the neat resin which is larger in the BASF blends, suggesting a lower crosslink density compared to the neat resin and ICI materials, in agreement with the calorimetric data. However, despite the possibly reduced crosslink density the E" and tan δ peak temperatures do not vary much between the materials. The intensity of tan δ would normally be

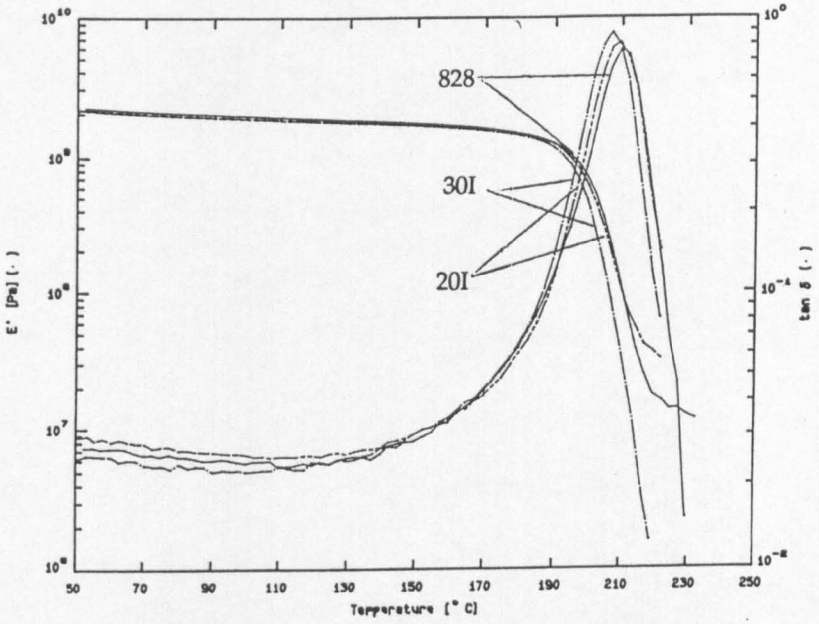

Figure 3.14: Tan δ curves of neat resin and ICI blends

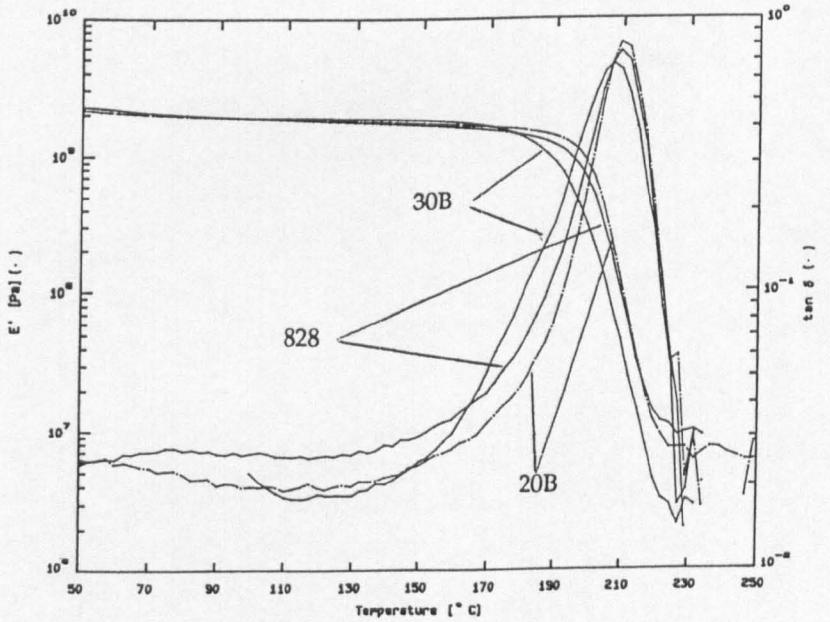

Figure 3.15: Tan δ curves of neat resin and BASF blends

expected to decrease in magnitude if the crosslink density is reduced, which it does in the ICI blends but not in the BASF blends. Mikolajczak et al (1987) reported that in an epoxy mixed with solvent, the strength of the glass transition relaxation decreased due to a small decrease in the number of crosslinks. The decrease in loss modulus maximum in the BASF blends is explained in terms of the fewer number of crosslinks.

Quantitative analysis of the data yields extra information. To characterise the glass transformation relaxations, a conventional Arrhenius analysis (Starkweather, 1981) and a power law analysis (Souletie and Thoulence, 1985) were used . The results of an Arrhenius analysis are shown in table 3.6.

Table 3.6: Arrhenius Activation Energy Data

Material	E_a (kJ/mol)	ΔH (kJ/mol)	ΔS (kJ/K/mol)	τ_o (s)	f_o (Hz)
828/DDS	871	869	3905	1.18 E -95	8.44 E94
20I	703	701	3048	6.28 E -77	1.59 E76
30I	703	701	3098	2.3 E -77	4.34 E76
20B	653	651	2809	2.15 E -77	4.64 E76
30B	677	676	2967	1.4 E -74	7.08 E73

Arrhenius analyses of experimental data pertaining to large scale chain motions are not reliable but are used here to indicate trends. The activation energies and enthalpies of the respective blends are reduced compared to the neat resin implying that perhaps the microscopic structure has greater freedom of movement . The greater reduction in the energy quantities has occurred in the BASF blends which perhaps supports the idea from the calorimetric data and the E' widths that these blends are the least highly crosslinked.

The activation entropy , which is a measure of the degree of cooperativity of a relaxation (Starkweather, 1981, Starkweather and Avakian, 1989) decreases with the amount of PES but by the greatest amount in the BASF blends. The reduction in the cooperativity can be explained in terms of the additional free volume introduced by the PES end groups and the unreacted epoxide end groups. That this ΔS is the smallest in the BASF blends suggests that the largest amount of free volume is introduced into these blends because of the

higher number of chain ends. The inaccuracies of the method are apparent from the high attempt frequencies, the energies of which are greater than the binding energy of a covalent bond but the analysis shows trends which are plausible.

A W-L-F analysis yields the results in table 3.7.

Table 3.7: W-L-F Data for Glass Transition Relaxations

Material	C_1	C_2(°C)	f_o/B	α_f/B	T_o(°C)
828	4.94	30.8	0.088	0.0029	160
20I	5.1	28.5	0.085	0.0029	157
30I	6.19	26.5	0.084	0.0027	158
20B	4.99	29.4	0.087	0.0029	157
30B	5.1	31.9	0.085	0.0027	158

The values of C_1 and C_2 are known to decrease with reductions in crosslink density (Gerard et al, 1991) but the data in table 3.7 imply that crosslink density is approximately the same within experimental error, the free volume as measured by f_o/B, remains constant and the temperature T_o also remains unchanged. These results seem a little unrealistic.

The power law data are contained in table 3.8.

Table 3.8: Power Law Data

Material	T^* (K)/(°C)	$z\upsilon$	τ^* (sX 10^{-7})	f^* (MHz)
828/DDS	475/202	3.26	12.4	0.806
20I	473/200	3.5	6.1	1.64
30I	468/195	4.6	.29	34.96
20B	475/202	3.57	2.85	3.51
30B	466/193	5.3	0.0042	238.66

This method of analysis is based on scaling laws for phase transitions so that the temperature T^* is a zero field phase transition temperature. In terms of polymers it may be thought of as a temperature at which the polymer

undergoes a transition, as in the Gibbs-DiMarzio theory and is perhaps equivalent to a frequency independent glass transition temperature. Alternatively, it can be thought of as analogous to the temperature T_0 of the Cohen and Turnbull theory (1959,1961) at which the viscosity becomes significantly high that large scale motions are hindered. The temperature T^* is seen to decrease by a very slight amount with PES content for both blend systems, the largest reduction occurring in the 30 phr blends. A reduction in T^* suggests that large scale molecular chain motions are able to persist to lower temperature as a result of increased molecular freedom, possibly because of reduced crosslinking and higher free volume. In the 20 phr blends the small reduction in T^* and the small increase in $z\upsilon$ suggest that there is little change in the degrees of freedom compared to the neat resin.

The relaxation time τ^* is longest in the neat resin but decreases with PES, more significantly so in the BASF blends. These results are somewhat in agreement with the calorimetric data, where similar glass transition temperatures for the blends and resin were observed but greater freedom of molecular motion was implied by the reduced enthalpy and entropy at the glass transition. Much the same behaviour is seen for T^* and τ^*, possibly because of the free volume effects of the PES coupled with a reinforcement of the epoxy network. In addition, the attempt frequency f^* increases rather dramatically in the blends, the largest increases occurring in the BASF blends but still remaining physically realistic.

A consistent increase in the scaling factor $z\upsilon$ with PES content is observed, marginally larger increases occurring in the BASF blends. This implies that under a change of applied stress field the relaxation peaks of the blends shift more than those of the neat resin at the same applied field and this obviously implies that the blends have more molecular freedom of motion in the glassy state. The fact that the scaling parameter is greater in the BASF blends in comparison to the equivalent ICI blends therefore suggests that the BASF blends are less highly crosslinked and possess higher molecular mobility.

3.1.4.2 Low Temperature Relaxations: the β Relaxation

The low temperature relaxations of the neat resin, together with the ICI and BASF blend relaxations are reproduced in figures 3.16 and 3.17 respectively.

The β relaxation in the neat resin is very broad and it is known that such broad relaxations in epoxy resins and other polyaromatics, can mask the more than one motion, including perhaps the phenyl rings (Pogany, 1970, Garroway et al, 1982, Dumais et al, 1986) as well as the crankshaft motion of the -CH_2-CH(OH)-O-CH_2- segments of the cured epoxy (Pogany, 1970, Chang et al, 1982b, Ochi et al, 1987).

In the ICI blends of fig 3.16 the addition of PES reduces the intensity of the right hand side of the peak significantly whilst the left hand side becomes a little narrower and reduces only slightly (and possibly negligibly) in intensity. Similar effects are observed for the BASF blends of fig 3.17 but the decreases are not as drastic as for the ICI counterparts. Given that the most severe reduction of intensity occurs in the right hand side of the peak it seems reasonable to associate this with the possible reduction of the number of -CH_2-CH(OH)-O-CH_2- segments with the left hand side associated with phenyl ring motions. Garroway et al (1982) reported a mechanical relaxation at -40°C and 6Hz and activation energy measurements of DMA together with NMR led them to assign this to the motion of phenyl groups.

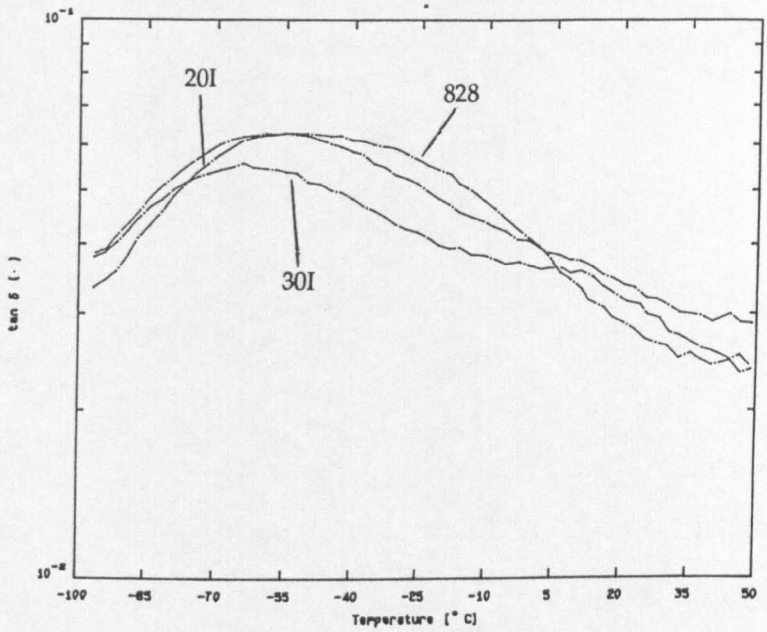

Figure 3.16: Secondary mechanical relaxations of neat resin and ICI blends

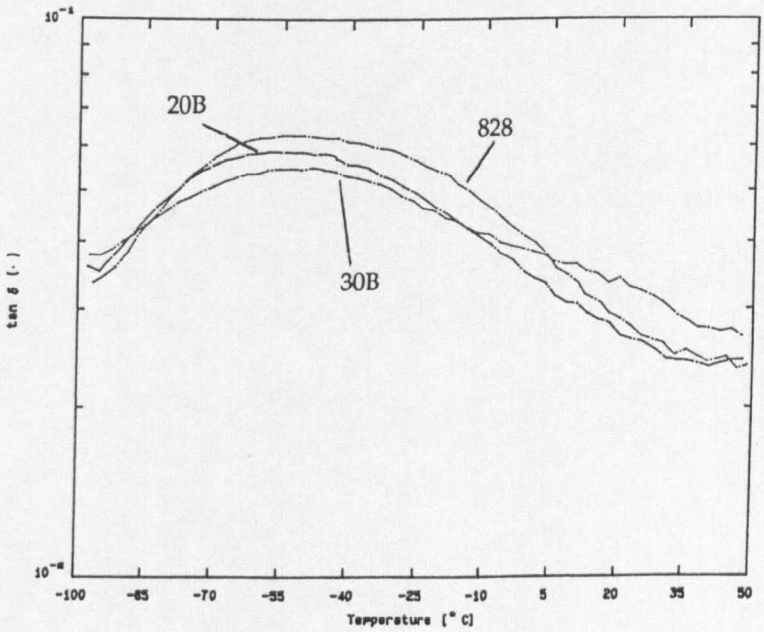

Figure 3.17: Secondary mechanical relaxations of neat resin and BASF blends

These observations are useful but a better feel for the effect of blending on the low temperature relaxations can be gained from a more quantitative analysis. For secondary relaxations activation energies calculated using an Arrhenius approach are appropriate and are shown in table 3.9.

Table 3.9: Arrhenius Data for β Relaxation

Material	E_a (kJ/mol)	ΔH (kJ/mol)	ΔS (J/Kmol)	$\tau_0(sx10^{15})$	f_0 (THz)
828/DDS	57+/-4	54+/-3.8	17.4+/-1.2	9.4	105
20I	56.6+/-4	54.8+/-4	38.3+/2.7	3.9	253
30I	63.3 +/-4.4	61.5+/-4.3	68.8+/5.5	0.03	38900
20B	58.3 +/-4.1	56.7+/-4	23.7+/1.9	4.5	220
30B	56.5 +/- 4	56.7+/-4	13.9+/1.3	1.7	595

The first observation is that the frequencies f_0 are very unrealistic so that the appropriateness is questionable but despite this the trends are important. The activation energies do not vary significantly amongst the materials but there are distinct differences in the activation entropies. The activation entropy for the neat cured resin is very low as is expected in a highly crosslinked structure where the segmental motion associated with this local relaxation is relatively unhindered. The elimination of some of the crosslinks removes some of the constraints on movement as well as introducing PES chains with which the segmental motions of the epoxy must interact. In the ICI blends the increase in activation entropy over that of the neat resin is large but a much reduced effect is seen in the BASF blends which show only small increases. Precisely why this should be is unclear. The relaxation times of equivalent blends are larger in the ICI materials, suggesting that the motions in these blends are faster.

A power law analysis yields the data in table 3.10.

Table 3.10: Power Law Data for the β Relaxation

Material	T^* (K)/(°C)	zυ	τ^* (ms)	f^*
828/DDS	201/-72	1.46	5330	187.6
20I	171/-102	7.6	1.82	54.94E6
30I	139/-134	20.7	0.00027	3700E6
20B	178/-95	4.52	0.011	90.9E6
30B	162/-111	9.7	0.331	3.02E6

The highest characteristic temperature T^* is obtained for the unmodified resin and this decreases with PES, most dramatically in the 30I blend. This is accompanied by increases in zυ which are largest for the ICI blends. The characteristic relaxation time is longest for the neat resin but decreases with PES most significantly in the ICI blends. The increase in zυ appears to be on a parallel with the reductions in τ^* but it appears that the low temperature relaxations of the ICI blends undergo a larger shift with change of frequency than the BASF blends, whereas for the glass transition region the reverse situation was observed. This suggests that the ease of the CH_2-CH(OH)-CH_2-O- rotation is greater in the ICI blends. It was shown by Enns and Gillham (1983) and Gupta and Brahatheeswaran (1991) that the free volume of a highly crosslinked epoxy resin in the glassy state is greater than the same less highly crosslinked resin, perhaps allowing at least the secondary relaxations more space in which to move, thereby allowing the segments on average, to experience less of a retarding potential from neighbouring molecules. The crosslinks do not play such a important role at low temperature where they are not dynamically active but at the glass transition they are able to reduce the shift under applied field resulting in lower scaling factors. The rate of thermal contraction of a highly crosslinked resin below the glass transition range was reported to be less than that for a less highly crosslinked resin (Gupta and Brahatheeswaran, 1991).

3.1.5 Dielectric Spectroscopy

3.1.5.1 Data at 25°C to 50°C

The dielectric spectra of the ICI and BASF blends at 25°C and 50°C are shown in figures 3.18-3.19 and 3.20-3.21 respectively. Table 3.11 shows the peak data obtained for the materials.

Table 3.11: Dielectric Peak Data

Material	f_β 25°C(Hz)	f_γ 25°C(Hz)	f_δ 25°C(Hz)	f_γ 50°C(Hz)	Shift ,ΔF_g (50°) (Hz)
828/DDS	70000	3200	———		———
20I	———	20000	———	33000	13000
30I	———	70000	15000		offscale
20B	———	28000	———	35000	7000
30B	———	100000	———	~130000	>30000

It seems that for the neat resin at 25°C that there are two relaxations or a single broad relaxation. The locations of these are 3200 Hz and 70000 Hz. In the 20I blend a high frequency relaxation is seen at about 20000 Hz and is better defined than in the neat resin and in the 30I blend a relaxation is seen at 70000 Hz. It is possible that the relaxations in the 20I blend at 20000 Hz and in the 30I blend at 70000 Hz may be the same as the 3200 motion in the resin, but shifted up field due to an increase in the molecular mobility (via larger holes) of the system allowing greater molecular freedom. The origin of the relaxation at 3200 lies perhaps in the motion of the -CH_2-CH(OH)-CH_2- O- segments , the freedom of motion of these groups increasing with the reduction in crosslink density. However, there also exists the possibility that the additional peaks observed in the blends are in fact associated with molecular motions of the PES, perhaps the polar sulphone group, hence their absence in the neat resin. Therefore, the peak at 3200 Hz may indeed be due to the CH_2-CH(OH)-CH_2-O- in the resin, but may be diminished in the blends whilst the remaining relaxations are caused by PES.

At 50°C (fig 3.19), the spectra change : the 70000 Hz relaxation of the neat resin appears to have been moved offscale to higher frequency whilst the relaxation at 3200 Hz has apparently shifted to 20000 Hz. In the 20I blend, the 20000 Hz motion has moved to 33000 Hz and in the 30I blend, the 70000 Hz

relaxation appears to have gone offscale and a lower frequency peak can now be observed.

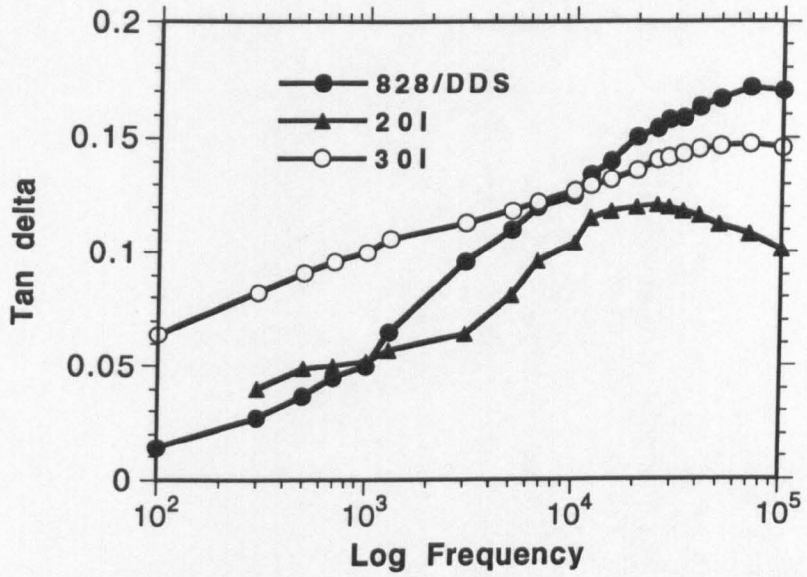

Figure 3.18: Dielectric spectra of unaged neat cured resin and ICI blends recorded at 25°C

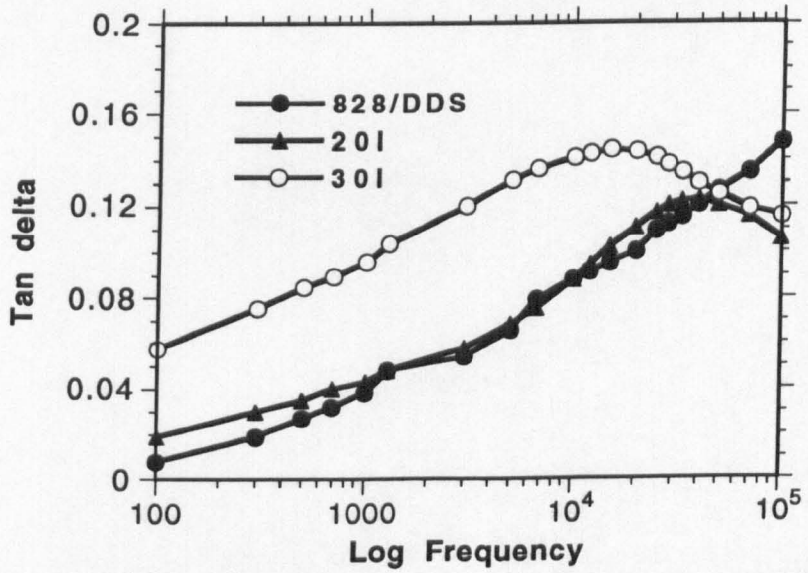

Figure 3.19: Dielectric spectra of unaged neat cured resin and ICI blends recorded at 50°C

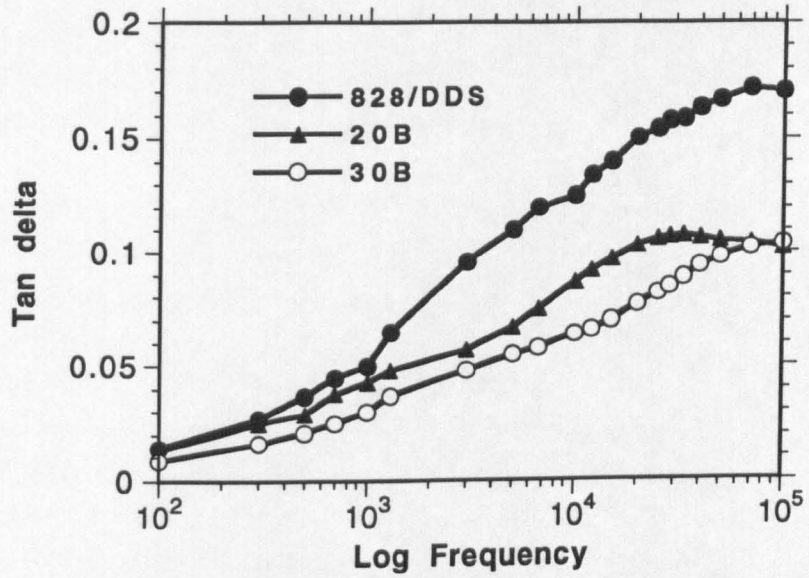

Figure 3.20: Dielectric spectra of unaged neat cured resin and BASF blends recorded at 25°C

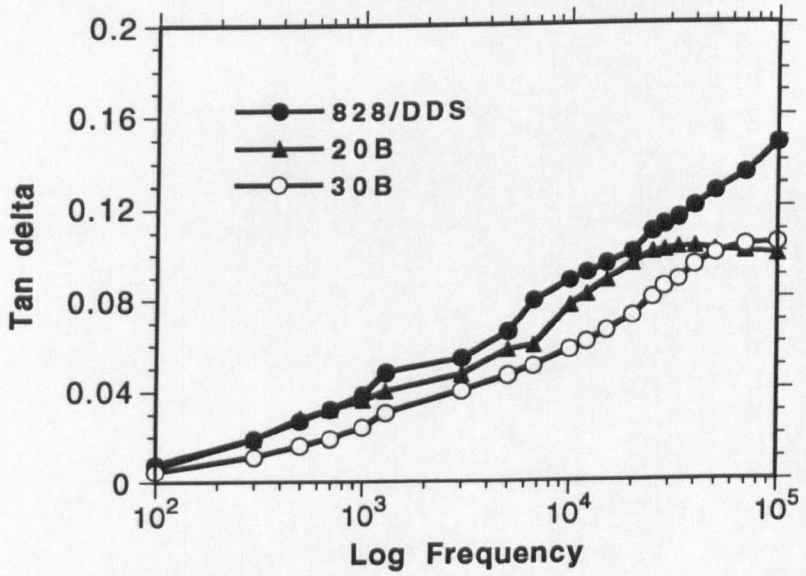

Figure 3.21: Dielectric spectra of unaged neat cured resin and BASF blends recorded at 50°C

Consider the spectra for the BASF materials. At 25°C effects similar to those of the ICI blends occur. The 20B blend has a relaxation at about 28000 Hz

which as in the case of the 20I blend appears to be derived from the neat resin. The 30B blend exhibits a similar relaxation but at 100000 Hz. Assuming these relaxations to be equivalent to those in the ICI materials, they are also shifted relative to the neat resin and the ICI counterpart blends. At 50°C the peaks in the 20B and 30B blends have shifted to higher frequency but in the 30B blend the shift is not as great as in the 30I blend.

Evidently, the molecular group or segment responsible for the peaks is polar but it is unusual to observe broadness in dielectric relaxations because they tend to be less co-operative than mechanical relaxations (Starkweather, 1981). The fact that the same or similar peaks appear in the ICI and BASF blends might be taken to indicate that these are caused by the same/similar molecular moieties although this is by no means certain. However , the relaxations in the BASF blends occur at slightly higher frequencies indicating that perhaps the microscopic structure offers more freedom of movement. It is tempting to try to correlate the peaks observed in the neat resin at 3200 Hz and the blends and to associate them with motion of the CH_2-CH(OH)-CH_2-O- segment but this leaves the higher frequency peaks unexplained. All the dielectric data appears to show in this case is that there is a definite increase in molecular mobility with PES presumably associated with an increase in total free volume or if the total free volume is nearly the same, a change in its distribution.

3.1.5.2 Dielectric Data at 200°C and above

The spectra obtained at 220°C for the ICI blends and the BASF blends are shown in figures 3.22 and 3.23 respectively. Several temperatures were used in order to shift the position of the spectra and enable analysis of the shifts to be carried out. Since these peaks occur at high temperature it is reasonable to conclude that they are connected with the glass transformation and large scale molecular motion.

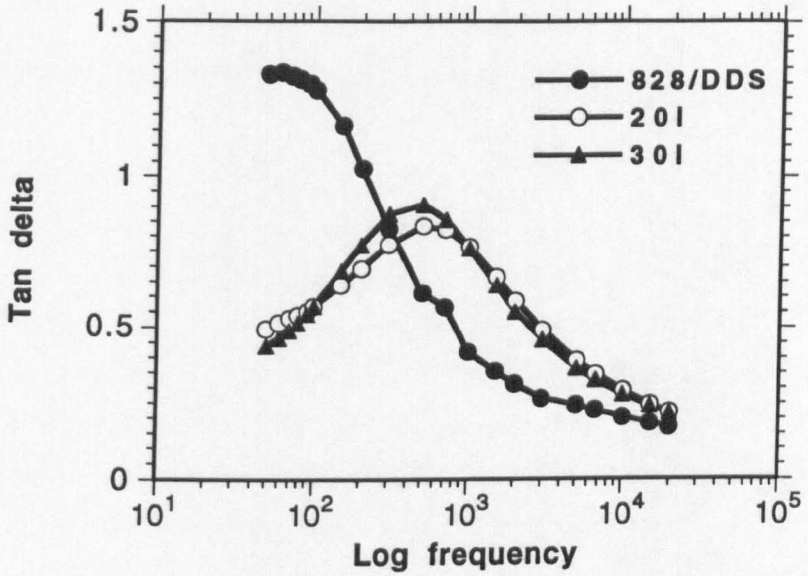

Figure 3.22: Dielectric spectra of unaged neat cured resin and ICI blends recorded at 230°C

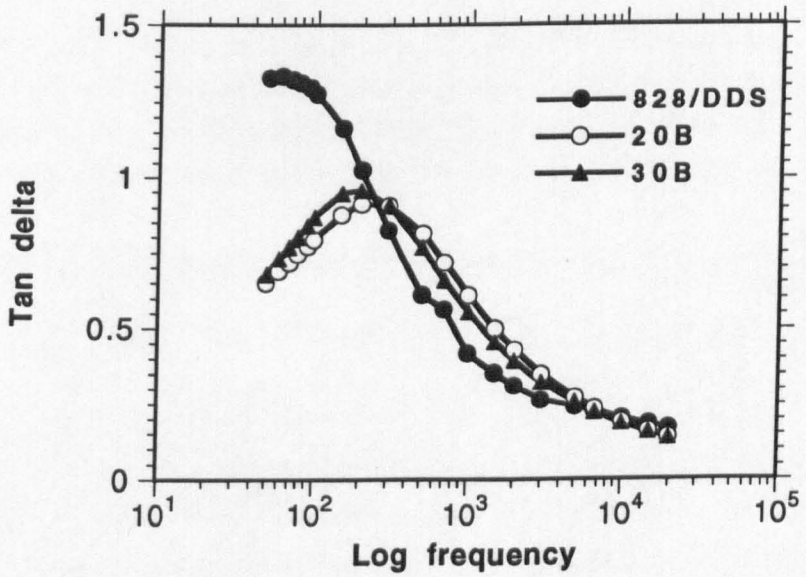

Figure 3.23: Dielectric spectra of unaged neat cured resin and BASF blends recorded at 230°C

The intensity of the relaxation of the resin is much larger for any of the blends and occurs at lower frequency, perhaps because of a more co-operative nature and smaller local free volume.

The peak positions of the materials at 230°C are shown in table 3.12.

Table 3.12: Dielectric Peak Frequencies at 230°C

Material	Peak Frequency (Hz)
828/DDS	60
20I	500
30I	500
20B	300
30B	400

The peak positions of the BASF blends are at a slightly lower frequency although the difference is not great and the data indicate little difference between the materials in terms of polar relaxations over the glass transformation.

3.1.5.3 Calculations Based on High Temperature Dielectric Data

It was only possible to utilise the peak shifts of the ICI blends in performing calculations with the dielectric data because insufficient data points were available for the BASF systems over the experimentally accessible frequency range. Table 3.13 shows the results for a power law analysis of the data.

Table 3.13: Power law Analysis of High Temperature Dielectric Data

Material	T^* (K)/(°C)	zυ	f^*	τ^* (ms)
828/DDS	479/206	1.03	4347.8	230
20I	462/189	1.6	26246.72	38.1
30I	454/181	2.2	73529.4	13.6

The temperature T^* decreases as expected with PES content but the increase in zυ is weak. The characteristic relaxation time also decreases with PES

content although the magnitude of the change is not as great as observed for the low temperature mechanical relaxations. If the temperature T^* corresponds to a temperature at which free motion of the molecular moiety ceases, then it appears to be rather high in the neat resin, at a temperature similar to the calorimetric glass transition or the peak temperature of the mechanical glass relaxation peak. However, the results suggest that a more mobile molecular structure is present in the blends, T^* decreasing quite significantly with PES. It is unfortunate and mysterious that similar data could not be obtained for the BASF blends. The lack of a shift in the peaks with temperature could be taken as an indication that the BASF blends are more highly crosslinked, but in the light of the data already presented this seems to be highly unlikely.

Rather tentatively, results of a W-L-F analysis of the data are included in table 3.14

Table 3.14: W-L-F Data for High Temperature Dielectric Relaxations

Material	C_1	C_2(°C)	T_o(°C)	T_r(°C)	C_1^r	C_2^r (°C)	f_r/B
828	0.534	47.75	192	215	1.121	22.75	0.38
20I	1.064	81.18	158	192	2.387	36.18	0.18
30I	2.546	81.97	158	184	7.204	28.97	0.06

The subscript 'r' refers to the calculated value of a quantity at a frequency of 69Hz, chosen for convenience. The trend is for c_1^o ,c_1^r , c_2^o and c_2^r to increase with the amount of PES and T_o is observed to decrease with the amount of PES, suggestive, as in the power law analysis, of a more mobile molecular structure. This simply confirms for the ICI blends that there is a common trend among the analyses even if some of the quantities calculated are not always feasible. However, f_r/B, which is a measure of the amount of free volume at temperature T_r, appears excessive in the neat resin but too small in the 30I blend.

3.1.5.4 Impact Data

It is interesting to examine the impact strengths of the materials in terms of the G_{IC}. Figure 3.24 shows some of the impact energy-BDZ plots typical of these systems and table 3.15 shows the complete set of data for all of the as cured materials.

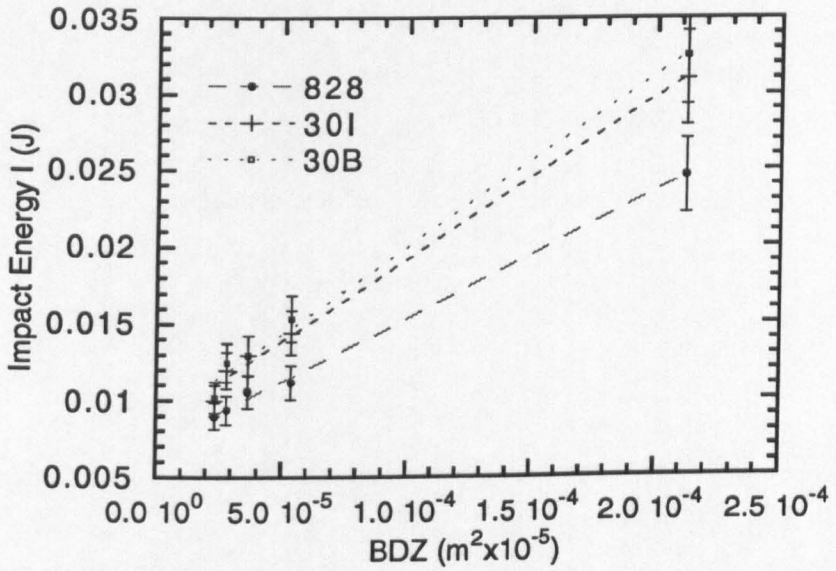

Figure 3.24: Impact energy plotted against BDZ for a selection of as cured materials

Table 3.15: Impact Energy of Resin and Resin Blends

Material	G_{IC} (J/m^2)
828/DDS	82
20I	90
30I	105
20B	98
30B	112

From figure 3.24, at large notch depths (small BDZ), the errors associated with the energy are such that there is litle difference between the blends 30I and 30B, but a significant although not much greater energy is absorbed by the blends relative to the unmodified resin. The relative closeness of the energy

values of the blends is maintained up to smaller notch depths (larger BDZ) but increases significantly in comparison to the unmodified resin. .This was also true of the 20I and 20B systems.

There is a slight increase in the toughness of the blends with PES content, apparently more so with the BASF material but within experimental errors shown in figure 3.24. It might be argued that the increases in G_{IC} are still significant and could result from the BASF blends containing more free volume and/or a different free volume distribution. In this thesis it is inferred that changes in free volume and free volume distribution are due to a reduction in crosslink density and in rubber toughened systems Yee and Pearson (1989) attributed the toughening effect as partly due to reduced crosslinking in the epoxy phase.

3.1.6 Discussion

Phase separation is not visible by means of SEM and the question arises why haven't the blends visibly phase separated? During the course of the work binary mixtures of epoxy and PES were observed to phase separate under a hot stage microscope when heated at various rates but since there was no way to record these events they have not been included in the results. Phase separation was observed at about 140°C when heated at 1°C/min, a manifestation of what is called Lower Critical Solution Temperature (LCST) behaviour. However, the same system containing DDS and heated at the same rate did not phase separate. Instead the DDS simply dissolved in the mixture at 130°C and on further heating even slowly, the blend simply cured.

Now it is a well documented fact that in initially miscible polymer blends there is a tendency for components to phase separate as the difference between their molecular weights increases and this fact has been exploited in the rubber toughened epoxy systems. In the Flory theory the combinatorial entropy term in the free energy of mixing equation

$$\Delta G_m = \Delta H_m - T(\Delta S_m^c + \Delta S_m^e)$$

and the free volume decrease monotonically as the difference in molecular weight increases (Olabisi et al, 1979). In this case since $\Delta S_m{}^e$ (the excess entropy of mixing) is believed to be generally small and $\Delta S_m{}^c$ will be small due to the increasing difficulty of maximising the conformations of the macromolecules, unless strong interactions exist to make ΔH_m negative the materials will become incompatible and phase separate.

The fact that they do not raises the possibility of strong interactions between the constituents. Strong interactions such as hydrogen bonding can be important in making blends mutually soluble and in the epoxy resin, DDS and PES there is an abundance of proton donors and acceptors for this to happen. At low temperatures in the mixture of only PES and epoxy monomer, both being polyethers containing similar molecular constituents are compatible and it is probably the molecular weight difference that comes into play at high temperature. The presence of the DDS however may change this situation. The only difference between a long macromolecule made up of DDS and epoxy monomer (assuming for a moment no branching) and the PES macromolecule at say a similar molecular weight is the presence of N

from the DDS and CH_3 from the epoxy monomer. The DDS contains a sulphone-aromatic combination similar to that of the PES and there is no reason why they should not be compatible at similar molecular weights. Added to this is the fact that even in the non-hydroxy terminated PES there is still ample opportunity for interactions via hydrogen bonding but not at the easiest sites, namely the chain ends. Since the crosslinking process is heterogeneous and the PES chains well dispersed in the mixture it can be envisaged that compatibility is maintained up to the point where the epoxy gels thereby entwining the PES in the network. Perhaps the molecular weight differences are somewhat offset by an attractive effect. The values of T_g calculated from the Flory-Fox rule for miscible blends (table 3.2) seem to provide a little support for the blends being miscible and single phase. However, it is clearly possible for the second phase to be of such a size that it is not detectable and unfortunately no clear evidence is available to clarify this situation.

3.1.6.1 A Qualitative Picture of the Structure of Epoxies

It is desirable to build up a picture of the microscopic physical structure of the blends based on the literature and the experimental results in this thesis. A starting point for such a picture must be the unmodified epoxy structure, which is known to be heterogeneous. It has been suggested by Oleinik (1982) that the structure of an epoxy consists of two kinds of holes, static holes which cannot be eliminated and are present because of molecular architecture in the crosslinked epoxy, and kinetic holes which are capable of dynamic motion and redistribution in the sense of the free volume theory of Cohen and Turnbull (1959). At any temperature below the glass transition the static holes will have a minimum size but one can envisage that they can be swollen to greater than this volume by kinetic holes . This is simply the idea of Cohen and Turnbull (1959) and Turnbull and Cohen (1961). However, the size of a static hole depends upon the local molecular architecture (fixed by chemical reaction) and the equilibrium size of the static hole can be achieved under some optimum condition dependent upon the conformation of the molecular chains in that region. Different static hole sizes will exist in different regions of the heterogeneous network and will be made up partly of kinetic holes, the amount depending upon the cooling rate. Therefore the distribution of hole sizes might be expected to depend upon the cooling rate and temperature and would also be expected to approach the equilibrium distribution at infinitely slow cooling rates.

The size and distribution of static holes must also depend upon the extent of chemical reaction and therefore the degree of crosslinking and the size of the moving segment at T_g, which decreases with crosslinking. It has also been suggested that the free volume in highly crosslinked samples is made up of a large number of small holes whilst in a less highly crosslinked sample there are a smaller number of larger holes (Oleinik, 1982, Gupta and Brahatheeswaran, 1991): i.e., the distribution of free volume changes. Oleinik (1982) also considered that the surface energy of the free volume of a highly crosslinked sample would therefore be greater because of the greater surface area. In this case there would be a larger driving force for elimination of this energy compared to a less highly crosslinked sample. Two samples of differing crosslink density but the same total free volume would therefore also have different driving forces for elimination of free volume. However despite the higher driving force in the more highly crosslinked sample the crosslinks slow down the conformational rearrangement and diffusion of the free volume and the number of static holes would also be greater than for a less crosslinked epoxy. These ideas have important consequences for the interpretation of the results for the blends, as discussed in the next section.

3.1.6.2 A Discussion of the General Effects of PES on Structure and its Potential Effects on Physical Ageing Behaviour

The heats of reaction shown in the results section show clearly that the PES reduces the extent of chemical reaction. This is related to the presence of the PES in the unreacted mixture, the effect of which is to increase the specific volume and free volume relative to the mixture of only epoxy and hardener (c.f. figure 3.25)

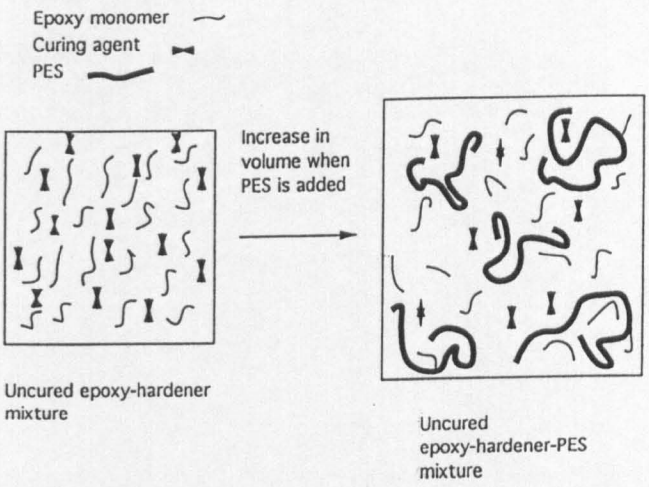

Figure 3.25: Schematic illustration of the effect of introducing PES into an uncured mixture of epoxy and hardener

It will be assumed that the PES chains exist as random coils in the mixture and that these are evenly distributed. Clearly the effect of the coils would be to introduce an excluded volume, the origin of the aforementioned effect on specific volume. At the curing temperature, it is possible that the PES chains form small domains too small to detect as phase separated regions, but irrespective of this, the presence of the PES will cause the hardener and epoxy to react around the PES coils giving rise to less crosslinking (c.f. figure 3.26). It seems clear that the PES retards the primary chemical reactions, which results in fewer CH_2-CH(OH)-CH_2-O- segments that form the crosslinks between the hardener and the epoxide molecule (Chang et al, 1982a).

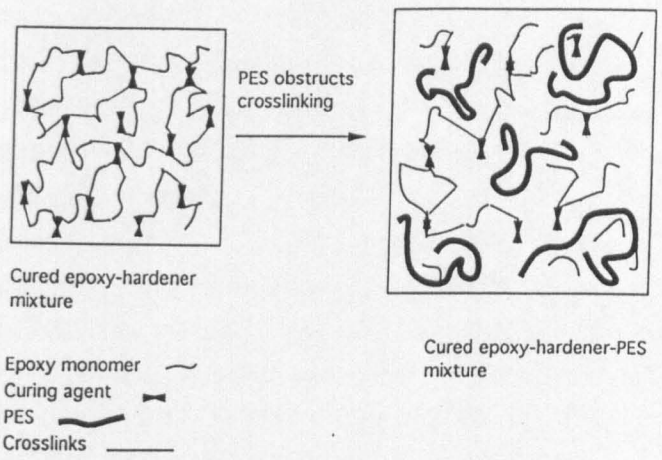

Figure 3.26: Schematic illustration of the effect of crosslinking an epoxy-PES blend in comparison to the unblended epoxy-hardener mixture

Irrespective of the type of end group, the PES chain ends must also affect the crosslinking reactions because they create extra free volume (Matsuoka 1992). The viscosity of the unreacted blends is much higher than the unreacted epoxy so that the speed with which the reactants diffuse is must be greatly reduced. The free volume per unit volume of material in the unreacted blends would then be greater than in the unreacted resin because of the PES. The PES appears to plasticise the epoxy, thereby reducing the heat of reaction and the crosslink density is expected to decrease in much the same way as in solvent-epoxy blends (Mikolajczak, 1987). A reduction in crosslink density with reduced extent of cure is a well known fact (Gerard et al, 1991, Gupta and Brahatheeswaran, 1991) and the unreacted epoxy chain ends and hardener will help create an overall higher level of free volume together with the PES chains and chain ends. Fewer crosslinks in the blends will have consequences for the contraction of the materials during cooling through the glass transition, a subject discussed both by Enns and Gillham (1983) and Gupta and Brahatheeswaran (1991).

The effects of less crosslinking in the blends are apparent from the heat capacity curves. As the amount of PES increases, so the heat capacity decreases and this is correlated with the reduction in crosslink density and thus with the reduced formation of the CH_2-CH(OH)-CH_2-O- segment, which is also responsible for the mechanical beta relaxation in many diepoxides

(Charlesworth, 1979, Ochi et al, 1982, 1986,1987). This is also the segment which is formed by the primary epoxide-hardener reaction . The work of Simha et al (1972), Goldstein (1976,1977), Johari (1980) and Bicerano (1991a,b) has shown that secondary relaxations contribute significantly to the number of degrees of freedom of a system because the unfreezing of these molecular motions demands energy. Reducing their number, whether by retarding chemical reactions or simply by physically 'pinning' the groups so they cannot move, removes an energy absorbing mechanism thereby requiring less heat to increase the temperature. A reduction in the peak magnitude of the low temperature mechanical relaxations with PES content confirms this idea and further support comes from the shift of the dielectric relaxations to higher frequencies (figures 3.18-3.21). This is confirmed also by reduced E''' widths (table 3.5) and from the Arrhenius and power law data (tables 3.6 and 3.8 respectively).

The slight increase in toughness of blends may also be associated with the reduction in crosslink density as suggested for rubber toughened systems by Yee and Smith (1989) but despite the crosslink density decrease, the T_g of the materials is similar. Looking at figure 3.25, one can imagine that perhaps the crosslink density effect is offset by some kind of reinforcement of the epoxy network by the PES domains.

It has been established that the crosslinking is reduced but what of its potential effects on physical ageing ? More crosslinking in an unmodified epoxy means a larger number of smaller holes than in less crosslinked structures (Gupta and Brahatheeswaran, 1991). This also means that the size of the moving segment at T_g decreases and that the network structure becomes stiffer. On the basis of Gupta and Brahatheeswaran (1991) it can be assumed that on cooling through the glass transition the blends will contract faster than the neat resin at temperatures below T_g. At such temperatures it might be expected that blends will have less free volume of larger average size with a more flexible epoxy network containing PES molecules dispersed throughout as random coils. The neat epoxy would contain a larger free volume of smaller average size (and according to Oleinik, 1982, a larger hole surface energy) and with a much stiffer network. On this basis the unfilled epoxy is expected to have a larger excess enthalpy, which combined with the larger excess free volume would lead to a greater thermodynamic driving force for physical ageing. However, it would be expected that physical

ageing in an unblended epoxy would be slowed down by the lower mobility of the molecules (caused by the crosslinks). During ageing one would expect also that cooperative movement between the molecules of an unblended epoxy would occur sooner because of the smaller average hole size. In summary, one expects the blends to reach equilibrium during physical ageing sooner than the unmodified epoxy.

3.1.6.3 Specific Effects of PES on Crosslink Density

The different ways in which the BASF E2010 and ICI 100P materials affect the blend structure will now be considered. Evidently the PES chains are capable of disrupting the normal crosslinking processes, which Raghava also suggested (1987) and the molecular weight of the PES plays an important part: the larger the mean molecular weight, the fewer the chain ends introduced but the larger the excluded volume. It can be assumed that the end groups of a molecular chain have a higher energy level and free volume than the same group at the interior of a chain so that end group effects might be expected to be more important (Matsuoka, 1992). In this case the BASF PES might be expected to cause the greatest reduction in crosslinking reactions, reducing the number of secondary relaxations and therefore the heat capacity. The nature of the end groups is also important and for the cure schedule studied there was no reaction between the hydroxyl end groups of the ICI PES and the epoxy but these end groups are capable of interaction with the epoxy by means of hydrogen bonding. This may provide another restraint on molecular freedom of the ICI blends in addition to the possibility that the higher molecular weight chains at the concentrations studied do not disrupt chemistry as much as smaller average molecular weight BASF PES chains. A reduction in crosslink density with reduced extent of cure is a well known fact (Gerard et al, 1991, Gupta and Brahatheeswaran, 1991) and the unreacted epoxy chain ends and hardener will help create an overall higher level of free volume together with the PES chains and chain ends. Fewer crosslinks in the blends will have consequences for the contraction of the materials during cooling through the glass transition (Enns and Gillham 1983, Gupta and Brahatheeswaran 1991.

It has been suggested that the ICI blends are more highly crosslinked than the BASF blends and below the glass transition more highly crosslinked epoxy resins are claimed to have a larger number of smaller holes than lesser crosslinked epoxies (Gupta and Brahatheeswaran, 1991). It is conceivable that

the ICI blends have a larger number of smaller holes (essentially a different distribution of free volume) than the BASF blends because of the higher degree of crosslinking. The evidence for this is the reduced heats of reaction and the lower β relaxation activity established from the heat capacity and mechanical spectroscopy. For the Arrhenius analysis of the mechanical spectra, the neat resin is the least co-operative in its molecular motions at T_g and has the shortest segment moving at this temperature. As the ICI PES is added the cooperativity increases but the activation energy remains the same. In the BASF blends the cooperativity remains at a similar to the neat resin. This can be explained in terms of the larger amount of free volume introduced by the BASF chains which are shorter on average than the ICI as well as extra free volume introduced by unreacted epoxy/hardener in these systems. There is also the possibility of greater interaction of the ICI PES with the epoxy network via hydrogen bonding, although this has not been substantiated by this investigation. The creation of substantially greater free volume in the BASF blends accounts for the lower cooperativity since there is more free space for molecular motion. The creation of this free volume also explains the power law data, the greater zv of the BASF blends being due to the extra free volume thermal expansion at the peak relaxation temperature.

The β relaxation is concerned with local motions and the larger activation entropy of the ICI blends is a reflection of the greater degree of packing due the PES. In the power law analysis however, zv is larger for the ICI blends and an explanation is not immediately obvious save that at the local level the precise details of the free volume and interactions are unknown. The low temperature dielectric data support the idea that for the local relaxations there is marginally greater freedom in the BASF blend. The high temperature data and the power law analysis also agree with intuition but unfortunately the W-L-F analysis is of little use.

In terms of physical ageing one clearly expects to see the neat epoxy relax more slowly, followed by the ICI blends and then the BASF blends. In the next section of this chapter this hypothesis will be tested.

3.2 Physically Aged 828-DDS Systems: Results

3.2.1 Calorimetric Data and Modelling

The heat capacity curves typically obtained for the neat resin are shown in figure 3.27 and curves of this type, identical except for the magnitude of the endotherm at different times, were obtained for the ICI and BASF blends.

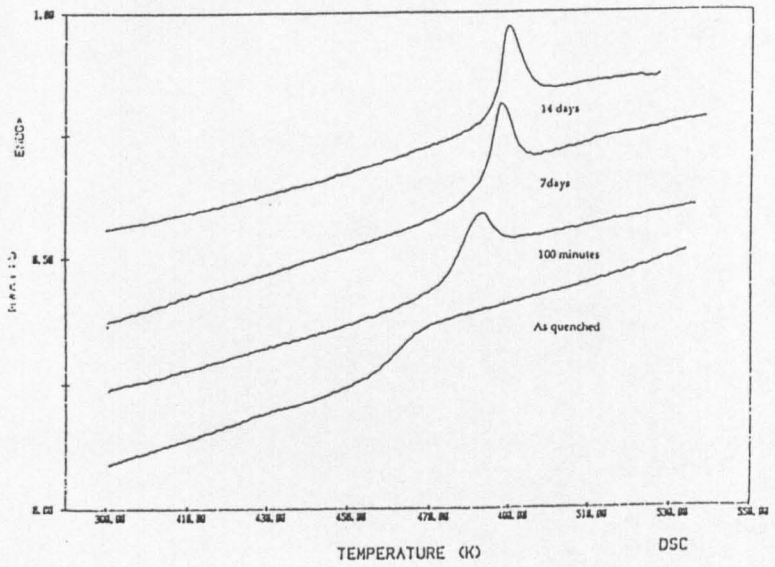

Figure 3.27: Heat capacity curves of neat resin annealed at 180°C

The characteristic feature of enthalpy relaxation, namely the development of an endothermic peak with time (Petrie, 1972, Struik, 1978, Ellis and Karasz, 1986, Lin et al, 1986, Plazek and Frund, 1990) is clearly visible in figure 3.27. Plotting the enthalpy relaxation against time yields the curves in fig 3.28 for ICI blends and fig 3.29 for BASF blends, both figures including the neat resin data for comparison.

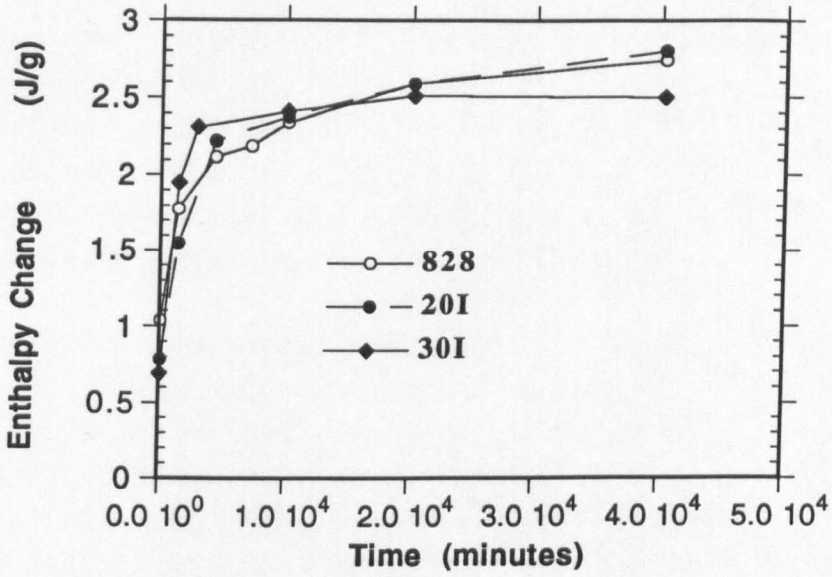

Figure 3.28: Enthalpy change of neat cured resin and ICI blends with annealing time at 180°C

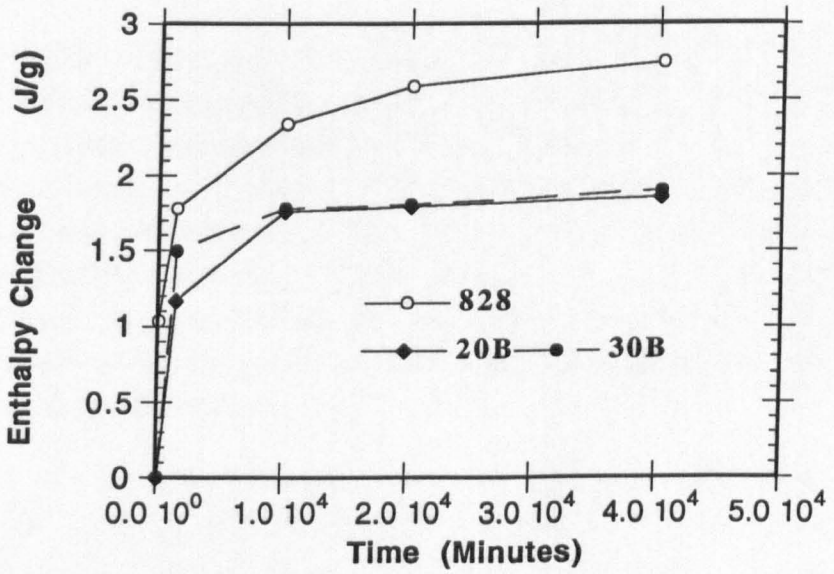

Figure 3.29: Enthalpy change of neat cured resin and BASF blends with annealing time at 180°C

In the ICI blends the early stages of the enthalpy relaxation (t<2000 minutes) appear similar in trajectory to the neat resin but as the amount of PES is increased , faster relaxation towards an equilibrium state appears to occur . At the longest ageing time the 30I resin appears to have relaxed into a near equilibrium state, the curve approaching a plateau with the loss of less excess enthalpy than the 20I blend. The 20I blend appears to relax faster than the 828 resin, also tending towards a plateau but with apparently more enthalpy to lose than the neat resin. The trajectory of the neat resin curve at the 40000 minute mark suggests that there is a lot more enthalpy to be lost.

The BASF blends in figure 3.29 clearly reach an equilibrium condition very rapidly in comparison to the neat resin, and do so on a similar time scale to the ICI blends but with the loss of a smaller amount of enthalpy . It is clear that both blend systems are able to relax much faster than the neat resin. The curves seem to suggest that the microscopic physical structure of the BASF blends is much more mobile than the ICI blends due to less crosslinking, a larger degree of free volume and/or different free volume distribution. It seems likely that conformational relaxation and the elimination of free volume are faster in the blends because of the reduction in crosslink density but that the BASF material, with a broader molecular weight distribution, a greater fraction of lower molecular weight material, lower M_n and therefore more chain ends, promotes faster physical ageing.

It is possible to put figures to the amount of enthalpy that must be lost in order to reach the equilibrium condition by curve fitting, although naturally such approaches make assumptions and are not always physically realistic models (Lindsey and Patterson, 1980). In this respect however two methods of simple data analysis were used, a single relaxation time curve fit to the data which is known to be physically unrealistic, and a curve fit using the Kohlrausch function which can be derived from a distribution of relaxation times approach (Lindsey and Patterson, 1980). The results of the Kohlrausch analysis are shown in table 3.16.

Table 3.16: Data Extracted from Curve Fitting to a Kohlrausch Form

Material	ΔH_e (J/g)	β	τ (minutes)
828/DDS	3.35	0.26	4699
20I	3.13	0.36	3269
30I	2.52	0.52	760
20I	1.93	0.41	1914
30I	2.26	0.15	913

The data obtained with the Kohlrausch fit for the neat resin and ICI blends shows that the amount of excess enthalpy ΔH_e, decreases as more PES is added, as does the characteristic relaxation time τ. The constant β, is small for the neat resin but as PES is added, β increases, signifying a change towards more linear behaviour. The changes in these constants support the idea that the degree of crosslinking in the ICI blends is reduced as the amount of PES increases and makes the physical structure more mobile, thereby allowing faster relaxation during annealing. The decrease in ΔH_e with PES content is presumably due to a more flexible structure which is able to eliminate more excess enthalpy during cooling. The values of theses constants and the way in which they change with ICI PES content make physical sense.

In the BASF blends ΔH_e decreases with PES as expected but although τ is less than in the neat resin and in the 20B blend is less than in the 20I blend, it is larger in the 30B blend than the 30I material. This is an unexpected result but β also changes in an unexpected manner, and is less in the BASF blends than in equivalent ICI blends. This suggests that the enthalpy relaxation in the BASF blends is more non-linear than in the ICI and for the 30B blend , the implication is that it is more non-linear than the neat resin. This does not make physical sense and does not agree with the results in the first section of this chapter.

A plot of log (ln $-\psi(t)$), where $\psi(t)$ is the relaxation function, against log t, where t is the ageing time, can be used to test the quality of the fitting, and should yield a straight line of slope β. This is shown in figure 3.30 where the agreement is very good in all cases. This however, is not a rigorous test since log-log plots invariably yield good straight line fits

A comparison of the experimental and fitted curves for the enthalpy relaxation of the resin is shown in figure 3.31. The data corresponding to the ICI blends are shown in figure 3.32 and those of the BASF blends in figure 3.33. Again agreement is very close.

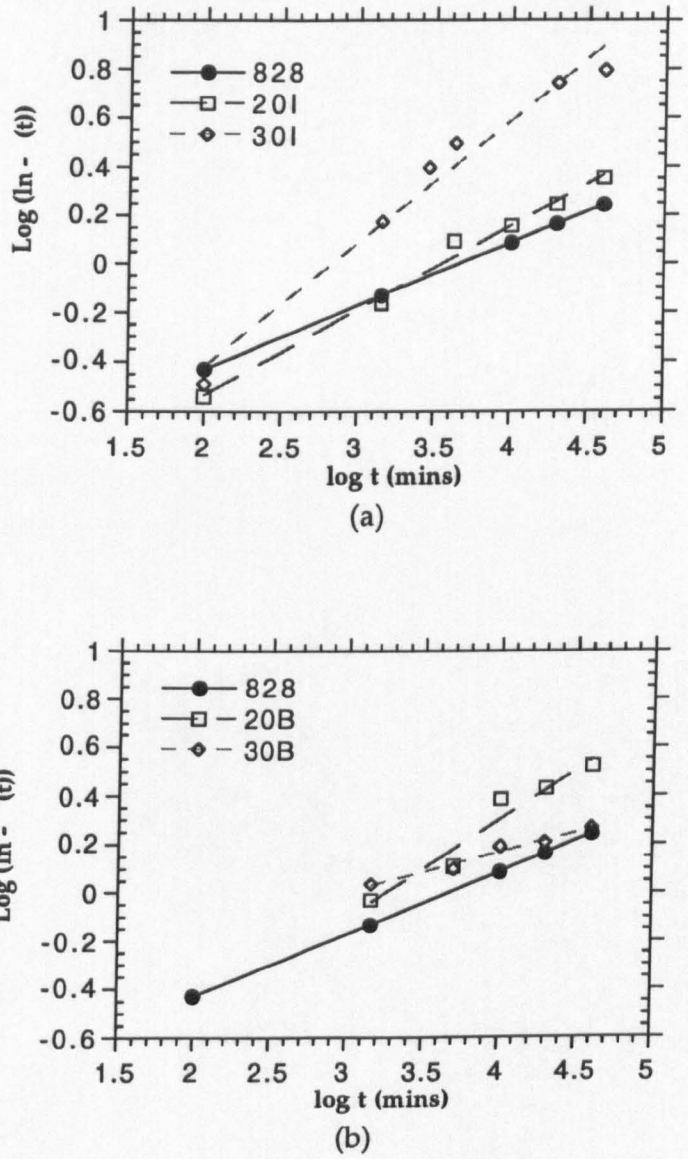

Figure 3.30: Plots of log (ln -ψ(t)) against log t for (a) neat resin and ICI blends (b) neat resin and BASF blends. Lines are results of linear curve fit and correspond to correlation of r=0.99,0.98,0.98 for neat resin , 20I and 30I blends respectively and r=0.98,0.97 for 20B and 30B blends respectively.

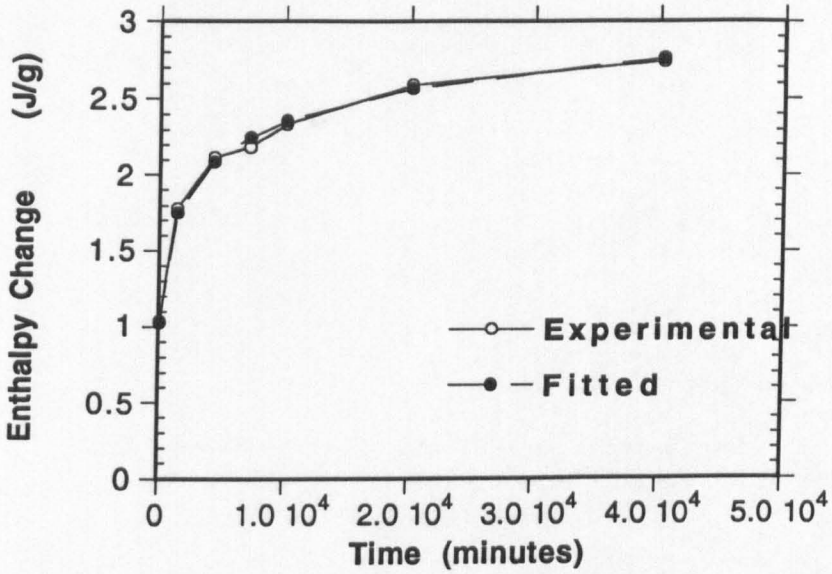

Figure 3.31: Comparison of experimental enthalpy data with Kohlrausch curve fitted enthalpy data for neat resin annealed at 180°C

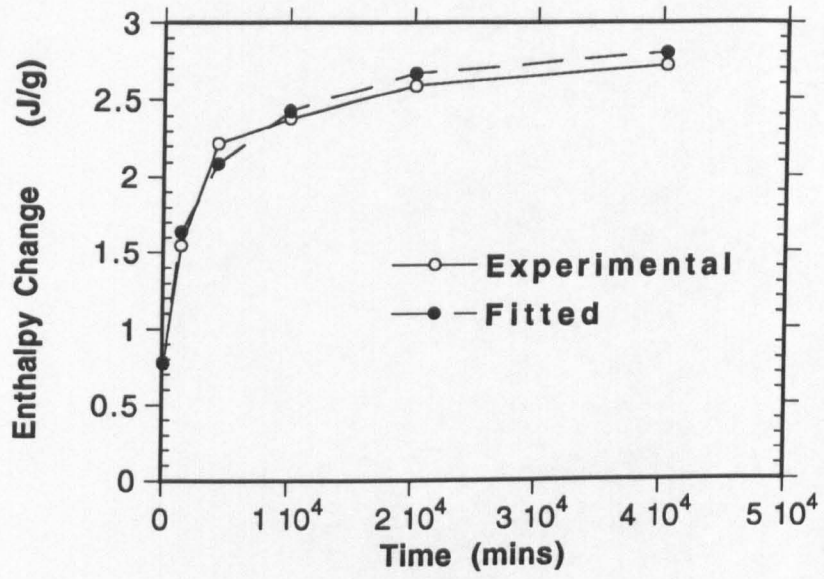

(a)

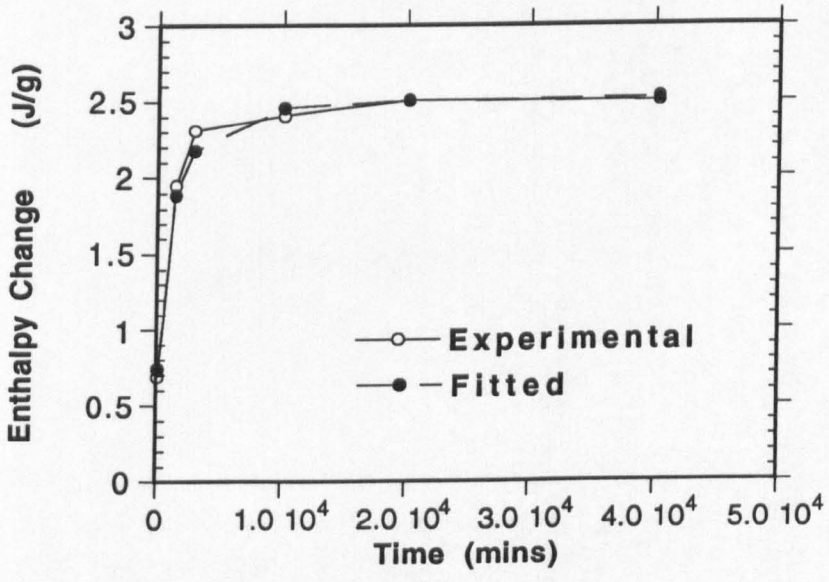

(b)

Figure 3.32: Comparison of experimental enthalpy data with Kohlrausch curve fitted enthalpy data for (a)20I blend annealed at 180°C(b)30I blend annealed at 180°C

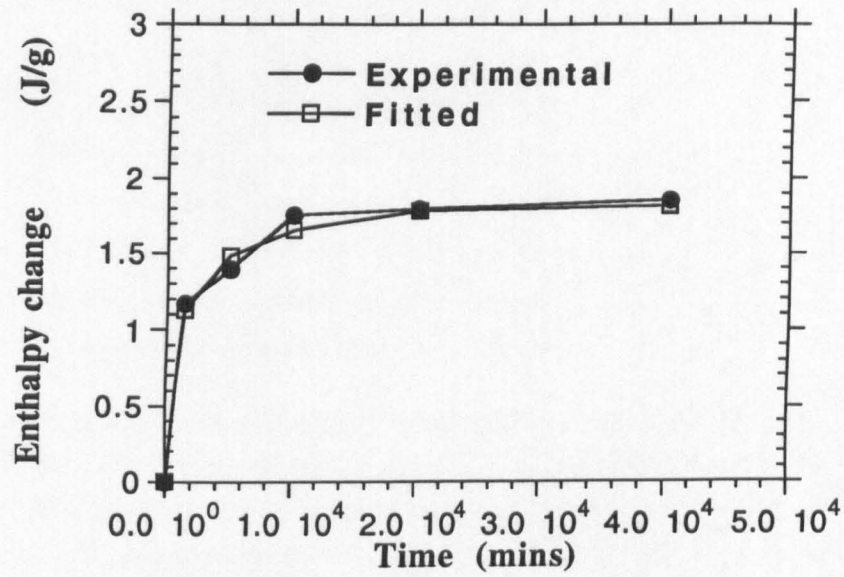

(a)

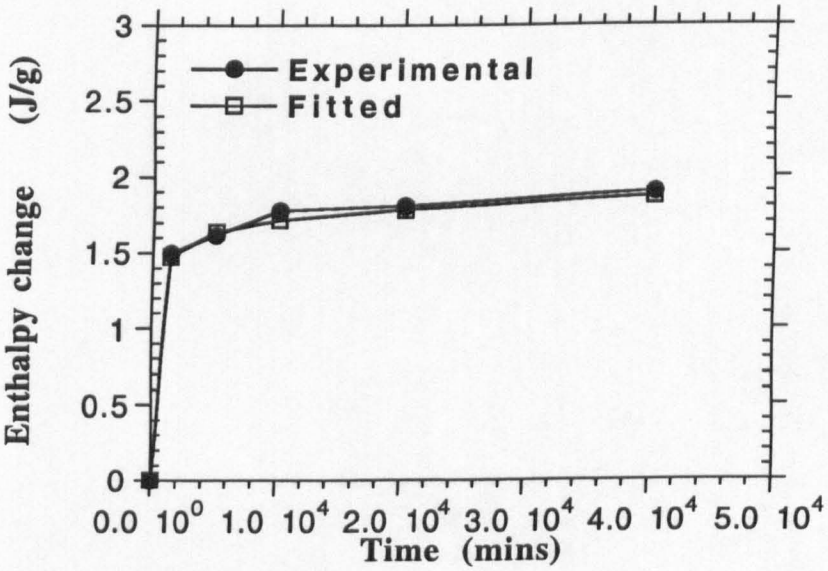

(b)

Figure 3.33: Comparison of experimental enthalpy data with Kohlrausch curve fitted enthalpy data for (a) 20Bblend annealed at 180°C(b) 30B blend annealed at 180°C

The data obtained from the exponential curve fit are shown in table 3.17.

Table 3.17: Data for Blends from Exponential Analysis

Material	ΔH_e (J/g)	τ (minutes)
828	2.36	770
20I	2.54	1497
30I	2.35	349
20B	1.73	1476
30B	1.77	786

The inadequacy of the exponential analysis for the epoxy resin and the ICI blends is evident because the values of ΔH_e fall below those obtained experimentally and makes no physical sense. In the case of the BASF blends ΔH_e also falls below measured values although τ shows plausible decreases with PES content.

3.2.2 Dynamic Mechanical Spectroscopy

3.2.2.1 The Glass Transition Region

The mechanical spectra of the various materials exhibit interesting changes when annealed. Figure 3.34 shows the changes that are observed in the glass relaxation region of the neat resin.

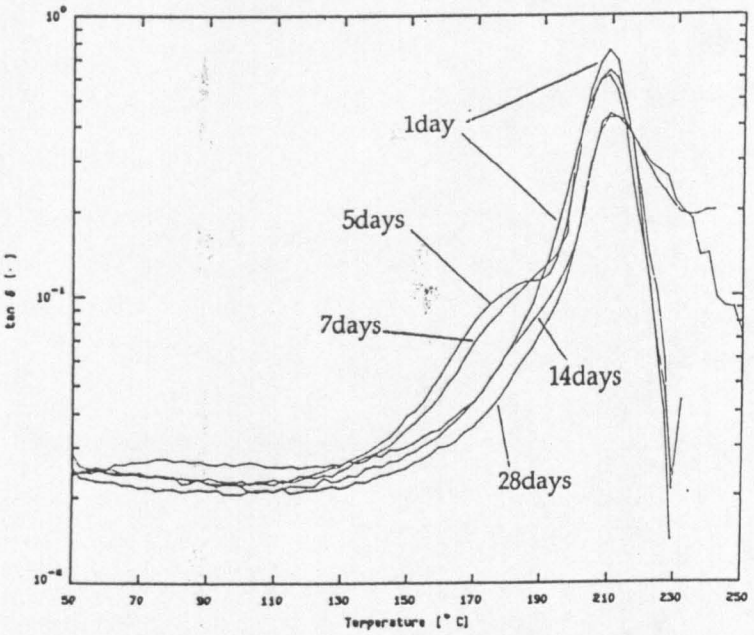

Figure 3.34: Dynamic mechanical spectra of aged resin

There is a gradual reduction in the intensity of the tan δ peak with ageing time as commonly observed (Kong et al, 1979, Kong, 1981, 1983a, 1983b, Chang and Brittain, 1982d, Pang and Gillham, 1989) but its peak position does not vary significantly as reported by some studies on epoxy resins (Kong, 1981). However, the shape of the peak undergoes some unexpected variation with time. At 5 days a shoulder, probably a second relaxation peak, is observed to the left of the main relaxation peak but this subsequently merges with the main peak at later times. At 7 days it has moved slightly but by 14 days it has merged, though not completely. It is interesting to note that the width of the main peak after the smaller peak has moved is larger than in the neat resin.

Similar effects are observed in the 20I and 30I blends in figures 3.35 and 3.36 respectively.

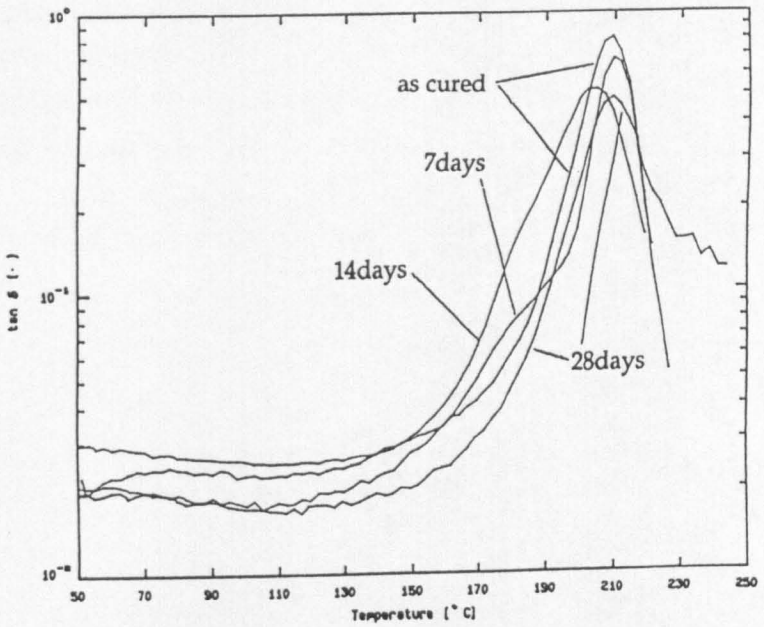

Figure 3.35: Dynamic mechanical spectra of aged 20I blend

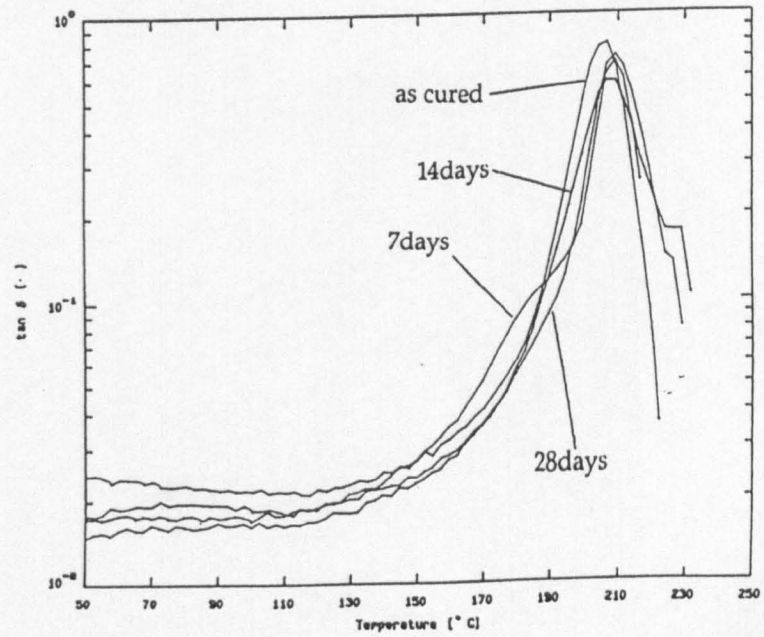

Figure 3.36: Dynamic mechanical spectra of aged 30I blend

In figure 3.35 the 20I blend undergoes similar reductions in peak intensity as does the 30I blend in figure 3.36 and both develop the characteristic shoulder to the right of the main relaxation peak, suggesting that the effect is due to the epoxy rather than the PES. The same observations apply to the 20B and 30B blends of figures 3.37 and 3.38 respectively except that in these blends, the relaxation seen as a shoulder is detectable even at 28 days.

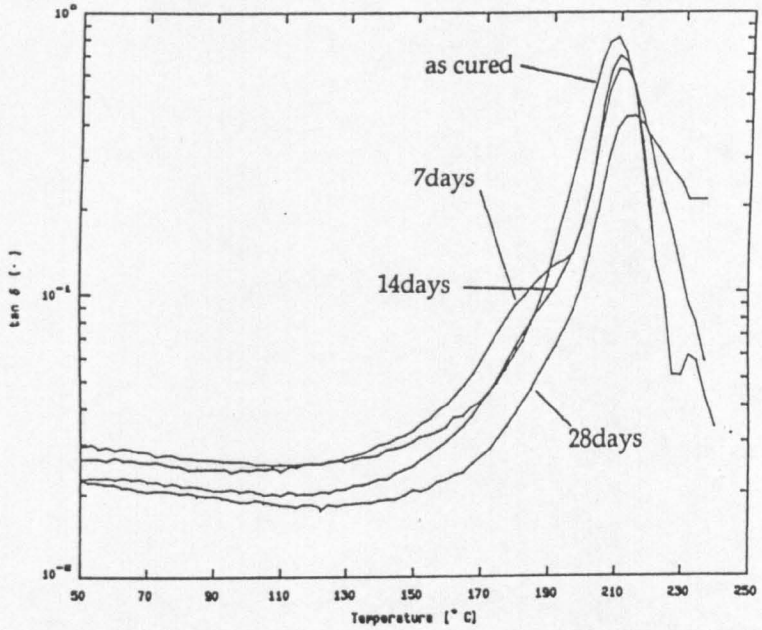

Figure 3.37: Dynamic mechanical spectra of aged 20B blend

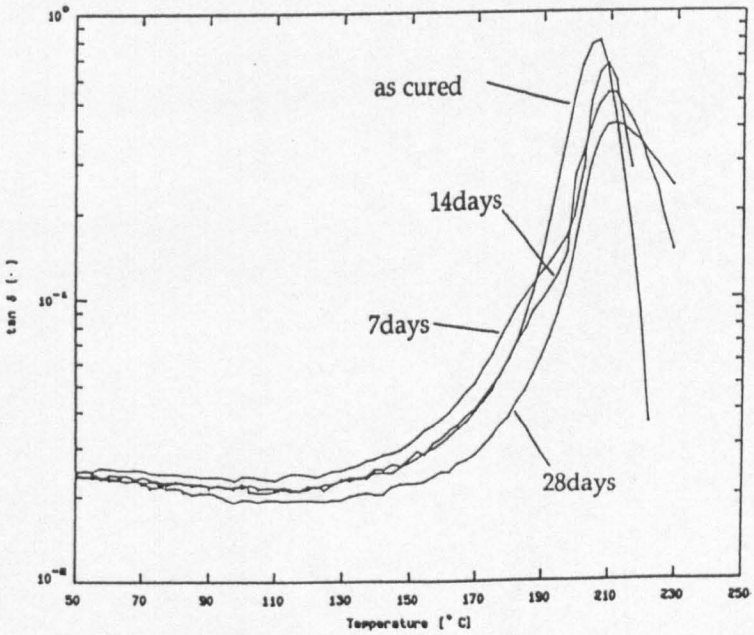

Figure 3.38: Dynamic mechanical spectra of aged 30B blend

Figure 3.39 shows the mechanical spectrum of 828/DDS aged, reequilibrated and compared to the as cured material and it is clear that they are not the same. This clearly suggests that chemical changes accompany physical ageing of epoxy resins.

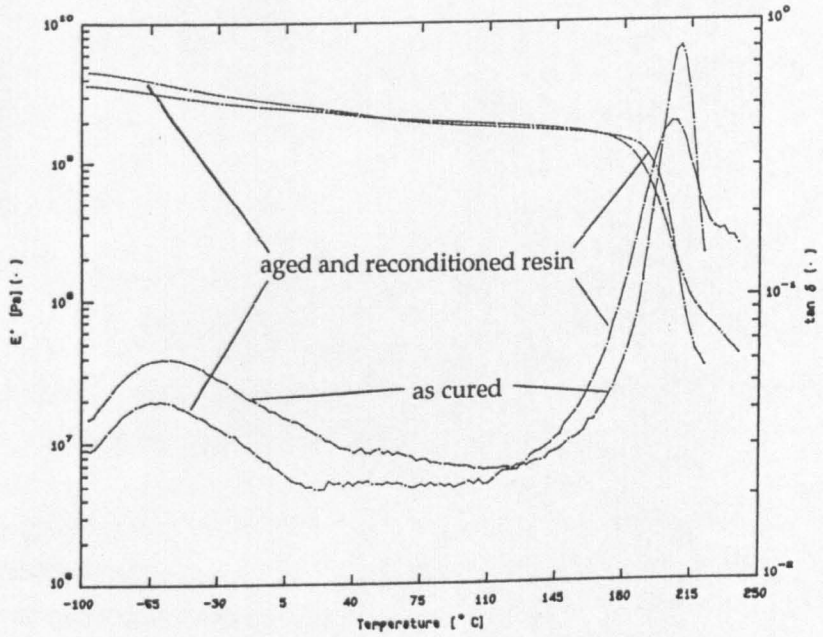

Figure 3.39: Dynamic mechanical spectrum of aged and reconditioned resin

The normalised intensities of the alpha relaxation are different for each material as a function of time and are shown in figure 3.40.

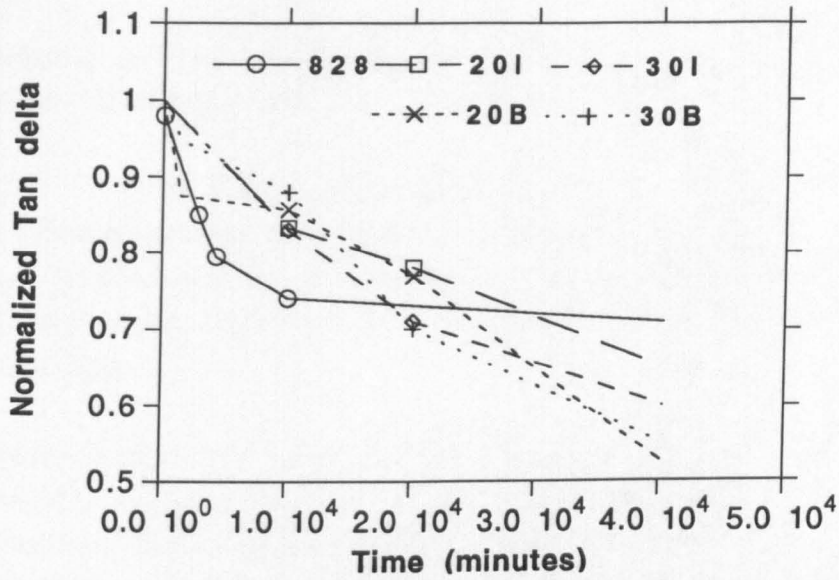

Figure 3.40: Comparison of normalised tan δ intensities as a function of annealing time at 180°C (lines are to guide the eye only)

From the graph it can be seen that the greatest initial decrease in the intensity occurs for the neat resin. In the calorimetric plots of enthalpy against time it was also observed that the greatest initial slope of the curve was found in the 828 data. It appears therefore that initially the neat resin relaxes fastest presumably because it is the furthest from equilibrium and therefore has a greater driving force . However, the rate of decrease of the intensity slows down drastically perhaps because of the greater number of constraints on molecular motion of the neat resin and this leads to the much larger intensity at long times.

At short times the next fastest relaxations appear in the 20I and 30I materials followed by the 20B and 30B materials. Given that the BASF materials are the least highly crosslinked materials it might be expected that the fastest initial relaxation rate would be found in these systems. However, the calorimetric data indicated that the largest amounts of excess enthalpy fall in the order 828>20I>30I>20B,30B and it is known that the driving force for relaxation is greater in those materials that are more perturbed from equilibrium, namely the resin and the ICI blends. Therefore it is to be expected that the curves suggest that the initial relaxation rates fall in the order found. At longer times however, the less constrained structure of the BASF blends enables relaxation

towards an equilibrium state to occur more easily so that the relative intensities of these blends are lowest, followed by the 20I, 30I and neat resin.

Analysis of aged mechanical data in terms of the power law was not possible because of insufficient data.

3.2.2.2 The β Relaxation Region

The effects of increased packing density are expected to be clearly manifested in the small scale motions of segments in the low temperature (high frequency) region. Figure 3.41 shows the change in the β relaxation peak for the neat resin.

There are clearly slight decreases in the intensity of the relaxation as often observed (Kong, 1981, Tant and Wilkes, 1981) but with a slight shift to lower temperature. These changes are also observed in the 20I and 30I curves of figures 3.42 and 3.43 respectively but the intensities of the relaxations at any time are lower than for the neat resin.

Similar trends are seen in the curves of the 20B and 30B relaxations in figures 3.44 and 3.45 respectively but they broaden more than the ICI blends and shift to slightly lower temperatures.

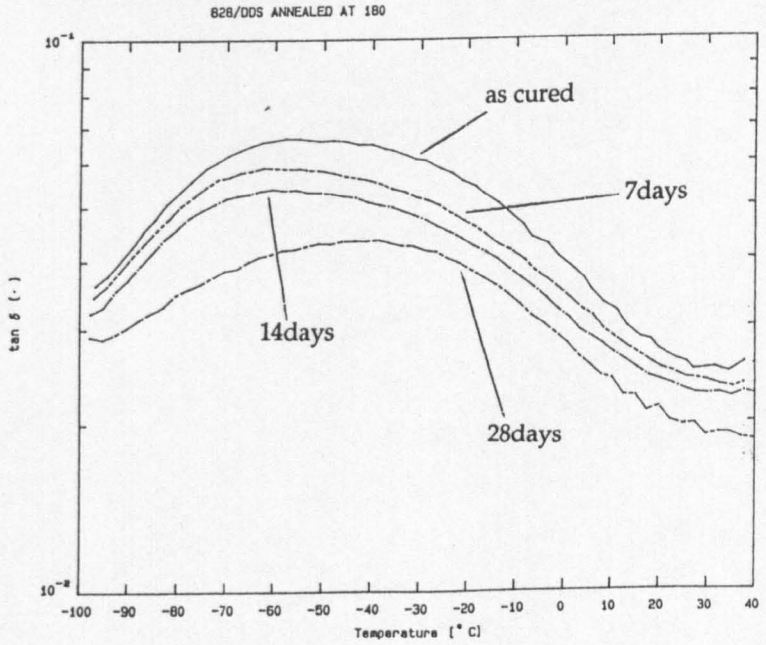

Figure 3.41: β relaxations of aged resin

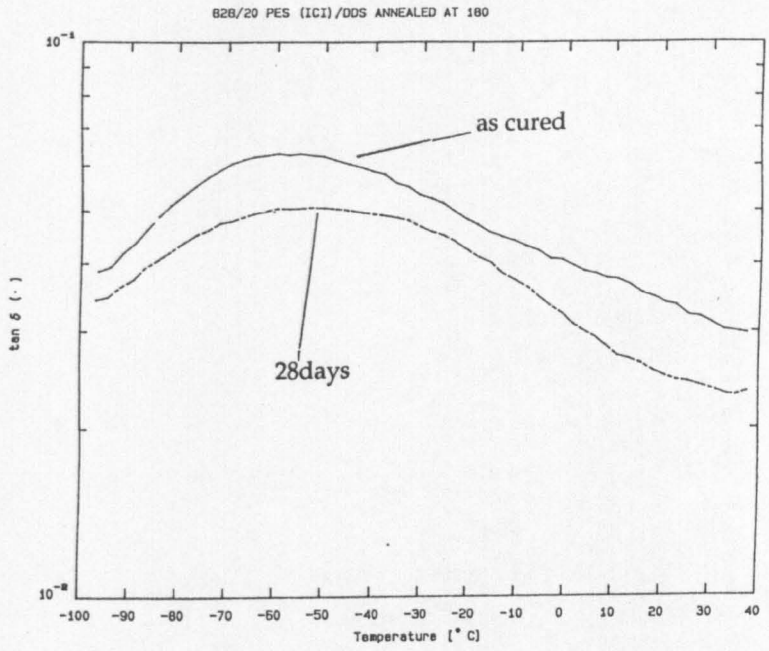

Figure 3.42: β relaxations of aged 20I blend

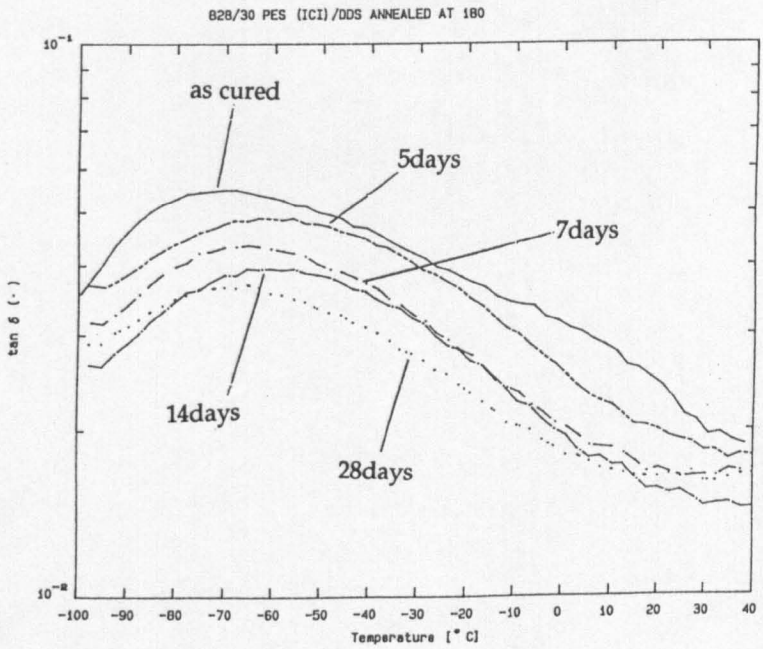

Figure 3.43: β relaxations of aged 30I blend

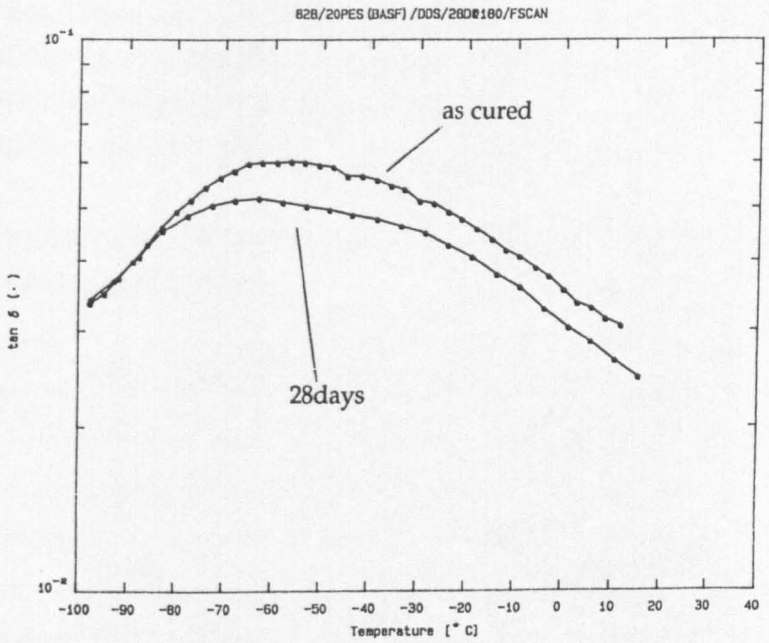

Figure 3.44: β relaxations of aged 20B blend

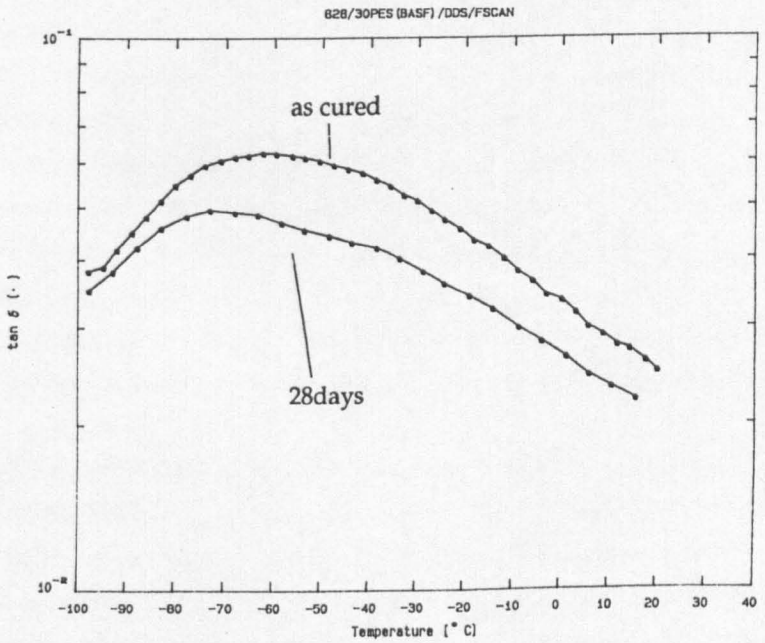

Figure 3.45: β relaxations of aged 30B blend

In fact, in contrast to the alpha relaxation there is a shift of the peak position towards lower temperatures in all materials. This would suggest that the activation energy and entropy decreases, an effect that would not be expected in a densifying system. Calculations of the activation energy using the method of Starkweather give the values shown in table 3.18.

Table 3.18: Activation Energy Data of Low Temperature Mechanical Relaxations of Aged Materials

Material	ΔE_a (kJ/mol)	ΔH(kJ/mol)	ΔS (J/K.mol)
828/DDS	54.7 (57)	51.6 (54)	19 (17.5)
20I	49.6 (56.6)	48 (54.8)	11.5 (38.23
30I	48.5 (63.3)	45.2 (61.5)	24.6 (68.8)
20B	71 (58.3)	69.2 (56.7)	149.1(23.7)
30B	61.3 (56.5)	59.6 (56.7)	68.2 (13.9)

For the neat resin there is little change in the activation energy and a slight increase in the activation entropy signifies increased cooperativity due to the denser packing. However, in the 20I blend the activation energy has decreased slightly, perhaps indicative of easier motion and the activation entropy has become less indicating that the molecular motion is less co-operative. The same is observed in the 30I blend but in the BASF blends there are significant differences. The activation energies of both 20B and 30B blends have increased slightly compared to the unaged material. There is a very large increase in the activation entropy of the 20B material but a more modest increase in the 30B blend. These results suggest that there is a large increase in cooperativity of the low temperature molecular motions at 28 days ageing in comparison to the ICI blends and the neat resin, the latter perhaps having been prevented from attaining a similar state by stronger constraints.

These results are not what is expected for the neat resin or ICI blends if the relaxation represents the motion of the CH_2-CH(OH)-CH_2-O- segments. This motion is expected to become more hindered as the densification proceeds with a loss of intensity and an increase in activation energy and entropy. That greater loss of intensity occurs on the lower side of the relaxation peak suggests that the relaxation of this segment is located below and hidden by the main relaxation, which is possibly due to a different part of the molecule, perhaps the phenyl rings (Pogany, 1970). These small rings might benefit

from the freezing out of some of the CH_2-CH(OH)-CH_2-O- motions during the early stages of ageing because more space becomes available for the movement of what is an extremely small group. No doubt at much longer times the phenyl ring groups will also be affected by the loss of free volume but perhaps at times much longer than those studied here. This would account for the observations. However, the 30I blend is almost in a state of equilibrium as observed from the calorimetric ageing data. It is possible that in the BASF blends the increasing cooperativity is because of the molecular weight effects of the BASF PES, which induce a different morphology on the physical structure. Power law analysis did not yield physically sensible or useful results for the annealed materials.

3.2.3 Dielectric Spectra

3.2.3.1 Data at 25° C

The dielectric spectra of the neat resin, 20I and 30 I blends are shown in figures 3.46. 3.47 and 3.48 respectively. In the neat resin it appears that any motions previously active within the experimental frequency range have moved to much lower frequencies or have been frozen out. In the 20I and 30I blends it is apparent that some degree of shift in what is thought to be the relaxation peaks is occurring and at the times investigated this is most easily observed in the 30I blend where a rather broad relaxation appears to have shifted down field. In the 20I blend there is a reduction in the intensity of the lower frequency region as well as the high frequency region. This effect is more pronounced in the 30I blend where the high frequency region reduces drastically.

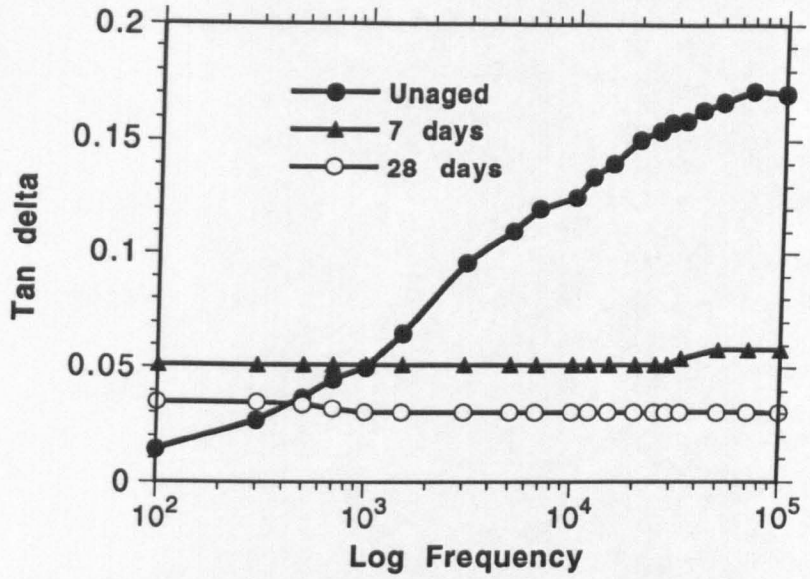

Figure 3.46: Dielectric spectra of neat resin recorded at 25°C after annealing at 180°C

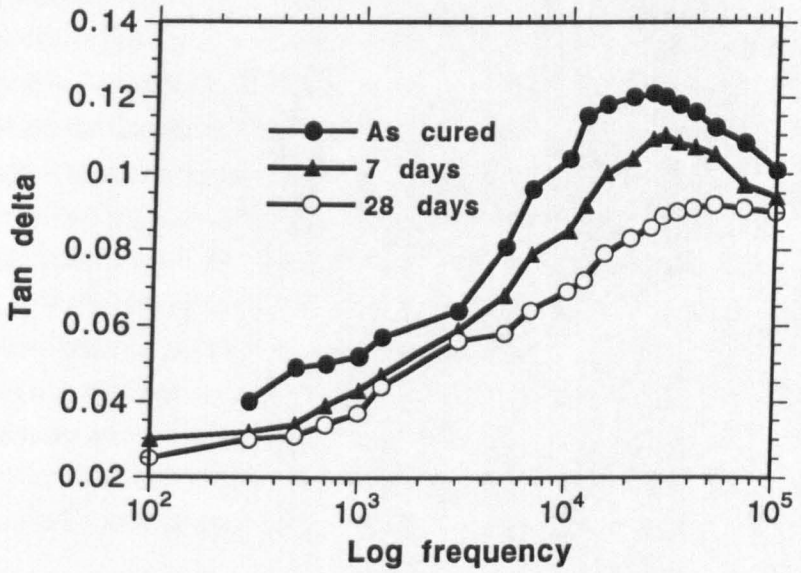

Figure 3.47: Dielectric spectra of 20I blend recorded at 25°C after annealing at 180°C

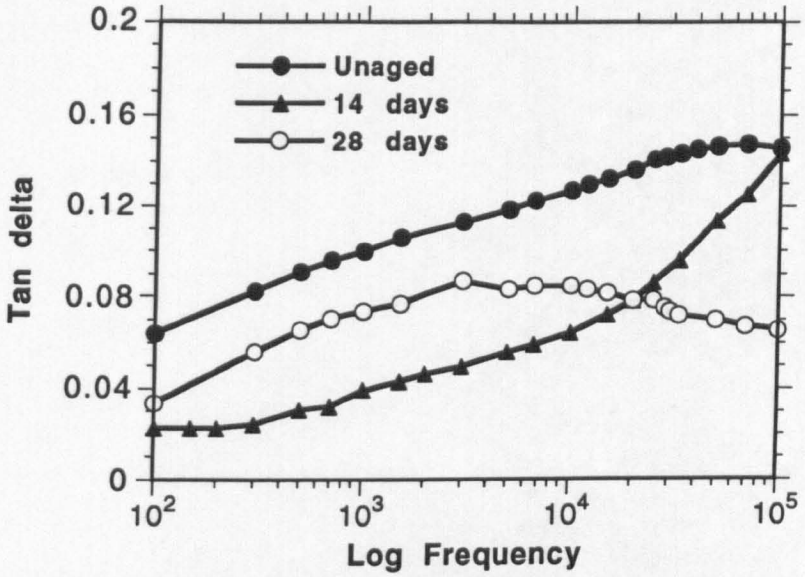

Figure 3.48: Dielectric spectra of 30I blend recorded at 25°C after annealing at 180°C

The spectra of the BASF blends are shown in figures 3.49 and 3.50. It is clear that initially there is a great reduction in intensity of the higher frequency region of the spectrum whilst another relaxation lower down remains unchanged but subsequent ageing reduces the intensity of the lower relaxation. In the 30B blend it is difficult to assess the reduction in intensity of the high frequency peak because it seems to reach a maximum outside the experimental frequency range, although it does seem to decrease. The lower frequency relaxation also decreases in intensity but compared to the 20B blend, it is weaker at the same annealing time. The implication is that annealing freezes out the local motions associated with these dielectric peaks but that the effect is stronger in the 30B blend, suggesting a local environment that permits more freedom of motion of molecular groups and better packing. A lower crosslink density in the BASF materials combined with a free volume distribution containing a larger number of big holes would explain these results.

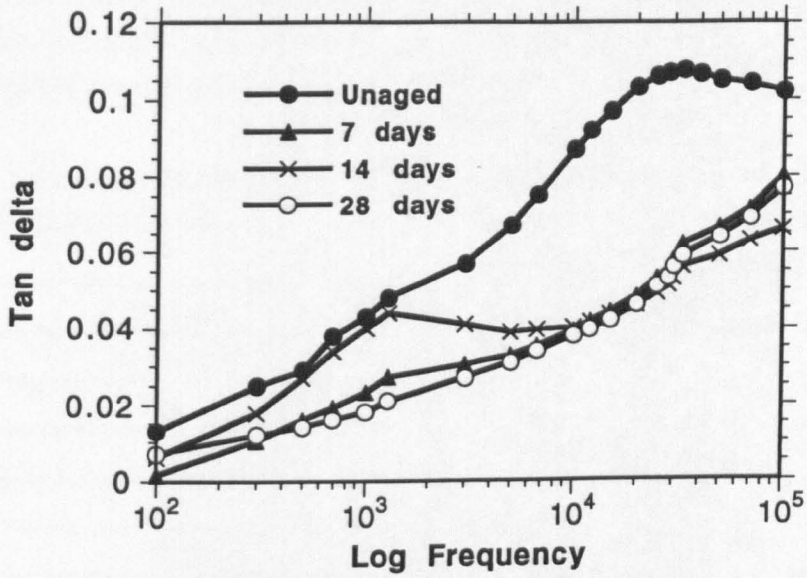

Figure 3.49: Dielectric spectra of 20B blend recorded at 25°C after annealing at 180°C

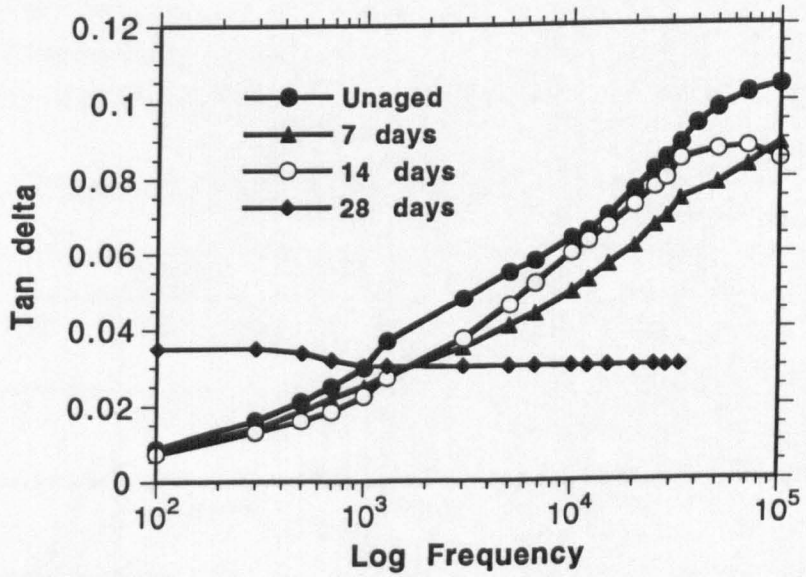

Figure 3.50: Dielectric spectra of 30B blend recorded at 25°C after annealing at 180°C

3.2.3.2 The Glass Transition Region

Increasing the temperature of measurement shifted the spectra to higher frequencies and enabled some calculations to be carried out. The spectra are not shown but the peak frequencies of the aged materials are shown in table 3.19 with the unaged frequencies in brackets.

Table 3.19: Dielectric Peak Frequencies of Materials after 28 days at 180° C and Recorded at 230°C

Material	Peak Frequency (Hz)
828/DDS	150 (60)
20I	300 (500)
30I	1000 (500)
20B	500 (300)
30B	500 (300)

Increasing the PES content in the ICI blends causes a shift in the peak frequency at the same temperature as the neat resin even after ageing, although the differences between the 20I and 30I blends are small. Compared to the unaged materials the aged materials exhibit larger peak frequencies at the same temperature, rather than showing a reduction as was expected. The data obtained from a power law analysis of the high temperature dielectric relaxations of the materials aged at 28 days is shown in table 3.20.

Table 3.20: Power Law Data for Dielectric Relaxation at 28 Days

Material	T^* (K)	t^*(minutes)	zυ
828/DDS	458.9(479.2)	1.79 E-3 (0.23E-3)	2.706(1.026)
20I	456.16(462)	2.648 E-6 (0.038 E-3)	2.588(1.593)
30I	452.01(454)	2.638 E-6 (0.0136 E-3)	2.2(2.166)
20B	466.7	5.314 E-5	0.856
30B	461.08	2.238 E-4	0.945

The numbers in brackets refer to the values of the quantities obtained in the unaged materials. In the ICI blends the temperature T^* decreases with PES content as already established in the unaged materials and this is accompanied by an increase in τ^* as expected if the material becomes more closely packed. However, $z\upsilon$ increases relative to the unaged materials when it is expected to decrease because it has been suggested that it is related to the degree of molecular freedom of motion. An analysis in terms of the WLF equation did not produce sensible results.

3.2.4 Impact Data

Figure 3.51 shows some of the impact energy-BDZ plots typical of the aged materials and table 3.21 shows the complete set of G_{IC} data. It is evident that physical ageing accompanied by perhaps some chemical changes leads to a significant deterioration in toughness.

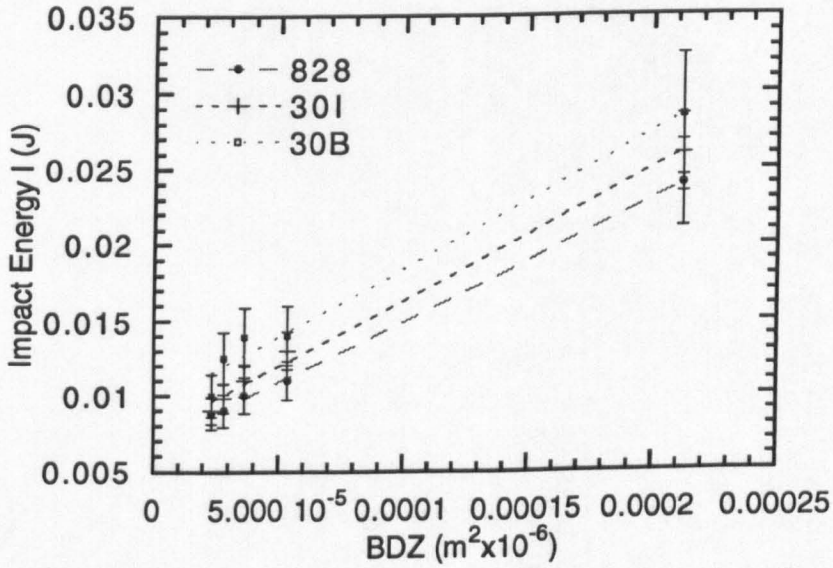

Figure 3.51: Impact energy plotted against BDZ for a selection of materials aged for 28 days at 180°C

Table 3.21: Impact Data of Materials Aged for 28 Days

Material	G_{IC} (J m^{-2})	% Decrease
828/DDS	74	10
20I	79	12
30I	89	15
20B	82	16
30B	91	19

The data show that the neat resin undergoes the least reduction in impact strength and that as the amount of PES in each blend increases from 20 phr to 30 phr, so the % decrease is greater. However, comparing equivalent blends, the largest decreases occur in the BASF material. These results are in agreement with the calorimetric and mechanical spectroscopy data of the aged materials.

3.2.5 Discussion

The heat capacity curves display the characteristic endotherm as evidence of physical ageing. It is interesting and potentially useful that some of the data can be fitted quite well using the Kohlrausch function. It would be useful to study isothermal annealing of these materials and materials like them in order to determine the potential lifetimes of adhesives under sustained use at certain temperatures. The fact that the initial trajectories of all the materials *appear* similar might suggest that the initial relaxation rates are also similar and it was suggested in the previous discussion that the smaller holes and higher hole surface energy of the more crosslinked materials might lead to similar initial relaxation rates, although clearly at such short times this is difficult to measure. The enthalpy relaxation curves indicate visually that the addition of PES reduces the amount of excess enthalpy and this is confirmed for the blends from the good agreement with the Kohlrausch curve fit. Visually the BASF blends have the least amount of excess enthalpy and relax very quickly when aged at the same temperature as the other materials. The constants determined form the Kohlrausch fit for the ICI blends show plausible trends. However, based on the results of section 3.2, one expects the β values for the BASF blends to be greater than in the equivalent ICI blends. In fact this is not the case and in the 30B blend the value of β is less than obtained for the resin, implying a greater degree of non-linearity. This does not seem to make physical sense and the quality of the fits to the BASF enthalpy data is good. However, it should be borne in mind that there are more rigorous methods of determining these constants as well as the time dependence of β and other associated structural parameters (Ngai et al, 1984-1988, Moynihan, 1976, Kovacs et al, 1979). The method chosen here is the simplest and is useful but clearly more comprehensive methods are required. Nevertheless, as expected the excess enthalpy of the BASF blends is consistent with the idea that the structure is more flexible in these materials and therefore able to relax faster. The values of τ also decrease in going from 20B to 30B, again an expected result. However, it is fair to say that in comparison to the exponential fitting, the Kohlrausch data are more physical and within each blend system the constants behave as expected.

The tan δ glass transformation relaxation intensities decrease universally with annealing as observed in other reports (Kong et al, 1979, Kong, 1981) although the peak positions do not vary greatly as reported in some of these works. The appearance of the shoulder in all of the materials is interesting.

Its appearance in the epoxy resin would suggest that it is in fact associated with heterogeneities in the network rather than being an effect induced purely by the presence of the PES. Given the non heterogeneity of the epoxy reactions it is quite possible that there are regions of low crosslink density or unreacted monomer which undergo phase separation from the bulk of the epoxy, explaining the shift to lower temperature (energy) but then undergo further chemical reaction which increases the crosslink density. As crosslinking proceeds so the material gradually remerges with the main peak. However, the increase in broadness of the neat resin and blend peaks after merging is suggestive of a change in the level of crosslinking, that it is increased by annealing. The weak mechanical spectroscopy peak associated with this small fraction of phase can remerge with the main glass transition peak if changes in conformation and the diffusion of free volume that occur during physical ageing permit a limited redistribution of segregated hardener and/or monomer which would allow a small amount of further chemical change. This means that the process of physical ageing occurs but is accompanied by and indeed may enhance further chemical reactions.

Physical ageing is a thermoreversible phenomenon but if chemical change has occurred the mechanical spectrum of a material as cured and a material which is aged, reconditioned and quenched will differ and this is confirmed by figure 3.38. Of course, this just confirms what is expected to be highly likely in a reactive material annealed at high temperature and similar ideas were expressed by Mijovic and Liang (1984). The effect of such chemical reactions should not however be overestimated and whilst they may be manifested as detectable changes, such changes are small and are simply exaggerated by plotting mechanical spectra on logarithmic scales (which is the intention). The bulk of the effects are still expected to be due to the physical ageing processes. It is interesting also that the shoulders appear to occur near to the annealing temperature before merging with the main peak. The cause of this relaxation peak is perhaps low crosslink density networks and low molecular weight unreacted material. The intensity of the peak is small and only appears the size it does because of the logarithmic scale and it is possible that this peak shifts down field as it phase separates from the more highly crosslinked network. Differences in molecular weight, even of networks can of course lead to incompatibility. This explanation is reminiscent of the argument of Kriebich and Schmidt (1979) and even neat epoxies are never totally cured so that it is possible. That this effect should

occur in the PES blends should be of no surprise because there is evidence from the heats of reaction that there is more unreacted material present in the blends because the PES disrupts crosslinking. The fact that the shoulder appears to peak near to the annealing temperature is perhaps because only material which has a glass transformation similar to the annealing temperature will separate. At lower temperatures this phenomenon might be the same.

An interesting observation is that the shoulder appears to persist for a slightly longer time in the BASF blends. Recalling that the BASF blends reduced the heats of reaction by the greatest amount, it is possible that in these blends there is more unreacted material. The small scale reactions must occur simultaneously with the physical ageing process, the latter reducing the free volume in the blends. The BASF blends are observed to relax in terms of enthalpy much faster, presumably also eliminating free volume at a faster rate and this may well slow down the process of any chemical reaction that occurs more than in the slower relaxing neat resin and ICI blends. The slower free volume relaxation in these materials will allow more mobility of low molecular weight material and lead to faster reaction of what little there is. The remerging of the shoulder is also explainable as the low molecular weight material undergoes further reaction, thereby achieving similar density to the main networks. That there is some chemical reaction is certain because the glass relaxation peak width becomes broader and the spectrum of an aged and reconditioned sample is not identical to the unaged spectra. Similar suggestions have been made by Mijovic and Liang (1987).

Whilst it is certain that chemical reactions occur the relaxation of the mechanical glass relaxation intensity (figure 3.39) follows similar trends to the enthalpy relaxation. The neat resin starts to relax fastest, but slows down rapidly, behaviour giving a little support to the qualitative discussion of section 3.1.5 . The neat resin is followed in terms of overall slowness by 20I, 30I and finally the BASF blends. It does seem that the qualitative model is reasonable because the enthalpy and mechanical spectra give a good degree of support. The mechanical β relaxation also reduces in intensity suggesting that there is a decrease in the number of segments capable of undergoing relaxation because of constraints imposed by increased local packing density and hence an increase in the strength of the potential experienced by a segment due to surrounding molecules. The changes are also observed to

occur more strongly to the left hand side of the peak, suggesting that it is a second relaxation hidden under the broad peak that is being affected most. This means that the activation energy measurements determine only the energy required to induce motion of the group responsible for the peak, and may give no indication of the activation energy for the second relaxation. Ageing clearly reveals the presence of these relaxations by freezing some of them out and previous workers have suggested the presence of more than one relaxation (Pogany, 1970, Garroway et al, 1982). The activation energy behaviour is a little unexpected with decreases in activation entropy occurring in the neat resin and ICI blends (unexpected) but increase in the activation energies and entropies of the BASF blends (expected). The latter case of increasing entropy is expected as space becomes more restricted (Starkweather, 1981, Starkweather and Avakian, 1989). Garroway et al (1982) reported a possible phenyl ring mechanical relaxation at -40°C although the molecular causes of the relaxations in this study were not pursued. It is possible that the left side of the peak is connected with the mechanical motions of the phenyl ring, the intensity of which is affected by packing density (Dumais et al, 1986) whilst the right side is more associated with the CH_2-CH(OH)-CH_2-O However, the situation is complicated by the presence of the PES.

The ambient (25°C) dielectric data also probes these high frequency (low temperature) relaxations and whilst in the unaged state it was not possible to say that there were two peaks, ageing has frozen out some of the relaxations and shown that in the blends at least, there are in fact two distinguishable relaxations. Again it is not possible to say exactly which relaxation is caused by which molecular group and since phenyl rings are not dielectrically active (McCrum et al, 1969) the dielectric spectra must be associated with polar groups such as the SO_2 or the CH_2-CH(OH)-CH_2-O . The freezing out effect is most rapid in the neat resin but the relaxations persist in the blends, even in the faster relaxing BASF blends. However, indirect confirmation of faster relaxation in the BASF blends compared to the ICI is the fact that the relaxations at 28 days in equivalent blends are more intense in the ICI systems. Comparing the ICI blends or the BASF blends shows again that increasing PES content leads to greater reductions in intensity with ageing.

The analyses of the dielectric relaxations in terms of the power law and W-L-F equations do not however make a great deal of sense, despite the apparent

agreement with intuition in assessing the behaviour of the as cured blends. The fact that with ageing the frequencies of the glass relaxations have increased (table 3.19) is certainly contrary to intuition. Further investigation is required.

The impact data confirm the information extracted from the enthalpy relaxation ,mechanical spectroscopy and ambient dielectric spectroscopy by showing that the blends relax faster than the resin. That the deterioration in impact energy is greatest in the BASF blends is evidence of a reduction in free volume and entropy giving rise to brittle behaviour as fewer molecular conformations are available due to a higher packing density, the latter also reducing molecular mobility. The lack of mobility leads to a slower response to the application of stresses and local regions of high stress build up because molecules cannot dissipate this energy. Ultimately in some regions of the materials the stress build up exceeds the strength of the material and brittle failure occurs. It would be useful to undertake more comprehensive impact studies in order to try to correlate a certain degree of enthalpy relaxation with a critical reduction in impact energy.

3.3 Summary

The effect of adding PES is to reduce the extent of chemical reactions by a small enough degree that the number of chemical crosslinks is reduced. The extent of this effect appears to be increased by the use of lower molecular weight PES containing chain terminations incapable of interaction with the epoxy. However, the glass transition ranges of the blends and the neat resin are similar for the compositions studied and agree well with the values calculated from the Flory -Fox rule of mixtures for miscible blends. This is not to say that the blends are truly single phase but rather that a second phase is not detectable with the techniques used.

The effect of the PES on physical ageing is that relaxation towards equilibrium during annealing is faster because of a suspected modification of the free volume distribution and reduced crosslinking. The curve fitting results suggest that because of the more flexible structure of the epoxy network in the blends at high temperature there is less excess enthalpy in the blends at sub glass transition temperatures and this is further reduced in those blends containing BASF lower molecular weight material with -Cl chain terminations.

The impact strength deteriorates faster in the blends and by a greater amount in the BASF blends, consistent with their lower crosslink density.

Chapter 4

The Effects of Annealing On Some Of The Properties of Two Phase Epoxy Resin-Polyethersulphone Blends

4.0 Introduction

In the previous chapter we were concerned with epoxy-PES blends in which a second phase was not detectable. In this chapter we investigate the characteristics of blends of epoxy resin and PES cured with a different hardener, DICY. When these blends are cured a second phase is clearly distinguishable with the analytical techniques employed. It is shown in this chapter that although these blends are not particularly tough and the particle sizes are rather large, significant changes occur when the materials are annealed at temperatures ranging from below the lower T_g phase to just under the T_g of the high temperature phase.

Why study this? The reason for this investigation is that two phase polymer blends are finding increasing use as a means to obtain a set of distinct material characteristics as cheaply as possible, thereby avoiding the use of a much more expensive 'pure' material. This philosophy has and still is applied extensively to blends of linear polymers and has also been applied to epoxy resins via a dispersed rubber phase in an epoxy matrix. More recently two

phase blends of epoxy resins and tough linear thermoplastics in which the thermoplastic is the minor phase have been developed with commercial applications in mind. Various reports have described the synthesis of epoxy-polyethersulphone blends in which there is no improvement in toughness (Bucknall and Partridge, 1983, 1986, Diamant and Maroum, 1985, Raghava, 1986, 1987) but other works have produced tough systems (Almen et al, 1988a,b, Sefton et al, 1987, Hedrick et al, 1991). However, these reports have only addressed the properties of the 'as cured' materials. It may be cause for concern that such epoxy systems, which contain PES, are in commercial use in helicopter rotor blades and composite panels and are sold by Ciba-Geigy and ICI. It would appear that more information is required concerning their high temperature performance and physical ageing behaviour. The materials studied in this chapter, although not commercially useful, exhibit deterioration of properties with high temperature annealing. This raises the question of how will other similar two phase blends behave when aged and will their properties also exhibit similar changes? The work presented in this chapter may provide some motivation for others to conduct similar investigations on commercial formulations.

4.1 Unannealed Materials: Results

4.1.1 Qualitative Assessment of the Degree of Cure

There are various techniques that can be used to determine the extent of cure (Manzione et al, 1981, Chang et al,1982a, Enns and Gillham, 1983) but in this case, in order to be sure that the materials were cured, the epoxide band at 910-915 cm^{-1} was examined. The FTIR spectra of the 30I and 30B blends are shown in figures 4.1 and 4.2 respectively.

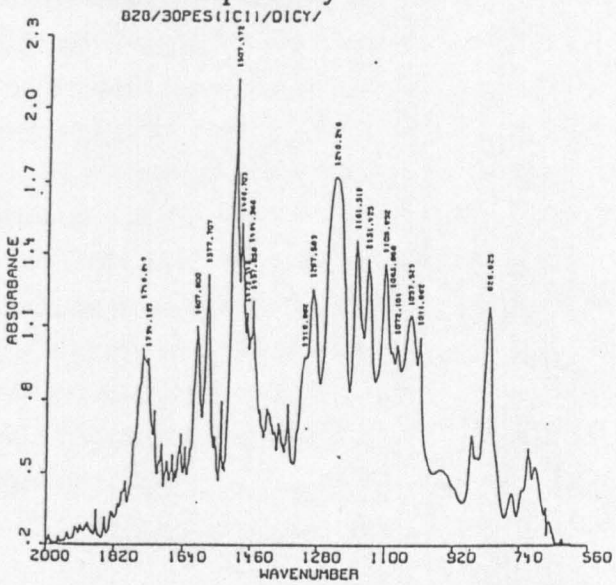

Figure 4.1: FTIR spectrum of 30I blend

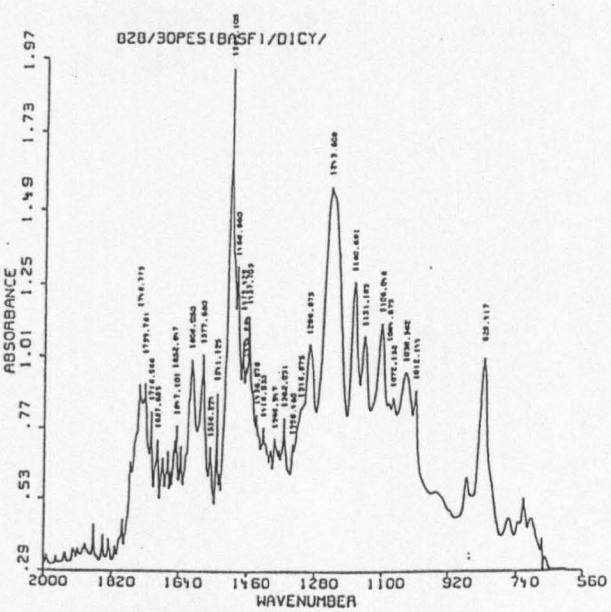

Figure 4.2: FTIR spectrum of 30B blend

The epoxide band is barely visible as a shoulder which is sufficient evidence for the assumption of an extent of cure in excess of 80-90%. Given that the cure schedule consists of exposure to 180°C for 16 hours it is reasonable to expect the materials to be as near to a fully cured state as possible. The temperature of 180°C used for the final cure is the maximum that could be used without the materials degrading.

The spectra are essentially the same although some of the peaks in the 30I blend appear stronger than their counterparts in the 30B blend. If there is a chemical reaction between the hydroxy end groups of the ICI PES and the epoxide ring there would be a change in the intensity of one of the ether bands relative to some other band that remains unchanged and can therefore be used as an internal control. In these blends the relative intensities of the bands with respect to the aromatic vibration at 1508 cm^{-1} remains the same. Therefore it is unlikely that any reaction occurs. It is difficult to draw any other conclusions from the IR spectra without the spectrum for the neat cured resin, which could not be obtained because of the difficulties of curing the system. With less than 30 phr PES the hardener DICY settles out because the viscosity of the blends is unable to maintain an even dispersion of hardener. In the unmodified system, it proved too difficult to produce a cured resin.

4.1.2 Calorimetry and Thermogravimetry

The heat capacity curves of the 30I and 30B blends are shown in figure 4.3 The heat capacities of the materials are similar and each exhibits two glass transformation regions indicating the presence of two phases (Olabisi et al, 1979, Fried, 1982).

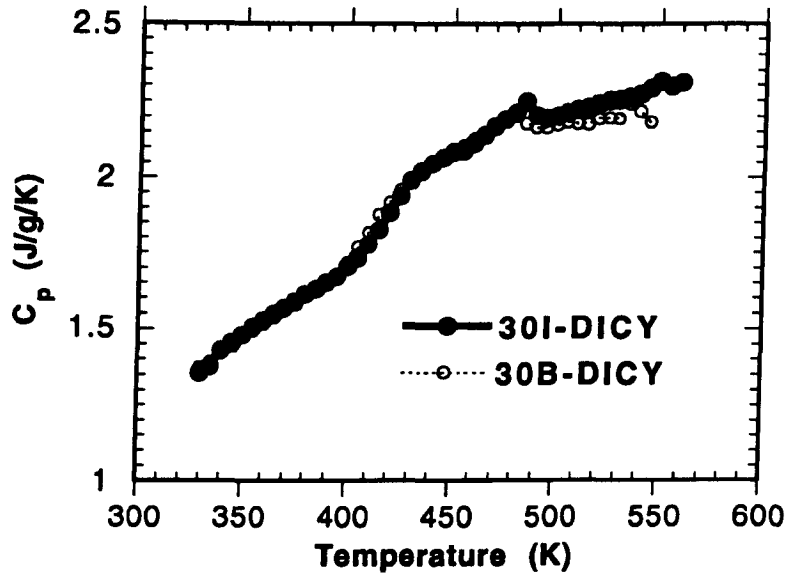

Figure 4.3: Heat capacities of 30I and 30B blends

The lower temperature glass transition is broad, somewhat typically of polymer blends and involves a significantly larger change in the heat capacity over the glass transformation than the high temperature phase, which is small and ill defined in both materials, but which shows evidence of physical ageing in the form of an endothermic peak. Table 4.1 summarises the temperature characteristics of the glass transition regions for these blends.

Table 4.1: Glass Transition Temperatures and Widths

Material	T_{g1o}(K)	T_{g2o}(K)	ΔT_{1o}(K)	ΔT_{2o}(K)
30I	403+/-5	416+/-3	35	----------
30B	396+/-6	409+/-4	34	----------

The onset of the glass transition is slightly higher in the ICI blends by an amount of the order of 7-8K but the temperature ranges over which the lower temperature glass transition occurs is about the same. The onset temperatures of the higher temperature phase were a little difficult to obtain because almost as soon as the lower transformation has been passed through the second starts and it was not possible to obtain any reasonable estimate of the breadth.

The size of the 'step' in the heat capacity as the transitions are passed through is a rough guide to the amount of phase involved in the main chain motions. It would appear that the lower temperature phase constitutes the larger part of the blends and since the minor component is PES it is reasonable to attribute the lower T_g to the epoxy phase, which presumably forms the matrix. The high temperature phase is then associated with the PES rich phase and the onset T_g as quoted in table 4.1 lies quite near to the PES T_g of 490K (220°C).

The calorimetric data for the glass transitions is shown in table 4.2.

Table 4.2: Calorimetric Data of Blends

Material	$\Delta H_1(T_{g1o})$ (J/g)	$\Delta H_2(T_{g2o})$ (J/g)
30I	5.9	1.01
30B	8.9	----------

The enthalpy change over the T_{g2} of the 30I blend was barely calculable but the change over the 30B range was too small and the start of this transition was merged with the end of the lower temperature transition.

The thermogravimetric curves of the blends are compared in figure 4.4 and it seems that the materials have similar thermal stabilities over the experimental temperature range.

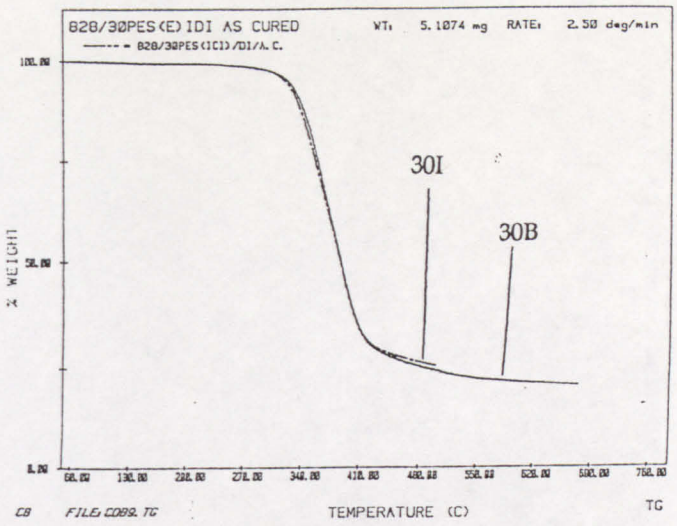

Figure 4.4: Thermogravimetric curves of 30I and 30B blends

4.1.3 SEM Micrographs

The SEM micrographs of fracture surfaces of the 30I and 30B blends are shown in figures 4.5 and 4.6 respectively.

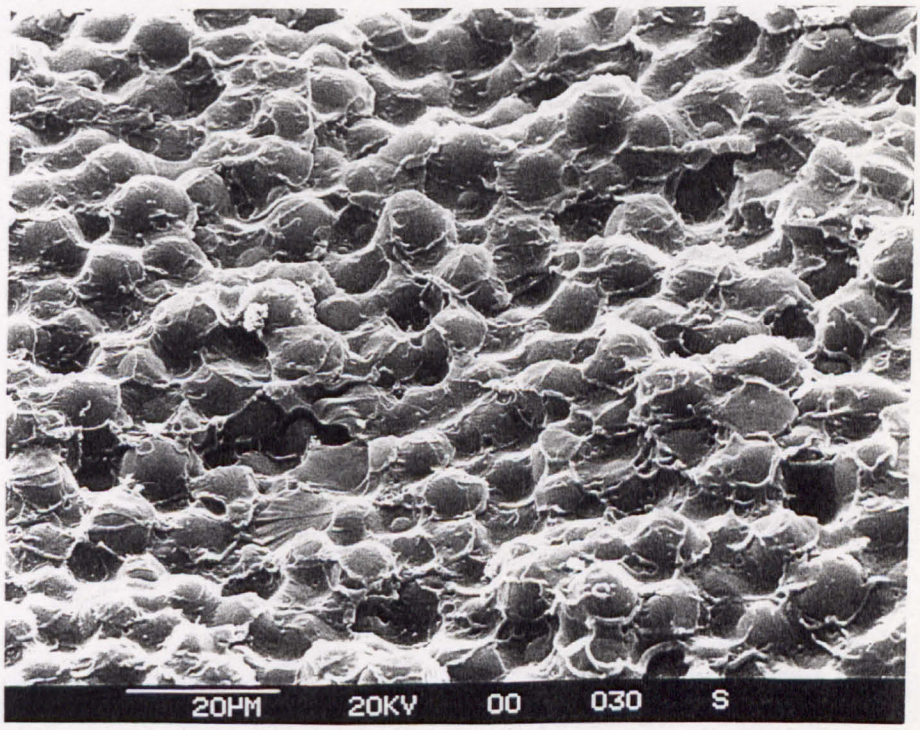

Figure 4.5: SEM micrograph of a typical fracture surface of a 30I blend

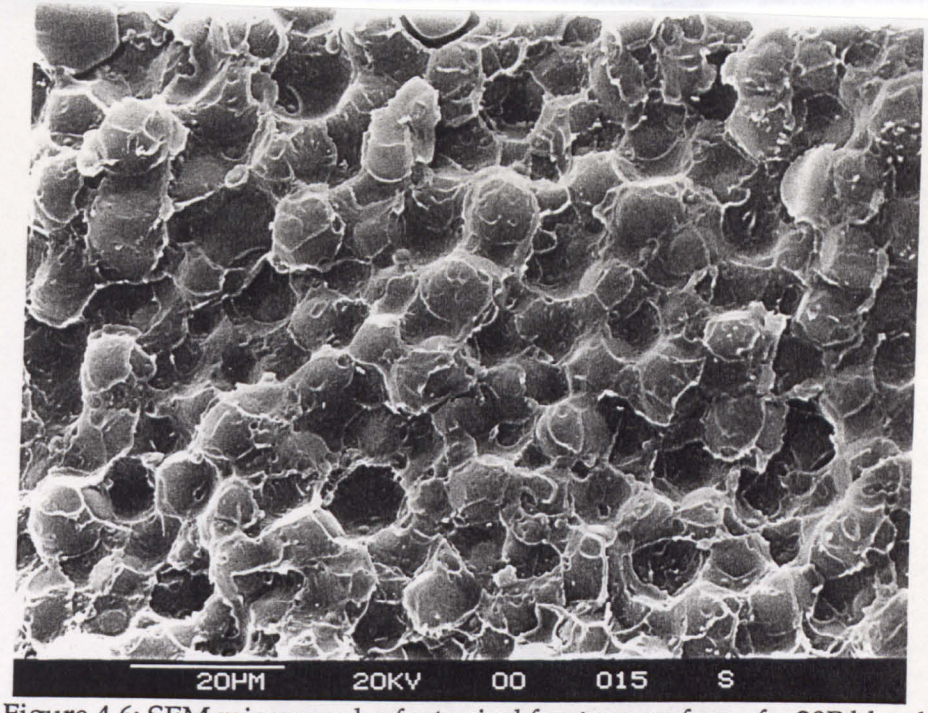

Figure 4.6: SEM micrograph of a typical fracture surface of a 30B blend

The micrographs clearly show that both blends have similar two phase morphologies. The microstructures resemble the micrographs of Bucknall and Partridge (1986) who also cured a DICY system, although the particle sizes in figure 4.5 are larger. The 30B blend microstructure contains very large particles embedded in a matrix which on closer inspection also contains a number of very small particles.

4.1.4 Mechanical Spectroscopy

The mechanical spectra of the blends are shown in figures 4.6 and 4.7 for the 30I and 30B blends respectively, and evidently there is also a great similarity between the two blends in terms of the dynamic mechanical response.

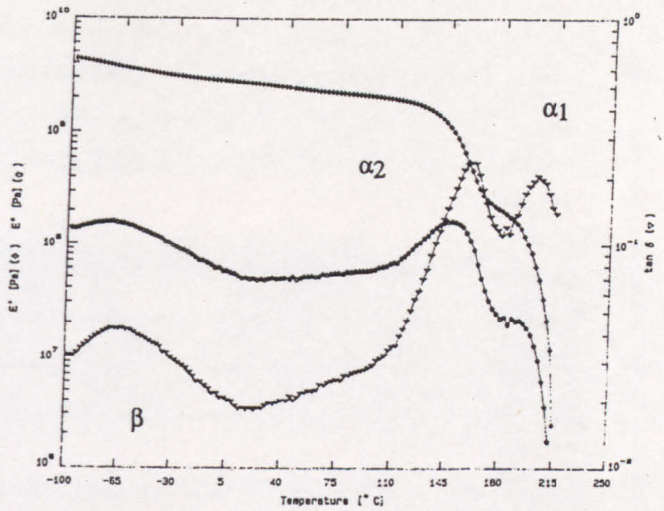

Figure 4.6: Dynamic mechanical spectrum of 30I blend

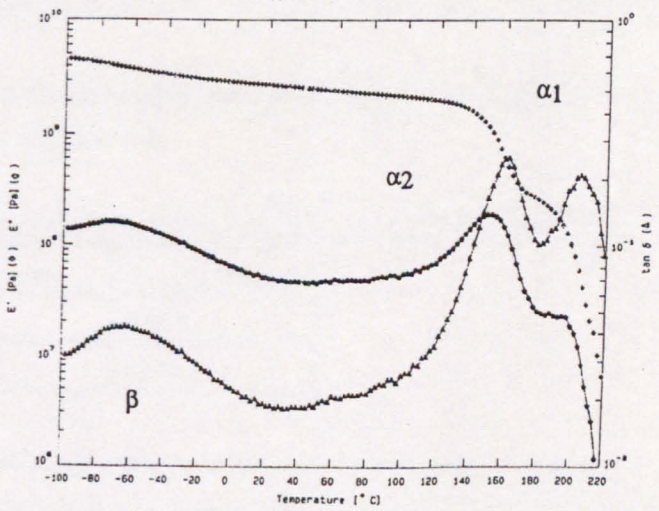

Figure 4.7: Dynamic mechanical spectrum of 30B blend

The presence of the two phase morphology is clearly indicated by the presence of the two high temperature relaxation peaks α_1 and α_2. The shapes of the relaxation peaks in each material are also similar. Table 4.3 shows the intensities of the tan δ peaks and in both blends it is such that $I_{\alpha 1} > I_{\alpha 2}$,which suggests that the fraction of the lower temperature phase is higher. It is also noticeable that at 1Hz $T_{\alpha 1}$ in the 30I blend is slightly higher than in the 30B blend whilst there is little difference between the $T_{\alpha 2}$ values.

Table 4.3: Dynamic Mechanical Characteristics of 30I and 30B Blends

Blend	T_β (°C)	I_β	$T_{\alpha 1}$(°C)	$I_{\alpha 1}$	$T_{\alpha 2}$(°C)	$I_{\alpha 2}$
30I	-62.9	0.043	162.4	0.243	204	0.208
30B	-67.5	0.055	157.1	0.26	202.3	0.19

It is clear also from table 4.3 that the intensity of the β relaxation is higher in the 30B blend and its peak temperature is lower a fact which suggests that there are more segmental -CH_2-CH(OH)-CH_2-O- rotations active in this material. This could be either because in the ICI material the crosslink density is lower, thereby giving rise to fewer of these segmental rotations or simply because a greater packing density in the ICI material prevents movement of these segments. There is also the possibility that the motion is connected with the PES low temperature relaxations. It is certain that in this instance the lack of data concerning the unmodified resin prepared under the same conditions hinders somewhat the interpretation of this data.

The apparent activation energies for the blend T_g's is useful for comparison and are shown in table 4.4.

Table 4.4: Apparent Activation Energies for T_g Relaxations

Blend	$E_{\alpha 1}$(kJ/mol)	$E_{\alpha 2}$(kJ/mol)
30I	103.9	108.3
30B	98.5	103.5

Although the data are not quantitatively correct because of the inappropriateness of Arrhenius analyses for glass transitions the data show that the activation energy of the 30I blend is marginally larger.

A W-L-F analysis of the data yields the values in table 4.5 and 4.6.

Table 4.5: W-L-F Data for α_1 Relaxation

Blend	C_1	C_2	T_o	f/B	α/B
30I	9.69+/-0.87	50.05+/-7.8	111.2+/-2.6	0.045	0.00096
30B	8.4+/-0.76	46.3+/-5.7	106+/-2	0.052	0.00112

Table 4.6: W-L-F Data for α_2 Relaxation

Blend	C_1	C_2	T_o	f/B	α_f/B
30I	6.48+/-0.56	24.67+/-1.9	162.8+/-9.5	0.067	0.0027
30B	5.5+/-0.5	22.1+/-2.1	157+/-10.1	0.079	0.0036

In both blends, the constants C_1 and C_2 and the divergence temperature T_o decrease in going from α_1 to α_2 as expected. It has been reported by Gerard et al (1991) that C_1 and C_2 are dependent upon crosslink density and decrease as crosslink density decreases. Therefore it appears as though it can be tentatively suggested that the 30B blend is of lower crosslink density than the 30I blend. The lower values of T_o in the 30B blend indicate that these relaxations are able to persist to slightly lower temperatures. The quantity f/B is a measure of the fractional free volume of the material at T_o and correctly shows that the fractional free volume for the lower relaxation is smallest. However, comparing the f/B values of each blend seems to indicate that the 30B blend has a slightly larger fractional free volume for both relaxations and a naturally a higher free volume expansion coefficient α_f/B. This is perhaps related to the molecular weight characteristics of the BASF PES which , because of its overall lower molecular weight, contains a larger number of chain ends which introduce a additional free volume. The nature of the chain ends is also important because the largely -OH terminations of the ICI PES are capable of hydrogen bonding with groups in the epoxy network. The largely -Cl terminations of the BASF PES are unable to interact and therefore one might expect that the fractional free volume surrounding a -Cl chain end is slightly greater than an -OH end group capable of molecular interaction.

Turning now to the activation energies of the β relaxations in table 4.7, it can be seen that the activation energy and derived quantities are less for the 30B blend showing that stress induced activation of segmental rotations is

marginally easier. This is an effect possibly connected with the increased fractional free volume in this blend.

4.1.6 Dielectric Spectroscopy

The dielectric spectra of the as cured 30I and 30B blends are shown in figure 4.8

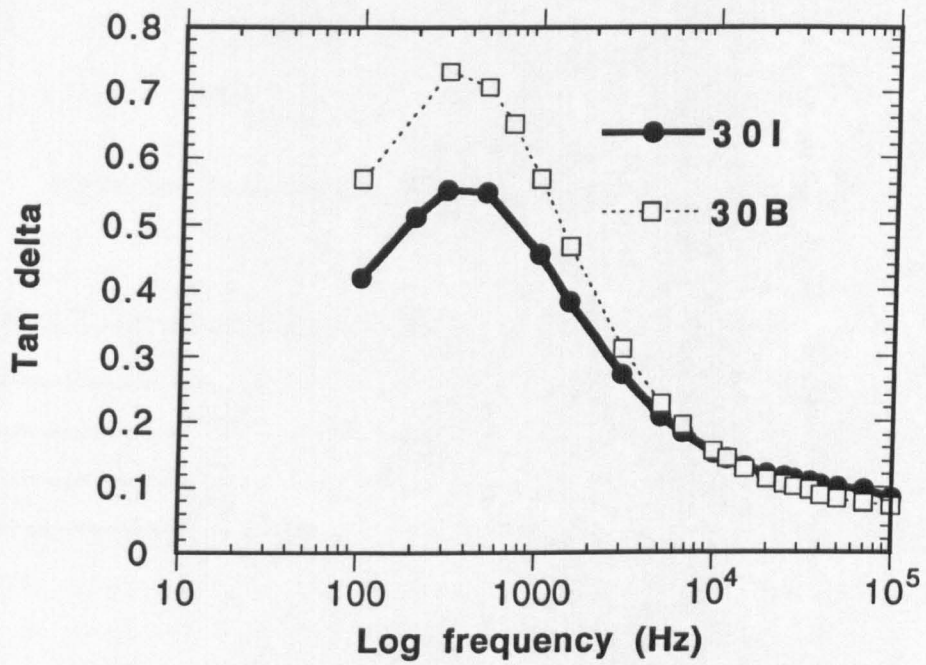

Figure 4.8: Dielectric spectra of as cured materials at 180°C

The spectra peak at similar frequencies but the 30B peak is the more intense. The peak is associated with the large scale chain motion of the lower temperature phase.

4.1.7 Impact Strengths

The impact energy-BDZ curves for the blends are shown in figure 4.9. From figure 4.9 and the critical strain energy release rates in table 4.7, it can be seen that the toughnesses are similar, and that G_{IC} is relatively low compared to other thermoplastic materials.

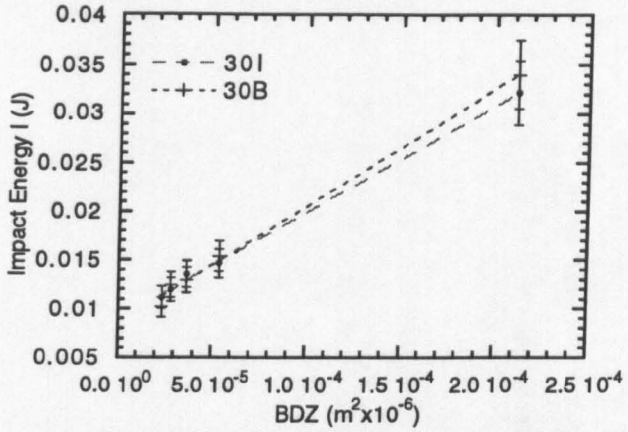

Figure 4.9: Impact energy plotted against BDZ for as cured blends

Table 4.7: G_{IC} values of as cured blends

Blend	$G_{IC}(J/m^2)$
30I	110
30B	120

4.2 Annealed Materials

4.2.1 Calorimetry

4.2.1.1 Data at 120°C

The heat capacity data for the ICI blends are shown in fig 4.10.

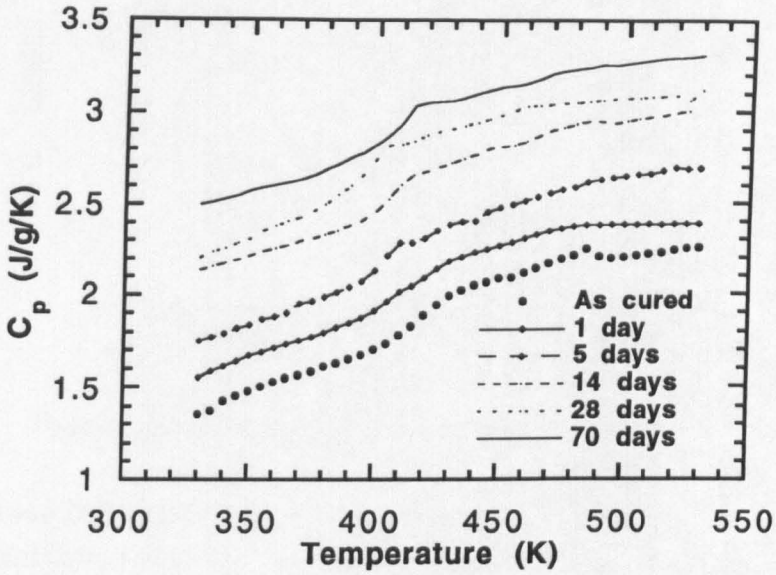

Figure 4.10: Heat capacity of 30I blend annealed at 120°C

The lower glass transformation region of the as cured material is quite broad and there appears to be some evidence of a small peak just before the onset. In the as cured material the high temperature phase shows some sign of physical ageing but it was not possible to recondition the material because had it been annealed above 180°C, the material would have degraded. Nevertheless, both glass transition regions are visible in the heat capacity curve. After annealing at 1 day the glass transitions become less well defined and 5 days is sufficient to render the upper transition barely visible but the lower transition remains in approximately the same position. At 14 days the upper transition is visible more clearly and remains so. The lower transition shifts slightly to lower temperature at 28 days but then shifts back at 70 days to its previous position but now has a broad tail.

The data for the BASF blend is shown in figure 4.11.

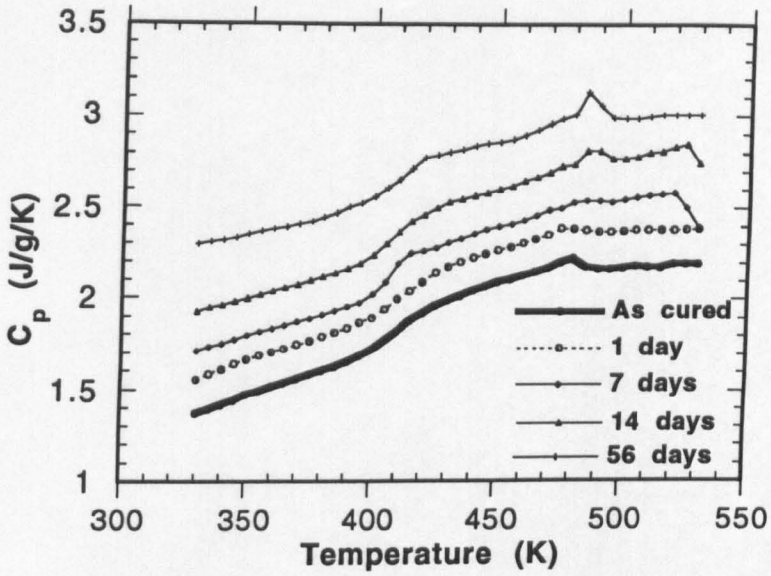

Figure 4.11: Heat capacity of 30B blend annealed at 120°C

The as cured 30B blend also exhibits some signs of physical ageing in the upper transition, still evident even after 1 day. The lower transition changes slightly in shape at 1 day but occupies a similar position to the as cured material. After 7 days the lower transition has become slightly more distinct but broadens again at 14 days with little change evident at 56 days. The upper transition has the physical ageing effect removed at 7 days but it reappears at 14 and 56 days.

4.2.1.2 Data at 180°C

The heat capacity data for the 30I blend are shown in figure 4.12.

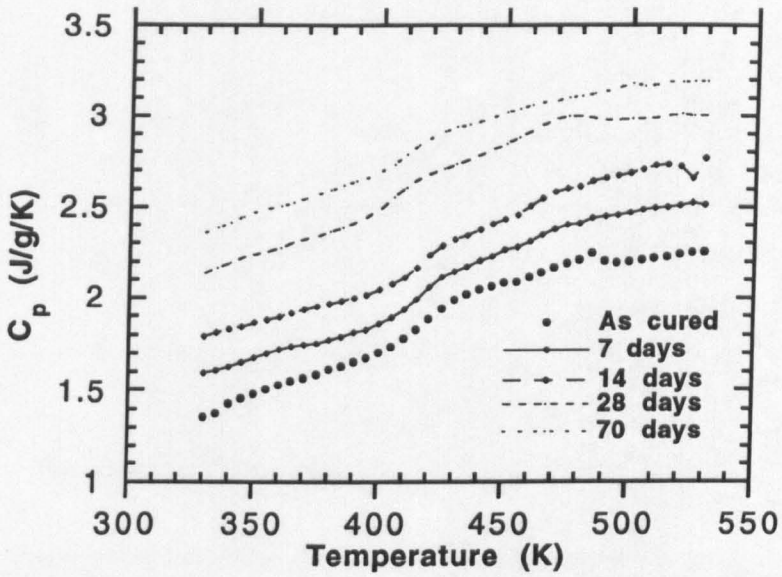

Figure 4.12: Heat capacity of 30I blend annealed at 180°C

The lower transition remains essentially unchanged until 28 days at which point it broadens and at 70 days it appears to have shifted slightly to higher temperature. However, during the annealing the height of the transition appears to become less while the upper transition gets stronger.

The heat capacity data for the 30B blend are shown in figure 4.13.

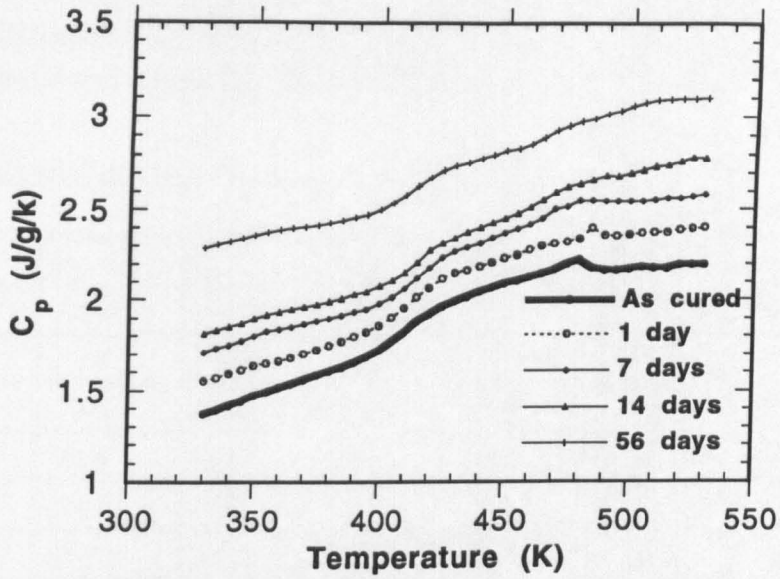

Figure 4.13: Heat capacity of 30B blend annealed at 180°C

There appears to be very little detectable change in the heat capacity curves of the 30B blend, except perhaps a small decrease in the height of the lower transition.

4.2.2 Mechanical Spectroscopy

4.2.2.1 Data at 120°C

The mechanical spectra for the 30I and 30B blends are shown in figures 4.14 and 4.15 respectively. The tan δ intensity and peak temperatures are shown in tables 4.7 and 4.8 for the 30I and 30B blends respectively.

Table 4.7: 30I Dynamic Mechanical Characteristics at 120°C

Time	T_β (°C)	I_β	$T_{\alpha 1}$(°C)	$I_{\alpha 1}$	$T_{\alpha 2}$(°C)	$I_{\alpha 2}$
0	-62.9	0.043	162.4	0.243	204	0.208
1 day	-71.7	0.056	160.5	0.200	200.4	0.154
7 days	-72.8	0.051	154.4	0.217	205.4	0.234
14 days	-74.4	0.05	147.8	0.195	200.4	0.196
28 days	-75.2	0.05	150.5	0.179	200.6	0.254
70 days	-77.7	0.042	152.3	0.14	194.9	0.163

Table 4.8: 30B Dynamic Mechanical Characteristics at 120°C

Time	T_β (°C)	I_β	$T_{\alpha 1}$(°C)	$I_{\alpha 1}$	$T_{\alpha 2}$(°C)	$I_{\alpha 2}$
0	-67.5	0.055	157.1	0.261	202.3	0.192
1 day	-64.8	0.059	152.2	0.209	194.6	0.223
7 days	-65.4	0.05	152.1	0.199	192.2	0.196
14 days	-67	0.04	150	0.210	198	0.192
28 days	-70	0.049	149.8	0.192	192.2	0.212
56 days	-75.3	0.047	142.2	0.192	192.2	0.215

Consider firstly the 30I blend. At 1 day the spectrum shows a shoulder to the left of the α_1 peak at about 120°C. The α_1 peak has also reduced in intensity. At 7 days the shoulder appears to have remerged with the α_1 relaxation although the relaxation has become broadened and reduced in temperature. At this point the α_2 peak has slightly increased in intensity. At 14 days the only effect seems to be some slight reductions in peak intensities and temperatures. At 28 days a second shoulder appears to the left of the α_1 peak which develops fully into a separate relaxation peak which appears at 120°C by 70 days.

TEXT BOUND INTO THE SPINE

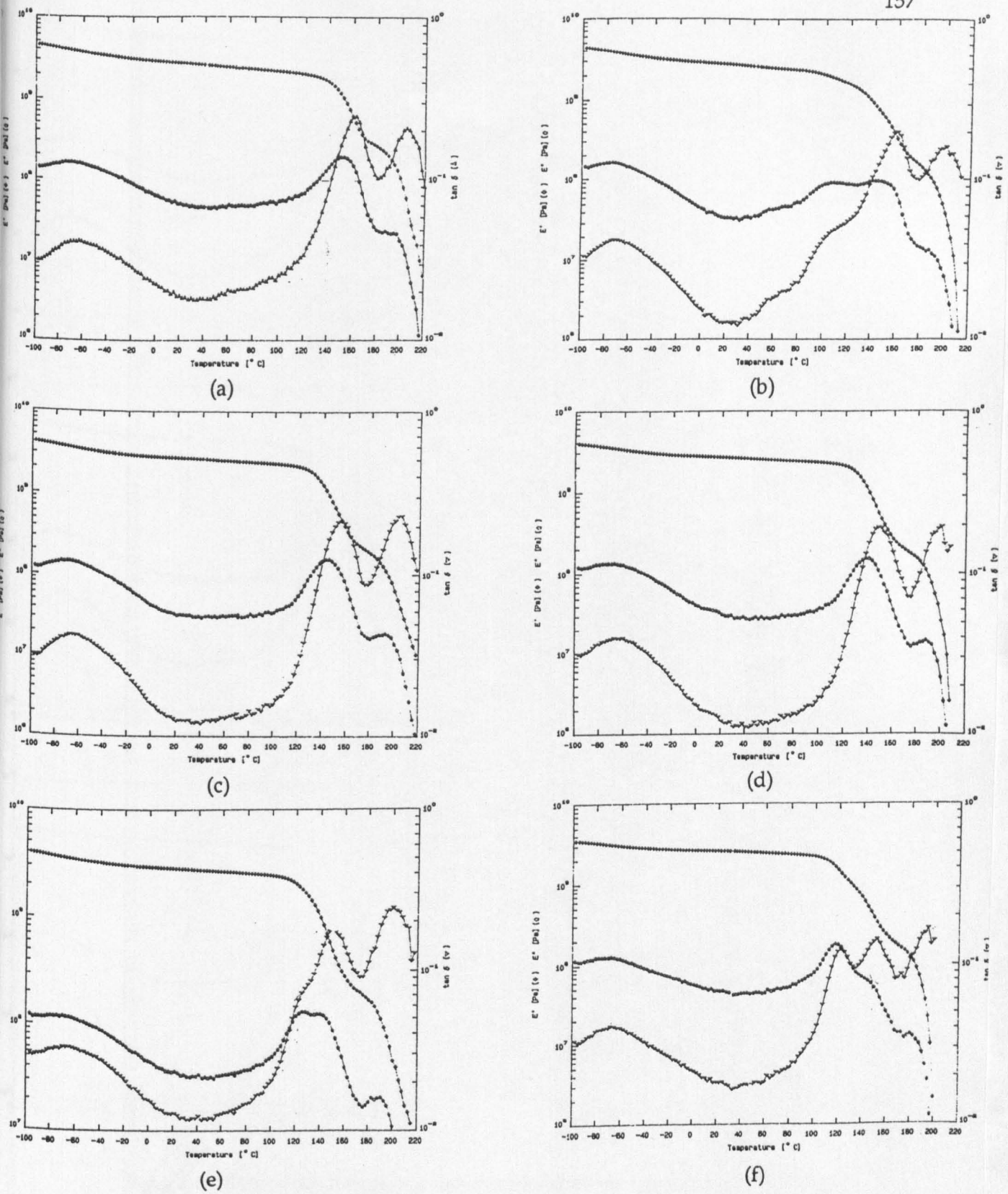

Figure 4.14: Dynamic mechanical spectra of 30I blend annealed at 120°C at (a) unannealed (b) 1 day (c) 7 days (d) 14 days (e) 28 days (f) 70 days

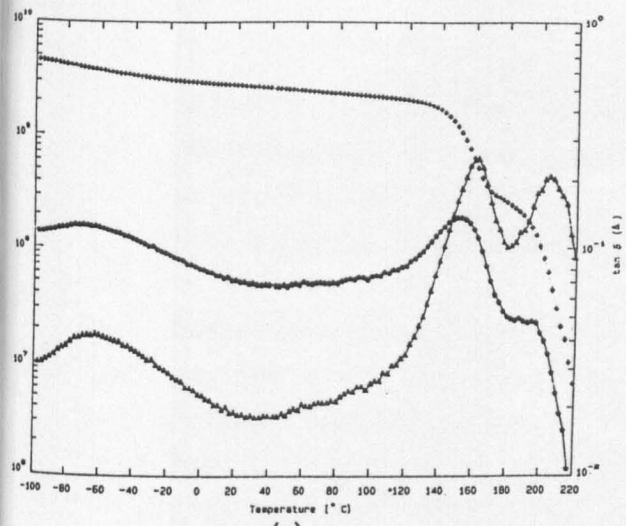

(a)

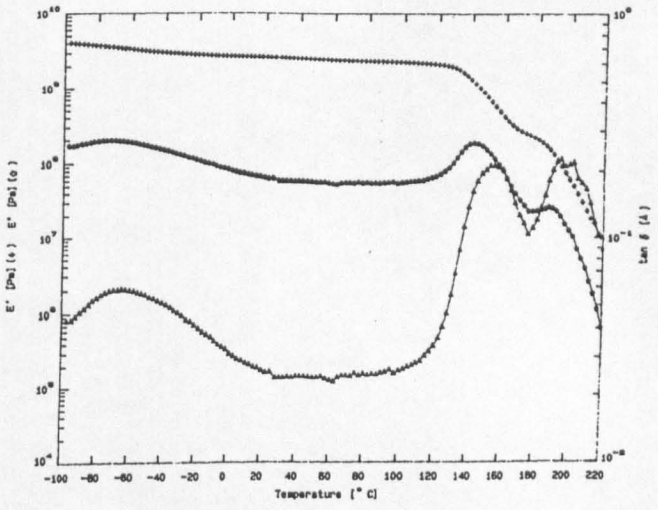

(b)

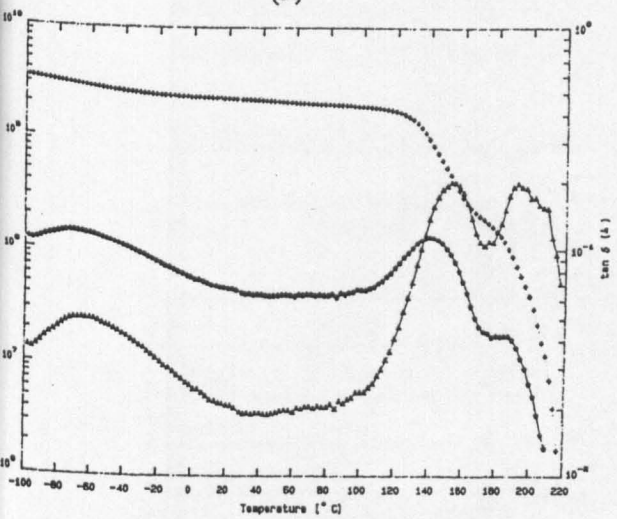

(c)

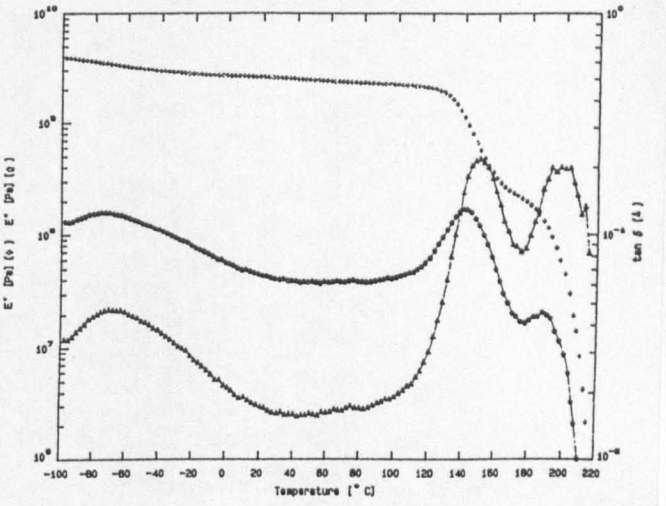

(d)

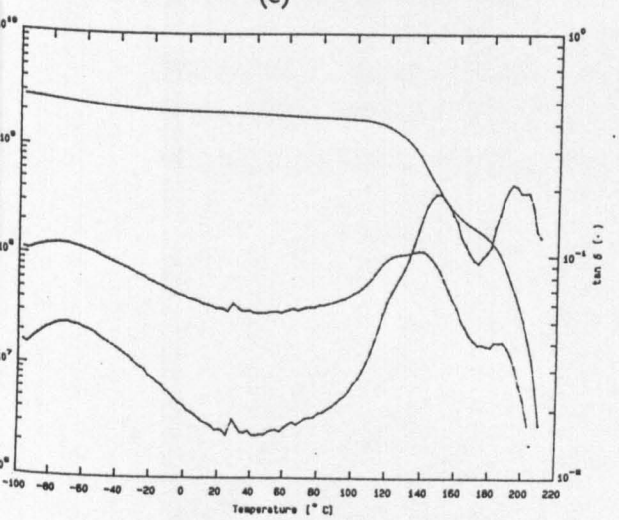

(e)

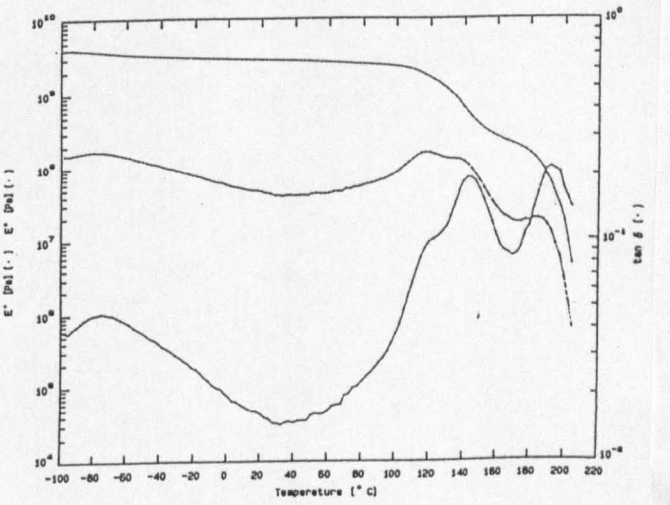

(f)

Figure 4.15: Dynamic mechanical spectra of 30B blend annealed at 120°C at (a) unannealed (b) 1 day (c) 7 days (d) 14 days (e) 28 days (f) 56 days

In the 30B blend there isn't a shoulder at 1 day but the α_1 peak has broadened relative to its initial shape suggesting perhaps that the shoulder has already appeared and merged. At 28 days a shoulder also appears to the left of the α_1 peak but is not as intense as in the 30I blend, perhaps because it is retarded.

In both blends the intensities of the α_1 and α_2 relaxations increase and decrease at various stages and the same is true of the peak temperatures although these ultimately decrease at longer times. The response of the β relaxation also involves variations in the intensity but there is a trend for the peak temperature to decrease as annealing proceeds. The activation energies after various ageing times are fairly constant but there are large changes in the activation entropy as shown in tables 4.9 for the 30I and 30B blends.

Table 4.9: β Relaxation Activation Energy Data

Time	30I E_a (kJ/mol)	30BE_a (kJ/mol)	30I ΔS (J/K/mol)	30B ΔS (J/K/mol)
0	58.5	54.6	57.03	53.4
1 day	62.6	58.5	77.3	69.7
7 days	61.7	63.2	65.3	73.4
14 days	67.7	68.4	109.95	98.6
28 days	54.2	56.6	34.7	56.2

The activation entropy is a measure of the degree of molecular cooperativity of the CH_2-CH(OH)-CH_2 -CH-O segmental relaxation and clearly this is varying significantly during the annealing process.

4.2.2.2 Data at 180°C

The mechanical spectra for the 30I and 30B materials are shown in figures 4.16 and 4.17 respectively and the mechanical spectroscopy data are shown in tables 4.10 and 4.11 for the 30I and 30B blends respectively.

Table 4.10: 30I Dynamic Mechanical Characteristics at 180°C

Time	T_β (°C)	I_β	$T_{\alpha 1}$(°C)	$I_{\alpha 1}$	$T_{\alpha 2}$(°C)	$I_{\alpha 2}$
0	-62.9	0.0426	162.4	0.24	204	0.21
1 day	-77.7	0.042	155.3	0.22	200	0.13
7 days	-74.9	0.037	158.2	0.22	189	0.17
14 days	-74.9	0.028	158	0.14	195	0.27
28 days	-74.8	0.023	158	0.09	210	0.33
70 days	-75.4	0.033	159	0.06	205	0.24

Table 4.11: 30B Dynamic Mechanical Characteristics at 180°C

Time	T_β (°C)	I_β	$T_{\alpha 1}$(°C)	$I_{\alpha 1}$	$T_{\alpha 2}$(°C)	$I_{\alpha 2}$
0	-67.5	0.055	157.1	0.26	202.3	0.19
1 day	-70.1	0.048	152	0.24	197	0.2
7 days	-71	0.047	158	0.21	———	———
14 days	-72.8	0.042	151	0.17	196	0.26
28 days	-77.5	0.039	152	0.12	207	0.37
70 days	-85.2	0.039	144	0.11	202	0.33

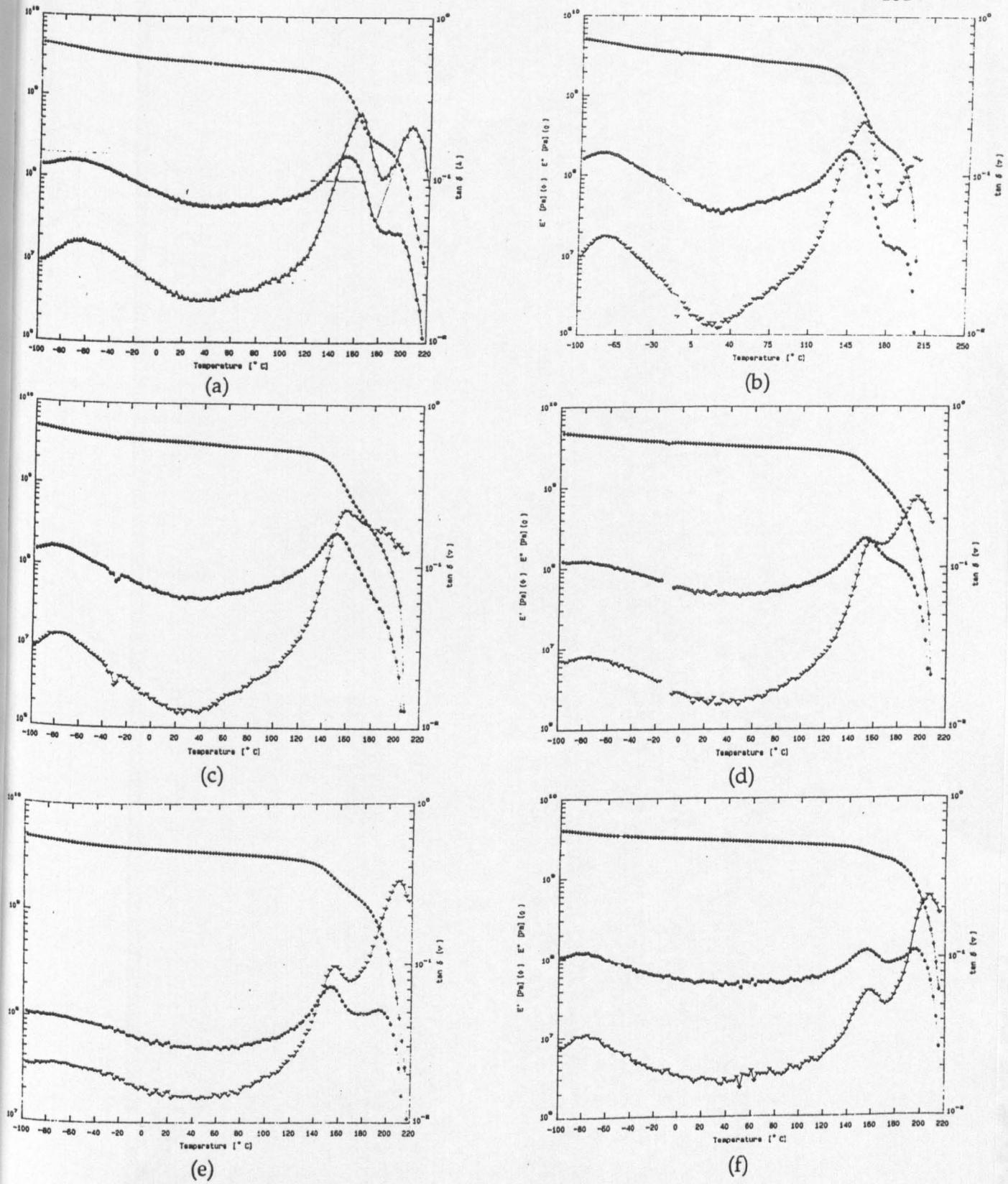

Figure 4.16: Dynamic mechanical spectra of 30I blend annealed at 180°C at (a) unannealed (b) 1 day (c) 7 days (d) 14 days (e) 28 days (f) 70 days

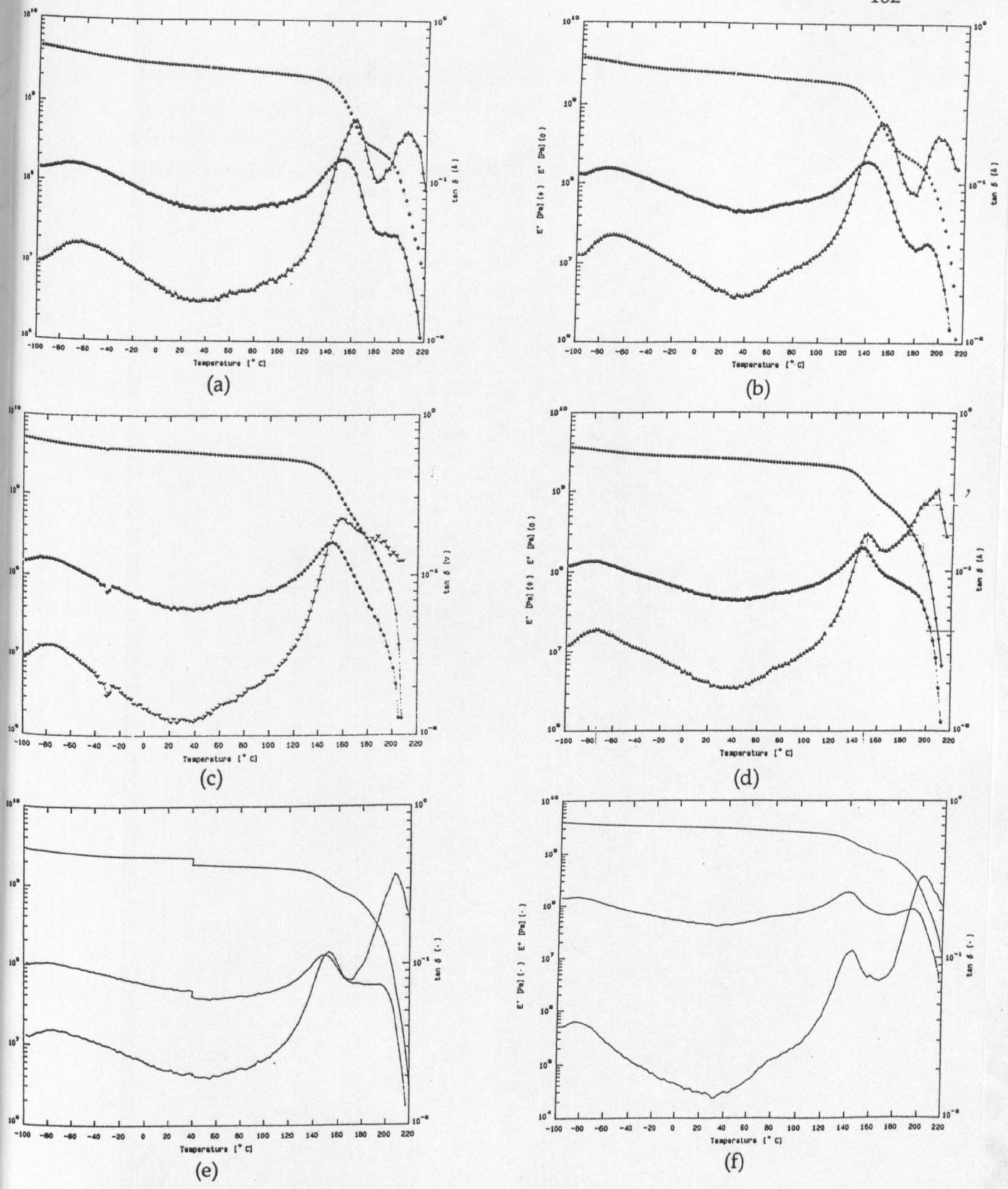

Figure 4.17: Dynamic mechanical spectra of 30B blend annealed at 180°C at (a) unannealed (b) 1 day (c) 7 days (d) 14 days (e) 28 days (f) 56 days

The responses of the systems are similar. In the 30I blend the temperature of α_1 remains approximately the same but its intensity reduces dramatically. At the same time the temperature of α_2 fluctuates considerably but the intensity increases significantly. The same applies to the 30B blends.

4.2.3 SEM Micrographs

4.2.3.1 Data at 120°C

The micrographs of the surfaces of the annealed 30I blend are shown in figure 4.18 where the morphology appears to undergo virtually no change. The same applies to the 30B blends in figure 4.19.

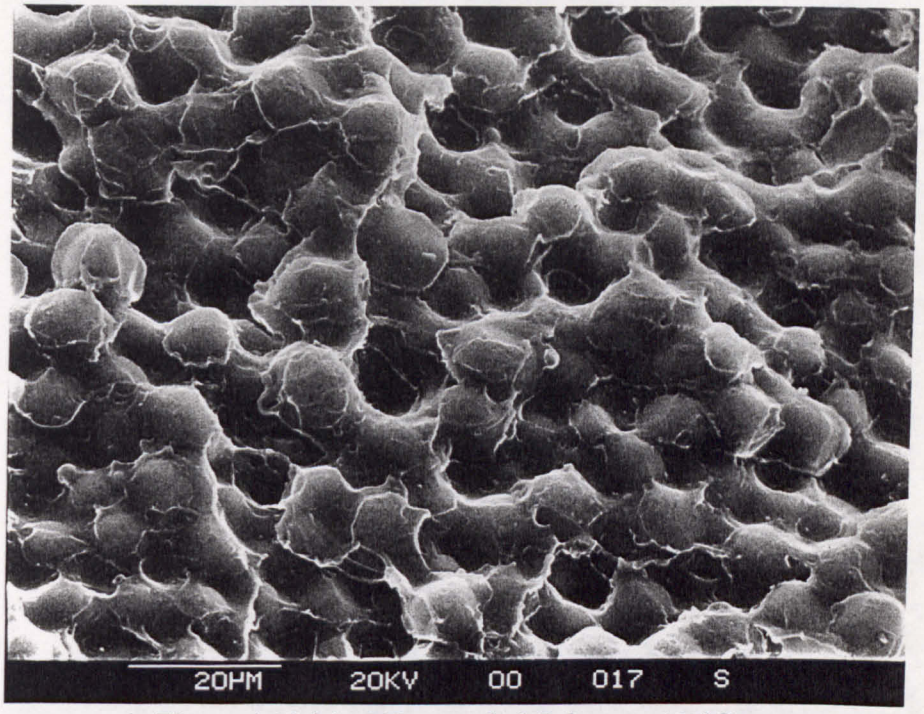

Figure 4.18 (a): 30I annealed 7 days at 120°C

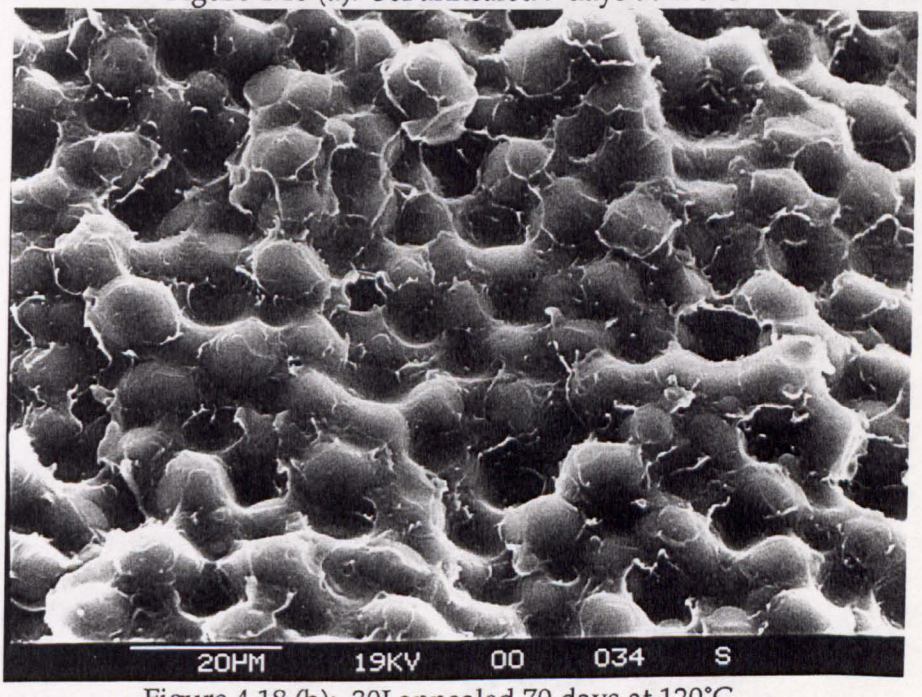

Figure 4.18 (b): 30I annealed 70 days at 120°C

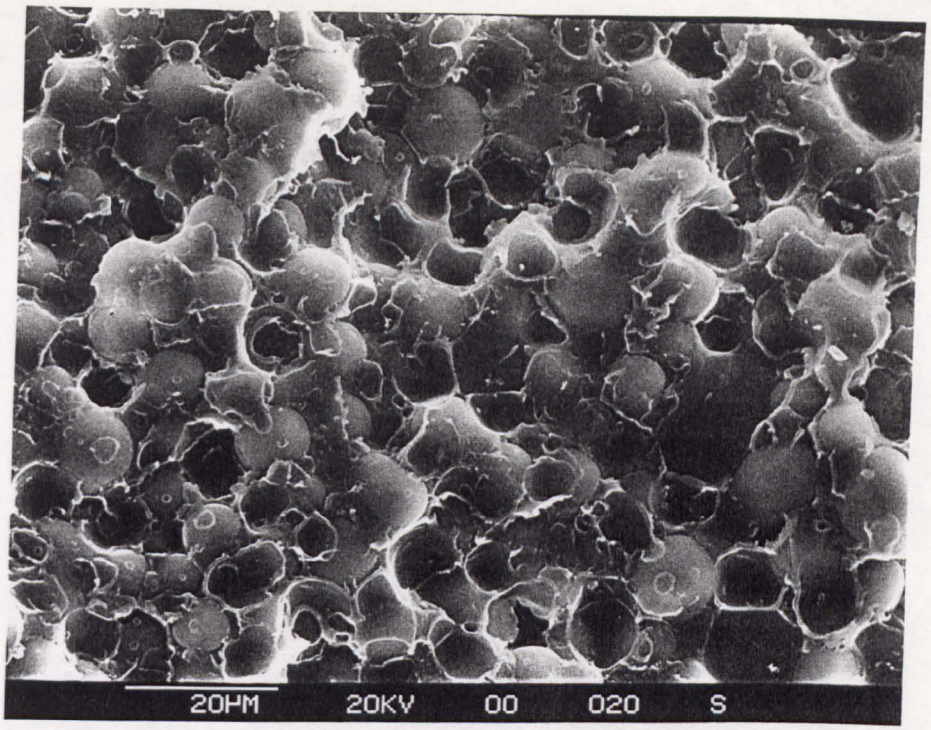

Figure 4.19 (a): 30B annealed 7 days at 120°C

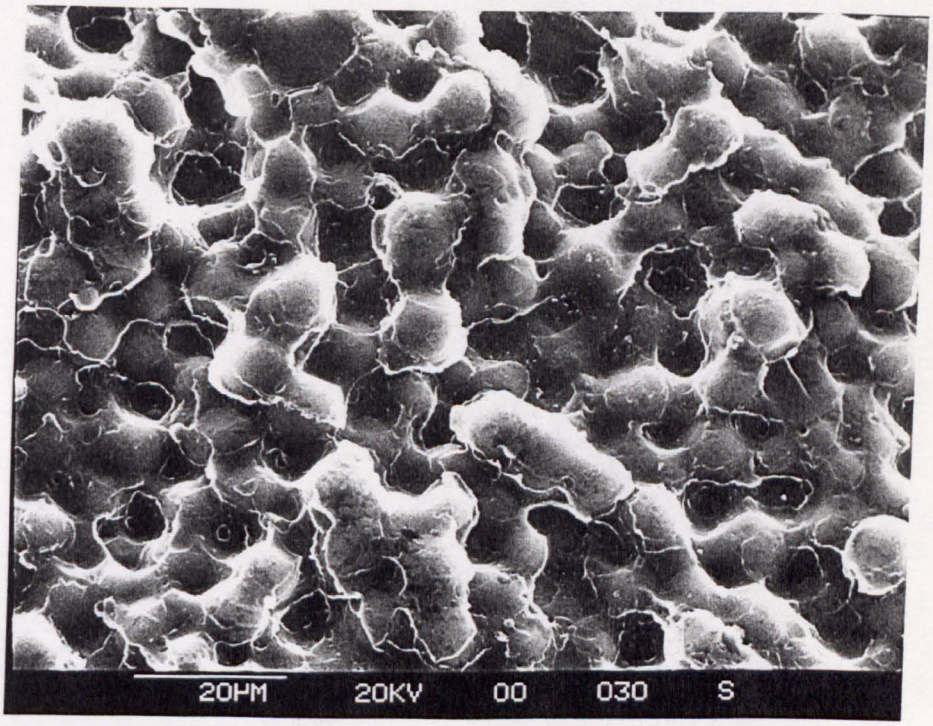

Figure 4.19 (b): 30B annealed 56 days at 120°C

4.2.3.2 Data at 180°C

The micrographs of 30I and 30B blends annealed at 180°C are shown in figures 4.20 and 4.21 respectively. There is little detectable change.

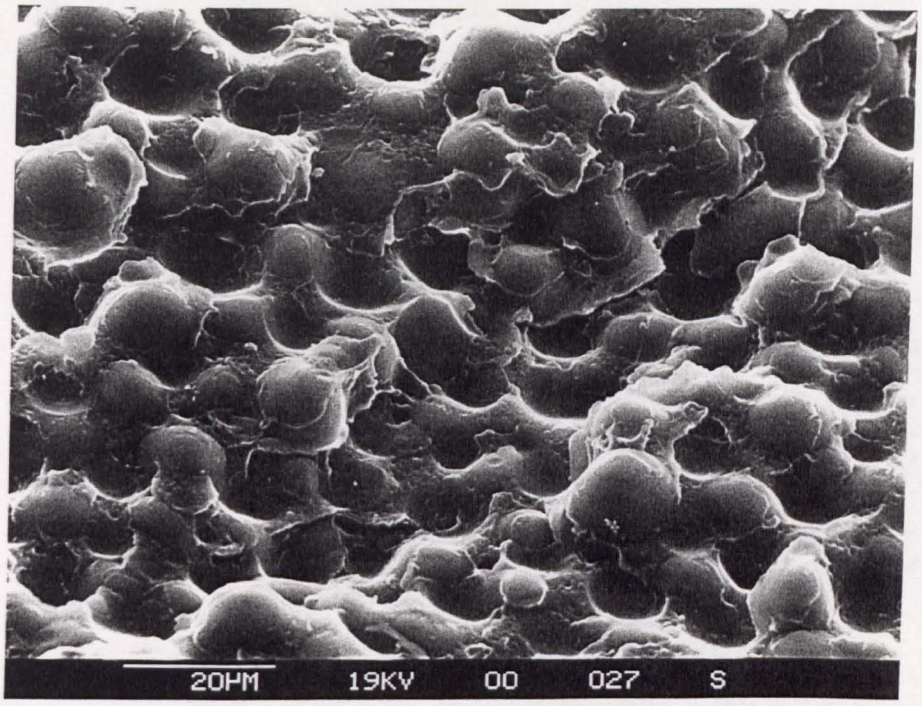

Figure 4.20 (a): 30I annealed 7 days at 180°C

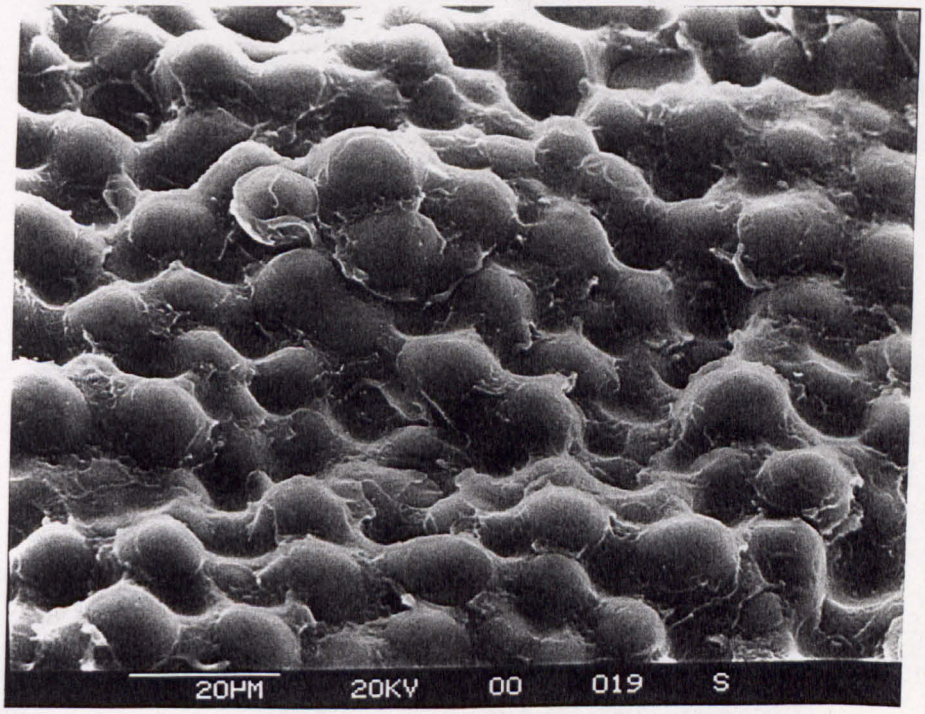

Figure 4.20 (b): 30I annealed 70 days at 160°C

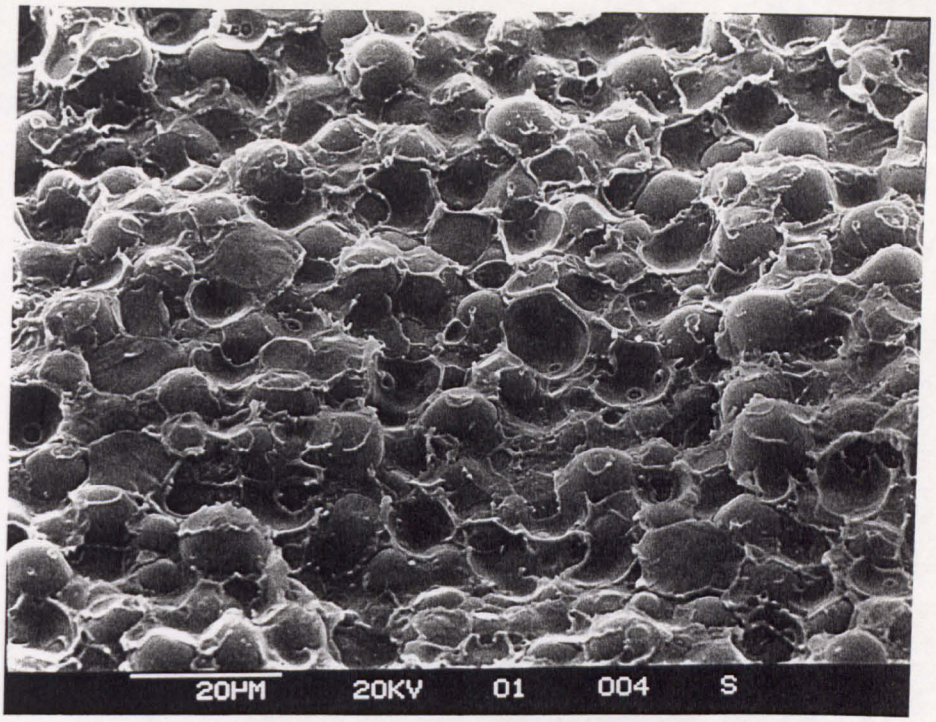

Figure 4.21 (a): 30B annealed 7 days at 180°C

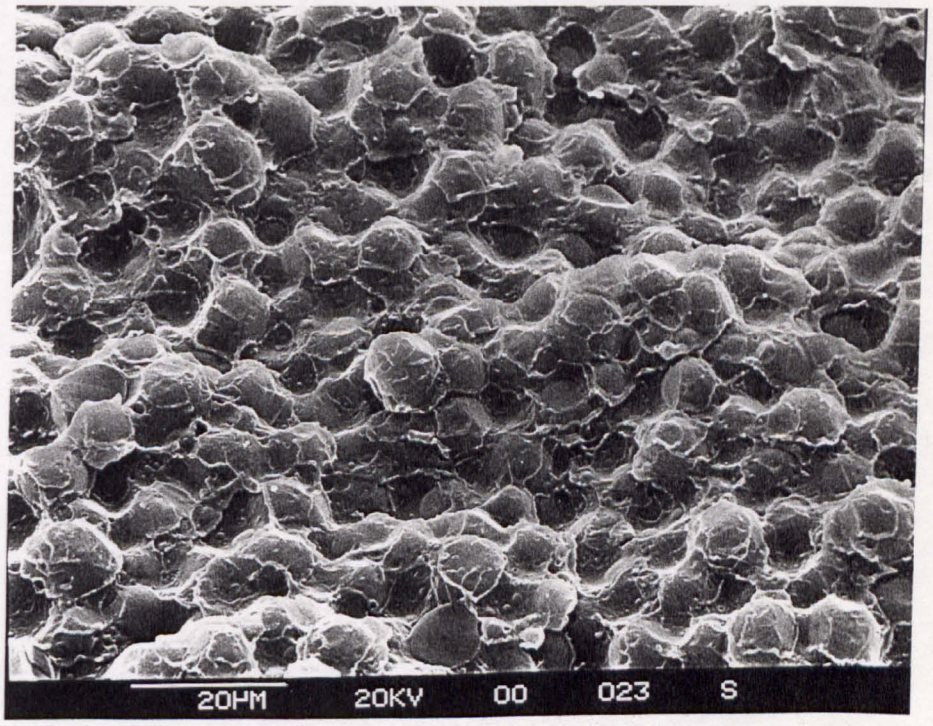

Figure 4.21 (b): 30B annealed 56 days at 180°C

4.2.4 Dielectric Spectroscopy

4.2.4.1 Data at 120°C

The spectra obtained for 30I and 30B are shown in figures 4.22 and 4.23 respectively.

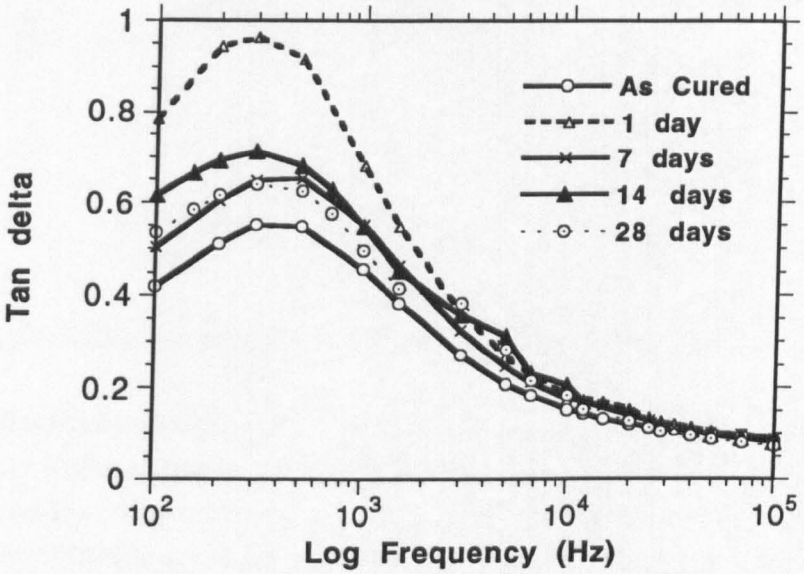

Figure 4.22: Dielectric spectra of annealed 30I blend collected at 120°C

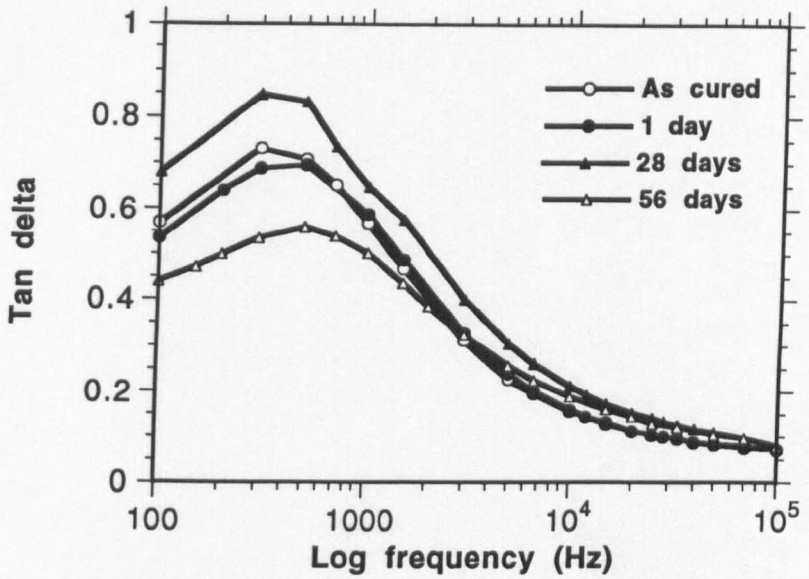

Figure 4.23: Dielectric spectra of annealed 30B blend collected at 120°C

Consider firstly the 30I blend. The initial response at 1 day is for the peak intensity to dramatically increase and then dramatically decrease at 7 days. This is followed by a slight increase at 14 days but then at 28 days the peak intensity settles to a similar value observed at 7 days.

In the 30B material at 1 day the peak intensity is similar to the as cured material but increases dramatically at 28 days followed by a dramatic decrease at 56 days.

4.2.4.2 Data at 140°C

The spectra obtained for 30I and 30B are shown in figures 4.24 and 4.25 respectively.

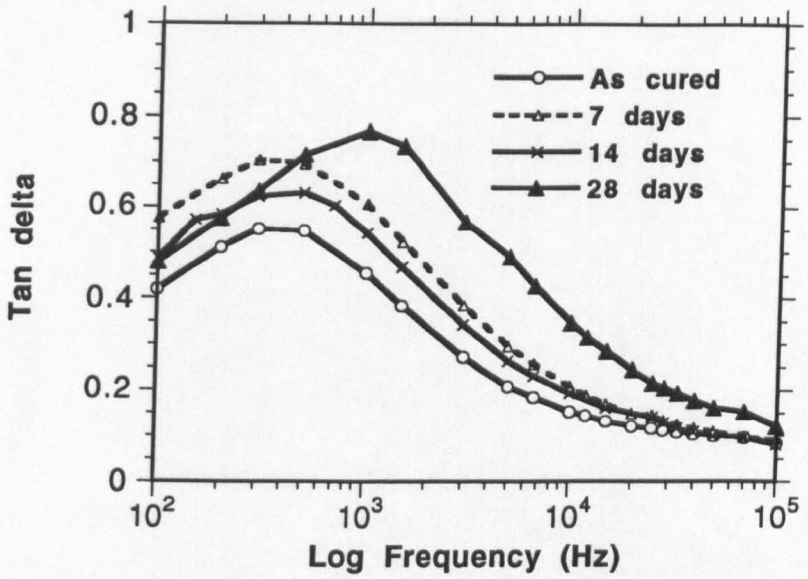

4.24: Dielectric spectra of annealed 30I blend collected at 140°C

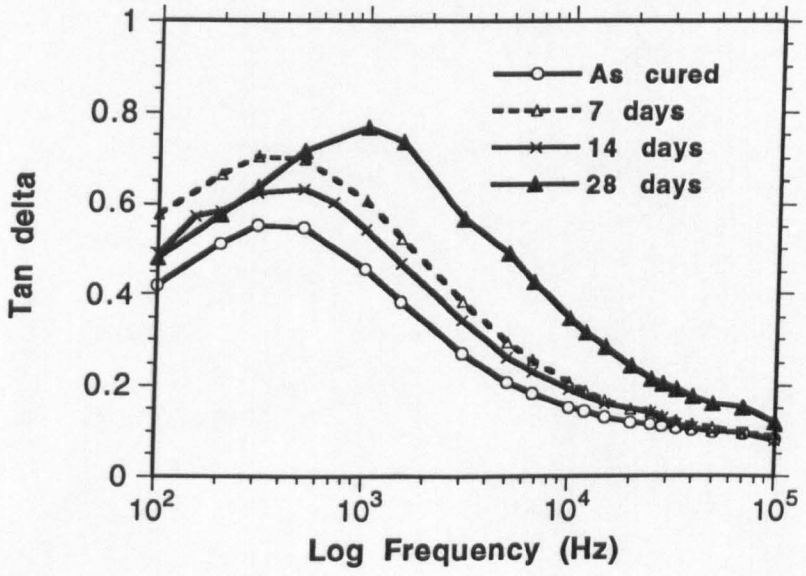

4.25: Dielectric spectra of annealed 30B blend collected at 140°C

4.2.4.3 Data at 160°C

The spectra obtained for 30I and 30B are shown in figures 4.26 and 4.27 respectively.

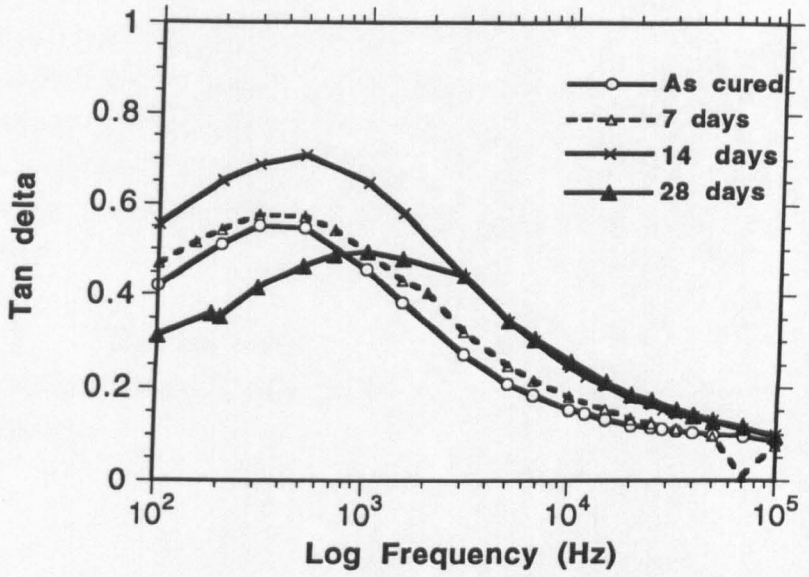

Figure 4.26: Dielectric spectra of annealed 30B blend collected at 160°C

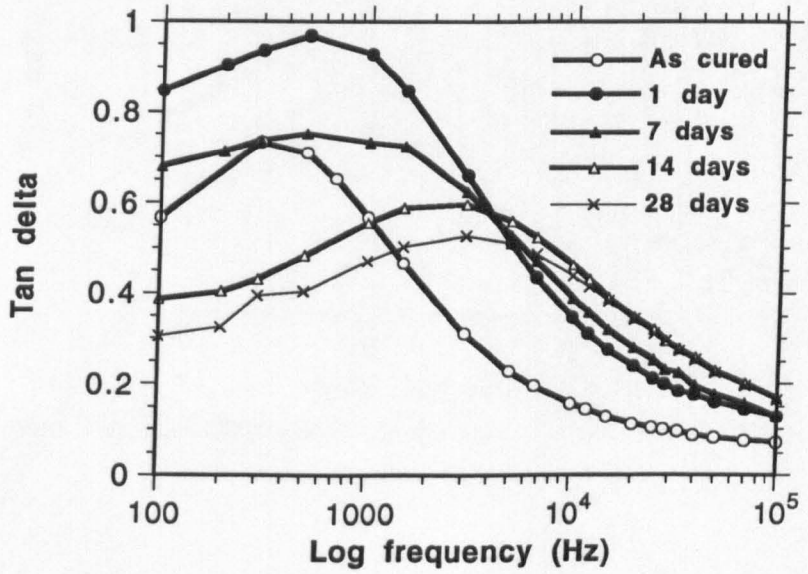

Figure 4.27: Dielectric spectra of annealed 30B blend collected at 160°C

In the 30I material annealing at 7 days increases the intensity by only a small amount but the peak broadens slightly. At 14 days the intensity increases dramatically and the peak broadens together with a slight shift to higher frequency. At 28 days the peak intensity drops to a value below the as cured material and shifts to higher frequency.

In the 30B material after 1 day there is a drastic increase in intensity and a s light shift to higher frequency and broadening of the peak. At 7 days the peak intensity drops but the peak is still very broad. At 14 days the peak drops in intensity to less than the as cured material and shifts to higher frequency. At 28 days the same peak appears to have only reduced further in intensity.

4.2.4.4 Data at 180°C

The spectra obtained for 30I and 30B are shown in figures 4.28 and 4.29 respectively.

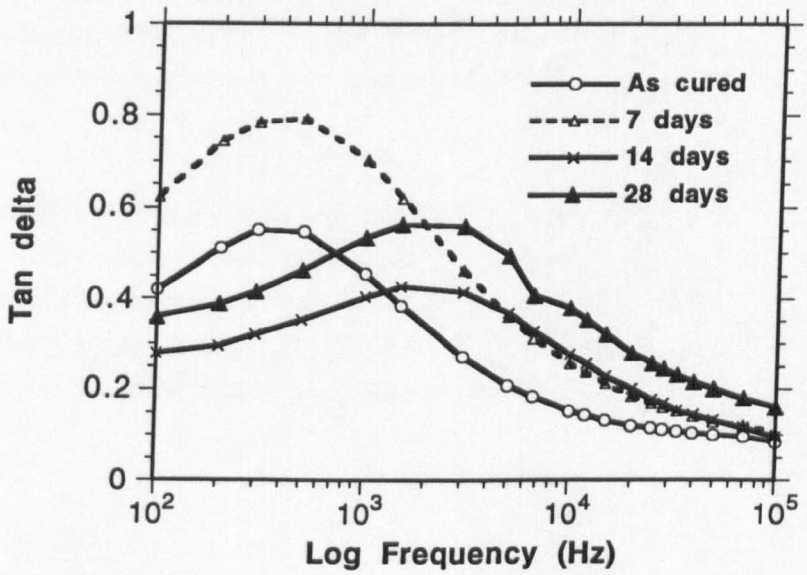

Figure 4.28: Dielectric spectra of annealed 30I blend collected at 180°C

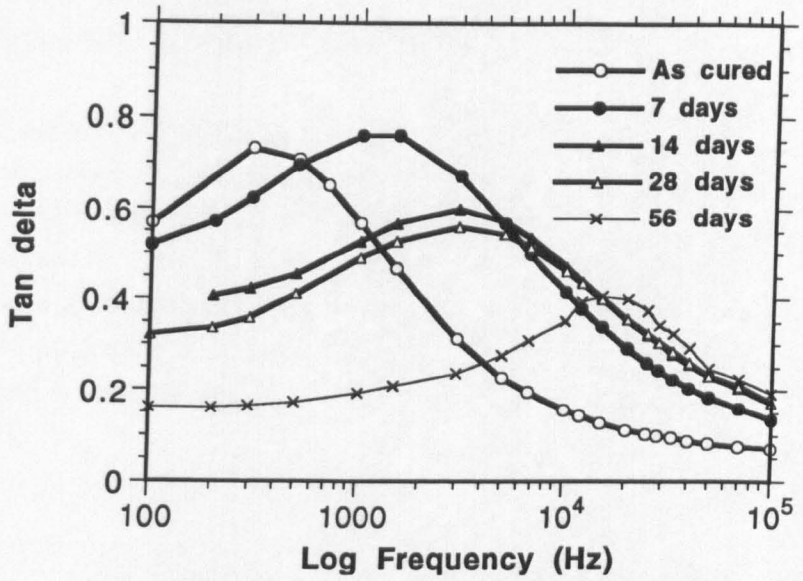

Figure 4.29: Dielectric spectra of annealed 30B blend collected at 180°C

In the 30I blend after 7 days the intensity of the peak increases greatly and the peak broadens but maintains a similar peak frequency. At 14 days the peak has reduced in intensity to less than the as cured material. The peak then increases in intensity and broadness at 28 days but maintains its peak position.

In the 30B blend at 7 days the peak shifts to higher frequency but the intensity increases by only a small amount. At 14 days the intensity reduces but the peak shifts to higher frequency. At 28 days the peak reduces in intensity but maintains a similar peak position and then at 56 days the peak intensity drops sharply but the peak frequency increases sharply.

4.2.5 Impact Strengths

Typical impact energy-BDZ plots are shown in figure 4.30. The errors are reasonable though they suggest that for the annealing times shown there is little actual difference between the blends at any temperature.

This is in fact confirmed from the variations in G_{IC} with annealing as shown for each material in tables 4.16 to 4.19 for temperatures from 120°C to 180°C respectively. At any particular temperature, the differences between the two materials as they are annealed is not significant but the decrease in the critical strain energy release rate with annealing agrees with other results which indicate microscopic changes. There seems to be little pattern in the variations of G_{IC} with temperature.

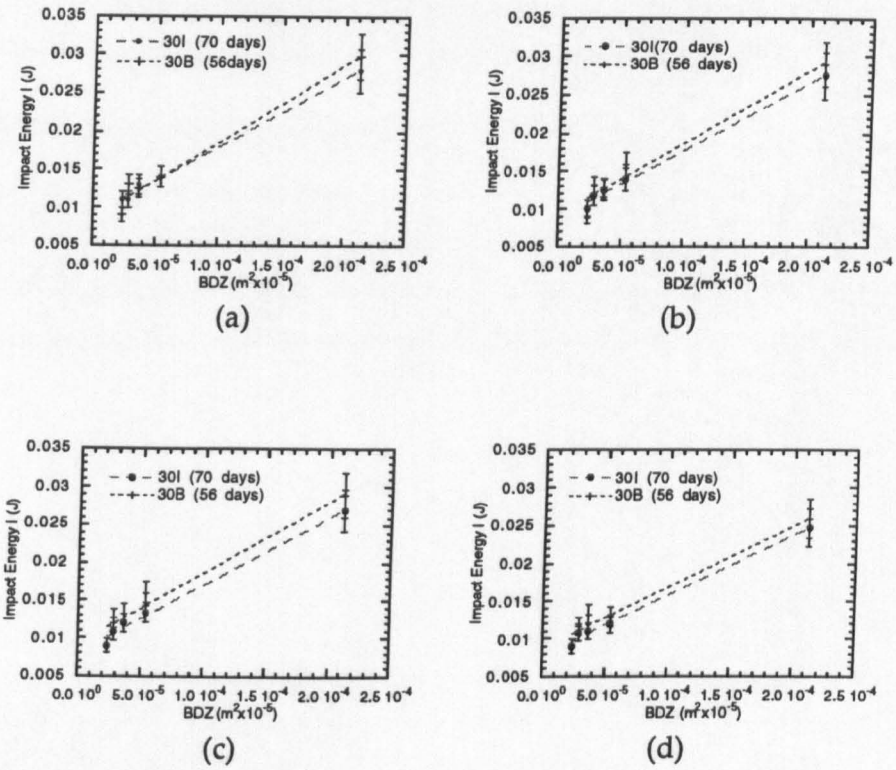

Figure 4.30: Impact energy plotted against BDZ for blends at selected annealing times. (a) 120°C (b) 140°C (c) 160°C (d) 180°C

Table 4.16: G_{IC} changes with annealing at 120°C

$G_{IC}(J/m^2)$				
Blend	As cured	28 days	56 days	70 days
30I	110	90	———	90
30B	120	100	100	———

Table 4.17: G_{IC} changes with annealing at 140°C

$G_{IC}(J/m^2)$				
Blend	As cured	28 days	56 days	70 days
30I	110	94	———	89
30B	120	100	93	———

Table 4.18: G_{IC} changes with annealing at 160°C

$G_{IC}(J/m^2)$				
Blend	As cured	28 days	56 days	70 days
30I	110	94	———	89
30B	120	105	92	———

Table 4.19: G_{IC} changes with annealing at 180°C

$G_{IC}(J/m^2)$				
Blend	As cured	28 days	56 days	70 days
30I	110	100	———	80
30B	120	100	80	———

4.3 Discussion

4.3.1 As Cured Materials

Although the heat capacity curves of the two blends are similar, the enthalpy change over the glass transition range is higher in the 30B blend. Since the change in enthalpy is given by $\Delta H = \Delta U + P\Delta V$, in passing through the glass transformation the enthalpy gained is due to a combination of internal energy increases and a change in the specific volume (density) of the material as it goes from glass to rubber. The latter quantity is rather dependent upon the degree of crosslinking and it is to be expected that the crosslinks will keep the material of higher crosslinked density more tightly packed in the rubbery state (Brahatheeswaran and Gupta, 1992). Therefore a lower crosslink density material passing through the glass transition will expand more than when the same material is more highly crosslinked. The 30I and 30B blends appear to be similar calorimetrically except for the greater enthalpy change of the latter, which may be associated with a greater volume change in the 30B blend due to lower crosslinking. The blends are of the same composition and were cured according to the same cure schedules but the glass transition temperatures obtained from DSC and the peak relaxation temperatures from dynamic mechanical spectroscopy are slightly higher in ICI blend, which also has a marginally higher apparent Arrhenius activation energy. The last two factors by themselves mean very little but a W-L-F analysis of the mechanical spectra shows also that the crosslink density or molecular weight of the lower temperature phase in the 30I material is marginally greater. The lower temperature phase is presumably primarily due to the epoxy phase. The constants C_1 and C_2 from the W-L-F analysis also indicate that the higher temperature phase of the 30I blend has a slightly higher molecular weight, assuming that in this phase there is a minor amount of crosslinked epoxy. This last result makes some sense since the ICI PES is of higher molecular weight. Fractional free volumes of the low and high temperature phases of the 30B blend are also larger than in the 30I material. With regard to the morphology of the blends, it seems possible that the lower molecular weight of the BASF PES may be the cause of the reduction in the crosslink density of the lower temperature phase and because of its lower molecular weight will be able to diffuse faster through a network whose reaction it has also retarded slightly. This may account for the large particles observed in the SEM micrographs. Clearly however, the process of phase separation in these materials is quite complex and at the cure temperature the higher temperature PES phase also physically ages slightly.

The morphology of a two phase blend is vitally important in determining its mechanical properties and a good degree of interphase mixing is required for significant stress transfer to occur across the interface without particles debonding. A typical density profile for two phases separated by an interface is shown in figure 4.31.

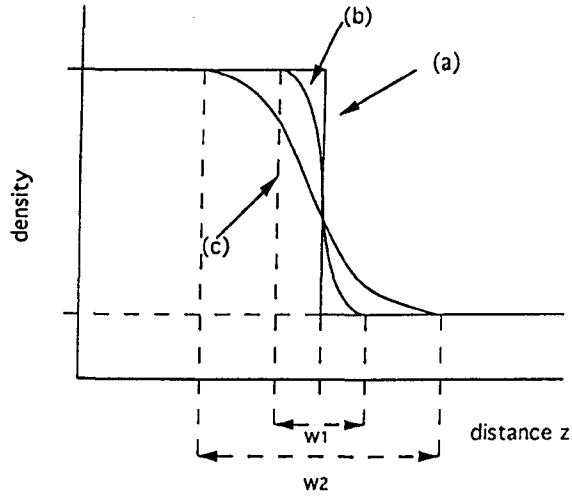

Figure 4.31: Typical interfacial density profile: (a) no interface (Chandler, 1987) (b) small degree of mixing at the interface (c) large degree mixing at the interface. The quantity w is the width of the interface which becomes larger as the polymers become more compatible.

The diagram shows that with no mixing at all 4.31(a)(an ideal case usually) there is a sharp boundary and a discontinuity in the density but in many polymer blends the change in density and therefore composition is continuous as in figures 4.31(b) and 4.31(c) and it is possible to characterise the interface by a width w. When the relative repulsions between the components is small (corresponding to low interfacial tension) the interphase width can be large, several nm, and in a finely dispersed system the amount of material mixed in the interfacial region can contribute significantly to the mechanical properties even if the bulk phases are quite pure. For a coarse dispersion however the smaller contact area even if the interphase width is the same as in a finely dispersed system, means a reduction in mechanical performance. The SEM micrographs of the as cured material show that the morphologies of both blends are different. The morphology of both blends is characterised by particles of ca.10- 15μm in diameter. This particle size is quite large compared to those reported for tough systems, typically 1-2μm

(Hedrick et al, 1991, Almen et al, 1988) but have been observed to be 2-4μm in two phase blends which were not tough (Bucknall and Partridge, 1983, 1986). Clearly the particle size is exceptionally large so that toughness is not really to be expected as indeed the G_{1C} values of table 4.7 show. However, the heat capacity curves show a broad transition in the lower temperature phase, which is presumably the epoxy phase. This broadness is characteristic of some degree of mixing but possibly only within the epoxy phase caused perhaps by rapid crosslinking preventing some of the PES from phase separating. The dynamic mechanical spectra suggest that the phases have similar volume fractions but this is not clear from the SEM micrographs, where the bulk of the microstructure appears to be particulate or from the heat capacity where the change over the glass transition region of the higher temperature phase (PES) is narrow. It was not possible to quantitatively analyse the PES composition of the matrix and particles. However, when the blends fracture the particles debond quite cleanly from the matrix, suggestive of a weak interface, narrow density profile and high interfacial tension between the phases.

The morphology does not indicate any detectable differences between the blends despite the differences in the molecular weights and chain terminations of the PES but the effect of these may be more important during the annealing of the blends.

4.4.2 Annealed Materials

During annealing the calorimetric curves show several interesting features. The glass transitions of the blends undergo changes when annealed and at 120°C the physical ageing peak in the high temperature phase of the 30I blend disappears at short times presumably due to a diffusional process, since the ageing effect cannot be erased at 120°C because this temperature is below the high temperature phase glass transition. At longer annealing times at this temperature it is possible to observed what appears to be an additional glass transition at around 380K (~100°C), possibly due to a third phase. This coincides with the appearance of a third relaxation in the dynamic mechanical spectrum of the 30I blend at 70 days and at this time the three relaxations appear to have similar intensities and perhaps similar volume fractions. The BASF blends respond similarly except that signs of physical ageing are retained throughout the annealing at 120°C and at 56 days it is also possible to

see what may be a possible third glass transition in the heat capacity curve and an additional relaxation peak in the DMA spectrum.

At other annealing temperatures the response of the ICI and BASF systems in terms of heat capacity and mechanical spectroscopy is similar. In all cases there is clearly a great deal of dynamic change as presumably the microscopic physical structure changes. The changes at the microscopic level are also revealed by the β relaxation activation energy data of table 4.9, which illustrate through the activation entropy changes that there is a great deal of change at a local level during annealing. The activation energy quantities for the annealed materials are not shown simply because they show the same variety of variations and only show that there are significant changes occurring at a microscopic level. Changes in the intensity of the mechanical spectra can be related to varying phase volume and/or volume fraction. The mechanical spectroscopy results could be interpreted as due to diffusion of phase mixed PES in the epoxy phase into the PES phase, thereby reducing the specific volume of the epoxy phase and accounting for the decrease in the α_2 relaxation intensity as the volume fraction is depleted by the departure of some of the PES.

There is clearly a driving force for the evolution of the blend properties towards a more stable thermodynamic state that differs considerably from the starting condition. In the as cured materials comment was made that the glass transitions appeared broad, characteristic of interphase mixing but this is probably as a result of the gelation of the epoxy trapping some of the thermoplastic phase in the network before it is able to diffuse away and form a more energetically or entropically stable morphology. Annealing simply allows the phase separation to continue very slowly and these changes are observable in the heat capacity curves as variations in the width and height of the glass transition ranges. These changes must be associated with compositional and density changes within the bulk phases and at the interfacial region where phase mixing may occur. An examination of the mechanical spectra clearly shows that there are major changes occurring to the microscopic structure and there must be a large thermodynamic driving force for the changes towards equilibrium morphologies characteristic of the annealing temperature, though the rates of change are inevitably slowed down by the network structure. This makes apparent the fact that as these systems cure there are two competing critical phenomena: the phase

separation of the PES and epoxy phases as the molecular weight of the epoxy increases and the gelation of the epoxy. The rate of chemical reaction of the short monomer and hardener molecules probably occurs much faster than the time allowed for the complete phase separation at the curing temperature. Clearly the as cured structure after curing at 180°C is not the same as the material after annealing at the same temperature. These changes must presumably involve a reduction in the degree of interphase mixing and a reduction in the interphase width as the systems seek to minimise the surface energies and tensions of the phases.

Despite the dramatic microscopic changes that the mechanical spectroscopy results seem to suggest, there is no evidence of these changes in the morphology of the fracture surfaces of the 30I and 30B blends, as the micrographs show. However, in the dielectric data, which probe the α_2 relaxation of the epoxy phase, this relaxation is reduced in intensity during annealing at 120°C but retains its peak position.. In the mechanical spectra the mechanical α_2 relaxation also reduced in intensity but shifts to a lower temperature by 10°C relative to its starting temperature of 157°C. The reduction in intensity in the dielectric relaxation agrees with the mechanical relaxation, suggesting a depletion of the PES content of the epoxy phase. At 140°C, 160°C and 180°C the dielectric relaxations decrease in intensity and shift to higher frequencies suggesting greater freedom of motion in the epoxy phase as some of the PES diffuses out and this is paralleled by reductions of intensity in the mechanical relaxations of the annealed materials. The changes registered by dielectric and dynamic mechanical spectroscopy and DSC are however reflected in the impact strengths, which decrease with annealing.

It seems clear that the microscopic changes that occur during annealing must be diffusional and naturally in polymer blends this is a slow process. In the 30I and 30B blends if the diffusion is due to the PES as it clearly must be since the epoxy is well cured, the PES chains are forced to move throughout a network structure which will slow them down considerably. The mechanism by which this might occur is described by DeGennes (1979) and Doi and Edwards (1986) and is termed reptation, which is the slow diffusion of a polymer chain along its own contour in the presence of topological constraints such as a network of fixed obstacles. Unfortunately insufficient time was available for further investigation but it seems a likely means of

diffusion of the PES and the reptation mechanism would account for the slowness of the diffusion process. However, it would be expected that the shorter average chain lengths of the BASF PES molecules might allow the processes to occur faster in the 30B blend. This does not seem to be the case from the results.

4.4 Summary

Mixing 828 difunctional epoxy monomer with a hardener, DICY and mixing this with PES forms a homogeneous solution. After removal of the solvent the system is still homogeneous but curing causes a second phase to be precipitated, seen as large spherical particles of 10-20μm in size under the SEM. The two phases are clearly detectable also by DSC and mechanical spectroscopy. The different types of PES (ICI or BASF) appear to make little difference to the morphology or other properties of the as cured material except that a slightly higher free volume in the BASF blends can be inferred from mechanical spectroscopy. In other respects the blends are virtually identical in terms of calorimetric and mechanical properties. The BASF blend has a marginally higher impact strength but not significant enough to be considered important.

Annealing the materials at temperatures from below the T_g of the lower temperature phase to below the high temperature phase T_g produces similar effects irrespective of the type of PES in the blend. At both extremes of temperature, the effect on properties appears similar. The mechanical spectra undergo significant changes which are not reflected in the morphology of fracture surfaces, but which are detectable as decreases in the impact strength and variations in the appearance of the heat capacity curves. There are continual fluctuations in the activation energy and entropy of the local relaxations, suggestive of microscopic changes.

The results indicate that although the materials appeared to be fully cured, curing was so rapid that it prevented complete phase separation which then continued more slowly during annealing.

Chapter 5

Conclusions

5.0 *Introduction*

A large amount of data has been presented in chapters 3 and 4. The purpose of this chapter is to summarise briefly the conclusions that can be drawn from the experimental and associated work.

5.1 Single Phase Systems Containing PES

On the basis of the work of chapter 5, the following can be concluded:

1). The addition of PES to an epoxy resin which is subsequently cured, does not necessarily result in a phase separated system. The fact that no PES phase was detectable by SEM combined with the heat capacity measurements and the good agreement obtained by use of the Flory-Fox equation, suggest that the blends are single phase. Even when reactions between the end groups of the epoxy are favoured, these will not occur to any detectable extent during the cure schedule, accounting for the similar properties of the blends made with -OH terminations and -Cl terminations. The reaction between -OH terminations on the PES and the epoxy resin must be carried out prior to curing if phase separation is to be expected.

2). Blending PES with the Epikote 828-DDS system reduced the heats of reaction of the blends relative to the neat resin, suggesting a reduction in the crosslink density of the network with increasing PES weight fraction. This is detectable also through the heat capacity of the cured materials. However, although the crosslink density is indirectly observed to decrease, it appears that similar glass transition temperatures result because the PES chains stiffen the network.

3). It was thought that the curing process might lead to the formation of a network faster than the PES could phase separate. Dynamic mechanical analysis suggests that there is a phase separation process occurring initially in all of the blends, but that this process is associated with low crosslink density regions in the main network, because it occurs also in the unmodified resin. The weak mechanical spectroscopy peak associated with this small fraction of phase subsequently remerges with the main glass transition peak. This can be attributed to the changes in conformation and the diffusion of free volume that occur during physical ageing. This could permit a limited redistribution of segregated hardener and/or monomer which could increase the crosslink density of these few regions, resulting in an increase in T_g of the less crosslinked regions and accounting for the remerging of the peak.

4). For the systems studied, an exponential model of the enthalpy relaxation is inadequate, but can be modelled well using the Kohlrausch function. Increasing PES content reduces the network stiffness and allows more conformational freedom. The reduced rigidity of the network allows faster relaxation leading to increased β and reduced τ, in agreement with the experimental data. Modelling of isothermal enthalpy relaxation is useful in assessing the suitability of materials for use at elevated temperatures and could assist in the selection and design of single phase blend systems. Furthermore, it appears that similar increases in network freedom are reflected by the scaling parameters in a power law analysis of the dynamic mechanical relaxations, the scaling parameters increasing with PES content.

5) The reduced crosslink density of the blends as PES is added may account for the slight increases in impact toughness. However, it should also be noted that although the blends appear to be slightly tougher, they physically age at faster rates and suffer more rapid deterioration of impact properties than the unmodified resin aged at the same temperature. This should be cause for

concern. Adhesive properties and tack may be improved as PES is added, but clearly the upper use temperature becomes lower. This is despite the fact that superficially, the unmodified epoxy and the blends have similar glass transition temperatures and other associated properties.

6) The foregoing conclusions suggest that in other single phase epoxy-thermoplastic blends, similar effects might be observed, particularly with regard to the reduction in the extent of crosslinking reactions and crosslink density.

5.2 Two Phase Systems Containing PES

On the basis of the work described in chapter 4, the following can be concluded;

1). In two phase systems, the use of which is now increasing, it appears that the materials studied are considerably affected by annealing. Although the materials have cured, the curing seems to have occurred so quickly as to freeze in some of the separating phase prior to complete phase separation.

2). Mechanical spectra and to a lesser extent, heat capacity measurements reveal that at a microscopic level, there are continuously ongoing changes as the materials slowly change during annealing. These changes produce no visible change in the morphology viewed in the SEM but quite large reductions in G_{IC} are observed. The changes are believed to be caused by internal rearrangements within the phases rather than further gross separation and are perhaps a manifestation of microphase rather than macroscopic phase changes.

3) The dramatic changes observed in the two phase systems are important, particularly because there is a growing interest in the use of epoxy resin-thermoplastic two phase systems. Although this work has been carried out using PES, similar effects may occur when other thermoplastic additives are used. Many studies describe the manufacture of such systems but none appear to have addressed the changes that occur when these systems are annealed. It is very important to catalogue such behaviour, especially in commercial two phase epoxy-thermoplastic blends where mechanical integrity is vitally important.

Chapter 6

Recommendations for Further Work

6.0 Introduction

Naturally, nothing can be totally conclusive without conducting exhaustive measurements and there remain many aspects of the work presented in this thesis which require further and more rigorous investigation, involving without question, techniques that were not accessible during the study period as well as more time. What follows are suggestions for future research related to the subject matter of this thesis.

6.1 Suggestions for Future Work Related to Chapter 3

Suggestions for further work are as follows:

1). An extensive study of the effects of varying molecular weight of the PES could be undertaken to examine in more detail the influence of the chain ends.

2). Similar experiments be conducted with other thermoplastic additives which give rise to single phase systems to see if the behaviour is general.

3) A more extensive impact testing programme would be useful for generating data at many temperatures/times, particularly with regard to the needs of engineers.

4) From the research point of view, it would be useful to characterise the as cured epoxy resin and blends by means of PAL (Deng et al, 1992), so that the free volume distribution of the materials prior to ageing could be compared. It would also be interesting to examine the changes in the free volume distribution in the aged materials and, if such measurements were possible, to follow the relaxation of the peak in the free volume distribution to see what functional form it fits best.

6) It would be useful to study enthalpy relaxation of epoxy-PES blends in more detail, at different temperatures and using more rigorous modelling to characterise the physical ageing behaviour and to compare this with free volume distribution data.

7) Mechanical spectroscopy might also be used to monitor changes in the microscopic structure during physical ageing by following changes in the W-L-F constants or the power law constants as a function of time.

6.2 Suggestions for Future Work Related to Chapter 4

It is suggested that:

1) The annealing behaviour of a system in which improved toughness is obtained by small PES rich particles (e.g. Hedrick et al, 1991) be studied to see the effects on mechanical properties. If physical ageing occurs , it would be interesting and useful to collect isothermal data concerning enthalpy and volume relaxation and mechanical properties.

2) The study should be extended to include systems which use other two-phase epoxy thermoplastic systems.

Appendix 1

A1.0: Remarks Concerning the Kohlrausch function obtained from a Distribution of Relaxation Times

The simplest approach (although not the only one, see Ngai et al, 1986) to justifying the use of the Kohlrausch function is by assuming the non-exponential relaxation function arises from a superposition of exponential relaxations. In a polymer this may amount to several different units in each macromolecule each type of unit exhibiting a different exponential relaxation time. Mathematically the function that describes the relaxation of a material property is expressed as the relaxation function $\phi(t)$, given by

$$\phi(t) = \exp-(t / \tau) \qquad \text{(A1.1)}$$

for single relaxing entity but by

$$\phi(t) = \int_0^\infty [\exp-(t / \tau)]\rho(\tau)d\tau \qquad \text{(A1.2)}$$

when many overlapping relaxation processes occur within the same system.

In equation (A1.2) the term

$$\int_0^\infty \rho(\tau)d\tau \qquad \text{(A1.3)}$$

is the normalisation condition and defines the Debye relaxation time distribution function. The quantity $\rho(\tau)$ is the Debye distribution of relaxation times, although it seems that it has no clear physical meaning.

Because of the wide time range covered, it is usual to express equation (A1.2) in terms of the logarithm of time

$$\phi(t) = \int_{-\infty}^{\infty} [\exp-(t / \tau)]\tau\rho(\tau)d\ln\tau \qquad \text{(A1.4)}$$

For many materials the macroscopic relaxation function is non exponential and can be well approximated by the relation

$$\phi(t) \approx \exp-(t / \tau_k)^\beta \qquad \text{(A1.5)}$$

which is called the Kohlrausch function where $0 \lhd \beta \leq 1$. If the relaxation function is considered to arise from a superposition of exponential relaxations then

$$\exp-(t/\tau_k)^{\beta} = \int_{-\infty}^{\infty}[\exp-(t/\tau)]\tau\rho(\tau)d\ln\tau \qquad \text{(A1.6)}$$

An average relaxation time which corresponds to the integrated area of the Kohlrausch function is given by

$$\langle\tau\rangle = \frac{\tau_k}{\beta}\Gamma\left[\frac{1}{\beta}\right] \qquad \text{(A1.7)}$$

with higher moments given by

$$\langle\tau^n\rangle = \frac{\tau_k^n}{\beta}\frac{\Gamma(n/\beta)}{\Gamma(n)} \qquad \text{(A1.8)}$$

Equation (A1.8) arises as a consequence of the definition of the moments of the distribution

$$\langle\tau^n\rangle = \int_0^{\infty}\tau^n\rho(\tau)d\tau = \frac{1}{\Gamma(n)}\int_0^{\infty}t^{n-1}\phi(t)dt \qquad \text{(A1.9)}$$

Equation (A1.9) can be arrived at by letting

$$\langle\tau^n\rangle = \frac{1}{\Gamma(n)}\int_0^{\infty}t^{n-1}\phi(t)dt \qquad \text{(A1.10)}$$

and inserting equation (A1.2) yields

$$\langle\tau^n\rangle = \frac{1}{\Gamma(n)}\int_0^{\infty}t^{n-1}\left[\int_0^{\infty}[\exp-(t/\tau)]\rho(\tau)d\tau\right]dt \qquad \text{(A1.11)}$$

Exchanging t^{n-1} for $\rho(\tau)$ and changing the order of integration yields

$$\langle\tau^n\rangle = \frac{1}{\Gamma(n)}\int_0^{\infty}\rho(\tau)\left[\int_0^{\infty}[\exp-(t/\tau)]t^{n-1}dt\right]d\tau \qquad \text{(A1.12)}$$

Using the definition of the gamma function as

$$\Gamma(n) = \int_0^\infty t^{n-1}[\exp -t]dt \qquad t \succ 0 \qquad \text{(A1.13)}$$

we obtain

$$\begin{aligned} \langle \tau^n \rangle &= \frac{1}{\Gamma(n)} \int_0^\infty \rho(\tau)\left[\Gamma(n)\tau^n\right]d\tau \\ &= \int_0^\infty \tau^n \rho(\tau) d\tau \end{aligned} \qquad \text{(A1.14)}$$

which defines the average relaxation time.

An average relaxation frequency can also be defined as (Lindsey and Patterson, 1980)

$$\langle \omega^n \rangle = \int_0^\infty \frac{1}{\tau^n}\rho(\tau)d\tau = (-1)^n \frac{d^n \phi(0)}{dt^n} \qquad \text{(A1.15)}$$

but the derivative of the Kohlrausch function is

$$\frac{d\phi(t)}{dt} = -\frac{\beta}{\tau_k}\left[\frac{t}{\tau_k}\right]^{\beta-1} \phi(t) \qquad \text{(A1.16)}$$

which diverges as $\tau \to 0$, thereby preventing the definition of an average relaxation frequency given by equation A1.15. Clearly there may be a problem in the physical interpretation of the Kohlrausch function when it is obtained from a distribution of relaxation times.

It is possible to obtain the distribution of relaxation times $\rho(\tau)$ in principle from the relaxation function by means of an inverse Laplace transform

$$\phi(t) = \int_0^{\infty} [\exp -(t/\tau)]\rho(\tau)d\tau$$

with $\chi = \frac{1}{\tau}$ then $d\tau = -\frac{1}{\chi^2}d\chi$

$$\phi(t) = \int_0^{\infty} [\exp - \chi t]\frac{\rho(1/\chi)}{\chi^2}d\chi$$

$$= \left(\frac{\rho(1/\chi)}{\chi^2}\right) \qquad \text{(A1.17)}$$

$\rho(\tau)$ is then given by

$$\rho(\tau) = \left(\frac{1}{\tau^2}\right) \qquad [\phi(t)]$$

There is no analytical solution for the Laplace or Fourier transforms of the Kohlrausch function, making difficult the calculation of a distribution of relaxation times or analysis of the Kohlrausch function in the frequency domain. This makes it necessary to use numerical or series methods to calculate $\rho(\tau)$ (Lindsey and Patterson, 1980).

A1.1: Interpretation of the Constants in the Kohlrausch Function

The constants in the Kohlrausch function can be obtained by a non-linear least squares fit using the Levenberg-Marquardt algorithm where χ^2 is minimised[1].

The relaxation time τ_K is simply the time at which the relaxation function $\phi(t)$ has decayed by 63% or (1-1/e). The β parameter in the Kohlrausch function determines the shape of the function and is interpreted as a measure of the non-exponential character of the relaxation function or as a measure of the variance of the distribution of relaxation times (Lindsey and Patterson, 1980). As β becomes smaller, so the distribution becomes broader but as β ->1, the relaxation process becomes more exponential and the distribution approaches the Debye distribution.

It is claimed by some that β is always time and temperature independent (Hodge, 1991) but this appears to vary with the system being studied, some systems displaying a temperature independent β, others exhibiting weak temperature dependence and some a strong temperature dependence (Ngai et al, 1987). However, one might expect the temperature dependence to be connected with the free volume at different temperatures. It also depends upon the physical quantity being measured and different β 's and τ_K's will generally be found from different physical measurements.

Physically however, a distribution of relaxation times makes sense in terms of the Cohen and Turnbull (1959) and Turnbull and Cohen (1961) ideas of the free volume theory. It seems logical also that during physical ageing the distribution of free volume and the distribution of relaxation times should change as a function of the density of the glass. One also envisages that exponential relaxation may persist for a short time in the sense of Ngai's theory, but that there will exist a point when sufficient free volume has been eliminated that the movements of molecules become strongly coupled. This could mean a change in the distribution of relaxation times detected via β.

Clearly, at some temperatures, probably high and close to the glass transition, the equilibrium state of packing may be such that molecules are not closely associated, and there is a high amount of equilibrium free volume. This could

---

[1]Press, W.H., Teukolksky, S.A., Vettering, W.T. and Flannery, B.P., "Numerical Recipes in Fortran", Cambridge University Press (1992)

lead to a time independent β and exponential relaxation at high temperatures (c.f figure A1.1)

However, as the ageing temperature is lowered, so the equilibrium state becomes increasingly one of greater packing density, so that the correlations between molecules become much more important. As densification proceeds so some molecular relaxations will be frozen out and this must change the distribution of relaxation times and presumably β would be expected to change also. However, since the fastest relaxing units will freeze out first, it is possible for β to remain unchanged but with changes occurring in the short relaxation part of the distribution accompanied by changes in the peak height which correspond to a reduced number of active relaxations.

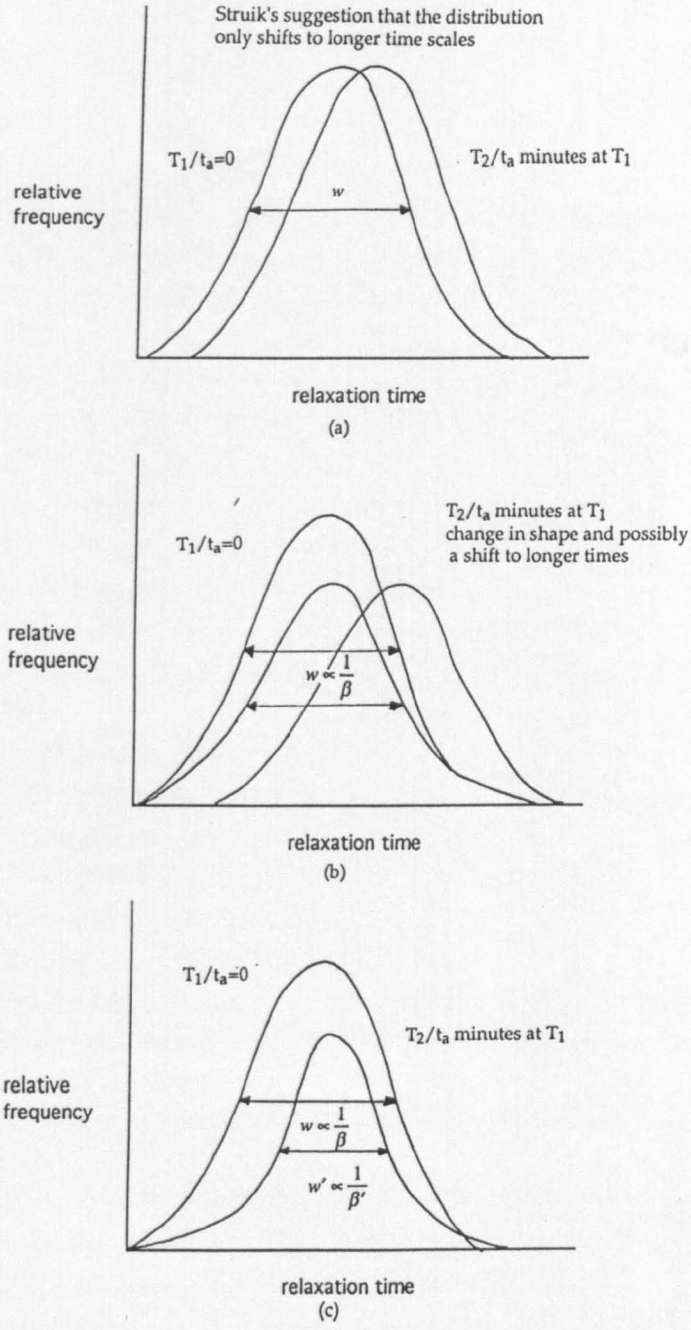

Figure A1.1: Hypothesised effects of temperature-time on the distribution of relaxation times: (a) Struik's suggestion that decreasing the sub-T_g temperature or ageing a glass below T_g simply shifts the spectrum of relaxation times. This may be valid at higher temperatures near to T_g. (b) It may be the case that decreasing the temperature and/or ageing the glass changes the shape of the spectrum as well as shifting the spectrum to longer times. If only the short relaxation times are frozen out, the change of shape does not have to change β .(c) At lower temperatures it is possible that β changes shape as well.

References

Adam, G. and Gibbs, J.H., J. Chem. Phys., **43** 139 (1965)

Allen, R.O. and Sanderson, P., Appl. Spectroscopy Reviews, **24(3,4)** 175 (1988)

Almen, G.R., Mackenzie, P., Malhotra, V., Maskell, R.K., McGrail, P.T., and Sefton, M.S., 20th International SAMPE Technical Conference, Sept. 27-29, (1988a)

Almen, G.R., Maskell, R.K., Malhotra, V., Sefton, M.S., McGrail, P.T. and Wilkinson, S.P., 33rd International SAMPE Symposium, Mar. 7-10, (1988b)

Almond, D.P., Bradell, O.G. and Harris, B., Polymer, **33(10)** 2234 (1992)

Angell, C.A and Sichina, W., Ann. N.Y. Acad. Sci., **279** 53 (1976)

Barlow, J.W. and Paul, D.R., Polym. Eng. Sci., **21** 985 (1981)

Bartenev, G.M., Polym. Sci. USSR, **3** 524 (1988)

Bascom, W.D. and Cottington, R.L., J. Adhesion, **7** 333 (1976)

Bascom, W.D., Ting, R.Y, Moulton, R.J., Riew, C.K. and Siebert, A.R., J. Mat. Sci., **16** 2657 (1981)

Baur, H., Rheologica Acta, **28** 333 (1989)

Bell, J.P. and McCavill, W.T., J. Appl. Polym. Sci., **18** 2243 (1974)

Bellamy, L.J., "Infra-Red Spectra of Complex Molecules", Volumes I and II, Chapman and Hall, (1976)

Bicerano, J., J. Polym. Sci., **29** 1329 (1991a)

Bicerano, J., J. Polym. Sci., **29** 1345 (1991b)

Binney, J.J., Dowrick, N.J., Fisher, A.J. and Newman, M.E.J., "The Theory of Critical Phenomena", Oxford Science Publications, Clarendon Press, Oxford (1992)

Brawer, S., "Relaxation in Viscous Liquids and Glasses", American Ceramic Society, (1985)

Breach, C.D., Folkes, M.J. and Barton, J.M., Polymer **33(14)** 3080 (1992)

Bubeck, R.A., Bales, S.E. and Lee, H.D., Polym. Eng. Sci., **24** 1142 (1984)

Bucknall, C.B. and Partridge, I.K., Brit. Polym. J., **15** 71 (1983)

Bucknall, C.B. and Partridge, I.K., Composites, **15(2)** 129 (1984)

Bucknall, C.B. and Partridge, I.K., Polym. Eng. Sci., **26** 54 (1986)

Cahn, J.W., J. Chem. Phys., **42** 93 (1965)

Callen, H.B., "Thermodynamics and an Introduction to Thermostatistics", 2nd Edn., Wiley (1985)

Chandler, D., "Introduction to Modern Statistical Mechanics", Oxford University Press, (1987)

Chang, T.D., Carr, S.H. and Brittain, J.O., Polym. Eng. Sci., **22** 1205 (1982a)

Chang, T.D., Carr, S.H. and Brittain, J.O., Polym. Eng. Sci., **22** 1213 (1982b)

Chang, T.D., Carr, S.H. and Brittain, J.O., Polym. Eng. Sci., **22** 1221 (1982c)

Charlesworth, J.M., J. Polym. Sci., **B17** 329 (1979)

Chow, T.S., Macromolecules, **22** 698 (1989a)

Chow, T.S., Macromolecules, **22** 701 (1989b)

Chow, T.S. and Prest, W.M., J. Appl. Phys., **53(10)** 6568 (1982)

Choy, I.C. and Plazek, D.J., J. Polym. Sci., **B24** 1303 (1986)

Cohen, M.H and Turnbull, D.J., J. Chem. Phys., **31** 1164 (1959)

Colmenero, J., Alegria, A., Alberdi, J.M., Alvarez, F. and Frick, B., Phys. Rev., **B44(14)** 7321 (1991)

Cukierman, S., Halary, J.L. and Lucien, M., Polym. Eng. Sci., **31** 1476 (1991)

Cusack, N.E., "The Physics of Structurally Disordered Matter", Adam Hilger, Bristol, (1987)

Davies, R.O. and Jones, G.O., Adv. Phys., **2** 370 (1953)

Dammant, F.R. and Kwei, T.K., J. Polym. Sci. A2, **5** 761 (1967)

DeBolt, M.A., Easteal, A.J., Macedo, P.B. and Moynihan, C.T., J. Amer. Cer. Soc., **59** 16 (1976)

De Gennes, P.G., "Scaling Concepts in Polymer Physics", Cornell University Press, (1979)

Deng, Q., Zandiehnadem, F. and Jean, Y.C., Macromolecules, **25** 1090 (1992)

Doi, M. and Edwards, S.F., "Theory of Polymer Dynamics", Oxford University Press, (1989)

Doolittle, A.K., J. Appl. Phys., **22** 1471 (1951)

Döll,W., in "Fractography", Ed. A.C. Roulin-Moloney, Elsevier (1989)

Diamant, Y., Marom, G. and Broutman, L., J. Appl. Polym. Sci., **26** 3015 (1981)

Dumais, J.J., Cholli, A.L., Jelinski, L.W., Hedrick, J.L. and McGrath, J.E., Polymer, **19** 1884 (1986)

Ehrenfest, P., Proc. Kon. Akad. Wetensch. Amsterdam, **36** 153 (1933)

Elliot, S.R., "Physics of Amorphous Materials", Longman Scientific, (1984)

Ellis, T.S. and Karasz, F.E., Polym. Eng. Sci., **26** 290 (1986)

Enns, B. and Gillham, J.K., J. Appl. Polym. Sci., **28** 2831 (1983)

Erath, E.H. and Robinson, M., J. Appl. Polym. Sci. C, **3** 65 (1969)

Ferry, J.D., "Viscoelastic Properties of Polymers", Wiley, (1980)

Flory, P.J., "Principles of Polymer Chemistry", Cornell University Press, Ithaca, (1953)

Fox, T.J. and Flory, P.J., J. Appl. Phys., **21** 581 (1950)

Fox, T.J. and Flory, P.J., J. Phys. Chem., **55** 221 (1951)

Fox, T.J. and Flory, P.J., J. Polym. Sci., **14** 315 (1954)

Fried, J.R. in "Developments in Polymer Characterisation", Ed. J.V. Dawkins, Applied Science, (1983)

Garroway, A.N., Ritchey, W.M. and Mainz, W.B., Macromolecules, **15** 1051 (1982)

Gerard, J., Galy, J., Pascault, J.P., Cukierman, S. and Halary, J.L., Polym. Eng.

Sci., **31** 615 (1991)

Gibbs, J.H. and DiMarzio, E.A., J. Chem. Phys., **28** 373 (1958)

Goldstein, M.J., J. Chem. Phys., **39** 3369 (1963)

Goldstein, M.J., J. Chem. Phys., **51** 3728 (1969)

Goldstein, M.J., J. Chem. Phys., **77** 667 (1973)

Goldstein, M.J., J. Chem. Phys., **64** 4767 (1976)

Goldstein, M.J., J. Chem. Phys., **67** 2246 (1977)

Grest, G.S. and Cohen, M.H., Adv. Chem. Phys., **48** 455 (1981)

Gupta, V.B. and Brahatheeswaran, C., Polymer, **32** 1875 (1991)

Gupta, P.K. and Moynihan, C.T., J. Chem. Phys., **65** 4136 (1976)

Hedrick, J.L., Yilgor, I., Jurek, M., Hedrick, J.C., Wilkes, G.L. and McGrath, J.E., Polymer, **32** 2020 (1991)

Hiltner, A. and Baer, E., Polymer, **15** 805 (1974)

Hirschfelder, J., Stevenson, D. and Eyring, H., J. Chem. Phys., **5** 896 (1935)

Hodge, I.M., J. Non-Crystalline Solids, **131** 435 (1991)

Hutchinson, J.M. and Kovacs, A.J., J. Polym. Sci., **B14** 1575 (1976)

Hutchinson, J.M. and Ruddy, M., J. Polym. Sci., **B26** 2341 (1988)

Jäckle, J., Rep. Prog. in Phys., **49** 171 (1986)

Johari, G.P., J. Chem. Phys., **58** 1766 (1973)

Johari, G.P., Phil. Mag., **41** 41 (1980)

Jonscher, A.K., Phys. Status. Solidi, **6** 585 (1977)

Kaiser, J., Makromol. Chem., **180** 573 (1979)

Kambour, R.P., Polym. Comm., **24** 292 (1983)

Kambour, R.P. and Matsumoto, D.S., Polym. Comm., **24** 297 (1983)

Kauzmann, W., Chem. Rev., **43** 219 (1948)

Kenyon, A.S. and Nielsen, L.E., J. Macromol. Chem., **A3** 275 (1969)

Kim, S.L, Skibo, M.D., Manson, J.A., Hertzberg, R.W. and Janiszewski, J., Polym. Eng. Sci., **18** 1093 (1978)

Kinloch, A.J. and Young, R.J., "Fracture Behaviour of Polymers", Applied Science (1983)

Kinloch, A.J., Shaw, S.J., Todd, D.A. and Hunston, D.L., Polymer, **24** 1341 (1983)

Kohlrausch, R., Pogg. Ann. Physik., **4-91** 56 (1854)

Kong, E.S.W., J. Appl. Phys., **52** 5921 (1981)

Kong, E.S.W., "Epoxy Resin Chemistry", Chapter 9, American Chemical Society Symposium (1983a)

Kong, E.S.W., 28th Nat. SAMPE Symposium, April 1-14th (1983b)

Kong, E.S.W., "Highly Crosslinked Polymers", Chapter 9, American Chemical Society Symposium (1984)

Kong, E.S.W., Wilkes, G.L., McGrath, J.E., Banthia, A.K., Mohajir, Y. and Tant,

M.R., Polym. Eng. Sci., **21** 943 (1981)

Kong, E.S.W., and Adamson, M.J., Polym. Comm., **24** 171 (1983)

Kong, E.S.W., Tant, M.R., Wilkes, G.L., Banthia, A.K. and McGrath, J.E., Polymer Preprints, **20** 531 (1979)

Kovacs, A.J., Fortschr. Hochpolymer Forsch., **3** 394 (1963)

Kovacs, A.J., Aklonis, J.J., Hutchinson, J.M. and Ramos, A.R., J. Polym. Sci. B, **17** 1097 (1979)

Kramer, E.J., Adv. Polym. Sci., **52/53** 1 (1983)

Kriebich, U.T. and Schmidt, R., J. Polym. Sci. Symp., **53** 177 (1975)

Kunz-Douglass, S., Beaumont, P.W.R. and Ashby, M.F., J. Mat Sci., **15** 1109 (1980)

Landi, V.R., Appl. Polym. Symp., **25** 223 (1974)

Lee, H. and Neville, K., "Handbook of Epoxy Resins", McGraw Hill, New York (1967)

Legrand, D.G., J. Appl. Polym. Sci., **13** 2129 (1969)

Lilley, J. and Holloway, D.G., Phil. Mag., **28** 215 (1973)

Lin, Y.G., Sautereau, H. and Pascault, J.P., J. Appl. Polym. Sci., **32** 4595 (1986)

Lindenmeyer, P.H., Polym. Eng. Sci., **21** 958 (1981)

Lindsay, C.P. and Patterson, G.D., J. Chem. Phys., **73** 3348 (1980)

MacKnight, W.J., Stoelting, J. and Karasz, F.E., Adv. Chem. Ser., **99** 26 (1971)

Mason, P., Polymer, **5** 625 (1964)

Matsuoka, S., J. Rheology, **30** 489 (1986)

Matsuoka, S., "Relaxation Phenomena in Polymers", Soc. Plastics Engineers, Hanser (1992)

Matsuoka, S. and Bair, H.E., J. Appl. Phys., **48** 4058 (1977)

Matsuoka, S., Bair, H.E., Bearder, S.S., Kern, H.E. and Ryan, T.T., Polym. Eng. Sci., **18** 1073 (1978)

Manzione, L.T., Gillham, J.K. and McPherson, C.A., J. Appl. Polym. Sci., **26** 889 (1981)

McCrum, N.G., Read, B.E. and Williams, G., "Anelastic and Dielectric Effects in Polymeric Solids", Dover, New York (1967)

Mijovic, J., J. Composite Materials, **19** 178 (1985)

Mijovic, J. and Kowstky, J.A., Polym. Eng. Sci., **24** 57 (1984)

Mijovic, J. and Liang, R.C., Polym. Eng. Sci., **24** 57 (1984)

Mikolajczak, G., Cavaille, J.Y. and Johari, G.P., Polymer, **28** 2023 (1987)

Morgan, R.J., J. Appl. Polym. Sci., **23** 2711 (1979)

Morgan, R.J. and O'Neal, J.E., " Chemistry and Properties of Crosslinked Polymers", Ed. S.S. Labana, Academic Press (1977a)

Morgan, R.J. and O'Neal, J.E., J. Mat. Sci., **12** 1966 (1977b)

Morgan, R.J. and O'Neal, J.E., Polym. Plast. Technol. Eng., **10** 49 (1978a)

Morgan, R.J. and O'Neal, J.E., J. Macromol. Sci. Phys., **B15** 139 (1978b)

Morgan, R.J. O'Neal, J.E. and Miller , D.B., J. Mat. Sci., **14** 109 (1979)

Mostovoy, S. and Ripling E.J., J. Appl. Polym. Sci., **10** 1351 (1966)

Narayanaswamy, O.S., J. Amer. Cer. Soc., **54** 491 (1971)

Nielsen, L.E., J. Appl. Polym. Sci., **47** 237 (1964)

Nielsen, L.E., J. Macromol. Sci., Rev. Macromol. Chem., **C3** 69 (1969)

Ngai, K.L., "Non-Debye Relaxation in Condensed Matter", Ed. T.V. Ramakrishnan and M. Raj Lakshimi, World Scientific (1987)

Ngai, K.L., Rajagopal, A.K. and Huang, C.Y., J. Appl. Phys. **55** 1714 (1984)

Ngai, K.L., Rajagopal, A.K. and Rendell, R.W., IEEE Trans. Elec. Ins., **EI 21** 313 (1986)

Ngai, K.L., Rajagopal, A.K. and Teitler, S., J. Chem. Phys., **88** 5086 (1988)

Ngai, K.L., Rendell, R.W., Rajagopal, A.K. and Teitler, S., Ann. New York Acad. Sci., **484** 150 (1986)

Ochi, M., Okasaki, M. and Shimbo, M., J. Polym. Sci., **B20** 689 (1982)

Ochi, M., Yoshizumi, M. and Shimbo, M., J. Polym. Sci., **B25** 1817 (1987)

Oleinik, E.F., Pure and Appl. Chem., **53** 1567 (1981)

Ophir, Z.H., Emerson, J.A. and Wilkes, G.L., J. Appl. Phys., **49** 5032 (1978)

Pang, K.P. and Gillham, J.K., J. Appl. Polym. Sci., **38** 2115 (1989)

Paul, D.R. and Altamirano, J.O., Adv. Chem. Ser., **142** 371 (1975)

Petrie, S.E.B., J. Polym. Sci. A-2, **10** 1255 (1972)

Plazek, D.J. and Frund, Z.N., J. Polym. Sci., **B28** 431 (1990)

Pogany, G.A., Polymer, **11** 66 (1970)

Raghava, R.S., J. Polym. Sci., **B25** 1017 (1987)

Raghava, R.S., J. Polym. Sci., **B26** 65 (1988)

Rajagopal, A.K., Teitler, S. and Ngai, K.L., J. Phys. C., **17** 6611 (1984)

Rajagopal, A.K., Ngai, K.L. and Teitler, S., J. Chem. Phys., **92** 243 (1990)

Rajagopal, A.K., Ngai, K.L. and Teitler, S., J. Non. Cryst. Solids, **131-133** 282 (1991)

Rehage, G. and Borchard, W. in "Physics of Glassy Polymers", Ed. R.N. Haward, Applied Science (1972)

Rendell, R.W., Lee, T.K. and Ngai, K.L., Polym. Eng. Sci., **24** 1104 (1984)

Richardson, M.J. and Saville, N.G., Polymer, **18** 413 (1977)

Rowe, E.H., Siebert, A.R. and Drake, R.S., Mod. Plast., **47** 110 (1970)

Scherer, G.W., "Relaxation in Glass and Composites", Wiley, New York (1986)

Sefton, M.S., McGrail, P.T., Peacock, J.A., Wilkinson, S.P., Crick, R.A., Davies, M. and Almen, G., 19th International SAMPE Technical Conference, Oct. 13-15th (1987)

Shaw, M.T., J. Appl. Polym. Sci., **18** 449 (1974)

Siebert, A.R. and Riew, C.K., Org. Plast. Chem., **31** 552 (1971)

Simha, R., Roe, J.M. and Nanda, V.S., J. Appl. Phys., **43** 4312 (1972)

Souletie, J. and Thoulence, J.L., Phys. Rev., **B32** 516 (1985)

Starkweather, H.W., Macromolecules, **14** 1277 (1981)

Starkweather, H.W. and Avakian, P., Macromolecules, **22** 4060 (1989)

Stoetling, J., Karasz, F.E. and MacKnight, W.J., Polym. Eng. Sci., **10** 133 (1970)

Struik, L.C.E., "Physical Ageing in Amorphous Polymers and other Materials", Elsevier (1978)

Sultan, J.N., Laible, R.C. and McGarry, F.J., Appl. Polym. Symp., **16** 27 (1971)

Sultan, J.N. and McGarry, F.J., J. Appl. Polym. Sci., **13** 29 (1979)

Tant, M.R. and Wilkes, G.L., Polym. Eng. Sci., **21** 874 (1981)

Ter Haar, D and Wergeland, H., "Elements of Thermodynamics", Addison-Wesley, London (1966)

Thomson, C.J., "Classical Equilibrium Statistical Mechanics", Oxford Science Publications (1988)

Tool, A.Q., J. Res., **34** 199 (1946)

Tool, A.Q., J. Am. Cer. Soc., **29** 240 (1946)

Turnbull, D. and Cohen, M.J., J. Chem. Phys., **34** 120 (1961)

Wannier, G.H., "Statistical Physics", Dover Publications (1966)

Whiting, D.A. and Kline, D.E., J. Appl. Polym. Sci., **18** 1043 (1974)

Williams, G., Cook, M. and Hains, P.J., J. Chem. Soc., Faraday Trans. II, **2** 1045 (1972)

Williams, M.L., Landel, R.F. and Ferry, J.D., J. Am. Chem. Soc., **77** 3701 (1955)

Williams, J.G., "Fracture Mechanics of Polymers", Ellis Horwood (1984)

Wu, Z., Jiang, D.Z., Seki, M. and Yosomiya, R., Die Angew. Makromol. Chemie, **160** 141 (1988)

Yamanaka, K. and Inoue, T., Polymer, **30** 662 (1989)

Yee, A.F., Polymer Preprints, **22(2)** 285 (1981)

Yee, A.F. and Pearson, R.A. in "Fractography", Ed. A.C. Roulin-Moloney, Elsevier (1989)

Yee, A.F. and Smith, S.A., Macromolecules, **14** 54 (1981)

Zabrzewski, G.A., Polymer, **14** 347 (1973)

Zarzycki, J., "Glasses and the Vitreous State", Cambridge University Press (1991)